



HAL
open science

Synthesis and evaluation of phosphorus polymers for the treatment of effluents contaminated by lanthanides and actinides

Xianyu Ding

► **To cite this version:**

Xianyu Ding. Synthesis and evaluation of phosphorus polymers for the treatment of effluents contaminated by lanthanides and actinides. Material chemistry. Université Montpellier, 2020. English. NNT : 2020MONT108 . tel-03329677

HAL Id: tel-03329677

<https://theses.hal.science/tel-03329677>

Submitted on 31 Aug 2021

HAL is a multi-disciplinary open access archive for the deposit and dissemination of scientific research documents, whether they are published or not. The documents may come from teaching and research institutions in France or abroad, or from public or private research centers.

L'archive ouverte pluridisciplinaire **HAL**, est destinée au dépôt et à la diffusion de documents scientifiques de niveau recherche, publiés ou non, émanant des établissements d'enseignement et de recherche français ou étrangers, des laboratoires publics ou privés.

THÈSE POUR OBTENIR LE GRADE DE DOCTEUR DE L'UNIVERSITÉ DE MONTPELLIER

En Chimie des matériaux

École doctorale Sciences Chimiques Balard ED459

Unité de recherche Institut Charles Gerhardt Montpellier UMR 5253

Synthèse et évaluation de polymères phosphorés pour le traitement d'effluents chargés en lanthanides et actinides

Présentée par Xianyu DING
Le 16 décembre 2020

Sous la direction de Sophie MONGE
et Bénédicte PRELOT

Devant le jury composé des

David BERGE-LEFRANC, Professeur, IMBE, Marseille

Olivier COLOMBANI, Maître de conférence-HDR, IMMM, Le Mans

Christophe DEN AUWER, Professeur, ICN, Nice

Catherine FAUR, Professeur, IEM, Montpellier

Bénédicte PRELOT, Directeur de recherche, ICGM, Montpellier

Sophie MONGE, Professeur, ICGM, Montpellier

Rapporteur

Rapporteur

Examineur

Examineur

Co-encadrant de thèse

Directeur de thèse



UNIVERSITÉ
DE MONTPELLIER

Thèse préparée au sein de l'Institut Charles Gerhardt de Montpellier

Université de Montpellier

Institut Charles Gerhardt, UMR 5253,

Place Eugène Bataillon, Bâtiment 17, cc 1702

34095 Montpellier cedex 5 - France

L'ensemble des travaux présentés dans ce manuscrit a
été financé par le programme « Chercheur d'avenir » de la Région
Languedoc-Roussillon



Synthèse et évaluation de polymères phosphorés pour le traitement d'effluents chargés en lanthanides et actinides

Les travaux de cette thèse concernent la synthèse de monomères et de polymères phosphorés et la caractérisation de leurs propriétés complexantes envers des lanthanides (Ln) et des actinides (An) (représentant des éléments radioactifs). Le polymère poly(diéthyl-6-(acrylamido)hexylcarbamoylmethyl phosphonate) (P(CPAAm6C)) et son dérivé mono-hydrolysé mhP(CPAAm6C), contenant des groupes carbamoylméthyl phosphonate, ont été évalués pour leur sorption de gadolinium (Gd(III)) et de thorium (Th(IV)), par dosage en solution et par calorimétrie de titrage pour déterminer les constantes de sorption et corrélérer avec les efficacités de séparation. Puis un nouveau monomère de type oxymethylphosphonate (DiAPC1) a été synthétisé et polymérisé. Les polymères avant et après hydrolyse, nommés poly(dimethyl(acryloyloxymethyl) phosphonate) (P(APC1)) et poly(acryloyloxymethyl acide phosphonique) (hP(APC1)) ont été évalués pour leurs interactions avec le cérium (Ce(III)) et le néodyme (Nd(III)). Enfin un autre monomère contenant une fonction polymérisable de type acrylamide et un groupement phosphonate, nommé diéthyl-2-(acrylamido)éthyl phosphonate (DAAmEP), a été utilisé afin d'obtenir le polymère P(DAAmEP) correspondant. Il a ensuite été hydrolysé afin d'aboutir à la forme acide phosphonique (hP(DAAMEP)). Les deux polymères ont été testés pour leur extraction du gadolinium (Gd(III)), du cérium (Ce(III)), du néodyme (Nd(III)) et du thorium (Th(IV)).

Mots clés: polymère ester phosphoné, polymère acide phosphonique, lanthanides, radio-éléments, sorption, constante de sorption, calorimétrie de titrage

Synthesis and evaluation of phosphorous polymers for the treatment of effluents contaminated by lanthanides and actinides

The work reported in this manuscript deals with the synthesis of phosphonic monomers and polymers, together with the characterization of their complexing properties for selected lanthanides (Ln) and actinides (An). The poly(diethyl-6-(acrylamido)hexylcarbamoylmethyl phosphonate) (P(CPAAm6C)) and its mono-hydrolyzed mhP(CPAAm6C) derivative, which contained carbamoylmethylphosphonate groups, were first evaluated for the sorption of

gadolinium (Gd(III)) and thorium (Th(IV)), using analytical and calorimetric (ITC) tools. Then, a new monomer oxymethylphosphonate (DiAPC1) was synthesized and polymerized. Polymers before and after hydrolysis, poly(dimethyl(acryloyloxymethyl) phosphonate) (P(APC1)) and poly(acryloyloxymethyl phosphonic acid) (hP(APC1)), were evaluated with cerium (Ce(III)) and neodymium (Nd(III)). Finally, another monomer containing acrylamide polymerizable group and phosphonate, named diethyl-2-(acrylamido)ethyl phosphonate (DAAmEP), was used to obtain P(DAAmEP) and then hydrolyzed leading to hP(DAAmEP). Both polymers were finally evaluated with gadolinium (Gd(III)), cerium (Ce(III)), neodymium (Nd(III)), and thorium (Th(IV)).

Keywords: phosphonated-based polymer, phosphonic acid-based polymer, lanthanides, radionuclides, sorption, binding constant, titration calorimetry

Table of contents

Acknowledgements	11
Abbreviation.....	12
Résumé français	14
General introduction	19

Chapter 1: Bibliography

Introduction	24
Part 1: Lanthanides and actinides.....	25
1.1. Lanthanides.....	25
1.1.1. General considerations	25
1.1.2. Resources and production	27
1.2. Actinides	27
1.2.1. General considerations	27
1.2.2. Properties and applications	28
1.2.3. Risks	28
1.3. Separation and recovery of lanthanides and actinides.....	29
1.3.1. Importance and challenges	29
1.3.2. Extraction techniques	30
1.4. Conclusion.....	32
Part 2: Water-soluble polymeric sorbents and thermosensitive property	33
2.1. Water-soluble polymeric sorbents.....	33
2.1.1. Main sorption functional groups.....	33
2.1.2. Phosphonic-acid based polymers for the sorption of metal ions	36

2.1.3. Regeneration and recycling of water-soluble polymeric sorbents	40
2.2. Thermosensitive property of polymeric sorbents	41
2.2.1. General considerations	41
2.2.2. Thermosensitive polymers	43
2.2.3. Thermosensitive phosphorus polymeric sorbents	45
2.3. Conclusion.....	47
Part 3: Interactions between water-soluble polymeric sorbents and metal ions in water	48
3.1. Study of metal ions solutions	48
3.1.1. Introduction of speciation.....	48
3.1.2. Speciation analysis techniques.....	49
3.2. Interaction study methods	51
3.3. Conclusion.....	53
Conclusion.....	54
Chapter 2: Comparison of Isothermal Titration Calorimetry (ITC) and Inductively Coupled Plasma Mass Spectroscopy (ICP-MS) to study sorption properties of polymers	
Introduction	57
1. Introduction	60
2. Experimental section	62
2.1. Materials.....	62
2.2. Synthesis of poly(6-(acrylamido)hexylcarbamoylmethyl phosphonic mono-acid) (mhP(CPAAm6C))	62
2.3. Characterization.....	63
2.4. Sorption experiments.....	64
2.4.1. Preparation of monomer and polymeric sorbents aqueous solutions	64

2.4.2. Preparation of metal ions aqueous solutions	64
2.4.3. Thermodynamics study based on Isothermal Titration Calorimetry (ITC)	65
2.4.4. Sorption experiments by dialysis coupled with Inductively Coupled Plasma Mass Spectrometry (ICP-MS)	65
3. Results and discussion	66
3.1. Synthesis and characterization of poly(6-(acrylamido)hexylcarbamoylmethyl phosphonic mono-acid) (mhP(CPAAm6C))	66
3.2. Sorption properties	68
4. Conclusion	81
Conclusion	83
Chapter 3: Oxymethylphosphonated-based monomers and polymers for the complexation of Cerium and Neodymium: evaluation by Isothermal Titration Calorimetry (ITC)	
Introduction	85
1. Introduction	91
2. Experimental section	93
2.1. Materials and methods	93
2.1.1. Materials	93
2.1.2. Characterizations	93
2.2. Synthesis	93
2.2.1. Synthesis of diisopropyl(acryloyloxymethyl) phosphonate monomer (DiAPC1)	94
2.2.2. Synthesis of dimethyl(acryloyloxymethyl) phosphonate monomer (APC1)	95
2.2.3. Synthesis of acryloyloxymethyl phosphonic acid monomer (hAPC1)	95
2.2.4. Synthesis of poly(diisopropyl(acryloyloxymethyl) phosphonate) (P(DiAPC1))	95
2.2.5. Synthesis of poly(dimethyl(acryloyloxymethyl) phosphonate) (P(APC1))	96

2.2.6. Synthesis of poly(acryloyloxymethyl phosphonic acid) (hP(APC1))	96
2.3. Sorption experiments with Isothermal Titration Calorimetry (ITC).....	96
2.3.1. Preparation of monomer and polymer aqueous solutions	96
2.3.2. Preparation of metal ions aqueous solutions	97
2.3.3. Isothermal Titration Calorimetry (ITC) experiments	97
3. Results and discussions.....	98
3.1. Synthesis of monomers and polymers.....	98
3.1.1. Synthesis of monomers.....	98
3.1.2. Synthesis of polymers	100
3.2. Sorption study.....	102
3.2.1. Sorption results with Ce(III).....	103
3.2.2. Sorption results with Nd(III).....	105
3.2.3. Complexation of hydrolyzed poly(acryloyloxymethyl phosphonate) (hP(APC1)) for Ce(III) and Nd(III) comparison	108
4. Conclusion	109
Appendix	111
Conclusion.....	116
Chapter 4: Thermosensitive phosphonate-based acrylamide polymers: complexation with Ln(III) and Th(IV) studied by Isothermal Titration Calorimetry (ITC)	
Introduction	119
1. Introduction	123
2. Experimental section	125
2.1. Materials and methods	125
2.2. Synthesis.....	126

2.2.1. Synthesis of poly(diethyl-2-(acrylamido)ethylphosphonate) (P(DAAmEP))	126
2.2.2. Synthesis of poly(2-(acrylamido)ethyl phosphonic acid) (hP(DAAmEP))	126
2.2.3. Synthesis of poly(6-(acrylamido)hexylcarbamoylmethyl phosphonic acid) (hP(CPAAm6C)).....	127
2.2.4. Synthesis of poly(acryloyloxymethyl phosphonic acid) (hP(APC1))	127
2.3. Sorption experiments by Isothermal Titration Calorimetry (ITC)	128
2.3.1. Preparation of metal ions and polymers aqueous solutions	128
2.3.2. Isothermal Titration Calorimetry (ITC) experiments	128
3. Results and discussion	129
3.1. Polymer synthesis	129
3.2. Sorption results of P(DAAmEP) and hP(DAAmEP) with Gd(III), Ce(III) and Nd(III)	133
3.3. Sorption results of P(DAAmEP) and hP(DAAmEP) with Th(IV)	137
3.4. Sorption results of hP(DAAmEP), hP(CPAAm6C) and hP(APC1) for Gd(III), Ce(III) and Nd(III).....	141
4. Conclusion	143
Conclusion.....	146
General conclusion and prospect.....	148
Supporting information	153
References	186

Acknowledgements

First of all, I would like to thank Dr Olivier Colombani and Pr David Bergé-Lefranc for accepting to judge my research work. I would also like to give my thanks to Pr Catherine Faur and Pr Christophe Den Auwer for being in my jury.

Then, I want to express my gratitude to my two directors of thesis, Sophie Monge and Bénédicte Prelot, for letting me do this thesis, for proposing me interesting training programs and for all the help and advices in my work. I want to give lots of thanks to Amine Geneste for his work and encouragement. I would also like to thank Dr Michel Meyer for welcoming me in his lab for two weeks, I have learned so much there.

There are many post-doc and PhD colleagues have given me support and help in my three years of work, Xavier Solimando, Hamza Chouirfa, Tarek Benkhaled... lots of thanks to them. I also thank all the permanents in our lab for their encouragement and the interesting discussions, which made my lab life more adorable. I would like to thank my dear friends, Loona Ferrié and Sofia Dominguez, for their understanding and encouragements, which made the three years less difficult, and so much joyful time we have passed together is the best memory for my life in France.

At last, I would like to give my deepest thanks to my parents for their support during my studies in France. It was not easy to bear five years of separation, but they have always understood and encouraged me. Without them, I would have not been willing to finish all the work.

Abbreviation

ACN: acetonitrile

CDCl₃: deuterated chloroform

CHCl₃: chloroform

D₂O: deuterium oxide

DCM: dichloromethane

DMAc: dimethylacetamide

DMSO: dimethyl sulfoxide

EtOH: ethanol

MeOH: methanol

Et₃N: triethylamine

TMSBr: trimethylsilyl bromide

CP: cloud point

M_n: number average molecular weight

Đ: dispersity

NMR: Nuclear Magnetic Resonance

SEC: Size Exclusion Chromatography

ITC: Isothermal Titration Calorimetry

ICP-MS: Inductively Coupled Plasma Mass spectrometry

APC1: dimethyl(acryloyloxymethyl) phosphonate

hAPC1: acryloyloxymethyl phosphonic acid

DiAPC1: diisopropyl(acryloyloxymethyl) phosphonate

CPAAm6C: diethyl-6-(acrylamido)hexylcarbamoylmethyl phosphonate

DAAmEP: diethyl-2-(acrylamido)ethyl phosphonate

P(APC1): poly(dimethyl(acryloyloxymethyl) phosphonate)

P(DiAPC1): poly(diisopropyl(acryloyloxymethyl) phosphonate)

hP(APC1): poly(acryloyloxymethyl phosphonic acid)

P(CPAAm6C): poly(diethyl-6-(acrylamido)hexylcarbamoylmethyl phosphonate)

mhP(CPAAm6C): poly(6-(acrylamido)hexylcarbamoylmethyl phosphonic mono-acid)

hP(CPAAm6C): poly(6-(acrylamido)hexylcarbamoylmethyl phosphonic acid)

P(DAAmEP): poly(diethyl-2-(acrylamido)ethyl phosphonate)

hP(DAAmEP): poly(2-(acrylamido)ethyl phosphonic acid)

REE: rare-earth element

Ln: lanthanide

An: actinide

Gd: gadolinium

Ce: cerium

Nd: neodymium

Th: thorium

U: uranium

Résumé français

Dans le monde d'aujourd'hui où les domaines technologiques et économiques évoluent très rapidement, la demande en certaines matières premières représente un enjeu d'importance croissante. Les éléments de type terres rares (REE) font partie des métaux dits 'technologiques' et constituent des ressources importantes dans les domaines de technologies de pointe. En conséquence, leur approvisionnement est à la fois stratégique et menacé. Actuellement, la Chine possède le quasi-monopole des ressources de terres rares. Selon les rapports du U.S. Geological Survey et le recensement récent en janvier 2020 des éléments concernés, la production de terres rares de la Chine représentait 65% de la production mondiale en 2019, et ses réserves représentaient environ 40% des réserves mondiales [1]. L'Union Européenne consomme de grandes quantités de métaux de terres rares pour les produits de haute technologie et la recherche. Toutefois, elle doit importer plus de 90% de ces métaux, principalement en provenance de Chine en raison du manque d'approvisionnement interne, ce qui rend les pays concernés économiquement dépendants [2]. En conséquence, depuis quelques années, les pays européens ont pris conscience de cette urgence d'améliorer la récupération et le recyclage des terres rares et donc de mieux contrôler les processus de séparation.

Ainsi, divers types de matériaux ont été développés pour extraire les métaux terres rares (REM) présents dans les effluents liquides, les lixiviats ou les solutions résultantes de la dissolution des minéraux monazitiques et des effluents industriels. Parmi tous les types de matériaux qui peuvent être utilisés, les polymères fonctionnalisés par des groupes chélatants ont montré leur efficacité de rétention dans certaines conditions. Cependant, l'une des difficultés rencontrées dans le recyclage des REE à l'aide de matériaux polymères est la présence d'autres contaminants compétiteurs dans les effluents à traiter. Ces contaminants sont principalement l'uranium, le thorium (présent en quantités relativement importantes) et leurs descendants produits par la filiation radioactive (y compris plusieurs isotopes du radium), qui peuvent également interagir au cours de l'extraction par les polymères.

Dans ce contexte, l'objectif de ce travail de thèse est de développer des polymères fonctionnels capables de complexer rapidement, efficacement et sélectivement le thorium, l'uranium (représentant les actinides), le gadolinium, le cérium et le néodyme (représentant les lanthanides). Dans un procédé idéal, ces polymères démontrant différents niveaux de sélectivité permettront d'une part la récupération d'éléments de terres rares (gadolinium, cérium, néodyme) et, d'autre part, l'élimination sélective des contaminants (thorium, uranium). En outre, l'étape de séparation sera également prise en considération, en fonction de la solubilité des polymères.

En effet, la mise en œuvre d'un matériau polymère donné dans un processus de traitement de l'eau doit d'abord être corrélée à sa solubilité. Des polymères sorbants hydrosolubles ont été largement utilisés dans des procédés de rétention en phase liquide (ou *LPR* pour *liquid-phase polymer-based retention*) [3], tandis que les polymères sorbants insolubles sont souvent utilisés dans des procédés mis en œuvre pour l'extraction dite en phase solide (ou *SPE* pour *Solid Phase Extraction*) [4-7], y compris les colonnes d'échange d'ions ou les processus de sorption à lit fixe. Les deux processus présentent des avantages et des inconvénients, tous liés au fait que l'état physique du polymère sorbant influence largement la capacité et la cinétique de sorption, ainsi que l'étape de séparation dans le procédé lui-même. Les polymères sorbants non solubles ont souvent été obtenus par fonctionnalisation de résines polymères [5, 8-10] qui ont été formulées sous forme de billes, de gels, de fibres, de membranes, de mousses ou d'éponges. En raison de leur insolubilité, ces matériaux permettent une séparation facile après l'étape de sorption. En outre, la polyvalence de la mise en forme de ces matériaux a facilité leur mise en œuvre dans des processus d'élution à travers des colonnes, des lits fixes [6, 11-18] ou des membranes [19-23]. De tels procédés ont été largement utilisés parce qu'ils combinent la rétention et la récupération des polluants ciblés, puis facilitent l'étape de séparation, et enfin consomment une faible quantité de solvants organiques [7]. La régénération de ces matériaux est aussi envisageable et réduit le volume de déchets du procédé [24]. Une telle régénération est le plus souvent réalisée par l'élution des matériaux avec une solution acide permettant la désorption des cations métalliques. Cependant, le maximum de sorption est atteint en quelques heures, ce qui signifie une cinétique de sorption lente et limitée par la diffusion de l'espèce métallique dans la solution [25]. La cinétique de sorption est un élément sensible

dans la conception d'un procédé de séparation du fait de son impact sur les différents débits et les temps de résidence. Pour les matériaux solides comme les billes par exemple, certaines espèces métalliques ne peuvent atteindre les sites de sorption en raison des effets de tortuosité, réduisant ainsi l'efficacité et la capacité de sorption du matériau. Dans ces conditions, les chaînes macromoléculaires ne sont pas déployées dans l'eau, réduisant ainsi la disponibilité des sites actifs. Il est possible de contourner cette contrainte de cinétique de sorption lente en utilisant des polymères hydrosolubles [26, 27]. Leur solubilité rend accessibles tous les sites de sorption pour faciliter le contact avec les polluants métalliques, conduisant à une sorption rapide (quelques minutes) [28, 29] et à des capacités de rétention élevées en fonction du nombre de site. Néanmoins, l'utilisation de polymères sorbants hydrosolubles nécessite une étape de séparation post-sorption habituellement réalisée par ultrafiltration [3, 30]. Le procédé d'ultrafiltration (PEUF) combiné aux polymères a été largement étudié, prouvant l'efficacité de cette technique pour l'élimination d'une très grande gamme de polluants. Cependant, il est parfois difficile à mettre en œuvre à l'échelle industrielle du fait qu'elle nécessite une pression relativement élevée, pouvant entraîner un encrassement important des membranes et des coûts d'exploitation élevés [31, 32].

Dans les travaux présentés ici, différents polymères phosphorés solubles dans l'eau ont été développés pour complexer sélectivement différents cations métalliques (radionucléides ou lanthanides). Par ailleurs, l'hydrosolubilité ou l'insolubilité des matériaux préparés ont été considérées. Dans le cas idéal, les matériaux polymères seront thermosensibles ou flocculants après sorption, permettant ainsi à la fois la sorption rapide (lorsqu'ils sont solubles dans l'eau) et une séparation aisée des complexes métal-polymères de la solution aqueuse (lorsqu'ils sont insolubles). Selon les résultats obtenus en termes de capacité de sorption, de sélectivité et de comportement thermosensible ou flocculant, un nouveau processus de traitement d'eau pourrait être proposé, permettant de séparer sélectivement les éléments de terres rares des radionucléides dans l'eau. Idéalement, ce processus, sans solvant organique, sera moins énergivore et moins coûteux que les solutions existantes.

Le premier chapitre du manuscrit rapporte la bibliographie sur les lanthanides et l'utilisation de polymères dans le traitement de l'eau. Une attention particulière a été accordée aux polymères thermosensibles. Le chapitre 2 décrit la poursuite des travaux du Dr

Gomes Rodrigues, avec la synthèse d'un polymère thermosensible complexant à base de phosphore, à savoir le poly(diéthyl-6-(acrylamido)hexylcarbamoylmethyl phosphonate) (P(CPAAm6C)). Le dérivé mono-acide (mhP(CPAAm6C)) a ensuite été préparé. La sorption du gadolinium (Gd(III), lanthanide) et du thorium (Th(IV), actinide) sur les deux polymères a été étudiée suivant une approche classique de sorption par analyse de solutions par spectrométrie de masse à plasma à couplée inductif (ICP-MS) et combinée à la calorimétrie de titration isotherme (ITC). Cela a permis d'évaluer les propriétés complexantes en déterminant les constantes d'interaction et les effets de sélectivité en système bicomposant, en tenant compte également du comportement thermosensible. La sélectivité pour le Th(IV) du polymère thermosensible P(CPAAm6C) dans le mélange de Gd(III) et Th(IV) a été confirmée par ITC et par sorption en membrane de dialyse. La sélectivité du polymère mono-hydrolysé mhP(CPAAm6C) pour le Gd(III) a été également montrée en utilisant cette même combinaison de techniques. Le chapitre 3 a été consacré à la synthèse, à la caractérisation et à l'évaluation de nouveaux polymères de type oxyméthylphosphonés solubles dans l'eau pour la sorption des lanthanides, à savoir le cérium (Ce(III)) et le néodyme (Nd(III)). Le poly(diisopropyl(acryloyloxyméthyl) phosphonate) (P(DiAPC1)) et le poly(diméthyle(acryloyloxyméthyle) phosphonate) (P(APC1)) ont été préparés et hydrolysés, ce qui a conduit à l'obtention du polymère hP(APC1). Les monomères DiAPC1 et APC1 ont également été hydrolysés et évalués pour étudier l'influence des groupes alkyloxy et hydroxy supportés par l'atome de phosphore et pour comparer les monomères aux polymères. Les propriétés complexantes du polymère portant le groupe acide phosphonique pour le Ce(III) et le Nd(III) ont été mis en évidence en ITC. Les polymères sous forme de diméthylphosphonate, et les monomères DiAPC1 et APC1 n'ont pas montré de propriétés complexantes pour le Ce(III) et le Nd(III). Enfin, dans le chapitre 4, des polyacrylamides thermosensibles à base de phosphore, le poly(diéthyl-2-(acrylamido)éthyl phosphonate) (P(DAAmEP)) et son dérivé hydrolysé (hP(DAAmEP)), ont été préparés, caractérisés et évalués pour la sorption des lanthanides et des radionucléides: Gd(III), Ce(III), Nd(III) et Th(IV)). Le hP(DAAmEP)) a montré une meilleure affinité pour le Gd(III), le Ce(III), le Nd(III) et le Th(IV) comparativement au P(DAAmEP)). Le complexe de hP(DAAmEP) avec le Th(IV) a flocculé dans une solution aqueuse à pH acide ou pH naturel. La sélectivité de hP(DAAmEP) envers les Ln(III) et le Th(IV) devra être vérifiée. Bien que le P(DAAmEP) ait montré une

Résumé français

efficacité de complexation relativement faible, sa thermosensibilité pourrait être intéressante. Enfin, les propriétés complexantes des trois polymères sous forme d'acide phosphonique développés précédemment, hP(DAAmEP), hP(CPAAm6C) and hP(APC1), ont été comparées pour le Gd(III), le Ce(III) et le Nd(III). Les matériaux hP(CPAAm6C) et hP(APC1) se sont avérés intéressants pour la sorption du Gd(III), du Ce(III) et du Nd(III).

General introduction

In today's world where the technology innovates so quickly and economy increases with a high speed, the demand for some raw materials is becoming a pressing issue. In such context, rare-earth elements (REEs) are among the metals so-called 'technological' metals, which are important resources in the top-technology fields. As a result, their supply is both strategic and threatened. Currently, China has almost the monopoly of rare-earth resources. According to U.S. Geological Survey's mineral commodity summaries in January 2020, documented rare-earths production of China represented 65% of the worldwide production in 2019, and its reserves was about 40% of the world [1]. Europe (EU) consumes high quantities of REEs for high-tech products and research; however, EU needs to import more than 90% of these metals mainly from China due to the lack of internal supply [2]. It makes it economically dependent in these related fields. European countries have therefore been aware of the urgency to better control the separation processes of REEs in order to enhance their recovery and recycling. Thus, various types of materials have been developed for removing REEs found in liquid effluents, leachates or solutions resulting from the dissolution of monazitic minerals and industrial effluent. Among all types of materials that can be used, polymers functionalized with different binding sites have shown efficiency and even selectivity in some cases. However, one of the difficulties encountered in recycling REEs using polymeric materials is the presence of other contaminants in aqueous solutions. These contaminants are mainly thorium, uranium (present in relatively significant amounts in the earth) and their descendants produced by radioactive parentage (including several radium isotopes), which can also interact with extracting polymers. In such context, the objective of this work was to develop functional polymers able to rapidly, efficiently and selectively complex thorium, uranium (representing actinides), gadolinium, cerium and neodymium (representing lanthanides). In the ideal targeted new process, these polymers demonstrating different selectivity will allow in the one hand the recovery of rare earth elements (gadolinium, cerium, neodymium) and in the other hand the selective removal of contaminants (thorium, uranium). Additionally, separation step will also be taken in consideration, depending on the polymer water solubility.

Indeed, the implementation of a given polymeric material in a water treatment process has to be first correlated to its solubility. Hydro-soluble polymeric sorbents were widely used in a process called 'liquid-phase polymer-based retention' [3] whereas insoluble polymeric sorbents were often employed in processes gathered under 'solid phase extraction' [4-7], including ion-exchange columns or fixed-bed sorption processes. Both processes had their advantages and drawbacks, all linked to the fact that the polymeric sorbent physical state could greatly influence the sorption capacity, the sorption kinetics, and the separation step of the process. Non-soluble polymeric sorbents were often obtained by functionalization of polymeric resins [5, 8-10] that was processed as beads, gels, fibers, membranes, foam or sponge. These materials allowed for the easy separation after the sorption step because of their insolubility. In addition, the versatility of the physical state of these materials facilitated their implementation in elution processes through packed columns, fixed-beds [6, 11-18] or membranes [19-23]. Such processes were widely used because they combined the removal and the recovery of the metallic pollution, facilitated the separation step, and consumed a low amount of organic solvents [7]. The regeneration of these materials was possible and reduced process wastes [24]. Such regeneration was most often achieved by the elution of materials with an acidic solution allowing desorption of the metallic cations. However, the maximum of sorption was reached in few hours meaning slow sorption kinetics limited by the diffusion of the metal species from the solution to the active sorption moieties of the polymeric sorbent [25]. Sorption kinetics was highly important at the process scale because it impacted the different flow rates and residence times. Some sorption-active sites could not be reached by metal species, thereby reducing the sorption capacity of the material because of its solid state and its tortuosity. Indeed, in such context, macromolecular chains were not extended in water, thus reducing the availability of active sites. It was possible to increase the slow sorption kinetics drawback by using a hydro-soluble polymeric sorbent [26, 27]. Its solubility ensured that all the sorption sites were in contact with the metallic pollutants leading to a rapid sorption of the species (few minutes) [28, 29] and to quantitative sorption capacity. Nevertheless, the use of hydro-soluble polymeric sorbents required a post-sorption separation step usually achieved by ultrafiltration [3, 30]. The Polymer Enhanced Ultrafiltration (PEUF) process has been widely studied, proving the efficiency of this technique for the elimination of a very large range of metallic pollution.

However, it was difficult to implement at an industrial scale because the ultrafiltration step required relatively high pressure, could lead to significant membrane fouling, and high operating costs [31, 32].

In the present work, different water-soluble phosphorous polymers will be developed to selectively complex different metal ions (radionuclides or lanthanides). Additionally, water-solubility or insolubility of the prepared materials will be considered. In the ideal case, polymeric materials will be either thermosensitive or flocculant after sorption, thus allowing both rapid sorption (when soluble in water) and easy separation of the metal-polymer complexes from aqueous solution (when insoluble). Depending on results obtained in terms of sorption capacity, selectivity, and thermosensitive or flocculating behaviour, new water process will be proposed allowing selectively separating lanthanides from radionuclides in water. Ideally, this process, without organic solvent, will be less energy consuming and less expensive than existing solutions.

First chapter of the manuscript reports bibliography about lanthanides and the use of polymers in water treatment. In particular, special attention will be paid to thermosensitive polymers. Chapter 2 describes the continuation of the work of Dr Donatien Gomes Rodrigues, with the synthesis of a thermosensitive and complexing phosphorous-based polymer, namely poly(diethyl-6-(acrylamido)hexylcarbamoymethyl phosphonate) (P(CPAAm6C)), which was then mono-hydrolyzed, thus leading to its mono-acid derivative (mhP(CPAAm6C)). Sorption of gadolinium (Gd(III), lanthanide) and thorium (Th(IV), actinide) on both polymers was studied by Isothermal Titration Calorimetry (ITC) and compared with results obtained by Inductively Coupled Plasma Mass Spectrometry (ICP-MS). This permitted to evaluate their complexing properties and to determine their selectivity, also considering the thermosensitive behaviour. Chapter 3 was devoted to the synthesis, characterization and evaluation of new water-soluble oxymethylphosphonated polymers for the sorption of two lanthanides, cerium (Ce) and neodymium (Nd). Poly(diisopropyl(acryloyloxymethyl) phosphonate) (P(DiAPC1)) and poly(dimethyl(acryloyloxymethyl) phosphonate) (P(APC1)) were prepared and hydrolyzed, leading to the same hP(APC1) polymer. DiAPC1 and APC1 monomers were also hydrolysed to obtain hAPC1 and evaluated to study the influence of the alkyloxy and hydroxy groups borne by the phosphorous atom, and to compare

General introduction

monomers and polymers. Finally, in the last chapter, phosphorous-based thermosensitive polyacrylamides, poly(diethyl-2-(acrylamido)ethyl phosphonate) (P(DAAmEP)) and its hydrolyzed derivative (hP(DAAmEP)) were prepared, characterized and evaluated for the sorption of lanthanides and radionuclides: gadolinium (Gd(III)), cerium (Ce(III)), neodymium (Nd(III)), and thorium (Th(IV)).

Chapter 1: Bibliography

Introduction

Bibliographic chapter is divided in three parts. First part deals with general considerations about lanthanides and actinides, and reports techniques currently used for the separation and recovery of lanthanides. In the second part, water-soluble polymers allowing the sorption of metal ions are considered. Thermosensitive polymers, in particular polymers showing a Lower Critical Solution Temperature (LCST), are described. Finally, interactions between water-soluble polymeric sorbents and metal ions in water are discussed in the last part. A special attention is paid to the techniques allowing characterizing the interactions between polymers and metal ions, including Isothermal Titration Calorimetry (ITC).

Part 1: Lanthanides and actinides

1.1. Lanthanides

1.1.1. General considerations

In Mendeleïev chemical periodic table (Figure 1), the elements in the 4f block from lanthanum (La) to lutetium (Lu) (57 to 71) are called the lanthanides, or lanthanoids. These 15 elements, together with scandium (Sc) and yttrium (Y) are given another well-known name, the rare-earth elements (REEs) or rare-earth metals (REMs), as defined by the International Union of Pure and Applied Chemistry. Considering that the REEs are mainly lanthanides, for practical reason, REEs in following text will refer to the lanthanide elements in the 4f block.

1 1A H Hydrogen 1.008	2 2A Li Lithium 6.941	3 3A Be Beryllium 9.0122	4 4A B Boron 10.811	5 5A C Carbon 12.011	6 6A N Nitrogen 14.007	7 7A O Oxygen 15.999	8 8A F Fluorine 18.9984	9 9A Ne Neon 20.1797	10 10A Na Sodium 22.98976928	11 11A Mg Magnesium 24.304	12 12A Al Aluminum 26.9815385	13 13A Si Silicon 28.0855	14 14A P Phosphorus 30.973761998	15 15A S Sulfur 32.06	16 16A Cl Chlorine 35.45	17 17A Ar Argon 39.948	18 18A K Potassium 39.0983	19 19A Ca Calcium 40.078	20 20A Sc Scandium 44.955912	21 3B Ti Titanium 47.88	22 4B V Vanadium 50.9415	23 5B Cr Chromium 51.9961	24 6B Mn Manganese 54.938044	25 7B Fe Iron 55.845	26 8B Co Cobalt 58.933194	27 9B Ni Nickel 58.6934	28 10B Cu Copper 63.546	29 11B Zn Zinc 65.38	30 12B Ga Gallium 69.723	31 13B Ge Germanium 72.63	32 14B As Arsenic 74.9216	33 15B Se Selenium 78.96	34 16B Br Bromine 79.904	35 17B Kr Krypton 83.798	36 18B Rb Rubidium 85.4678	37 19B Sr Strontium 87.62	38 20B Y Yttrium 88.90584	39 21B Zr Zirconium 91.224	40 22B Nb Niobium 92.90637	41 23B Mo Molybdenum 95.94	42 24B Tc Technetium 98	43 25B Ru Ruthenium 101.07	44 26B Rh Rhodium 102.90550	45 27B Pd Palladium 106.42	46 28B Ag Silver 107.8682	47 29B Cd Cadmium 112.411	48 30B In Indium 114.818	49 31B Sn Tin 118.710	50 32B Sb Antimony 121.757	51 33B Te Tellurium 127.603	52 34B I Iodine 126.90447	53 35B Xe Xenon 131.29	54 36B Cs Cesium 132.90545196	55 37B Ba Barium 137.327	56 38B La Lanthanoids 138.90547	57 39B Hf Hafnium 178.49	58 40B Ta Tantalum 180.94788	59 41B W Tungsten 183.84	60 42B Re Rhenium 186.207	61 43B Os Osmium 190.23	62 44B Ir Iridium 192.222	63 45B Pt Platinum 195.084	64 46B Au Gold 196.966569	65 47B Hg Mercury 200.59	66 48B Tl Thallium 204.38	67 49B Pb Lead 207.2	68 50B Bi Bismuth 208.9804	69 51B Po Polonium 209	70 52B At Astatine (210)	71 53B Rn Radon (222)	72 54B Fr Francium (223)	73 55B Ra Radium (226)	74 56B Rf Rutherfordium (261)	75 57B Db Dubnium (262)	76 58B Sg Seaborgium (266)	77 59B Bh Bohrium (264)	78 60B Hs Hassium (277)	79 61B Mt Meitnerium (276)	80 62B Ds Darmstadtium (285)	81 63B Rg Roentgenium (289)	82 64B Cn Copernicium (285)	83 65B Nh Nihonium (284)	84 66B Fl Flerovium (289)	85 67B Mc Moscovium (288)	86 68B Lv Livermorium (293)	87 69B Ts Tennessine (294)	88 70B Og Oganesson (294)
57 La Lanthanum 138.90547	58 Ce Cerium 140.12	59 Pr Praseodymium 140.90766	60 Nd Neodymium 144.242	61 Pm Promethium (145)	62 Sm Samarium 150.36	63 Eu Europium 151.964	64 Gd Gadolinium 157.25	65 Tb Terbium 158.92534	66 Dy Dysprosium 162.500	67 Ho Holmium 164.93033	68 Er Erbium 167.259	69 Tm Thulium 168.93402	70 Yb Ytterbium 173.054	71 Lu Lutetium 174.967																																																																									
89 Ac Actinium (227)	90 Th Thorium 232.0377	91 Pa Protactinium 231.03688	92 U Uranium 238.02891	93 Np Neptunium (237)	94 Pu Plutonium (244)	95 Am Americium (243)	96 Cm Curium (247)	97 Bk Berkelium (247)	98 Cf Californium (251)	99 Es Einsteinium (252)	100 Fm Fermium (257)	101 Md Mendelevium (258)	102 No Nobelium (259)	103 Lr Lawrencium (260)																																																																									

Figure 1. Mendeleïev periodic Table of the elements [33]

(a) Electronic configuration and main properties of lanthanides

The lanthanides are widely used in various fields owing to their excellent physical and chemical properties. These properties are due to their electronic configuration in the ground state. Two types of electronic configurations exist for lanthanide elements: $[Xe]4f^n6s^2$ and $[Xe]4f^{n-1}5d^16s^2$, where $[Xe]$ represents the electronic configuration of xenon, and n number goes from 1 to 14 [34]. The electronic configuration that the lanthanide elements adopt

depends on the relative energy level of these two electronic configurations for each element. According to the principle of the lowest energy, the electronic configuration with lowest energy level is generally adopted. La, Ce and Gd belong to the $[\text{Xe}]4f^{n-1}5d^16s^2$; Pr, Nd, Pm, Sm, Eu, Tb, Dy, Ho, Er, Tm, Yt and Lu belong to the $[\text{Xe}]4f^n6s^2$ type [35]. Sc and Y are also considered as rare-earth elements due to their similar electronic configuration with lanthanide elements, whose outermost electrons are with the $(n-1)d^1ns^2$ configuration [34]. Another reason for the similar chemical properties of Sc and Y to lanthanide elements is the 'lanthanide contraction' (ionic radius of lanthanides decreases with increasing atomic number) [34]. Due to the special electronic configurations, REEs are highly electropositive: they tend to lose three electrons and exhibit a trivalent state [34]. Since the 4f shell is unfilled, different arrangements of 4f electrons bring different energy levels. The transition of 4f electrons between the various energy levels could generate numerous absorption and emission spectra, which is the origin of specific photo-physical properties of lanthanide elements. Additionally, the orbital contribution of trivalent lanthanides brings their magnetic properties [35]. Lanthanide cations tend to form chemical bonds with atoms of hard base, due to their hard acid character from the point of view of soft-hard acid-base theory [34].

(b) Applications of lanthanides

Lanthanide compounds, complexes, nanoparticles as guests in microporous hosts materials are used in different fields, such as lighter flints, super-conductors [36], hydrogen storage [37], iron and steel production [38], permanent magnets [39], lasers [40], telecommunications and magneto-optic data recording [35]. They give also lots of contribution in medical applications: Magnetic Resonance Imaging (MRI) contrast agents, hypophosphatemic agents for kidney dialysis patients, luminescent probes in cell studies and for palliation of bone pain in osteosarcoma and anticancer agents [34, 41, 42]. In the field of nuclear application, lanthanide compounds can be used as fuel cells and fuel additives [43]. In synthetic organic chemistry, lanthanides reagents are used for simple functional group transformations, in selective carbon-carbon bond forming reactions [44-47], or as initiators and catalysts in ring-opening polymerizations [48-50].

1.1.2. Resources and production

In contrast to their name, the REEs are broadly distributed in the Earth's crust, but in relatively small concentrations (10-300 ppm) and always in mixture with other species. Due to lack of knowledge and appropriate processes, it is difficult to separate these elements. All the REEs exist in natural state in basalts, granites, clays or silicate rocks [51], except for promethium. Because of their electropositive nature, REEs are generally found under oxidized, carbonate, phosphate and silicate forms in the nature. Cerium (Ce) is the most abundant lanthanide elements in the Earth's crust, with abundance of 60-68 ppm. For neodymium (Nd) and gadolinium (Gd), abundance is about 30-35 ppm and 5-10 ppm, respectively. Lanthanum (La) has a similar level than neodymium. The other lanthanides are less than 10 ppm in the Earth's crust [35, 51].

Lanthanides (the main REEs) production from minerals can be achieved using more than hundreds of types of minerals all over the world. The mineral initially mined as a primary product was a rare-earth fluorocarbonate mineral in Canada. Monazite, a phosphate mineral, was produced as a separated concentrate or associated as an accessory mineral in heavy-mineral concentrates [1]. In 2019, the evaluation of the rare-earth worldwide reserves showed that China took 36%, Brazil and Vietnam both got 18%, followed by Russia, India, Australia, Greenland and United States; the other countries or regions represented less than 0.9 million metric tons of rare-earth oxides. Concerning the REEs production, about 62% was produced by China, the following being United States, Burma and Australia, which produced respectively 12.2%, 10.3% and 9.9% of REEs [1]. These data showed that the REEs resources are mainly owned by few countries.

1.2. Actinides

1.2.1. General considerations

As shown in the periodic table of the elements (Figure 1), there is a series of elements in the 5f block (below the lanthanides) called actinides, going from actinium (Ac, 89) to lawrencium (Lr, 103). These elements attracted people attention due to their specific properties and radioactivity. An element is called radioactive when its nucleus is not stable and releases energy spontaneously in the form of radiation alpha, gamma or beta in order to

reach its stable state. This process is called the decay phenomena. Among the actinides, only the first 4 elements (actinium (Ac), thorium (Th), protactinium (Pa) and uranium (U)) can be found in a natural state. The others are heavier and can only be artificially produced in a nuclear reactor [52, 53]. Herein, only the actinides with natural states will be investigated, especially thorium (Th) and uranium (U). The latter are both long-lived elements and can be found in the earth in relatively significant amounts. As a result, they were chosen to be studied in the present work. Th is mainly found in (IV) oxidation state. Furthermore, U exhibits oxidation states of (III), (IV), (V), and (VI). Most of compounds are in the (IV) and (VI) states [54]. The main thorium ore is monazite (around 10%), the main uranium ore is U_3O_8 , usually known as pitchblende [52].

1.2.2. Properties and applications

The specific electronic configuration of actinides brings them unique physical and chemical properties. Actinide ions and related compounds possess particular thermodynamic, optical, electronic, magnetic properties and chemical reactivity, which arise from the spin and orbital angular momenta of the unpaired electrons [52, 55-57]. With the development of nuclear energy, these actinides and other radioactive elements made the most important contribution to some technological issues, related to water-cooled reactors, reprocessing of spent nuclear fuel and high-level radioactive wastes, and fuel evolution during final radioactive waste disposal [58, 59]. In addition, they have been intensively applied in the study of ultra-high-density data storage, spintronics and Quantum Information Processing (QIP) owing to f-elements single-ion magnets (f-SIMs) [60, 61].

1.2.3. Risks

As previously mentioned, all the actinides are radioactive, and sometimes intensely. As a result, these elements and their derivatives can damage living organisms and ecosystems. For humans, the radionuclides damage various organs of the body or tissues and caused cancers. The complex kinetics depended on the nature of the metabolic processes. For ecosystems, these pollutants were able to lead to biochemical, physiological and behavioural alterations of organisms [62, 63], and brought irreparable damages. The chemical and radiotoxicity of radionuclides is one of the biggest challenges. In particular, it is important to

'control' nuclear energy [64], especially disposal of nuclear waste materials, notably in the case of high-level waste from the cores of reactors and nuclear weapons [54]. It is thus needed to pay attention to processing and treatment of actinides and other radioactive elements.

1.3. Separation and recovery of lanthanides and actinides

1.3.1. Importance and challenges

The separation of metal ions and their recovery plays a key role in various industrial activities, from potable water production, detoxification process of waste effluent to leaching and recovery of metals from ores [65]. The separation and recovery of the crucial metal cations attract attention for numerous reasons. Indeed, the decrease in grade of the available ores, or limited sources in some areas and countries makes imperative to recover crucial metals. In addition, high costs of production and strict environmental regulations make important to find efficient methods for processing waste solutions containing metal ions, even at very low concentrations [66]. However, a series of challenges can be encountered in the process of metal ions recovery. In the case of lanthanides and actinides, the low concentrations and the complexity of mixtures in effluent are amongst the most common problems in their recovery processes [67]. Additionally, in the case of individual separation of the lanthanides, another challenge is related to the similar physicochemical properties of the various lanthanide elements. It is not only due to the chemical identification of the electronic arrangements in the outer electron shells (5s and 5p), but also to the contraction effect (lanthanide contraction) caused by the 4f orbital. Thus, the difference in separation factors is too low to separate a single lanthanide element from its adjacent neighbour [51, 68]. The same problems are found in the separation of actinides [53]. For radioactive effluent, another challenging issue is the stabilization and solidification of soluble radioactive nuclides found in wastewater, which are critical for final disposal [69]. Moreover, the potential risk of human exposure to water radiation should also be taken into consideration in selecting, designing and operating the radioactive effluent treatment process. Finally, the separation process for both lanthanides and actinides is complicated by the variability of the effluent, including the solution composition, pH, temperature and the presence of organic substances [5].

1.3.2. Extraction techniques

In industrial lanthanides production from mineral resources, the general processes to obtain saleable lanthanide compounds or defined mixture include mineral treatment, extraction of lanthanides, separation of the lanthanides to individual, and refining [51, 70]. Most common methods used to extract lanthanides from mineral solutions are chemical/bioleaching [71, 72], chemical and biological precipitation [73] and solvent extraction [5, 74]. In the step of individual separation, the two historical methods, fractional crystallization and fractional precipitation were both almost replaced by solvent extraction in large-scale treatment [75]. These two fractional separation methods were indeed inefficient and labour intensive, probably because of the small difference in the valence states of the different REEs [70]. Indeed, as reported in the properties of REEs, they generally exhibit (III) valence, but Ce, Pr and Tb have also (IV) valence and Eu, Sm and Yb can exist in (II) valence. Thus, these REE species can be purified through selective oxidation or reduction [68, 70]. However, the method of solvent extraction is based on another difference in properties of REEs. This difference is related to the lanthanide contraction phenomenon, which leads to various acidity levels for REEs. This brings differences in solubility property, ionic hydrolysis and complexation [70]. In solvent extraction method, REEs aqueous solution is firstly mixed with an organic solvent, which permits the formation of complexes with REE ions. The ions are then extracted from organic phase to aqueous solution where the REE ions have higher solubility; this step is often called stripping. This process should be repeated many times until reaching the required purity [70]. The advantages of solvent extraction are fast kinetics, high capacities, and selectivity for some targeted REE ions. However, this process involves contamination of aqueous phase by organic solvent and a large volume of organic solvent is needed for diluting effluent [5], which is expensive and environmentally unfriendly.

Another separation method based on polymer sorption has been recently much studied and applied in REEs recovery. Two types of polymeric sorbents were considered, employing resins heterogeneous systems or water-soluble polymeric sorbents. The use of resins was based on similar principle as solvent extraction, with functional groups borne by the polymeric insoluble materials capable of complexation or ion exchange [5, 51]. This specific process is called Solid Phase Extraction (SPE) process [76]. Since targeted metal ion is bound

to the functional groups of polymer particles, there is no loss of extractant into the aqueous phase. The other advantage is that these materials can be regenerated and easily reused for continuous processes. On the reverse, one of the main disadvantages of this method is the slower kinetics compared to solvent extraction, because of lower accessibility of sorption sites in resins [5, 66, 77]. Nevertheless, SPE process can be improved with the enhancement of the accessibility by increasing the porosity or decreasing the bead size or cross-linking degree [5, 78, 79]. At last, REE compounds can be recovered or released with an appropriate eluent. In order to avoid the heterogeneous two-phase system, another widely used technology is the separation process based on water-soluble polymeric sorbents. It employs water-soluble polymers containing appropriate functional groups to bind with metal ions of interest. Purified effluent is then produced with the help of ultrafiltration (UF) membrane [65]. This process is called Polymer Enhanced Ultrafiltration (PEUF). Metal ions bound to soluble polymers are separated from non-bound metals through membrane filtration. This method is also known as the Liquid-phase Polymer-based Retention (LPR) technique [66, 76, 80, 81]. At the end, pure REE compounds can be isolated using acidic medium. This method using water-soluble polymers exhibits both advantages of high kinetics and good efficiency. However, the use of ultrafiltration technique generally increases the cost of purification, even with latest generation of development for ultrafiltration techniques in the recent years. This makes the application in industrial scales not very convenient. Other chemical techniques, such as electrolytic reduction, bio-precipitation [82], adsorption by nanomaterials [83], and biosorption [84] are also developed to produce lanthanide products with high-purity.

When actinides separation is concerned, the REEs processing can be an environmental hazardous operation because of the presence of radioactive contaminants. The decontamination of radioactive effluent is thus getting more and more attention for further treatment or in the case of incidental situation. As for lanthanides, various chemical, physical, biological and combined methods have been developed for removing radioactive metals from effluent, such as chemical precipitation, adsorption, advanced oxidation process, evaporation, electrodialysis, and membrane filtration [57, 69, 85, 86]. Among these various techniques, polymeric sorbents in association with complexation or ion exchange are known for their selectivity, together with favourable areas of contact, stable structures and good

regeneration for radioactive waste treatment [69]. The challenges in the separation of actinides are similar with that in lanthanides separation, thus the developed polymers require high selectivity and capacity. In addition, the radiation stability of polymers needs also to be considered to avoid the degradation of polymers because of the radiolysis effect in the radioactive effluent [87, 88].

1.4. Conclusion

The important role of lanthanides in the modern industry and technology development is well-known, owing to their good physicochemical properties. Lanthanides are therefore regarded as a key resource over the world; however, only few countries possess rich lanthanides resources together with great production capacity. Herein, the separation and recovery of lanthanides from industrial effluent or natural mineral solution is attracting more and more attention. One of the challenges in the separation and recovery of lanthanides is that they are often accompanied by radioactive metal ions in the solution, especially actinides. Thus, the actinides removal has to be jointly considered. Concerning the procedures allowing the separation and the recovery of lanthanides and actinides, another big challenge is related to the difficulties of separating these ions into individual phases, because of their pretty similar chemical and physical properties. As a consequence, technologies permitting selectivity for lanthanide or actinide ions have been much demanded. Currently, the main techniques applied for separating these metal ions include fractional precipitation, solvent extraction and polymer sorption. Concerning the latter, the resins based heterogenous systems or the combination of water-soluble polymeric sorbents with ultra-filtration offer another possibility to recover separately and efficiently lanthanide and actinide ions.

In the reported work, new ideal procedure will deal with the development of a more selective, more efficient and solvent free technique, ideally combining rapid sorption and easy separation step. This objective can be notably reached using water-soluble thermosensitive polymers.

Part 2: Water-soluble polymeric sorbents and thermosensitive property

2.1. Water-soluble polymeric sorbents

As reported in the first part of this chapter, the use of water-soluble polymeric sorbents bearing metal-ion specific sorption groups, in conjunction with membrane filtration, is an interesting method to remove or recover metal ions from effluent. Owing to their efficiency and selectivity for removing metals from water [76], they have attracted much attention. In addition, natural or bio-sourced materials, and hybrid materials were also of interest in hazardous metal removal [89, 90]. Water-soluble synthetic polymeric sorbents are the focus of this work. The sorption moieties in polymeric sorbents are the key for their optimized sorption performance. Some functional groups proved to be efficient for the sorption of many metal ions, such as O-donors (alcohols, crown ethers), N-donors (amines, amides) and acidic moieties (carboxylic acids, phosphonic acids, sulfonic acids) [76]. A donor atom has at least one lone pair of electrons in its outermost energy level, and this lone pair of electrons can be donated to metal ions to form coordination complexes.

2.1.1. Main sorption functional groups

In order to better understand the sorption mechanism between functional moieties and metal ions, together with their selectivity, the knowledge about sorption groups borne by polymeric sorbents is important. Table 1 shows the functional moieties often used to design polymeric sorbents.

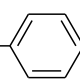
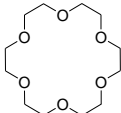

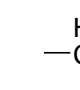

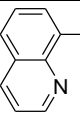
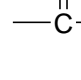
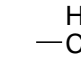

Types	Molecule type	Functional groups in polymeric sorbents
O-donors	Alcohols	$\text{---C}^{\text{H}_2}\text{---OH}$
	Ketones	$\text{---C}^{\text{H}_2}\text{---C}^{\text{O}}\text{---C}^{\text{H}_2}\text{---CH}^{\text{O}}$, $\text{---C}^{\text{O}}\text{---C}^{\text{O}}\text{---O---R}'$, $\text{---C}^{\text{O}}\text{---C}^{\text{O}}\text{---NH}_2$
	Esters	$\text{H}_2\text{C---C}^{\text{H}}\text{---O---C}^{\text{O}}\text{---}$ 
	Crown ethers	
S-donors	Thiols	$\text{---C}^{\text{H}}\text{---C}^{\text{H}}\text{---SH}$, $\text{---C}^{\text{H}}\text{---C}^{\text{H}}\text{---O---C}^{\text{H}_2}\text{---C}^{\text{H}_2}\text{---SH}$, $\text{---C}^{\text{H}}\text{---C}^{\text{H}}\text{---C}^{\text{S}}\text{---N---}$
	Thiocyanate	$\text{---C}^{\text{H}_2}\text{---C}^{\text{H}_2}\text{---S---C}\equiv\text{N}$
N-donors	Amines	$\text{---C}^{\text{H}_2}\text{---C}^{\text{H}_2}\text{---NH}_2$, $\text{---C}^{\text{H}_2}\text{---}$  $\text{---C}^{\text{H}_2}\text{---N---C}^{\text{H}_2}\text{---}$
	Nitrogen heterocyclic	$\text{---C}^{\text{H}_2}\text{---}$  , $\text{---C}^{\text{H}_2}\text{---}$  ---N=N--- 
	Amides	$\text{---C}^{\text{O}}\text{---N---R}$, $\text{---C}^{\text{O}}\text{---N---}$  $\text{---N---C}^{\text{O}}\text{---}$
	Amidines	$\text{HN}=\text{C}^{\text{H}}\text{---NH}_2$
	Imines	$\text{HO---N}=\text{C}^{\text{H}}\text{---NH}_2$, $\text{HN}=\text{C}^{\text{H}}\text{---NH}_2$, $\text{HN}=\text{C}^{\text{H}_2}\text{---S---}$
Acidic groups	Carboxylic acids	$\text{---C}^{\text{H}_2}\text{---C}^{\text{H}}\text{---C}^{\text{O}}\text{---OH}$, $\text{HO---C}^{\text{O}}\text{---C}^{\text{H}_2}\text{---N---C}^{\text{H}_2}\text{---C}^{\text{O}}\text{---OH}$
	Phosphonic acids	$\text{---C}^{\text{H}_2}\text{---C}^{\text{H}_2}\text{---P}^{\text{O}}\text{---OH}$, $\text{---C}^{\text{H}_2}\text{---}$  $\text{---O---C}^{\text{H}_2}\text{---P}^{\text{O}}\text{---OH}$
	Sulfonic acids	$\text{---C}^{\text{H}_2}\text{---}$  $\text{---S}^{\text{O}}\text{---OH}$

Table 1. Functional groups allowing the sorption of metal ions [76, 91]

So far, sorption moieties the most used include amines, amides, crown ethers, alcohols, carboxylic, sulfonic and phosphonic acids [76]. The sorption function owes mainly to free

electron pair in nitrogen and oxygen atom, which can bind metal ions through complexation reaction. Additionally, the affinity and capacity of these groups is affected by electronic environment. Another mechanism allowing the sorption of various metal species is ion-exchange. This is mainly encountered for the polymers bearing charged functional groups. However, compared to complexation reaction, ion-exchange reaction is regulated by charge conservation and is then relatively weak and reversible [76]. Figure 2 shows the differences between the two types of sorption mechanisms with the example of phosphonic acid complexing moiety.

Figure 2. Ion-exchange and complexation mechanisms [76]

For N-donors, the free electron pair of nitrogen atom is able to form stable complexes with metal ions. However, the stability of the complexes formed between nitrogen atoms and metal ions strongly depends on pH. Because almost all the amino groups are protonated at low pH, their affinity for the metal ions is poor and the stability of the complex is low. As the pH increases, both affinity and stability of the polymer-metal complexes increase [66]. On the contrary, water-soluble polymers with acidic groups such as sulfonate groups favor the electrostatic interaction between the functional groups and metal ions [66]. In the case of phosphonic acid, its sorption property arises from the free electron pair of its three oxygen atoms which can be engaged in coordination bonds formation [92]. Due to the acidity of phosphonic acid, it is usually deprotonated in water. This can be therefore used to increase the water solubility of organic compounds, polymers, or ligands [92, 93]. Among all the functional groups that can be borne by polymers, acidic groups appear to be of great

interest. In particular, phosphonic acid-based polymers proved to be efficient for the sorption of different metal ions.

2.1.2. Phosphonic-acid based polymers for the sorption of metal ions

Developed polymers in the present work are polymeric sorbents bearing phosphonate moieties, including phosphonic acid groups. Phosphonic acids ($R-PO_3H_2$) were one of the most studied for metal-ion removal. Compared to carboxylic acids, phosphonic acids are diacids, meaning that they exhibit two dissociation constants ($pK_{a1}=2-3$ and $pK_{a2}=6-7$) [94, 95]. They are dissociated ($R-PO_3H^-$ and $R-PO_3^{2-}$) in an aqueous solution as shown in Figure 3.

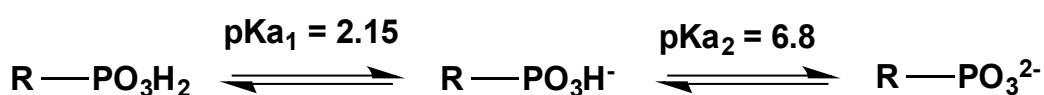
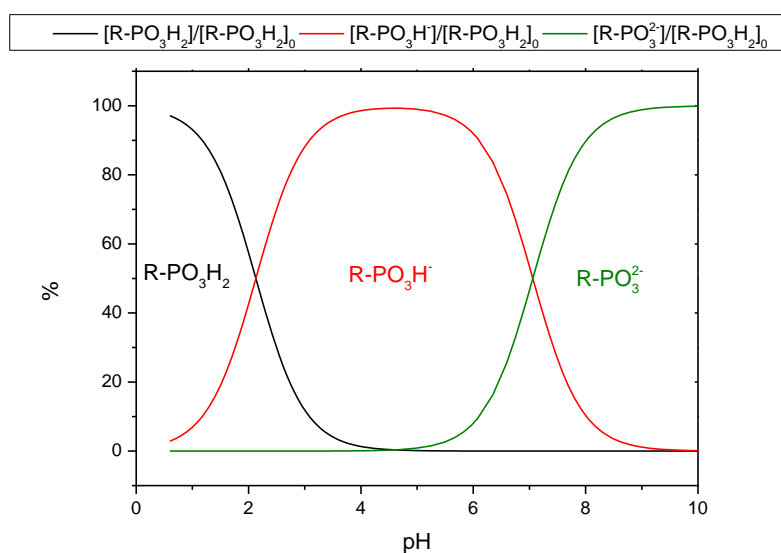


Figure 3. Dissociation equilibria, acidity constants, and regression curves of phosphonic acid moieties [76]

According to its pK_a constants, the sorption capacity of phosphonic acids at low pH was interesting compared to other functional groups. Phosphonic acids were dissociated for pH values higher than or equal to 2, which increased electrostatic interactions with metal ions [9, 96-101]. In this pH range, the polymers bearing phosphonic acid moieties were negatively charged, and the competition between cations and H^+ ions was quite low [13, 102]. The negative charges increased the hydrophilic character of the polymer and facilitated the approach of cations leading to faster sorption. The cases of pH values between 2 and 7 and

those higher than 7 (Figure 4) had to be considered separately. When the pH was between pK_{a1} and pK_{a2} , only one hydroxyl was dissociated involving the presence of two different mechanisms. In this pH range, phosphonic acid behaved as a polychelator with the complexation of metal ions and as a polyelectrolyte with the electrostatic interactions with positively charged ions. The adsorption for a pH higher than 7 resulted from electrostatic forces because the two acid functions were dissociated. When the pH was lower than 2, the functional groups were not dissociated and were able to form coordination bonds with metal ions even if the capacity sorption decreased [97, 98, 100, 103].

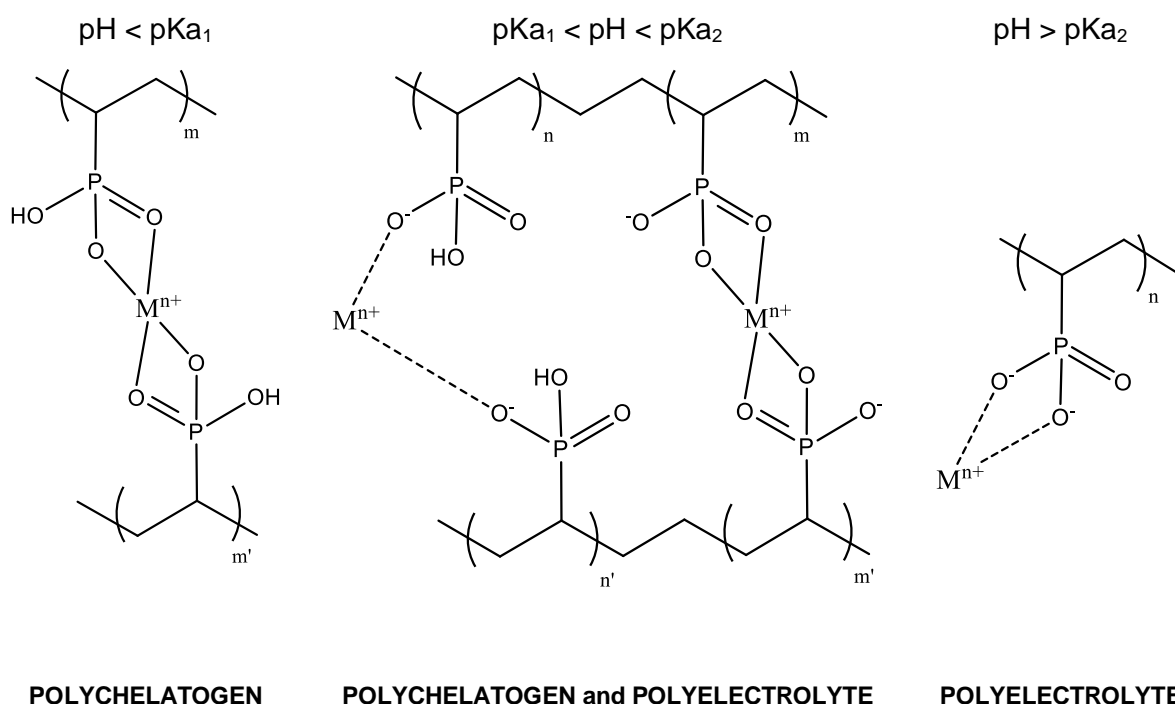


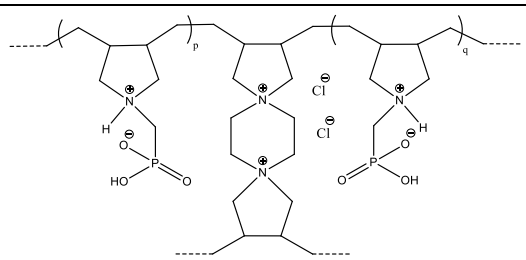
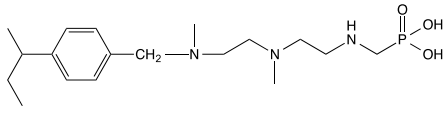
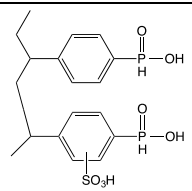
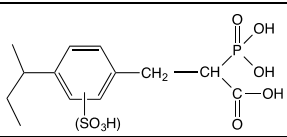
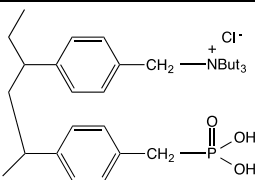
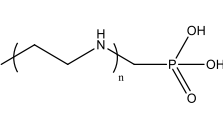
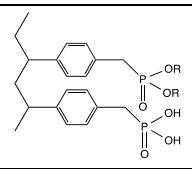
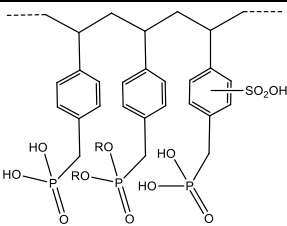
Figure 4. Possible mechanisms of cation sorption for polymeric sorbents bearing phosphonic acid moieties [76]

As for carboxylic groups, the sorption with phosphonic acid was not equivalent for the different cations. Phosphonic acids were hard acids with a better affinity for hard metal ions compared to that of soft acids. Thus, the phosphonic acid moieties had higher selectivity for metal ions such as Fe(III), Cu(II), and Cr(III) than for soft cations such as Ca(II) and Mg(II) [104]. This result was also consistent with cation valences because a higher metal-ion valence led to better sorption properties. Tokuyama *et al* [103] showed that the adsorption of divalent cations by phosphonic groups was significantly lower than that of trivalent

cations. These affinity differences gave phosphonic acids good selectivity properties, particularly at pH values below 2. Some examples of the use of phosphonic acid derivatives for metal-ion removal are given in Table 2.

Different polymeric sorbents exhibiting various physical states and containing phosphonic acids were synthesized for targeted separation processes. Polyethylenimine backbone was mainly used because of its good water solubility when applied to the recovery of metals such as Fe(III), U(IV) [105-107], and Cu(II) [100]. In the case of U(VI), obtained experimental capacity was $39.66 \text{ mg}\cdot\text{g}^{-1}$, and proved to be higher than those obtained with chelate modified solid phase extraction as Amberlite[®], gel-amide, or gel-benzamide. The sorption capacity of the phosphonic acid polymer toward Cu(II) was $85.69 \text{ mg}\cdot\text{g}^{-1}$. Furthermore, several authors investigated the synthesis of water insoluble polymers as beads [108], resin [109], fibres [97], or gels [110]. Tokuyama *et al* [103] described the synthesis of gels having the capacity to chelate In(III) and Zn(II) ions. The amount adsorbed of In(III) ions was 0.15 mmol per gram of wet gel. Prabhakaran *et al* [102, 111] chemically modified an Amberlite resin[®] with a phosphonic derivative for the selective complexation of U(VI), Th(IV), and La(III). Sorption capacities were equal to 1.38, 1.33, and $0.75 \text{ mmol}\cdot\text{g}^{-1}$ at optimum pH, respectively. Phosphonic acid-based soluble polymers were also considered for the selective sorption of Gd(III) [112]. Usually, in the case of carboxylic acids, commercial polymers were available and used as chelating agents, whereas phosphonic derivatives had to be specifically synthesized to create more complicated structures (Table 2). Several experimental methods to obtain polymeric structures with cation-removal properties were reported. Among these different strategies, the modification of commercial polymers by phosphorylation according to the Kabachnik-Fields reaction [113] and the development of new functional monomers were prevalent. Different chelating ligands were combined in the same polymeric structure to remove different metal ions. For instance, Liu *et al* [97] associated phosphonic and amine groups in fibrous structures for the complexation of metal ions, and Vasudevan *et al* [114] combined sulfonic and phosphoric groups in cross-linked methacrylate-based membranes for the recovery of U(VI) in seawater. Alexandratos *et al* developed several bifunctional resins based on polystyrene. Among all examples, bifunctional polymer supported aminomethylphosphonated [115], quaternary amine phosphonic acid resins [116], combination of phosphonic acid groups and carboxylic acid groups on polystyrene (with or

without sulfonic acid groups) [117], sulfonated and phosphonic acid [5] or diphosphonic acid [118] supported on polystyrene proved to be of interest for the sorption of different metal cations.

Functional materials	Physical state	Target cations	Ref
	resin	Pb(II), Cu(II)	[96]
	resin	Pb(II)	[115]
	resin	Eu(III)	[5]
	resin	Cu(II), Cd(II), Pb(II), Eu(III)	[117]
	resin	Hg(II)	[116]
	water-soluble polymer	Cu(II)	[100]
	bead	Ca(II), Cu(II), Ni(II)	[9]
	bead	Eu(III), Fe(III)	[99]

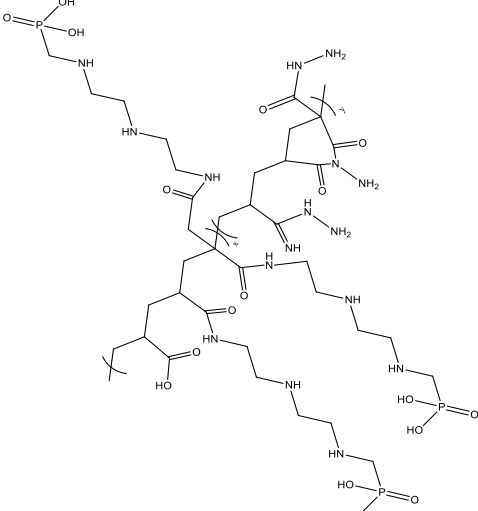
 <p>The image shows a complex chemical structure of a polymeric sorbent. It features a central polymer backbone with several side chains. One prominent side chain is a phosphonic acid moiety, represented as a phosphorus atom double-bonded to an oxygen and single-bonded to two hydroxyl groups, connected to a methylene group which is further linked to a primary amine group (-NH-CH2-CH2-NH-). Another side chain contains a secondary amine group (-NH-) linked to a methylene group, which is then connected to a carbonyl group (-C(=O)-). A third side chain features a tertiary amine group (-N-) linked to a methylene group, which is then connected to a carbonyl group. The structure also includes a carboxylic acid group (-COOH) and a hydroxyl group (-OH) on the main chain. The overall structure is highly branched and complex, indicating a multi-functional polymer.</p>	fiber	<p>Ag(I), Cu(II), Pb(II), Zn(II), Co(II), Ni(II), Hg(II), Cd(II), Mn(II), Cr(III)</p>	[97]
--	-------	---	------

Table 2. Polymeric sorbents bearing phosphonic acid moieties and cations targeted [76]

In the present contribution, we report the development of water-soluble phosphorous-based materials for the sorption of radionuclides or lanthanides. In the ideal case, developed polymers will also show thermosensitive or flocculating behaviour in order to facilitate the separation step. Once metal-polymer complexes recovered, it is important to consider the regeneration step allowing the reusability of the polymeric material.

2.1.3. Regeneration and recycling of water-soluble polymeric sorbents

Due to relatively high cost of synthesis of polymeric sorbents in general, their regeneration and reusability became a crucial issue for industrial applications. Regeneration and recovery of complexed metal ions were often carried out using regeneration agents, such as acids, alkalis and chelating agents [75, 76]. The choice of regeneration agents depended on the type of functional groups. Some examples of the polymeric sorbents bearing typical sorption moieties will be given to explain this regeneration process. For example, chitosan-*g*-poly(acrylic acid) with crosslinked polymeric networks was synthesized to recover Ni(II) [119]. Its sorption capacity was evaluated at 54.47 mg·g⁻¹. With 1 mol·L⁻¹ hydrochloric acid (HCl) solution as regeneration agent, the interaction between carboxylate and Ni(II) was weakened due to the protonation of carboxylate groups in acidic conditions. Therefore, Ni(II) was released from the polymer and total recovery of Ni(II) could reach 95%. The study of sorption/desorption cycles was also carried out. The results showed that the sorption capacity was still 83% after six cycles, which demonstrated the excellent reusability

of the polymeric sorbent. HCl solution was found to be a good regeneration agent who may be used in many cases. $0.1 \text{ mol}\cdot\text{L}^{-1}$ dilute HCl proved to be relatively efficient for releasing Cd(II) from phosphonate-treated rice husk with 54% desorption [120]. Apart from hydrochloric acid, sulfuric acid was also used as regeneration agent. In a study of heavy metals removal using poly(*N-n*-propylacrylamide-*stat*-hydrolyzed (dimethoxyphosphoryl) methyl-2-methacrylate), sulfonic acid (H_2SO_4) was used in regeneration step [121]. Al(III), Ni(II) and Cd(II) were all completely desorbed at pH=1. Even after four cycles of sorption/desorption, the results were almost as good as at the beginning. Another example of phosphonic acid containing polymer dealt with poly(ethylene glycol methacrylate phosphate-*co*-2-acrylamido-2-methyl-1-propane sulfonate) membrane. Its complex with Fe(III) could be treated with $0.2 \text{ mol}\cdot\text{L}^{-1}$ disodium salt of EDTA. The recovery rate of Fe(III) was proved to be 100%.

To conclude, the regeneration agents for stripping metal ions from polymeric sorbents were mainly acidic solutions; the main reason was that acidic solutions led to the easy and efficient protonation of the functional groups, which was the key to desorb and release metal ions.

2.2. Thermosensitive property of polymeric sorbents

2.2.1. General considerations

Thermosensitive (or temperature-responding) polymers show at least one physicochemical property varying when changing the temperature. In the present study, thermosensitive property proved to be of great interest, as it allowed an easy separation of the metal-polymer complexes from the aqueous solution as a function of the temperature. Most of the applications of thermosensitive polymers are based on this temperature-responding solubility character with a hydrophobic-hydrophilic balance depending on the temperature. When temperature changes around a critical temperature, the polymeric chains collapse or expand to respond to the new adjustments of the hydrophobic or hydrophilic interactions between the polymeric chains and the aqueous media, respectively. There are two types of phase behaviours of thermosensitive polymers characterized by two temperatures of interest called Upper-Critical Solution Temperature (UCST) or Lower-Critical

Solution Temperature (LCST), when the polymer solubility increases or decreases with the temperature, respectively [122]. The polymers with LCST are soluble at low temperature and become insoluble at high temperature whereas the polymers with UCST behave in the opposite way. Figure 5 shows both behaviours of polymer chains as a function of the temperature.

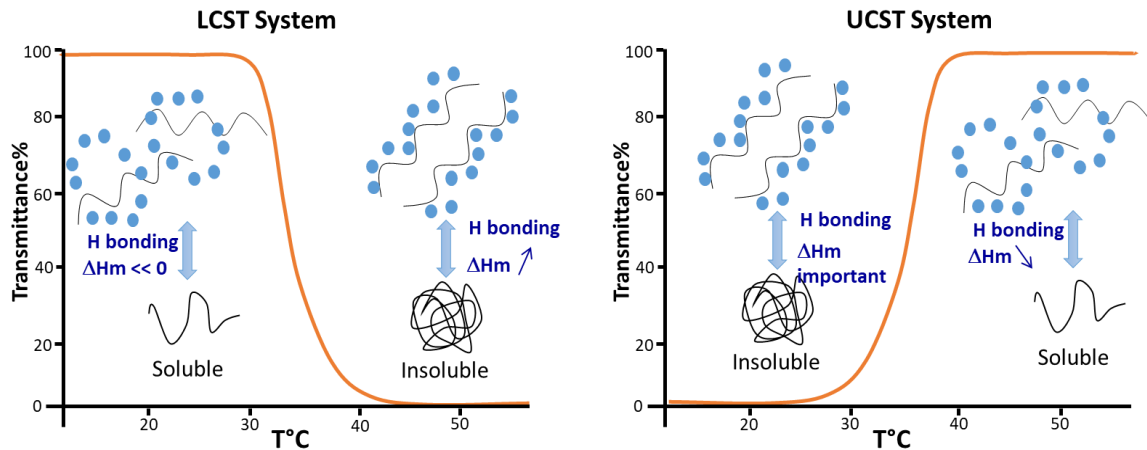


Figure 5. LCST and UCST systems: transmittance of a polymer aqueous solutions decreases with temperature increasing for polymers with Lower Critical Solution Temperature (LCST), but increases for a polymer with Upper Critical Solution Temperature (UCST)

The mechanism of different temperature-responding behaviours is related to the chemical structure of polymers. Concerning polymers showing a LCST, poly(N-isopropylacrylamide) (PNiPAAm) (Figure 6) can be given as an example. Below the LCST, two types of H-bonding interactions exist with water due to the presence of acceptors of hydrogen bonds and donors of hydrogen bonds in the polymeric structure. Indeed, as indicated in Figure 6, two lone pairs of the oxygen atom and the lone pair of the nitrogen atom of the amide bond are acceptors of hydrogen bonds whereas the hydrogen attached covalently to the nitrogen atom is a donor of hydrogen bonds. Additionally, the solidity of hydrogen bonds depends on the energy of a hydrogen bond, which is connected with temperature. As temperature increases, molecules move more strongly and cannot stay at stable position from one another, which weakens the hydrogen bonds [123]. Thus, interaction of water molecules with the pendant groups becomes weaker as temperature increases in this case. Another effect is that the increase in temperature strengthens the

intensity of the hydrophobic effects upon two hydrophobic solutes aggregate. The isopropyl alkyl group attached on the secondary amide group of PNiPAAm is hydrophobic. As temperature increases, the polymer chains are no longer hydrated as well as they were at lower temperature, and the hydrophobic effect becomes predominant. Therefore, polymer-polymer interactions are stronger than polymer-water interactions, and polymer becomes insoluble in water [123].

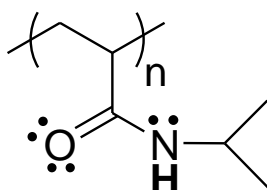


Figure 6. Chemical structure of poly(N-isopropylacrylamide) (PNiPAAm) thermosensitive polymer showing O, N as acceptors and H in -NH as donor for H-bonding in water

The transition temperature of a thermosensitive polymer in water media is one of the most important parameters to be taken into account when considering its applications under a given set of conditions [124]. The thermo-responsive polymers showing LCST have been studied more intensively than those with UCST. The temperature-responding character brings dramatic changes in morphology, shape and sol-gel transitions of polymeric sorbents. In addition, thermosensitive polymers can be synthesized in different forms such as hydrogels [125, 126], micro and nanoparticles [123], film, micelle and micelle-inspired materials. Owing to these special characters and possible architectures, the applications of thermosensitive polymers are increasing. For instance, they were already employed in separation and purification [127], electronic engineering [128, 129], as scaffolds in tissue engineering [130, 131] and especially in drug delivery and biomedical field [123, 132-135].

2.2.2. Thermosensitive polymers

The most studied polymers showing thermosensitivity are N-substituted poly(meth)acrylamide, poly(N-vinylalkylamide), poly(lactam/pyrrolidone/pyrrolidine) and poly(alkyloxide) (often copolymerized) [124]. Chemical structures of these representative polymers and their LCST values are listed in Table 3. These polymers have been intensively studied and applied in various fields. Transition temperatures of thermosensitive polymers

reported in literature are often not an absolute value. Indeed, the transition temperatures depend on the concentration in aqueous solution. For PNiPAAm (Figure 6 and Table 3), the thermal transitions of its intra- and intermolecular hydrogen bonding slightly decreased with increasing concentrations [124]. There are several other factors influencing the thermo-responding behaviour of thermosensitive polymers in aqueous solution. Chemical structure is the primary parameter. For example, for a series of polyacrylamides containing different N-ester-substitutes, their thermo-behaviour in aqueous solution depends on N-ester-substitute [136]. With the increase of carbon number in the N-ester-substitutes from 0 to 3, the thermo-responding behaviour of these polymers in water varied from totally soluble to insoluble with LCST decreasing. The second factor that can be considered is the molar mass of polymers. Molecular weight dependence of the LCST was studied in the case of poly(N,N-diethylacrylamide) [137]. By studying 11 polymer samples with an average molecular weight (M_n) going from $9.6 \cdot 10^3$ to $1.3 \cdot 10^6 \text{ g} \cdot \text{mol}^{-1}$, the transition temperatures in aqueous solution proved to decrease with the increase of M_n . When the molecular weight reached about $2 \cdot 10^5 \text{ g} \cdot \text{mol}^{-1}$, LCST remained constant. This indicated that the impact of molecular weight on LCST values is limited to low molecular weight polymers. Water solution composition can also influence transition temperatures of thermosensitive polymers, as the presence of salts and their concentrations [124]. Additionally, the transition temperatures of thermosensitive polymers can be modified by incorporating hydrophilic or hydrophobic co-monomers or by end group transformations [138, 139].

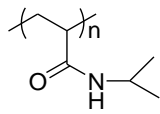
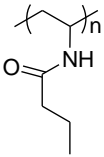
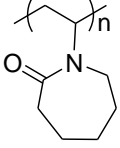
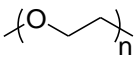
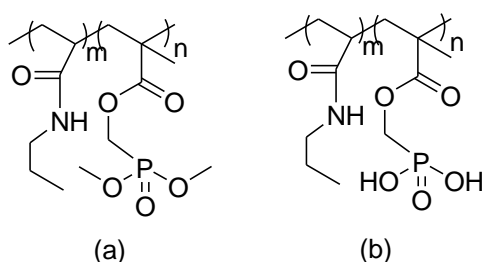
Polymers	Structures	LCST (°C)
poly(N-isopropylacrylamide) (PNIPAAm)		32
poly(N-vinylisobutyramide) (PNVBA)		32
poly(N-vinyl caprolactam) (PVCa)		25-35
poly(ethylene glycol) (PEG)		85

Table 3. Chemical structures of thermosensitive polymers and their Lower Critical Solution Temperature values (LCST) [140-143]

2.2.3. Thermosensitive phosphorus polymeric sorbents

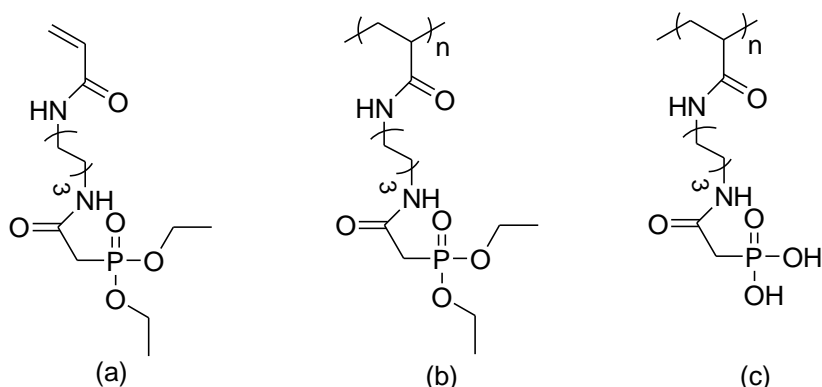
As described previously, the disadvantage of the use of water-soluble polymeric sorbents in conjunction with ultra-filtration led to a high cost of phases separation by ultrafiltration. In order to simplify the phase separation and keep simultaneously the rapid sorption of water-soluble polymeric sorbents and an easy filtration, thermosensitive property of water-soluble polymers was explored. The separation of polymer-metal complexes from solution was performed through precipitation of polymers by changing solution temperature. Therefore, the main idea was to develop valuable (co)polymers combining the sorption efficiency and thermosensitive property. The previous works carried out in our team will be described to evidence the performance of synthesized polymeric sorbents and the recent progress in this field. Innovative poly(N-*n*-propylacrylamide-*stat*-(dimethoxyphosphoryl)methyl 2-methylacrylate) (P(NnPAAm-*stat*-MAPC1)) (Scheme 1(a)) was prepared by free radical polymerization. MAPC1 moieties were then hydrolysed to afford phosphonic acid complexing groups. Resulting P(NnPAAm-*stat*-*h*MAPC1) copolymers (Scheme 1(b)) were characterized and used for metal ions sorption [127, 144, 145]. These copolymers showed

different LCST values depending on the molar ratio of both monomers. Copolymer with 20% of phosphonic acid groups was selected as it combined relatively high content of complexing groups with appropriate LCST value (around 25 °C). Sorption experiments demonstrated its efficiency for the complexation of Ni(II), Cd(II) and Al(III) metal ions. Thermosensitive character of the copolymer allowed an easy separation of the polymer-metal complexes in particular in the case of Al(III). Experimental results led to the development of a new process for the removal of heavy metals from wastewaters named 'Thermosensitive polymer Enhanced Filtration' (TEF process) [144].



Scheme 1. Chemical structures of thermosensitive copolymers poly(*N-n*-propylacrylamide-*stat*-(dimethoxyphosphoryl)methyl 2-methylacrylate) (P(NnPAAm-*stat*-MAPC1)) (a) and its hydrolysed derivative P(NnPAAm-*stat*-*h*MAPC1) (b) [127]

More recently, another phosphonate-based acrylamide monomer containing valuable carbamoylmethylphosphonate moiety was developed (Scheme 2(a)) [146]. This original monomer was then polymerized by free radical polymerization to obtain poly(diethyl-6-(acrylamido)hexylcarbamoylmethyl phosphonate) (P(CPAAm6C)) homopolymer (Scheme 2(b)). Owing to both acrylamide and phosphonate groups, this homopolymer was the first example in the literature showing a combination of thermosensitivity and complexation properties. LCST was measured at around 42 °C in milli-Q water. Its sorption of gadolinium (Gd(III)) proved to be efficient below and above the critical temperature, shown by infrared spectroscopy and ICP-MS characterization before and after the complexation [146, 147]. The P(CPAAm6C) was the first thermosensitive homopolymer used to improve water treatment procedure. For a further study of sorption property, its hydrolysed derivative hP(CPAAm6C) (Scheme 2(c)) was also tested with Gd(III). A better capacity for Gd(III) sorption under the same experimental conditions was proved. The hydrolysed polymer was relatively selective of Gd(III) in Gd/Ni mixtures, however, hP(CPAAm6C) was not thermosensitive [148].



Scheme 2. Chemical structures of monomer diethyl-6-(acrylamido)hexylcarbamoylmethyl phosphonate (CPAAM6C) (a), the P(CPAAM6C) homopolymer (LCST=42 °C) (b) and its hydrolyzed hP(CPAAM6C) derivative (c) [112, 146]

Side to gadolinium (Gd), P(CPAAM6C) and hP(CPAAM6C) were also considered for the sorption of uranium (U) and thorium (Th). In the most recent work [149], the complexing results of P(CPAAM6C) and hP(CPAAM6C) in the Gd/Th/U mixture aqueous solution were reported. P(CPAAM6C) showed stronger affinity for Th(IV) compared to Gd(III) and U(VI), its sorption capacity for Th(IV) was higher than 1.5 mmol·g⁻¹. hP(CPAAM6C) showed selective flocculation property for U(VI), its sorption capacity for U(VI) was higher than 2.75 mmol·g⁻¹.

2.3. Conclusion

Polymeric sorbents play an important role in metal ions removal, with both advantages of good selectivity and reusable performance. The sorption property of these polymers is brought by the functional groups borne by the polymers, which ensure metal ions sorption by complexation or ion-exchange interactions. Among all the functional groups known and studied, phosphonic groups attracted the most our attention as it proved to be efficient for the complexation of metal ions. In order to facilitate the phase separation, it is proposed to combine the sorption property and thermosensitivity of water-soluble polymers, especially those showing a LCST. These thermosensitive polymeric sorbents showed great interest to ensure phase separation through precipitating the polymer-metal complexes by heating aqueous solution above the LCST of the polymer. At last, for regenerating polymeric sorbents, some classic regeneration agents can be used, as acids and alkalis.

Part 3: Interactions between water-soluble polymeric sorbents and metal ions in water

3.1. Study of metal ions solutions

3.1.1. Introduction of speciation

Knowing the nature of various metal ion species in aqueous solutions is an important issue because the toxicity, mobility, bioavailability, bioaccumulation and interactions between metal ions and organic compounds depend on their chemical forms [150, 151]. Therefore, in the study of metal ions separation and recovery processes, which is based on the interaction between polymeric sorbents and metal ions present in effluent, this knowledge becomes important. Insoluble metal species or metal cations strongly associated with anions have lower to form chelation bond with the ligands in polymers [91]. Herein, it is mandatory and important for us to make sure that the target metal cation is present as free species in aqueous solution under the studied experimental conditions, without forming precipitated or crystallized solids.

The complexity of states of lanthanides and actinides in nature is first reported. Among these states, it exists two forms of particulate (not soluble in water) and soluble phase in effluent. Soluble phase includes hydrated ions, inorganic and organic complexes, and species associated with heterogeneous colloidal dispersions. Insoluble phase is mainly the undissolved mineral matrix containing related elements. In order to identify and determine physical-chemical forms of target metal elements in aqueous solution under given conditions, speciation measurement/analysis was proposed.

Speciation study is mandatory not only for water treatment, but also for investigating the transport of elements in the environment and the study on harmful effects on living organisms [152-156]. For example, in oil production, metals occur in crude oil in a great variety of complexed forms. These metals are important constituents even with minor quantity [157], since they affect the refining and production operations, and participate in geochemical processes. The roles of metals are thought to be related to their chemical state, which requires speciation analysis. The speciation of metal ions is influenced by several factors, as pH, temperature, anions, ligands [158, 159], ... Among all the impact factors, pH is

thought to be the most important one. For instance, in a study on Fe(II) and Fe(III) in natural geothermal water in Iceland, the Fe(II) and Fe(III) speciation and Fe_{total} concentration were proved to be largely influenced by the pH [154]. In the pH range of 7-9, the Fe_{total} concentration was lower than $2 \mu\text{mol}\cdot\text{L}^{-1}$ with Fe(III) predominating; Fe(II) became the major moiety at pH below 3 with Fe_{total} concentration increasing. In another study, the speciation of Al(III) in drinking water also proved to mainly depend on the pH [160], the proportion of Al(III) was found more important at pH=4 than that at higher or lower pH value. These studies show the noticeable influence of pH on the metal ions speciation and this will have an influence on the studied properties (sorption, transport, etc.). Additionally, this impact of pH depends on the metal ions. Some metal ions or species are relatively stable under large range of pH, whereas others vary more with the pH changes. Temperature is another important impact factor for metal ions speciation, which is of course related to the chemical thermodynamic properties of metal ions [161, 162]. The presence of organic species could also impact metal ions speciation [163, 164]. For example, a study about the influence of ethylenediamine disuccinic acid (EDDS, an isomer of EDTA) on speciation of dissolved metals in contaminated soils was carried out [163]. A batch of extraction experiments using four field-contaminated soils with pH variation from 4.7 to 7.2 demonstrated that the addition of EDDS increased total metal concentrations in the soil extracts, the influenced metals were Al, Cu, Fe, Ni and Zn. However, the free metal concentrations of Cu, Ni and Zn decreased with the addition of EDDS.

3.1.2. Speciation analysis techniques

The difficulty in identifying natures or forms of lanthanide and actinide species is generally caused by their weak concentrations in natural water or industrial effluent [165]. The development of coupled techniques, based on a separation system combined with a highly sensitive and selective atomic detector, makes possible the study of metal speciation analysis [166]. However, it is quite impossible to determine systematically the speciation with analytical chemistry methods alone and they have to be combined with spectroscopic methods, potentiometric measurement or polarography and so on [167, 168]. Simulating metal speciation is the main way to obtain the complete description of the different species in a given system. Chemical speciation modelling is a convenient way to know the

distribution of species of a metal element before further study, and to properly design measurements conditions. Chemical speciation models are based on mass balance and thermodynamic equilibrium constants of the chemical species in aqueous solution [167]. The determination of thermodynamic constants requires various experiments for quantifying proton concentrations, metal ion concentrations, ligand concentration and metal ions/ligand using spectroscopic methods, electromotive force, light spectrophotometry, or nuclear magnetic resonance [169, 170]. The measurement should be performed at equilibrium state. All this give access to the thermodynamic constants of a given element, which can be found in dedicated database.

Publicly available modeling software incorporates multicomponent thermodynamic equilibrium speciation modeling, which has been explained in details in the work of Morel and Morgan [171]. In the past years, various speciation codes have been developed, together with a wide range of reaction thermodynamic databases for computation [172]. For instance, MEDUSA is a common freeware for directly obtaining the diagrams of metal speciation, excluding organic compounds. For example, in a study of heavy metal cations adsorption on silica using flow microcalorimetry by Lantenois *et al* [173], the adsorption isotherm experiments of Pb(II) and Cd(II) on Spherosil must be fixed at a pH in order to avoid the pH range where the ions hydrolysis and precipitation occurred. For fixing the pH in experiments, MEDUSA using thermodynamic constants from Wateq4f database was therefore used to calculate the speciation of lead and cadmium nitrates in the experimental conditions. According to the speciation diagrams obtained, the hydrolysis of Pb(II) and Cd(II) occurs at pH equal to 5.5, and 8, respectively. Thus, the adsorption experimental pH condition was fixed at 5 for Pb(II) and 7 for Cd(II) without appearance of ions hydrolysis or precipitation, and then only adsorption was considered, and surface precipitation could be excluded.

Another versatile software, PHREEQC, is designed to perform a wide variety of aqueous geochemical calculations [174]. For example, it was used in a study of the effect of presence of DTPA organic ligand on Eu(III) sorption onto quartz at different pH [175]. In this study, batch sorption experiments and surface sorption simulation were carried out. In the surface complexation modelling, in order to establish the surface reactions between Eu(III) and DTPA

at different pH, the species of Eu(III), DTPA and 1:1 Eu(III)-DTPA were defined and calculated by using PHREEQC with Nagra/PSI chemical Thermodynamic database. Furthermore, the thermodynamic equilibrium constants ($\log K$) of the surface complexation reactions were optimized by fitting the simulated sorption curves to the experimental data using PHREEQC coupled with another program called PEST. Batch sorption experiments showed that the presence of DTPA brought higher sorption of Eu(III) on quartz at acidic and neutral pH, but lower sorption at basic pH. The modelling results showed the formation of $\equiv\text{QOHEuDTPA}^{2-}$ ($\equiv\text{QOH}$ represents quartz sand) at acidic and neutral pH and the formation of EuDTPA^{2-} at basic pH, which explained the different sorption results at different pH between Eu(III) and DTPA in batch experiments. Other modeling programs are also often used in speciation analysis, such as Hyss and Visual MINTEQ, which can be used to calculate metal speciation, solubility equilibria and metal sorption in aqueous systems. In general, all these programs have advantages and limits, the choice depends on the studied objects and systems.

3.2. Interaction study methods

As previously reported, various interactions between functional polymers and metal cations make possible the formation of complexes showing different forms. The driving forces include forces of electrostatic attraction, hydrogen and coordination bonds. The studies of the structures of complexes and the complexation processes in aqueous solutions can be carried out with various physicochemical analytical methods. In order to obtain an insight into the structure of polymer-metal-ion complexes, many techniques have been employed, including light scattering, nanoparticle tracking analysis, cryo-transmission electron microscopy, atomic force microscopy, small-angle neutron scattering, analytical velocity sedimentation, straight leg raising test, extended X-Ray absorption fine structure and luminescence methods [176]. Other techniques, such as potentiometric titration, isothermal titration calorimetry and surface plasmon resonance, make possible to access the type of interactions between polymers and metal cations [176].

In this work, Isothermal Titration Calorimetry (ITC) has been chosen to study the complexation property of the synthesized polymers with selected lanthanide and actinide ions. It was selected for its easy operation and the information that could be extracted. As a tool for characterizing molecular interactions, ITC is able to provide thermodynamics

parameters (affinity, stoichiometry, enthalpy) of the interactions [177, 178]. These parameters are calculated from the heat variation measured during the titration process, which is based on the heat release (exothermic) or heat absorption (endothermic) for the interactions between two components [178, 179]. The case without thermic variation is very rare in the binding interactions between ligands and metal ions. This approach is this used to rapidly and indirectly evaluate the sorption efficiency, and above all to compare the complexing property of various materials. ITC has been widely used in the study of binding reaction between metal ions and organic ligands. For example, ITC was used to determine thermodynamics of Al(III), Cr(III) and Pb(II) binding to chitin biopolymer [180]. In this study, the sorption performance with chitin were then compared with those determined with activated carbon. The ITC results demonstrated two distinct binding sites on chitin for all the three metal ions. The interactions between the three metal ions and chitin showed higher Gibbs free energy changes (ΔG) than that with activated carbon. Another thermodynamic and structural study dealt with the complexation of Nd(III), Eu(III) and Am(III) with malate [181], where ITC was also used to achieve the study. Apart from the thermodynamic parameters of changes of enthalpy, entropy and Gibbs free energy, two complexes with 1:1 and 1:2 metal/malate stoichiometry were determined by ITC for the three ions. In addition, the complexing constants of 1:1 and 1:2 Nd(III)/malate obtained by ITC were then used to extrapolate the stability constants in zero ionic strength condition. Stability constant of 6 and 9, for 1:1 and 1:2 Nd/malate, was obtained, respectively. ITC is not only useful in metal ions sorption study, but also in the study of interactions between polyelectrolytes. An example is a study about the influence of ionic strength and charge density on the interaction between ϵ -polylysine (positive charge) and a series of polyanions containing acrylamide by Lounis *et al* [182], ITC was used to determine binding constants and stoichiometry of the interactions at different ionic strengths and at different polyanions density. These ITC results could be used to model and predict the binding parameters at any ionic strength or any polyanion charge density. The results of entropy and enthalpy obtained from ITC confirmed the entropically driven character of the interactions. Finally, ITC experiments were carried out to study the sorption of different metal ions onto poly(vinyl alcohol) (PVA)-based polymers bearing ethylene diamine tetraacetic acid (EDTA) as chelating agent. The hydro-soluble PVA1(EDTA)_{15%} polymer was tested with Co(II), Ni(II), Zn(II), Pb(II), Cd(II) and Cu(II) using ITC.

It showed good selectivity for Ni(II), Cu(II) and Pb(II) by comparing the binding constants obtained by ITC [183].

3.3. Conclusion

To study the interactions between the water-soluble polymeric sorbents and target metal cations, it is important to know the different species that can be encountered for the studied metal ions in aqueous solution at different pH, and to fix an experimental pH value, in order to simplify the studied system, also avoiding the precipitation phenomenon. Speciation analysis is generally carried out with simulation methods by using different software adapted to studied systems. The interactions between water-soluble polymeric sorbents and metal ions are related to two different mechanisms, electrostatic forces and formation of coordinating bonds. Additionally, their interactions are influenced by polymer chains, the position of functional groups and solution physicochemical conditions (pH, temperature, etc). ITC, as the selected method in this work for studying the interactions between polymers and metal ions, possesses the advantage of providing thermodynamic parameters of the interactions. This technique also allows comparing the complexing property of the different synthesized water-soluble polymeric sorbents.

Conclusion

The important role of the REEs in advanced technology developments is undoubted. Thus, purification and separation techniques for REEs have been intensively studied. Phosphorous water-soluble polymers have attracted people attention owing to the complexation property of phosphonic oxygen for Ln(III) reported in the literature [74, 112, 184] and various properties brought by polymeric structures.

The aim of the present work is to synthesize original new polymers for the selective complexation of lanthanides or actinides. In case of success, experimental results obtained will lead to the development of an innovative process to purify and separate REEs. The strategy is to separate and to isolate the REEs individually through the selectivity of specifically designed phosphorous polymers from effluents. Considering the usual presence of actinide elements in the effluents (thorium and uranium), we will first design phosphorous polymers capable to selectively complex the actinides. Then, thermosensitivity will be used to achieve the complexes separation in aqueous solution by heating the solution above the LCST of the polymer and then precipitating the polymer-metal complexes. As polymers can also in some cases flocculate after sorption, this property will be considered to permit an easy filtration step. Once actinide contaminants removed, another polymeric sorbent will be used for the selective sorption of lanthanides. Ideally, this polymer will also be thermosensitive to favor the filtration step. Figure 7 reports the principle of the procedure to be developed in the present work. Two water-soluble phosphorous polymers able to selectively complex Th(IV) and U(VI) will be synthesized. Polymer 1 was thermosensitive and selective for Th(IV), polymer 2 flocculated with U(VI) in aqueous solution. Therefore, the complexes of polymer 2 and U(VI) can be isolated by filtration at the first time, and the complexes of polymer 1 with Th(IV) can be isolated by precipitating after heating. Mono-hydrolyzed derivative from polymer 1 will also be studied in order to evaluate its selectivity. Then, a third oxymethylphosphorous-based polymer will be necessary to complex the lanthanides (Gd, Nd and Ce) selectively, with thermosensitive or flocculating property. The structure intended of this third polymer is shown in Figure 7 as polymer 3. Further study of interactions between polymers and metal ions is also one of the

objectives of the present work, the obtained information of their relative selectivity being used for better designing the polymeric sorbents.

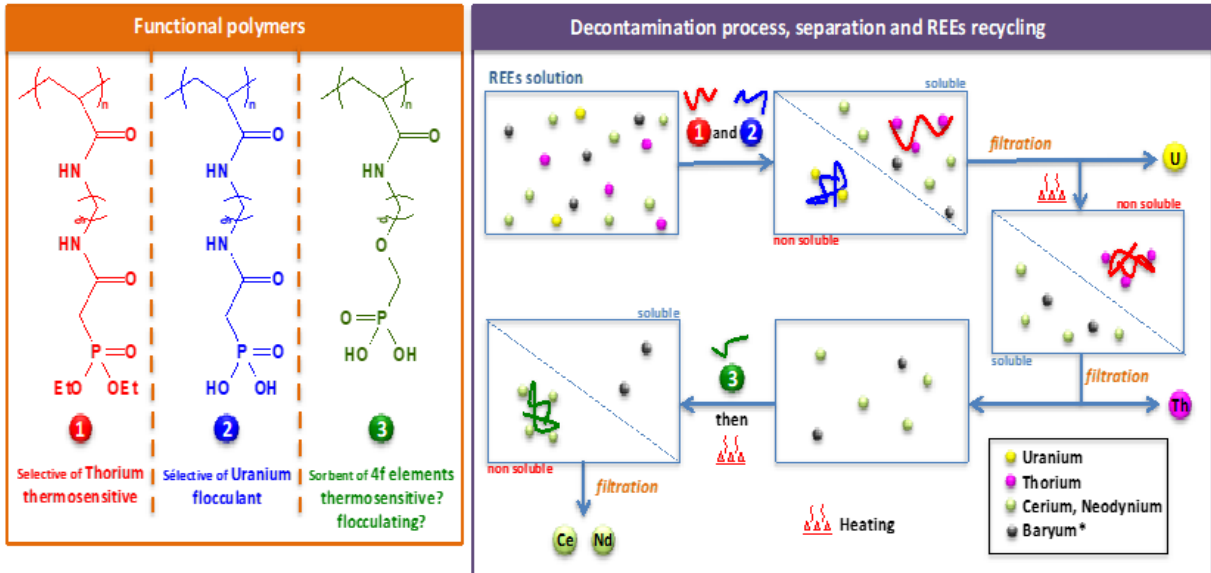


Figure 7. Designed phosphorous polymers and ideal process to be developed for separating and isolating REEs from phosphorous water-soluble polymeric sorbents

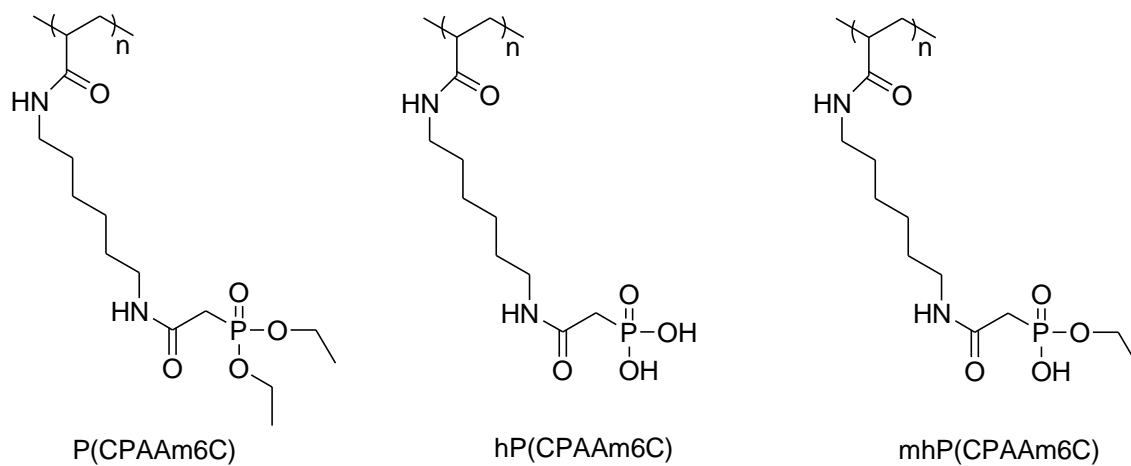
Chapter 2: Comparison of Isothermal Titration Calorimetry (ITC) and Inductively Coupled Plasma Mass Spectroscopy (ICP-MS) to study sorption properties of polymers

Introduction

Both thermosensitive and chelating homopolymer, namely poly(diethyl-6-(acrylamido)hexylcarbamoylmethyl phosphonate) (P(CPAAm6C)) (Scheme 3), was recently developed in our group (thesis of Dr D. Gomes Rodrigues) [146]. This polyacrylamide homopolymer showed a thermosensitive behaviour with a cloud point value measured at 42 °C. Additionally, P(CPAAm6C) bore a valuable carbamoylmethylphosphonate function, able to efficiently complex metal ions. For instance, in a mixture containing 86% mol of gadolinium (Gd), 10% mol of thorium (Th) and 4% mol of uranium (U), P(CPAAm6C) proved to be selective for Th(IV) [149]. As the polymer was also thermosensitive, it was easy to convert it to insoluble state above the cloud point, thus leading to an easy separation from the aqueous effluent. Full hydrolysis of the P(CPAAm6C) was also achieved to produce a new polymer (hP(CPAAm6C)) (Scheme 3) with diphosphonic acid groups. As hP(CPAAm6C) was highly hydrophilic, it was not thermosensitive anymore. Nevertheless, it was demonstrated that this polymer flocculated once complexing with metallic cations [149]. In a similar 86/10/4% mol of Gd/Th/U mixture aqueous solution, it was shown that hP(CPAAm6C) was selective for U(VI) even when its proportion in the cation mixture was very low (4%). Moreover, polymer precipitated in the aqueous solution when U(VI) was complexed, confirming the flocculating character of the polymer.

These experimental results of sorption were obtained from solution analysis using Inductively Coupled Plasma Mass Spectrometry (ICP-MS). Another valuable analysis technique that appeared interesting to employ was Isothermal Titration Calorimetry (ITC) as it notably gives information about the sorption of metal ions onto functional groups of polymers using low quantities of materials. Moreover, ITC could provide information in addition to those given by ICP-MS. As sorption of gadolinium and thorium onto P(CPAAm6C) was studied by ICP-MS, we decided to achieve ITC experiments using these metal ions. Uranium was also studied but it was impossible to afford results due to the complicated speciation system of uranyl and thus the difficulty to establish the mechanism and fit the experimental data. Additionally, as selectivity depended on the chemical nature of the phosphorus-based complexing group, mono-hydrolysis of P(CPAAm6C) was carried out,

leading to mhP(CPAAm6C) mono-phosphonic acid derivative (Scheme 3). Complexation of gadolinium and thorium onto mhP(CPAAm6C) was also studied. Results obtained by thermodynamic approach (ITC) and solution analysis (ICP-MS) were compared. All experimental results obtained were reported and discussed in the following scientific article.



Scheme 3. Chemical structures of poly(diethyl-6-(acrylamido)hexylcarbamoylmethyl phosphonate) (P(CPAAm6C)), its fully hydrolyzed derivative (hP(CPAAm6C)) and its mono-hydrolyzed derivative (mhP(CPAAm6C))

Development of chelating phosphorous polymers, and evidence of their complexation properties using combination of analytical and thermodynamic approaches

Abstract: Poly(diethyl-6-(acrylamido)hexylcarbamoylmethyl phosphonate) (P(CPAAm6C)), phosphonate-based polyacrylamide homopolymer, proved to be of great interest as it combined thermosensitivity with complexing properties due to polyacrylamide nature and carbamoylphosphonated moiety, respectively. In particular, P(CPAAm6C) revealed interesting chelating properties for some lanthanides and radionuclides, *e.g.* gadolinium (Gd), thorium (Th) and uranium (U). In the present study, poly(diethyl-6-(acrylamido)hexylcarbamoylmethyl phosphonate) was mono-hydrolyzed to lead to the mhP(CPAAm6C) polymer. The sorption properties of both polymers were tested for the lanthanides removal from nuclear effluents. In particular, separation of Gd and Th was investigated by combining two complementary tools based on thermodynamic and analytical studies: Isothermal Titration Calorimetry (ITC) and Inductively Coupled Plasma Mass spectroscopy (ICP-MS), respectively.

The diethyl phosphonate group borne by the polymer kept its chelating property, with similar binding constant compared to the monomer, the polymer being more easily handled in a sorption process. In addition, direct measurements of binding constants have proved that the selectivity for Th(IV) of the P(CPAAm6C) polymer in the mixture of Th(IV) with Gd(III), previously demonstrated by standard sorption study, was confirmed. For the phosphonic mono-acid group found in the mono-hydrolyzed mhP(CPAAm6C) polymer in contact with Th(IV), two successive reactions were necessary to fit the ITC data. In the mixture of Th(IV) with Gd(III), direct thermodynamic analysis as well as retention experiments in dialysis membrane have evidenced that the mhP(CPAAm6C) polymer was selective for Gd(III).

Keywords: phosphorous-based polymers, gadolinium, thorium, thermodynamic study, ICP-MS, ITC

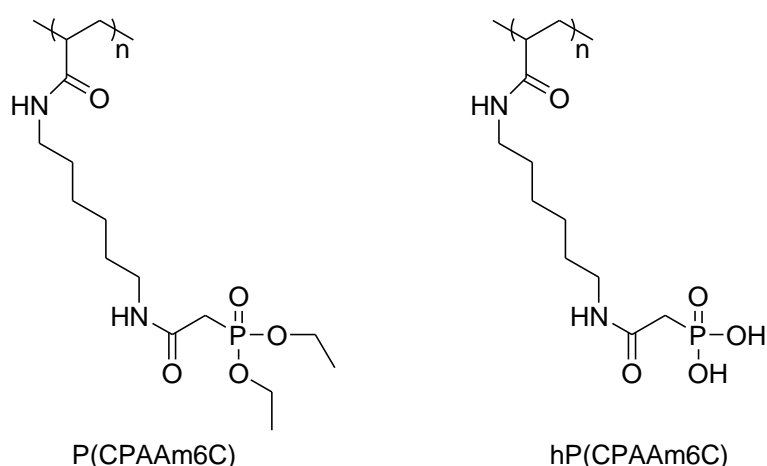
1. Introduction

The abundant applications of rare-earth elements (REEs), mostly the lanthanides, in high technologies make them continuing attracting people attention. Lanthanide compounds, complexes, nanoparticles as guests in microporous hosts materials are used in different fields owing to their excellent physical and chemical properties, such as lighter flints, superconductors [36], hydrogen storage [37], iron and steel production [38], permanent magnets [39], lasers [40], telecommunications and magneto-optic data recording [35]. In contrast to their intensive demand, the resources in REEs in many countries or regions are limited. Thus, separating and recovery techniques of REEs are currently being intensively studied. Different methods to separate REEs from mineral and industrial effluent have been developed, including solvent extraction, Solid Phase Extraction (SPE) [5, 51, 76] using non-water-soluble polymeric sorbents, and Polymer Enhanced Ultrafiltration (PEUF) [65] with water-soluble polymeric sorbents. Solvent extraction methods showed disadvantages such as important consumption of solvent, many times repetition needed to obtain pure product and relatively bad selectivity. The SPE methods generally have slow kinetics and bad efficiency. In the PEUF procedures, water-soluble polymers functionalized with different complexing sites showed efficiency, fast kinetics and selectivity in some cases. However, one of the difficulties encountered in recycling REEs using polymeric materials is the presence of other contaminants in aqueous solutions. These contaminants are mainly thorium (Th), uranium (U) (present in relatively significant amounts in the earth) and their descendants produced by radioactive parentage (including several radium isotopes), which can also interact with extracting polymers.

To date, some water-soluble polymers have been reported to be able to complex the lanthanides (Ln, the majority of REEs) or actinides (An, radioactive). Bisset *et al* [185] reported a water-soluble polymer that contained primary hydroxamic acid binding group which proved to be selective for Th(IV) over Fe(III) at pH=1. Some polyacrylate polymers could complex uranyl ions [186]. Polycarboxylic and aminocarboxylic acids have been successfully used to complex Ln and An [186, 187]. Phosphonic group also proved to be good sorbent for some Ln and An [187, 188], and showed better selectivity for Ln [189]. Even if some polymers showed interesting results, it is still valuable to develop new materials that

could be involved in REEs recovery process. In particular, water-soluble phosphorous-based polymeric sorbents, which demonstrated some selectivity for different metal ions, are wished to be developed. In an ideal case, these polymers will allow recovering the REEs and/or removing contaminants. In addition, separation of metal-polymer complexes must also be taken in consideration, depending on the polymer water solubility. It would be relevant to avoid ultrafiltration, notably to decrease the cost of the process. An example dealt with functionalized thermosensitive phosphonic acid-based copolymer, named P(*Nn*PAAm-*stat-h*MAPC1) [95, 127, 190], which proved to be able to selectively complex Al(III) over Ni(II), Cd(II) and Ca(II). The resulting metal-polymer complexes were precipitated by heating the aqueous solution above the polymer Lower Critical Solution Temperature (LCST) [127].

The objective of the present work was to develop and/or study phosphorous polymers able to efficiently and selectively complex gadolinium (Gd, lanthanide, representing the REEs) or thorium (Th, actinide, representing the contaminants) combining two complementary tools based on thermodynamic and analytical studies: Isothermal Titration Calorimetry (ITC) and Inductively Coupled Plasma Mass spectroscopy (ICP-MS), respectively. For such purpose, poly(diethyl-6-(acrylamido)hexylcarbamoymethyl phosphonate) (P(CPAAm6C)) (Scheme 4) was used as starting material. This homopolymer was the first example in the literature showing a combination of thermosensitivity and complexation properties, with a cloud point (CP) measured at 42 °C in milli-Q water [146]. This polymer allowed an efficient sorption of Gd(III) below and above the CP, and proved to be selective for Gd(III) over Ni(II) [147]. The metal-P(CPAAm6C) complexes could be precipitated by heating the aqueous solution over the CP, which allowed using microfiltration for the separation step. For a further study of sorption property, P(CPAAm6C) was fully hydrolysed to lead to hP(CPAAm6C) derivative (Scheme 4), which was also tested with Gd(III). A better capacity for Gd(III) sorption in Gd/Ni mixture was proved, however, hP(CPAAm6C) was not thermosensitive [148]. In a most recent work [149], the complexing property of P(CPAAm6C) and hP(CPAAm6C) in the Gd/Th/U aqueous solutions mixture (86/10/4% in moles) was studied. P(CPAAm6C) showed stronger affinity for Th(IV) compared to Gd(III) and U(VI), its sorption capacity for Th(IV) was higher than 1.5 mmol·g⁻¹. hP(CPAAm6C) showed selective flocculation property for U(VI), its sorption capacity for U(VI) was higher than 2.75 mmol·g⁻¹.



Scheme 4. Thermosensitive poly(diethyl-6-(acrylamido)hexylcarbamoylmethyl phosphonate) (P(CPAAm6C)) polymer (left) and its hydrolyzed hP(CPAAm6C) derivative (right)

In this present work, the mono-hydrolysis of P(CPAAm6C) was carried out, leading to mhP(CPAAm6C) polymer. Its complexing properties towards Gd(III) and Th(IV) were studied and compared with that of P(CPAAm6C) using a combination of analytical and thermodynamic approaches. Isothermal Titration Calorimetry (ITC) technique was used to evaluate the thermodynamic parameters (mainly binding constants) and thus get an insight of the selectivity. The ITC results dealing with P(CPAAm6C) and mhP(CPAAm6C) for Gd(III) or Th(IV) complexation were compared with those obtained from dialysis sorption experiments coupled with ICP-MS, to check the selectivity of both polymers with Gd(III) and Th(IV).

2. Experimental section

2.1. Materials

Solvents were purchased from Aldrich and were used without further purification. Gadolinium(III) nitrate hexahydrate ($\text{Gd}(\text{NO}_3)_3 \cdot 6\text{H}_2\text{O}$, Aldrich, 99.99% metal basis trace), $(\text{Th}(\text{NO}_3)_4 \cdot \text{H}_2\text{O}$, puriss. spez. Aktivität: $0.0467 \text{ uCi} \cdot \text{g}^{-1}$), HNO_3 (Carlo Erba), KOH (Honeywell, $\geq 85\%$) were used as received. Aqueous solutions used for sorption experiments were prepared with Milli-Q water of $18.2 \text{ M}\Omega \cdot \text{cm}$.

2.2. Synthesis of poly(6-(acrylamido)hexylcarbamoylmethyl phosphonic mono-acid) (mhP(CPAAm6C))

Poly(diethyl-6-(acrylamido)hexylcarbamoylmethyl phosphonate) (P(CPAAm6C)) was prepared according to already published procedure [146], by polymerizing the diethyl-6-(acrylamido)hexylcarbamoylmethyl phosphonate (CPAAm6C) monomer by free radical polymerization. The mono-hydrolyzed mhP(CPAAm6C) polymer was then prepared starting from P(CPAAm6C). The full procedure is described as follows. P(CPAAm6C) (0.8 g, 2.3 mmol) was dissolved in ethanol (EtOH) (10 mL). Then, a potassium hydroxide solution prepared with KOH (3.86 g, 68 mmol) dissolved in distilled water (12 mL) was added into the polymer solution. The reaction was kept stirring at 90 °C under reflux overnight. EtOH was evaporated after the reaction. The product was then purified by dialysis using a 3.5 kD cut-off membrane and then dried using lyophilization to lead to a white powder (0.75 g, yield: 100%).

^1H NMR (400 MHz, δ (ppm), D_2O): 1.16-1.20 (m, $-\text{CHCH}_2$, $-\text{NHCH}_2\text{CH}_2\text{CH}_2$, $-\text{OCH}_2\text{CH}_3$); 1.28-1.61 (m, $-\text{COCH}$, $-\text{NHCH}_2\text{CH}_2$); 2.61-2.67 (m, $-\text{PO}_3\text{CH}_2$); 2.92-3.12 (m, $-\text{NHCH}_2$); 3.85-3.89 (m, $-\text{OCH}_2\text{CH}_3$)

^{31}P NMR (400 MHz, δ (ppm), D_2O): 16.23 ppm (Figure SI 2)

2.3. Characterization

Nuclear Magnetic Resonance (NMR) was carried out with Bruker Avance 400 (400 MHz) to record ^1H and ^{31}P NMR spectra with D_2O as deuterated solvent purchased from Eurisotop. For ^1H NMR, chemical shifts were referenced to the corresponding hydrogenated solvent residual peak at 4.79 ppm. H_3PO_4 was used as a reference for ^{31}P NMR.

Size Exclusion Chromatography (SEC) was performed with PL-GPC 50 (Agilent), equipped with a refractive index (RI) detector. PolarGel M column was used at 50 °C with a flow of 0.8 $\text{mL}\cdot\text{min}^{-1}$ calibrated with PMMA standards. Elution solvent used was DMAc (+0.1wt% LiCl).

Cloud point (CP) was determined using UV visible measurements, performed with PerkinElmer Lambda 35 UV/VIS spectrometer coupled with PerkinElmer Peltier temperature programmer system. The aqueous solutions of polymers ($10\text{ g}\cdot\text{L}^{-1}$) were prepared by dissolution of P(CPAAm6C) (30 mg) or mhP(CPAAm6V) (30 mg) in Milli-Q water (3 mL). The CP determination was set in a temperature region from 25 to 65 °C with temperature ramp of $0.1\text{ }^\circ\text{C}\cdot\text{min}^{-1}$. The wavelength was fixed as 500 nm.

2.4. Sorption experiments

2.4.1. Preparation of monomer and polymeric sorbents aqueous solutions

CPAAm6C monomer aqueous solution of $31 \text{ mmol}\cdot\text{L}^{-1}$ was prepared by dissolving CPAAm6C in Milli-Q water. Various solutions of polymers were prepared at two concentrations (14.3 and $31 \text{ mmol}\cdot\text{L}^{-1}$) depending on the systems to be studied and the analysis to be carried out. For the polymers, the concentrations were expressed taking into account the concentrations of the monomer unit, and solutions were prepared by directly dissolving one of the selected polymers in Milli-Q water. The pH of all solutions was modified to $\text{pH}=1$ with $1 \text{ mol}\cdot\text{L}^{-1}$ HNO_3 solution (prepared from 65% HNO_3 dilution). Due to the subsequent dilution after acidification, special attention has been paid to reevaluate the effective concentration. In particular, new concentrations of all solutions after pH modification were recalculated to consider updated parameters before thermodynamic data treatment. In sorption experiments based on dialysis, the polymer aqueous solution concentration in the inner part of the tube was $14.3 \text{ mmol}\cdot\text{L}^{-1}$.

2.4.2. Preparation of metal ions aqueous solutions

For Isothermal Titration Calorimetric (ITC) experiments, single Gd(III) aqueous solutions or Th(IV) aqueous solutions at various concentrations (63 or $17 \text{ mmol}\cdot\text{L}^{-1}$) were prepared to obtain optimal experimental signals depending on the ligand/metal couple. Gd(III) and Th(IV) aqueous solutions were prepared by dissolving respectively gadolinium(III) nitrate or thorium(IV) nitrate in Milli-Q water. The pH of the solutions was then modified to $\text{pH}=1$ using the same $1 \text{ mol}\cdot\text{L}^{-1}$ HNO_3 . As done for the polymeric sorbent solutions, new concentrations of the solutions after pH modification were accurately recalculated.

For sorption experiment based on dialysis, solutions containing mixture of Gd(III) and Th(IV) with a fixed percentage (89.6% and 10.4% in moles, respectively) were prepared at three various concentrations (1.4 , 5.7 and $14.3 \text{ mmol}\cdot\text{L}^{-1}$). These concentrations corresponded to 0.1 eq, 0.4 eq and 1 eq related to the concentration of polymer aqueous solution inside the dialysis tube ($14.3 \text{ mmol}\cdot\text{L}^{-1}$ expressed for the monomer moiety). The mixed metal ions solutions were prepared by dissolving both salts (gadolinium nitrate and thorium nitrate) in Milli-Q water and the pH was adjusted to $\text{pH}=1$.

2.4.3. Thermodynamics study based on Isothermal Titration Calorimetry (ITC)

Isothermal Titration Calorimetry (ITC) experiments were performed with a TAM III multi-channel calorimetric device equipped with Nanocalorimeters and Micro Reaction System composed of a computer-controlled micro-syringe injection device. A stock solution of metal ion was injected in a controlled manner to stainless steel sample ampoule serving as a calorimetric cell. The sample cell was filled with the ligand solution for a sorption experiment. Similar experiment was performed with metal successive injection in the solvent (acidified aqueous solution without ligand), in order to remove the thermal effect due to the dilution. The initial volume in the cell (of the ligand or of the acidified water) was 800 μL . Measurements were carried out at 298 K. A complete experiment consisted in a series of 25 injections of 10 μL (injection duration of 10 seconds). The time between two injections was 45 minutes to ensure a complete return to the baseline before the next injection. Homogeneity of the solutions was maintained using a gold stirrer at 95 rpm.

2.4.4. Sorption experiments by dialysis coupled with Inductively Coupled Plasma Mass Spectrometry (ICP-MS)

The dialysis sorption experiments were performed by immersing a dialysis membrane tube (cut-off equals to 2 kD) containing 10 mL of P(CPAAm6C) or mhP(CPAAm6C) aqueous solution of 14.35 $\text{mmol}\cdot\text{L}^{-1}$ into a 100 mL mixture aqueous solution of $\text{Gd}(\text{NO}_3)_3\cdot 6\text{H}_2\text{O}$ and $\text{Th}(\text{NO}_3)_4\cdot\text{H}_2\text{O}$. All the dialysis experiments were kept stirring for 24 hours at room temperature to completely reach the thermodynamic equilibrium where the concentrations of ions in the dialysis tube and in the bulk could be considered as equal. Solutions in the bulk were sampled before and after the dialysis. Concentrations of each metal ion were determined by Inductively Coupled Plasma Mass Spectrometry (ICP-MS) after appropriate dilution.

The ICP-MS was an AA Thermo Scientific ICE3000. Depending on the metal ions type, the spectrometer was calibrated with different standard solutions. For Gd(III), the concentrations of standard solutions were 0, 350, 400, 500, 600 and 650 ppb. They were prepared by diluting a $\text{Gd}(\text{NO}_3)_3\cdot 6\text{H}_2\text{O}$ solution with an initial concentration of 1000 $\text{mg}\cdot\text{L}^{-1}$. For Th(IV), 0, 0.1, 1, 10, 30 and 75 ppb standard solutions were prepared by diluting a $\text{Th}(\text{NO}_3)_4\cdot\text{H}_2\text{O}$ solution with an initial concentration of 1000 $\text{mg}\cdot\text{L}^{-1}$.

3. Results and discussion

3.1. Synthesis and characterization of poly(6-(acrylamido)hexylcarbamoylmethyl phosphonic mono-acid) (mhP(CPAAm6C))

Poly(diethyl-6-(acrylamido)hexylcarbamoylmethyl phosphonate) (P(CPAAm6C)) was prepared by free radical polymerization of the corresponding diethyl-6-(acrylamido)hexylcarbamoylmethyl phosphonate (CPAAm6C) monomer, as already reported in a previous publication [146]. P(CPAAm6C) was characterized by size exclusion chromatography (SEC) in dimethylacetamide (DMAc), using PMMA standards. The molecular weight (M_n) and the polymerization dispersity (\mathcal{D}) were determined to be equal to 16000 $\text{g}\cdot\text{mol}^{-1}$ and 1.6, respectively (see Supporting information, Figure SI 3). The polymer before and after hydrolysis was also characterized with ^1H and ^{31}P NMR in deuterated water. ^1H NMR of P(CPAAm6C) homopolymer (Figure 8) demonstrated that the polymerization was successful, notably with signals at 1.26-1.29 ppm and 4.12 ppm, corresponding to the methyl and methylene of the ethoxy group borne by the phosphorous atom, respectively. ^{31}P NMR spectrum showed a signal at 24.29 ppm (see Supporting information, Figure SI 1). Then, P(CPAAm6C) homopolymer was mono-hydrolyzed using a potassium hydroxide solution at 90 °C overnight (Scheme 5). After evaporation of the solvent, mhP(CPAAm6C) mono-hydrolyzed polymer was purified by dialysis and obtained after lyophilization. ^1H NMR (Figure 9) allowed proving that the reaction worked, as spectrum showed similar shifts for corresponding protons, with half of protons corresponding to $-\text{OCH}_2\text{CH}_3$ ethoxy group around 1.17 and 3.86 ppm removed by the hydrolysis reaction. ^{31}P NMR spectrum (see Supporting information, Figure SI 2) showed a shift from 24.29 ppm on the starting polymer to 16.23 ppm after hydrolysis.

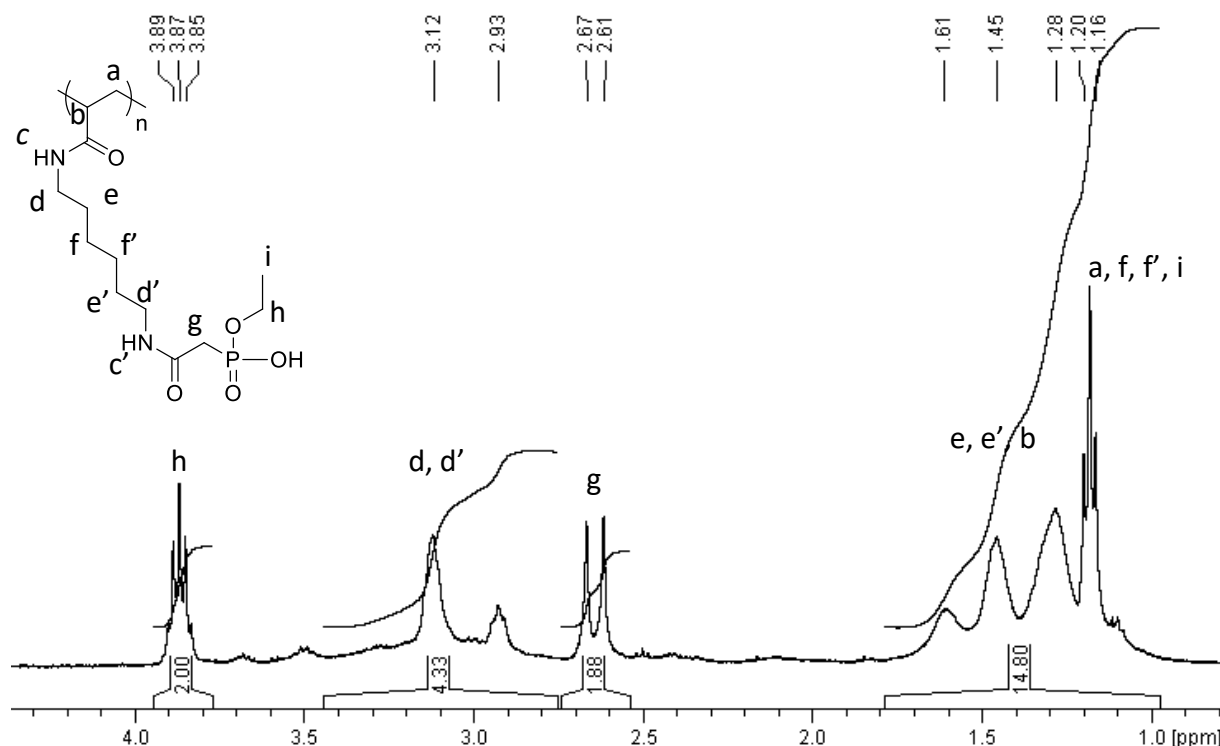


Figure 9. ^1H NMR spectra (400 MHz, D_2O) of poly(6-(acrylamido)hexylcarbamoylmethyl phosphonic mono-acid) (mhP(CPAAm6C))

It is important to notice that it was impossible to determine mhP(CPAAm6C) mono-hydrolyzed polymer molecular weight by size exclusion chromatography as the phosphonic acid group in mhP(CPAAm6C) could damage the column. Concerning the thermosensitivity, UV-Visible experiments were carried out to determine the potential cloud point (CP) for both P(CPAAm6C) and mhP(CPAAm6C) polymers. For P(CPAAm6C), the evolution of the transmittance as a function of the temperature (see Supporting information, Figure SI 4) allowed determining a cloud point equal to 43 °C whereas no cloud point was detected for mhP(CPAAm6C), indicating that mono-hydrolyzed polymer was not thermosensitive but fully soluble in water due to the presence of mono-acid groups.

3.2. Sorption properties

Thermodynamics of the complexation of the initial CPAAm6C, and of P(CPAAm6C) and mhP(CPAAm6C) polymers in interaction with Gd(III) or Th(IV) was studied using Isotherm Titration Calorimetry (ITC). After appropriate data treatment, binding constants were

calculated, and the various affinities between polymers and ions were compared to differentiate the separation efficiency. Dialysis coupled with ICP-MS was then used to assess the selectivity of the polymers with Gd(III) and Th(IV).

As mentioned in the experimental part, all ITC measurements were carried out at pH=1, for the sorbent and for the solvent alone. This was in connection with the application of the separation process to extract lanthanides dissolved from ores in acidic media [191, 192]. At pH=1, the speciation of Gd(III) and Th(IV) (see Supporting information, Figure SI 5 to Figure SI 8) has revealed that no solids were present, and that only free species had to be considered. For Gd(III), the main species at pH=1 were Gd^{3+} and $GdNO_3^{2+}$. Depending on the concentration in the solution to be injected, the repartition between Gd^{3+} and $GdNO_3^{2+}$ was in the range 80-20% for the lowest concentration to 60-40% for the highest concentration, respectively. For Th(IV), the main species at pH=1 were $ThNO_3^{3+}$ and Th^{4+} , Th^{4+} being the minor moiety. The repartition was more strongly impacted by the concentration compared to Gd(III) since the ratio between Th^{4+} and $ThNO_3^{3+}$ was 25-75% for the lowest concentration to 8-92% for the highest one, respectively.

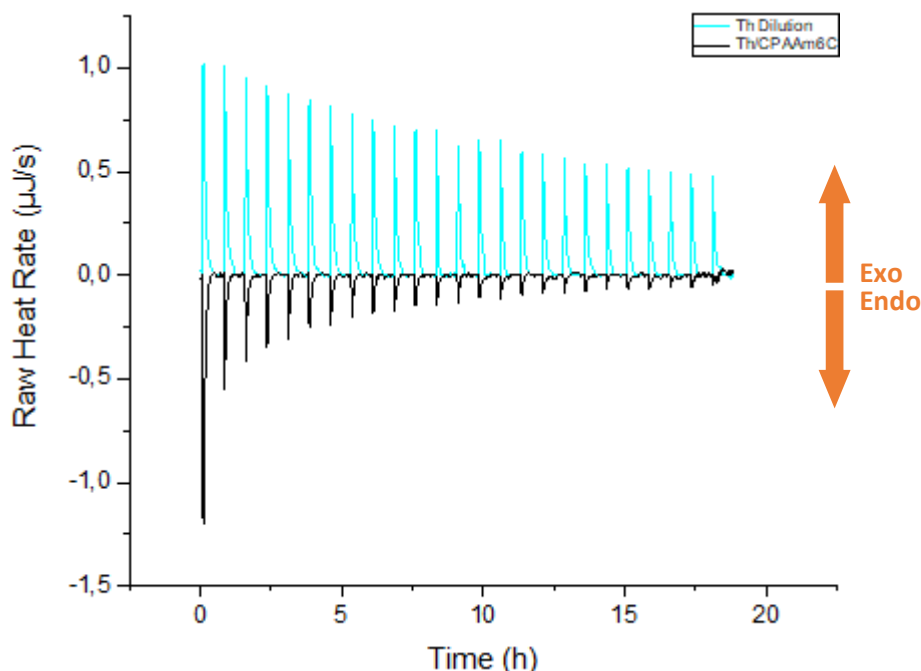


Figure 10. Processed thermal profiles for the Th(IV) ITC experiment of the CPAAm6C monomer aqueous solution of 31 mmol L^{-1} (sorption experiment) and acidified Milli-Q water (dilution experiment) titrated by $Th(NO_3)_4 \cdot H_2O$ aqueous solution of $63 \text{ mmol} \cdot L^{-1}$. Experiments carried out at 298 K and pH=1, with 25 successive injections recorded with $10 \mu\text{L}$ for each injection of Th(IV) stock solution into $800 \mu\text{L}$ of CPAAm6C solution or acidified Milli-Q water.

Firstly, the sorption of CPAAm6C has been characterized for Th(IV) and compared to the corresponding polymer. Figure 10 illustrates the raw ITC thermograms for the CPAAm6C/Th(IV) system, with the superposition of the sorption experiment at pH=1 together with the dilution measured on acidified Milli-Q water. The successive injections resulted in a raw heat rate record as a function of time. The sorption experiment between Th(IV) and CPAAm6C showed endothermic signals starting at $-1.2 \mu\text{J}\cdot\text{s}^{-1}$. The intensity rapidly decreased, and the flow rate reached a constant value of $-0.2 \mu\text{J}\cdot\text{s}^{-1}$ for the 10-12 last injections. This indicated that after 15 injections, no more heat transfer occurred when Th(IV) was added in the system. The dilution of Th(IV) showed exothermic signals starting with an intensity about $1 \mu\text{J}\cdot\text{s}^{-1}$. The subsequent injection slowly and regularly decreased and reached a constant value for the 5 last peaks at around $0.5 \mu\text{J}\cdot\text{s}^{-1}$. The clear difference between sorption and dilution obviously showed that the injected Th(IV) interacted with CPAAm6C.

Similar experiment was performed on the P(CPAAm6C) polymer based on the CPAAm6C unit. Figure 11 illustrates the raw ITC thermograms for the P(CPAAm6C)/Th(IV) system, with the superposition of the sorption and the dilution experiments at pH 1. The sorption heat flow was endothermic with the first peak at $-1 \mu\text{J}\cdot\text{s}^{-1}$, and the intensity of the subsequent injections rapidly decreased. The flow rate was then constant after 15 injections, meaning that the sorption was complete. The dilution of Th(IV) was similar to the one described in Figure 10. The comparison of sorption and dilution contributions evidenced the interactions between Th(IV) and P(CPAAm6C). In addition, the comparison between the curve corresponding to CPAAm6C and P(CPAAm6C) in interaction with Th(IV) exhibited large resemblances. The superposition of the two thermograms (Figure 12) confirmed that the signals were analogous. Thus, the chelating properties of the carbamoylmethyl phosphonate was not changed when the ligand was free in CPAAm6C or in the P(CPAAm6C) polymer. The polymer chains did not hinder nor modify the ligand property, and the complexation behavior was preserved. In addition, considering the thermosensitivity of P(CPAAm6C), it is obviously possible to use the material in a separation cycle.

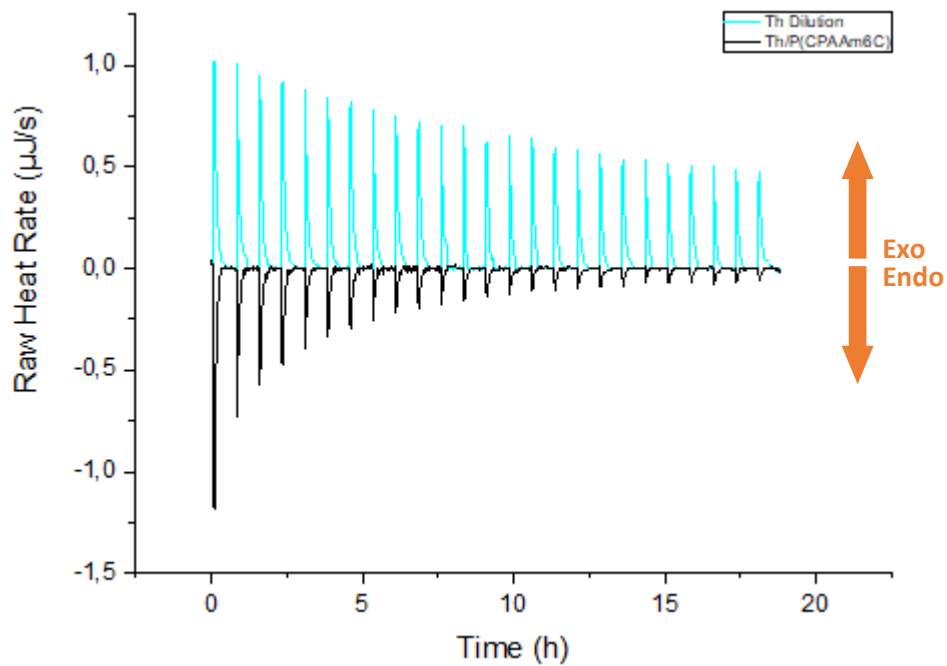


Figure 11. Processed thermal profiles for the Th(IV) ITC experiment of the P(CPAAm6C) polymer aqueous solution of 31 mmol L^{-1} (sorption experiment) and acidified Milli-Q water (dilution experiment) titrated by $\text{Th}(\text{NO}_3)_4 \cdot \text{H}_2\text{O}$ aqueous solution of 63 mmol L^{-1} . Experiments carried out at 298 K and $\text{pH}=1$, with 25 successive injections recorded with $10 \text{ }\mu\text{L}$ for each injection of Th(IV) stock solution into $800 \text{ }\mu\text{L}$ of P(CPAAm6C) solution or acidified Milli-Q water.

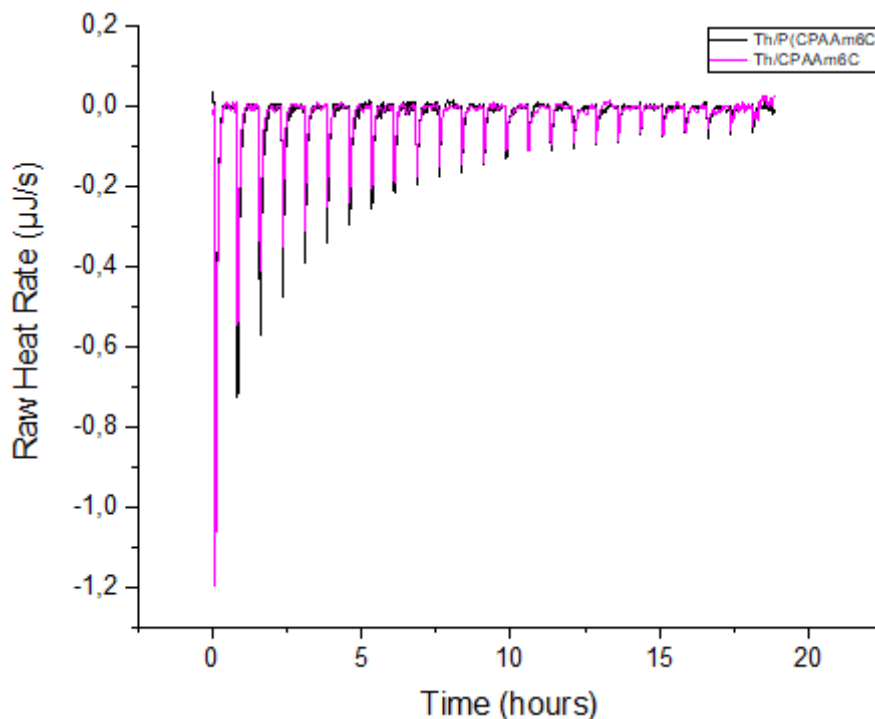


Figure 12. Comparison of the processed thermal profiles for the Th(IV) ITC sorption experiments of the CPAAm6C monomer or the P(CPAAm6C) polymer aqueous solution of 31 mmol L^{-1} and titrated by $\text{Th}(\text{NO}_3)_4 \cdot \text{H}_2\text{O}$ of 63 mmol L^{-1} . Experiments carried out at 298 K and $\text{pH}=1$, with 25 successive injections recorded with $10 \text{ }\mu\text{L}$ for each injection of Th(IV) stock solution into $800 \text{ }\mu\text{L}$ of monomer or polymer solution.

Quantitative parameters have been extracted from the ITC heat data. The signal of the heat ($\text{kJ}\cdot\text{mol}^{-1}$) as a function of the mole ratio could be fitted. The Nanoanalyze software supplied by TA Waters was used to extract statistics results of binding constants, enthalpy and stoichiometry. The independent model, based on the interaction of n ligands with a macromolecule that has one binding site, has been used to fit the data and extract thermodynamic parameter. In the present study, all the curves did not exhibit the well-known standard sigmoid shape and this made the fitting and the complete calculation complex, and made the interpretation difficult. The enthalpy and the stoichiometry will not be discussed. Only the binding constant will be carefully described and correlated with the quantification of sorption using dialysis membrane. The fitted ITC heat data for P(CPAAm6C) and CPAAm6C are shown in Figure 13 and in Supporting information (see Supporting information, Figure SI 9), respectively. The obtained parameters (mainly binding constant (K_a)) of each complexation interaction calculated by fitting corresponding ITC heat data of the sorption experiments of mhP(CPAAm6C), P(CPAAm6C), and CPAAm6C with Gd(III) and Th(IV) are summarized in Table 4.

Test	Cations	Sorbents	K_a (M^{-1})
1	Gd	P(CPAAm6C)	$2.2\cdot 10^1$
2		mhP(CPAAm6C)	$5.0\cdot 10^4$
3	Th	CPAAm6C	$5.3\cdot 10^2$
4		P(CPAAm6C)	$4.0\cdot 10^2$
5		mhP(CPAAm6C)	$1.2\cdot 10^4$
	$4.8\cdot 10^4$		

Table 4. Binding constant (K_a) at 298 K and pH=1 of interactions of CPAAm6C monomer, P(CPAAm6C) and mhP(CPAAm6C) polymers with Gd(III) and Th(IV), results calculated with independent model in Nanoanalyze for test 1-4; successive binding sites model with the Levenberg–Marquardt non-linear curve-fitting algorithm for the test 5.

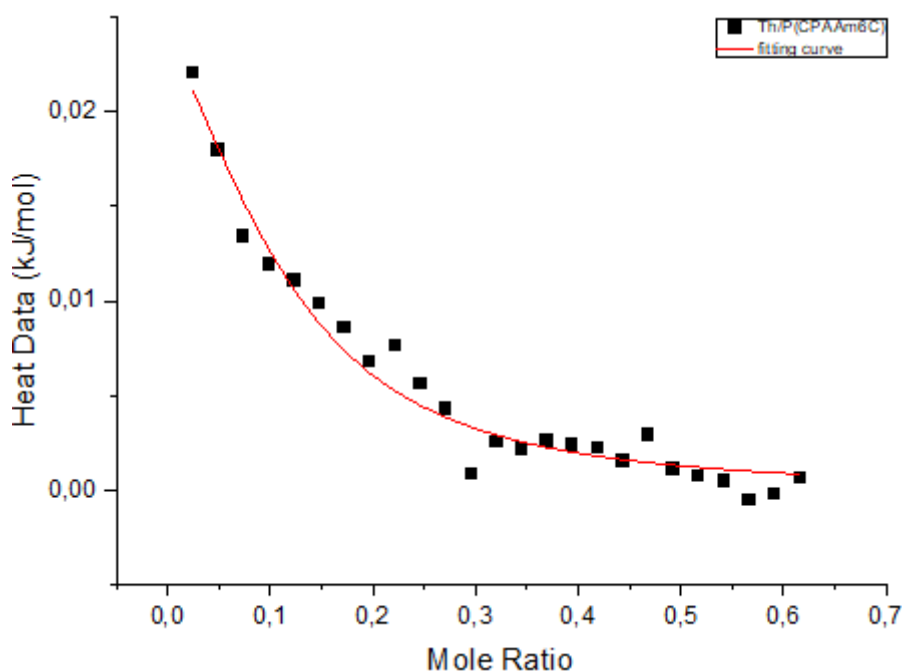


Figure 13. Heat data corresponding to the Th(IV) ITC experiment (298 K and pH=1) of the P(CPAAm6C) polymer ($31 \text{ mmol}\cdot\text{L}^{-1}$) aqueous solution titrated by $\text{Th}(\text{NO}_3)_4\cdot\text{H}_2\text{O}$ ($63 \text{ mmol}\cdot\text{L}^{-1}$) stock solution, together with the fitting curve obtained with 'independent model' in Nanoanalyze software.

In addition to the correspondence between thermograms, the K_a value of complexation of Th(IV) with the CPAAm6C monomer and that with the P(CPAAm6C) homopolymer were very similar, with $5.2\cdot 10^2$ and $4.0\cdot 10^2$, respectively. This showed that polymer chains did not influence the complexing property of the ligands. For the stoichiometry (n), the shape of the experimental data for CPAAm6C (Figure 10) did not provide acceptable calculation, and the n value was too weak to be determined correctly.

Similar approach was followed for the P(CPAAm6C) polymer in interaction with Gd(III). The thermogram of the sorption and the dilution experiments are shown in Figure SI 10. The fitted ITC heat data (Figure 14) gave access to the binding constant in the applied conditions summarized in Table 4.

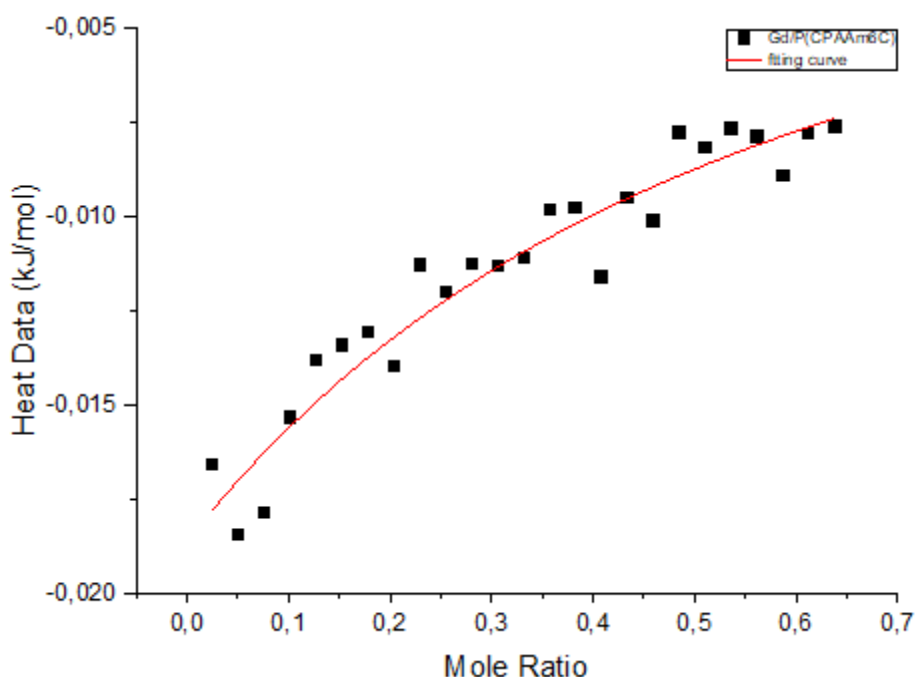


Figure 14. Heat data corresponding to the Gd(III) ITC experiment (298 K and pH=1) of the P(CPAAm6C) polymer ($31 \text{ mmol}\cdot\text{L}^{-1}$) aqueous solution titrated by $\text{Gd}(\text{NO}_3)_3\cdot 6\text{H}_2\text{O}$ ($63 \text{ mmol}\cdot\text{L}^{-1}$) stock solution, together with the fitting curve obtained with 'independent model' in Nanoanalyze software.

For P(CPAAm6C), its binding constant (K_a) for Th(IV) was higher than that for Gd(III) (Table 4), which indicated its better affinity for Th(IV). In terms of stoichiometry between the cation and the ligand, the determination had to be considered cautiously. Indeed, this value was determined from the inflexion of the curve representing the heat flow as a function of molar ratio. In both cases, this change of slope was not clearly identified. The stoichiometry was estimated between 5 and 10 ligands for 1 cation. Nevertheless, no clear interpretation about the number of ligands per cation could be done. In addition, it is important to consider that Th(IV) was mainly in the ThNO_3^{3+} form compared to Gd(III), which was mainly present in Gd^{3+} moiety.

In order to corroborate the affinity tendency, sorption experiments based on a dialysis procedure were carried out with different concentration ratios between metal ions and P(CPAAm6C) at pH 1. The results are shown in Table 5 and describe the percentage of Gd(III) or Th(IV) complexed by P(CPAAm6C) for different concentration ratios depending on the quantity of ligand. The concentration ratio was $[C_{\text{total}}]/[P]$, expressed taking into account the ratio between the initial concentration of all cations related to the total amount of CPAAm6C.

For the ratio $[C_{\text{total}}]/[P]=0.1$, the percentage of Gd(III) complexed was 25% and Th(IV) complexed was 75%. When the ions concentration was increased to $[C_{\text{total}}]/[P]=0.4$, the proportion of Gd(III) complexed by the polymer was only 13%, and that of Th(IV) was 87%. In both cases, P(CPAAm6C) showed a preferential sorption for Th(IV). In addition, the sorption of Th(IV) increased with increasing concentration. To conclude, both ITC and dialysis sorption experiments demonstrated the selectivity of P(CPAAm6C) for Th(IV) in the mixture of Gd(III) and Th(IV).

$[C_{\text{total}}]/[P]$	$[\text{Gd}_{\text{absorbed}}]/[\text{C}_{\text{absorbed}}]$	$[\text{Th}_{\text{absorbed}}]/[\text{C}_{\text{absorbed}}]$
0.1	25%	75%
0.4	13%	87%

Table 5. Dialysis sorption of poly(diethyl-6-(acrylamido)hexylcarbamoylmethyl phosphonate) (P(CPAAm6C)) aqueous solution ($14.35 \text{ mmol}\cdot\text{L}^{-1}$) carried out at pH=1 in the mixture aqueous solutions of $\text{Gd}(\text{NO}_3)_3\cdot 6\text{H}_2\text{O}$ (89.6%) and $\text{Th}(\text{NO}_3)_4\cdot \text{H}_2\text{O}$ (10.4%) of $1.43 \text{ mmol}\cdot\text{L}^{-1}$ (0.1 eq) or $5.72 \text{ mmol}\cdot\text{L}^{-1}$ (0.4 eq) after 24 hours.

In the second part of the work, the impact of the mono-hydrolysis has been studied. The mhP(CPAAm6C) polymer has been used in ITC and sorption experiments by dialysis, for Gd(III) and Th(IV). Figure 15 illustrates the raw ITC thermograms of the sorption experiments of mhP(CPAAm6C) with Gd(III) and Th(IV). As done for P(CPAAm6C), the results of calorimetric titration were carried out at 298 K and pH=1 for Gd(III) (Figure 15(a)) or Th(IV) (Figure 15(b)) stock aqueous solutions injected into acidified Milli-Q water (dilution experiments) and into mhP(CPAAm6C) aqueous solution (sorption experiments).

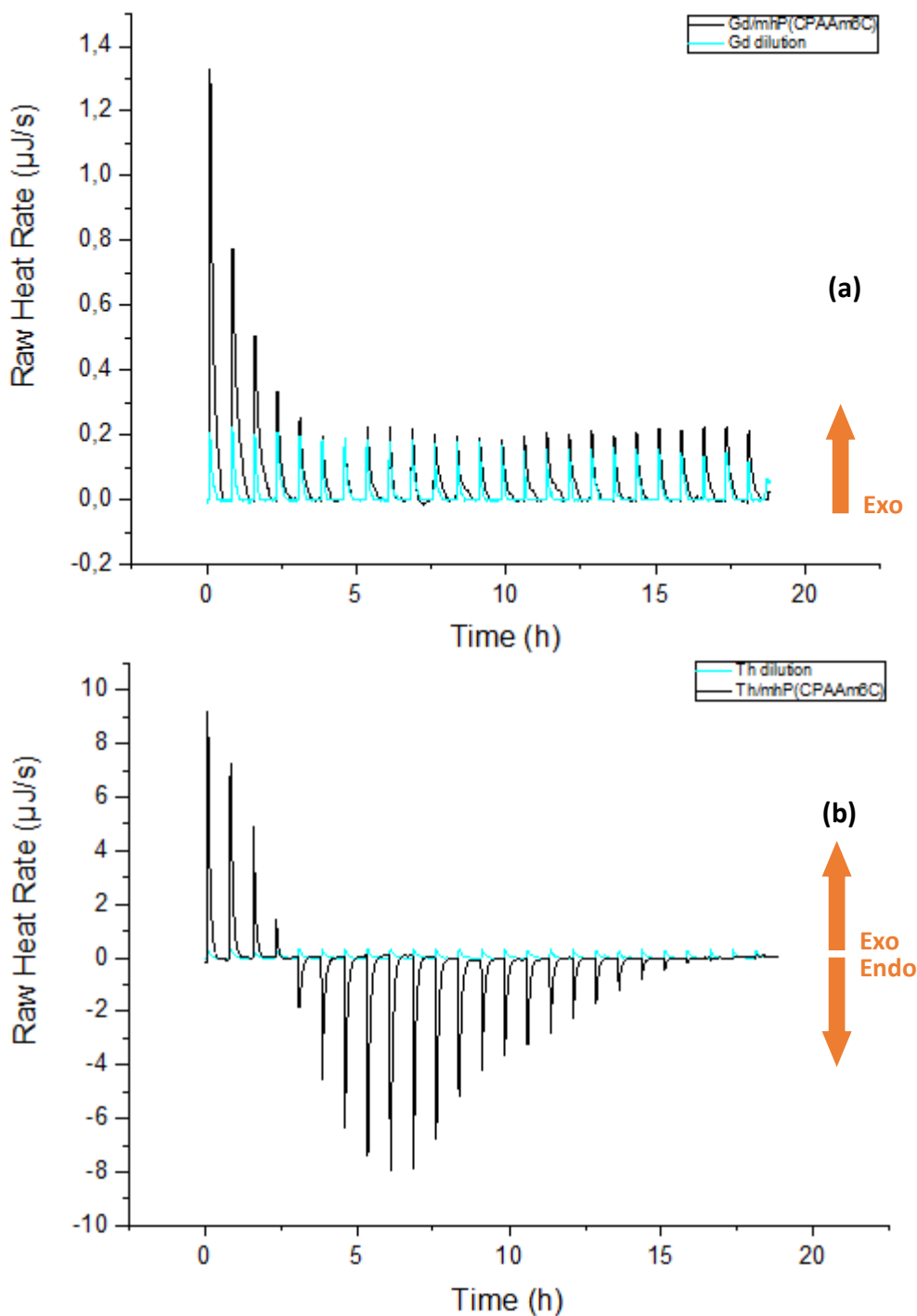
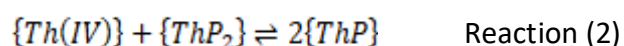
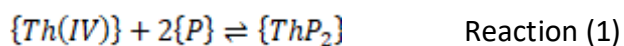


Figure 15. Processed thermal profiles for the Gd(III) or Th(IV) ITC experiment of the mhP(CPAAm6C) polymer aqueous solution of $14.3 \text{ mmol}\cdot\text{L}^{-1}$ (sorption experiment) and acidified Milli-Q water (dilution experiment) titrated by (a) $\text{Gd}(\text{NO}_3)_3\cdot 6\text{H}_2\text{O}$ stock solution of $63 \text{ mmol}\cdot\text{L}^{-1}$ and (b) $\text{Th}(\text{NO}_3)_4\cdot\text{H}_2\text{O}$ of $17 \text{ mmol}\cdot\text{L}^{-1}$. Experiments carried out at 298 K and $\text{pH}=1$, with 25 successive injections recorded with $10 \mu\text{L}$ for each injection of Gd(III) or Th(IV) stock solution into $800 \mu\text{L}$ of mhP(CPAAm6C) polymer solution or acidified Milli-Q water.

On the one hand, as shown in Figure 15(a), the dilution of Gd(III) showed exothermic signals of an intensity about $0.2 \mu\text{J}\cdot\text{s}^{-1}$ for each injection without variation; the sorption experiment between Gd(III) and mhP(CPAAm6C) showed exothermic signals with a decreasing tendency for the first injections. Then only dilution effect of Gd(III) remained till the end. On the other hand, the sorption experiment of mhP(CPAAm6C) for Th(IV) (Figure 15(b)) showed two tendencies. Firstly, it showed exothermic character with decreasing tendency, and then the global heat effect turned to endothermic with increasing intensity down to the 9th injection. Then, the endothermic signals decreased (in absolute value), until no variation of the intensity for the last peaks. The succession of the two tendencies in the signals indicated that two reactions contributed to the interaction mechanism [193]. Indeed, this has already been observed in previous studies for low cost sorbent dealing with the ability of the chitin biopolymer to bind metal ions as Al(III), Cr(III), and Pb(II) [180], as well as for potential separation reagents such as diamide derivatives of bipyridinedicarboxylate and phenanthrolinedicarboxylate for the removal of Nd(III) and Eu(III) [194], or for efficient reprocessing of high level nuclear wastes with phosphorylated calixarenes for the recognition elements such as Eu(III), Am(III), UO₂(II), Th(IV) [195]. In our case, the reactions involved Th(IV) and mhP(CPAAm6C).

Based on the binding studies of phosphonic acid or amine containing molecules [196, 197], the binding constants (K_a) and the stoichiometry (n) of the complexation between Th(IV) and the mhP(CPAAm6C) mono-hydrolyzed polymer was estimated by fitting experimental ITC data with a successive binding sites model using the Levenberg-Marquardt non-linear curve-fitting algorithm [196]. This model takes into account the formation of two successive complexes during the sorption between Th(IV) species and mhP(CPAAm6C).



To establish the relevant equation reactions, mhP(CPAAm6C) is indicated $\{P\}$, whereas for Th(IV) moieties, since the exact species involved in the mechanism were not identified, they are noted $\{\text{Th(IV)}\}$. At the beginning of titration, the reaction (1) was favourable since it corresponded to the situation where there was an excess of phosphonic group $\{P\}$ in the cell;

as Th(IV) moieties were added, the reaction (2) became dominant. The sorption experiment between Th(IV) and mhP(CPAAm6C) was the only case in the present which showed two tendencies in the experimental signals, the ITC data of the other sorption experiments were fitted with the independent model. The ITC heat data of mhP(CPAAm6C) for Gd(III) and Th(IV) together with the fitting curves are shown in Figure 16 and Figure 17. The binding constants (K_a) are summarized in Table 4.

As mentioned above for mhP(CPAAm6C), there were two successive reactions in its complexation with Th(IV). The two K_a values obtained with successive binding sites model corresponded respectively to the binding constant of the formation of $\{ThP_2\}$, with $K_a \approx 1.2 \cdot 10^4 \text{ M}^{-1}$ and the formation of $\{ThP\}$, $K_a \approx 4.8 \cdot 10^4 \text{ M}^{-1}$. The first constant for Th(IV) was smaller compared to the K_a of mhP(CPAAm6C) for Gd(III) of $5.0 \cdot 10^4 \text{ M}^{-1}$. In addition, this K_a ($5.0 \cdot 10^4$) value of Gd(III) binding to the phosphonic mono-acid moieties in mhP(CPAAm6C) was compared to the one reported by Pailloux *et al* [198], who estimated the binding between Gd(III) and a [(hydroxyphenylcarbonyl) methyl]phosphonic acid with $\log K_{(MLH)} = 6.2$. Our lower constant could be explained by several reasons, such as the monohydrolyzed form, the acrylamide group, or the polymeric structure. Nevertheless, even with only phosphonic mono-acid in the mhP(CPAAm6C), it showed also good affinity for Gd(III).

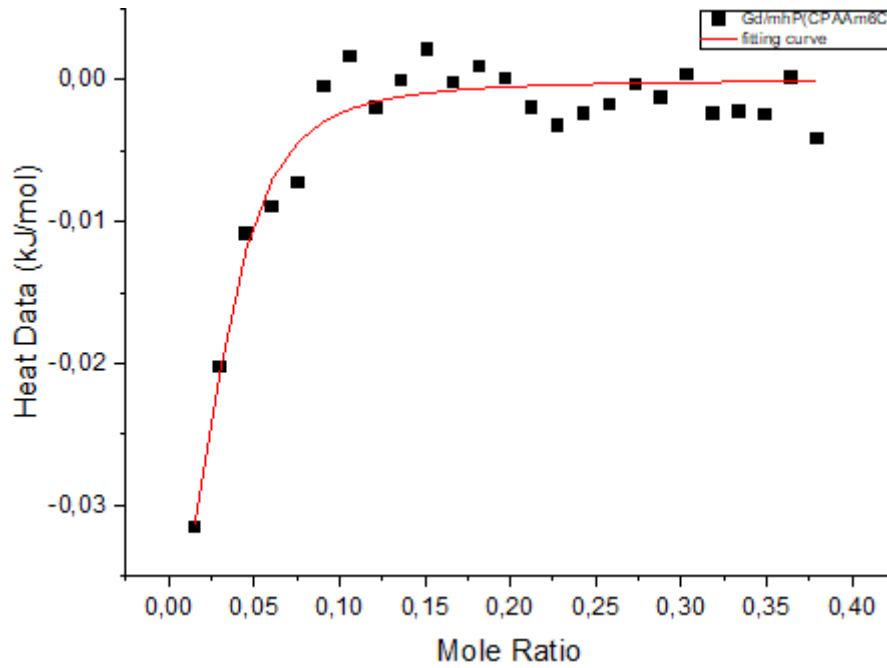


Figure 16. Heat data corresponding to the Gd(III) ITC experiment (298 K and pH=1) of the mhP(CPAAm6C) polymer ($14.3 \text{ mmol}\cdot\text{L}^{-1}$) aqueous solution titrated by $\text{Gd}(\text{NO}_3)_3\cdot 6\text{H}_2\text{O}$ ($17 \text{ mmol}\cdot\text{L}^{-1}$) stock solution, together with the fitting curve obtained with 'independent model' in Nanoanalyze software.

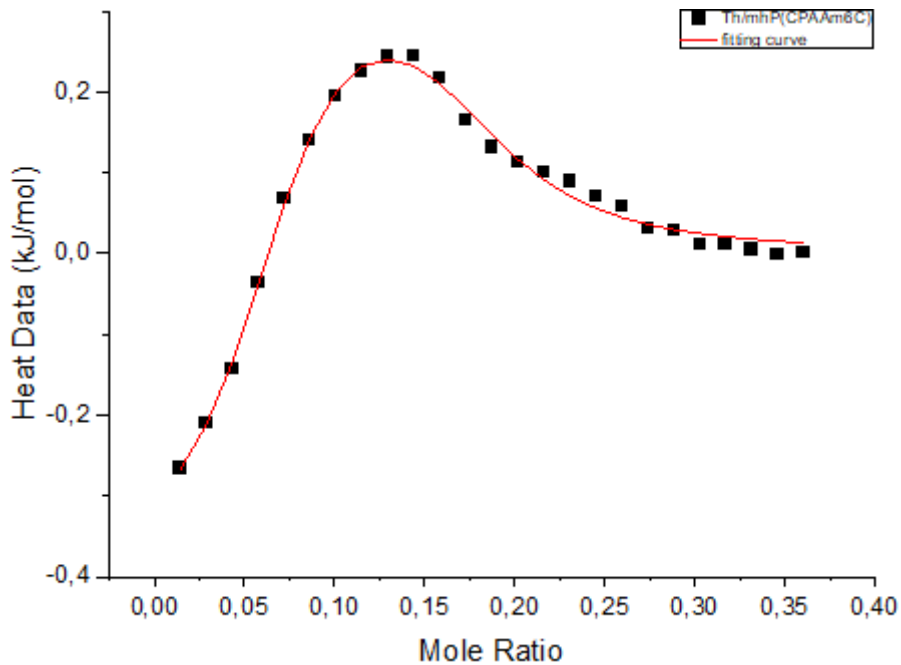


Figure 17. Heat data corresponding to the Th(IV) ITC experiment (298 K and pH=1) of the mhP(CPAAm6C) polymer ($14.3 \text{ mmol}\cdot\text{L}^{-1}$) aqueous solution titrated by $\text{Th}(\text{NO}_3)_4\cdot\text{H}_2\text{O}$ ($17 \text{ mmol}\cdot\text{L}^{-1}$) stock solution, together with the fitting curve obtained with 'successive binding sites model' using the Levenberg–Marquardt non-linear curve-fitting algorithm in Microsoft Excel.

Another group of dialysis sorption experiments under condition of pH=1 of mhP(CPAAm6C) with Gd(III) and Th(IV) mixture solutions was carried out to verify the selectivity of mhP(CPAAm6C). The results are displayed in Table 6. It showed the proportions of Gd(III) and Th(IV) complexed at different concentration ratios, expressed as the ratio between the amount of all ions and the quantity of ligand in mhP(CPAAm6C) polymer. At the concentration ratio equal to 0.1, complexed Gd(III) represented 81% and complexed Th(IV) was 19%. When the concentration ratio was increased to 1, complexed Gd(III) was slightly higher (89%) whereas Th(IV) complexed decreased to 11%. In both cases, mhP(CPAAm6C) showed selectivity for Gd(III), with higher sorption of Gd(III) for increasing concentration ratio. The selectivity of mhP(CPAAm6C) for Gd(III) in the mixture aqueous solutions of Gd(III) and Th(IV) was evidenced. This was confirmed by both the binding constant and the proportions of cations complexed. The binding constant of mhP(CPAAm6C) for Gd(III) was 4 times higher than that of the 1st reaction for Th(IV), and of the same range order for the 2nd reaction. The first reaction corresponded to the case where the polymer was in excess compared to the cation, which was the case for the $[C_{total}]/[mhP]=0.1$. Furthermore, in the equimolar system, the final repartition between $Gd_{absorbed}$ and $Th_{absorbed}$ was close to the concentration ratio in the initial solution. In such a case, both ions were equally complexed, which was in line with the value of constant in a first approximation, in particular for the 2nd reaction of Th(IV), when the cations were highly concentrated.

$[C_{total}]/[mhP]$	$[Gd_{absorbed}]/[C_{absorbed}]$	$[Th_{absorbed}]/[C_{absorbed}]$
0.1	81%	19%
1	89%	11%

Table 6. Dialysis sorption of poly(6-(acrylamido)hexylcarbamoylmethyl phosphonic mono-acid) (mhP(CPAAm6C)) aqueous solution ($14.35 \text{ mmol}\cdot\text{L}^{-1}$) carried out at pH=1 in the mixture aqueous solutions of $Gd(NO_3)_3\cdot 6H_2O$ (89.6%) and $Th(NO_3)_4\cdot H_2O$ (10.4%) of $1.43 \text{ mmol}\cdot\text{L}^{-1}$ (0.1 eq) or $14.3 \text{ mmol}\cdot\text{L}^{-1}$ (1 eq) after 24 hours.

Both ITC and dialysis sorption experiments have shown the ability of P(CPAAm6C) and mhP(CPAAm6C) to complex Gd(III) and Th(IV). In particular, P(CPAAm6C) was selective for Th(IV) and mhP(CPAAm6C) was selective for Gd(III). Indeed, the

carbamoylmethylphosphonate moieties in the P(CPAAm6C) and mhP(CPAAm6C) (Scheme 5) are known for their properties to sorb the Ln(III) and An, particularly for the extraction of transuranium elements in the TRUEX process for example [199-201]. The metal cation interacts with the phosphoryl oxygen while the carbonyl oxygen acts as an external buffer by binding a proton [202, 203]. The intramolecular buffering effect could explain the property of the carbamoylmethylphosphonate moieties in complexing the Ln(III) and the An. Concerning the ion-ligand affinities, hard-soft acid-base theory has to be considered as important factor. Lanthanide and actinide cations are hard Lewis acids thus tend to bind with hard Lewis bases. The lanthanide cations tend to form ionic bond, whereas the actinide ones could form covalent bond [204]. This difference in interaction bonds makes the actinides more easily extracted by softer donor atoms compared to lanthanides [189]. In this context, many studies have focused on using soft donor ligands to extract the An [205, 206]. For instance, Mazzanti *et al* has reported that tris[(2-pyrazinyl)methyl]amine (a neutral N-donor ligand) formed shorter covalent bond with U(III) compared to with La(III) [205]. Herein, the phosphonated ester group in P(CPAAm6C), having a softer character than the phosphonic mono-acid in mhP(CPAAm6C), showed selectivity for Th(IV) whereas mhP(CPAAm6C) showed selectivity for Gd(III).

4. Conclusion

In a previous work, starting from phosphonate-based acrylamide monomer, the poly(diethyl-6-(acrylamido)hexylcarbamoylmethyl phosphonate) (P(CPAAm6C)) polymer had been developed. Owing to both acrylamide and phosphonate groups, this homopolymer was the first example in the literature showing a combination of thermosensitivity and complexation properties. In addition to a cloud point, it notably showed selectivity for Th(IV) over Gd(III). In the present study, the mono-hydrolyzed derivative of P(CPAAm6C), named mhP(CPAAm6C), was synthesized, and its complexing property with Gd(III) and Th(IV) was investigated and compared with that of P(CPAAm6C) homopolymer. In addition to the evaluation of sorption using dialysis membrane and ICP-MS as analytical tool, Isothermal Titration Calorimetry (ITC) technique was selected. The binding constants of the CPAAm6C monomer and the P(CPAAm6C) polymer were similar, meaning that the polymer form of the

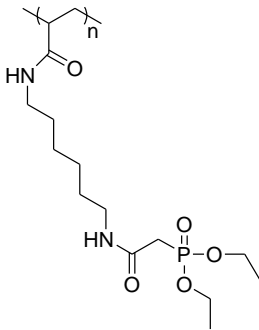
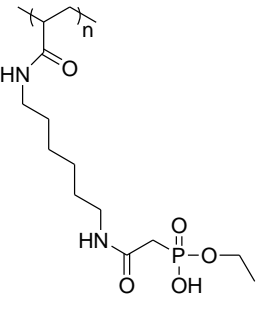
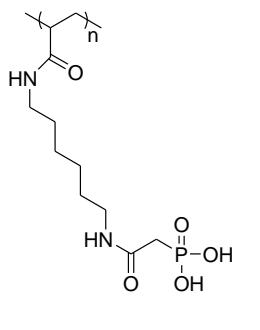
ligand did not modify the sorption, the polymer being more easily handled in a sorption process.

The selectivity of the diethyl phosphonate group in P(CPAAm6C) for Th(IV) over Gd(III), observed previously using dialysis sorption experiments coupled with ICP-MS dosage technique, was confirmed using direct measurement of the binding constant, the constant of Th(IV) being higher than Gd(III) one. On the other hand, for both types of measurements (ITC and sorption in dialysis membrane), the mhP(CPAAm6C), polymer which contained mono-phosphonic acid group, was slightly more in favor for Gd(III) in the mixture of Gd(III) and Th(IV). The selectivity of its mono-hydrolyzed mhP(CPAAm6C) polymer for Gd(III) in the mixture of Gd/Th aqueous solution was also demonstrated. These results on polymeric sorbents open the way to innovative materials for the treatment of contaminated effluents.

Conclusion

In this chapter, we reported the synthesis and study of a mono-phosphonic acid-based polymer (mhP(CPAAm6C)), prepared from poly(diethyl-6-(acrylamido)hexylcarbamoylmethyl phosphonate) (P(CPAAm6C)). Whereas P(CPAAm6C) proved to be thermosensitive with a cloud point measured at 43 °C in Milli-Q water, mhP(CPAAm6C) proved to be fully soluble in water whatever the temperature. Both polymers were investigated for the sorption of gadolinium(III) and thorium(IV). For such purpose, we decided to perform a combination of analytical and thermodynamic approaches using Inductively Coupled Plasma Mass Spectroscopy (ICP-MS), and Isothermal Titration Calorimetry (ITC), respectively. These methods allowed determining that P(CPAAm6C) was selective for Th(IV) whereas mhP(CPAAm6C) was selective for Gd(III). It is important to notice that the fully hydrolyzed polymer (hP(CPAAm6C)) was already studied by ICP-MS and proved to selectively flocculate with U(VI). This allowed us to conclude that selectivity strongly depended on the nature of the phosphorous-based complexing group. We also demonstrated that ITC was a valuable tool to study sorption of cations on polymers allowing confirming sorption selectivity results. Finally, last valuable results obtained concerning mhP(CPAAm6C) is that the latter flocculated when complexing metal cation, in particular when aqueous solutions contained U(VI). This would make the separation step easier to achieve by filtration.

From all results obtained, when an 86/10/4% in moles of Gd/Th/U mixture aqueous solution (pH=1) was used, corresponding to the concentrations obtained by dissolution of monazite mineral, we concluded on selectivity:

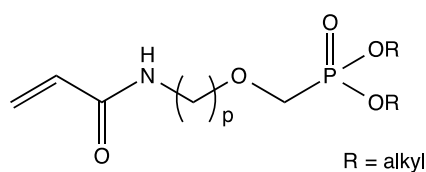
Polymeric chemical structure	 P(CPAAm6C)	 mhP(CPAAm6C)	 hP(CPAAm6C)
Selectivity for	Thorium	Gadolinium	Uranium
Character	Thermosensitive	Flocculating	Flocculating

**Chapter 3: Oxymethylphosphonated-based monomers and
polymers for the complexation of Cerium and Neodymium:
evaluation by Isothermal Titration Calorimetry (ITC)**

Introduction

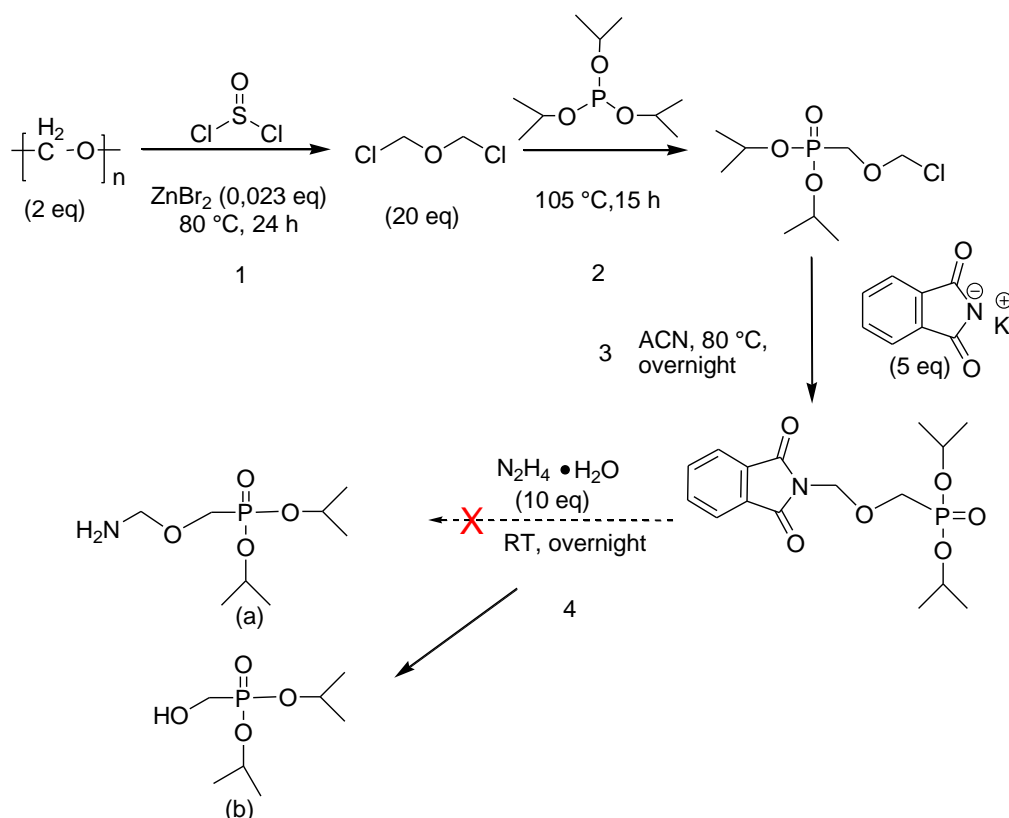
As mentioned in the chapter 2, a thermosensitive phosphonated homopolymer, poly(diethyl-6-(acrylamido)hexylcarbamoylmethyl phosphonate) (P(CPAAm6C)), showed selectivity in complexing thorium (Th(IV)) over gadolinium (Gd(III)) and uranium (U(VI)) in the mixture of the three cations aqueous solutions at acidic pH [149]. On the reverse, fully hydrolyzed polymer derived from P(CPAAm6C), namely hP(CPAAm6C), has proved to be selective for U(VI) under the same condition. As a result, we can conclude that both polymers are able to remove contaminants from effluents (results obtained by Dr Gomes Rodrigues). We have developed mono-hydrolyzed mhP(CPAAm6C) derivative, which proved to be selective for Gd(III), meaning that it could be potentially used to complex the lanthanides. Unfortunately, it was not thermosensitive but showed flocculating behavior (maybe induced by some uranium complexation) once complexed Gd(III).

In the present chapter, we report the work carried out to develop thermosensitive polymers able to selectively complex the REEs. For such purpose, we first designed the chemical structure of a new monomer (Scheme 6) that could be employed to prepare potentially thermosensitive polymers able to complex the REEs selectively. This monomer structure contained an oxymethyl phosphonate group and an acrylamide group, to bring complexing property for REEs and to favor thermosensitivity, respectively. Free radical polymerization of the monomer will be used to limit polymerization costs.



Scheme 6. Targeted chemical structure of a new monomer leading, in the ideal case, to thermosensitive and chelating polymers (in particular, $p=1$)

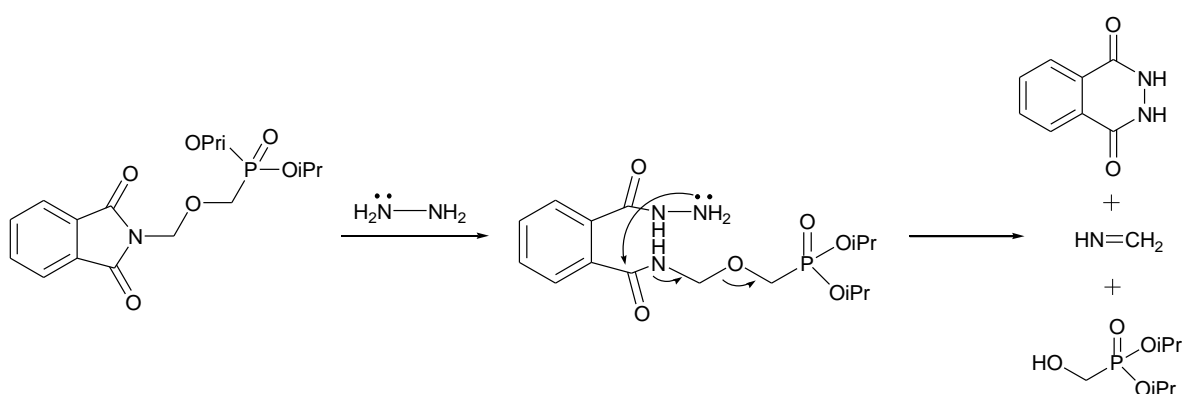
Unfortunately, the synthesis of the targeted acrylamide bearing oxymethylphosphonated group was difficult to perform. We tested different procedures, which were unsuccessful. For instance, the following synthesis pathway was designed to obtain the acrylamide phosphonate monomer (Scheme 7).



Scheme 7. Designed reactional pathway for the synthesis of the targeted (aminomethoxy)methyl phosphonate that could lead to acrylamide phosphonate monomer by acryloylation

The two first steps were carried out as already described in the literature by Pav [207] and Fild [208], respectively. In the first step, paraformaldehyde and thionyl chloride were mixed in the presence of zinc bromide. The reaction lasted one day at 80 °C. Bis(chloromethyl)ether (BCME) was obtained after cryo-distillation at room temperature with a 77% yield. Characterization was achieved by ^1H NMR (see Appendix, Figure Appendix 1). Then, BCME was heated under reflux in the presence of triisopropyl phosphite during 15 hours, allowing the synthesis of diisopropyl(chloromethoxy)methyl phosphonate (DiCMP) with a 60% yield. Product was successfully characterized by ^1H and ^{31}P NMR (see Appendix, Figure Appendix 2 and Figure Appendix 3, respectively). Mass spectroscopy (electrospray ionization in positive mode) also showed a peak at $m/z=245$, corresponding to the molecular weight of the DiCMP (see Appendix, Figure Appendix 4). In the third step, Gabriel reaction was achieved in anhydrous acetonitrile under nitrogen atmosphere overnight at 80 °C, in the presence of potassium phthalimide and hydrazine to obtain diisopropyl [(1,3-dioxisoindol-

2-yl)methoxy] methyl phosphonate (DiOMP). The latter was obtained with a yield equal to 80% and characterized by ^1H and ^{31}P NMR (see Appendix, Figure Appendix 5 and Figure Appendix 6, respectively) and by mass spectroscopy (see Appendix, Figure Appendix 7), demonstrating the obtaining of the targeted DiOMP. ^1H NMR spectrum notably showed the presence of aromatic protons at 7.3-7.5 ppm. Unfortunately, in the second step of the Gabriel Reaction using hydrazine or potassium hydroxide, a rearrangement led to the obtaining of the diisopropyl hydroxymethyl phosphonate (DihMP) instead of the diisopropyl(aminomethoxy)methyl phosphonate (Scheme 8).



Scheme 8. Rearrangement occurring during the second step of the Gabriel reaction

The rearrangement was due to the electro-attracting effect of the phosphonated moiety. This reaction was confirmed by ^1H NMR (Figure 18), which only showed the presence of the methylene in α of the hydroxyl group at 3.85 ppm. Isopropoxy groups borne by the phosphorus atom was also found around 4.75 and 1.3 ppm for the methine and methyl groups, respectively. Mass spectroscopy (electrospray ionization in positive mode) (Figure 19) also allowed to prove that diisopropyl hydroxymethyl phosphonate was obtained with a peak at $m/z=197$, corresponding to the molecular weight of the DihMP.

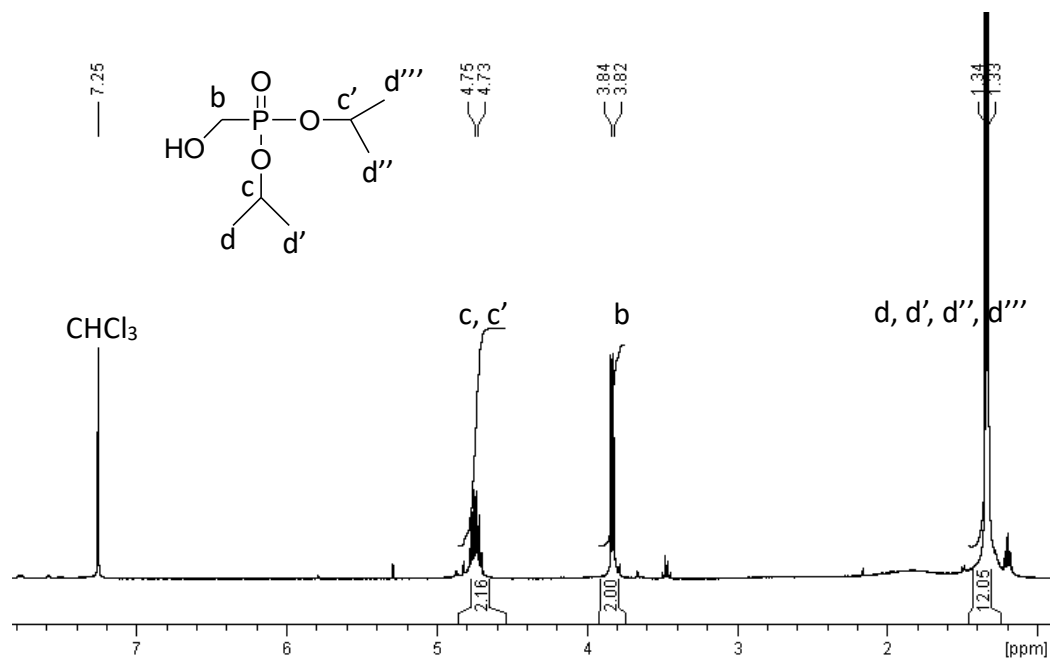


Figure 18. ^1H NMR spectrum (400 MHz, CDCl_3) of diisopropyl hydroxymethyl phosphonate (DihMP) obtained after the second step of the Gabriel reaction

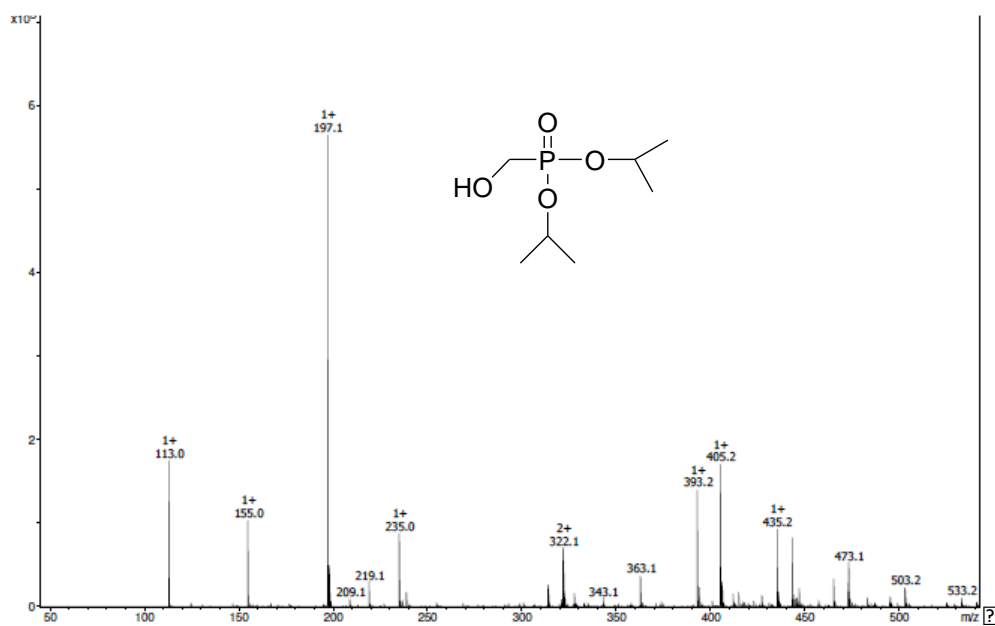
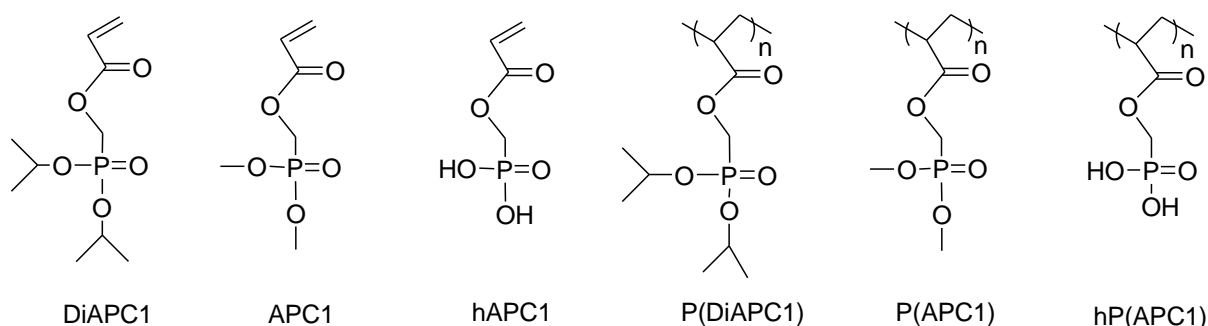


Figure 19. Mass spectrum in positive mode of diisopropyl hydroxymethyl phosphonate (DihMP) by micrOTOF-Q instrument, ion source: ESI, intensity $\times 10^5$; product at $m/z=197.1$.

As a consequence, we worked with other oxymethylphosphonated derivatives, in particular with phosphonated ester acrylate monomers, namely diisopropyl(acryloyloxymethyl) phosphonate (DiAPC1) and dimethyl(acryloyloxymethyl)

phosphonate (APC1) (Scheme 9). These monomers were polymerized by free radical polymerization to lead to P(DiAPC1) and P(APC1), respectively (Scheme 9). Additionally, both DiAPC1 and APC1 were hydrolyzed, thus leading to the same hAPC1 monomer (Scheme 9). Finally, P(DiAPC1) and P(APC1) polymers were also hydrolyzed leading to the same hP(APC1) polymer (Scheme 9). Complexing properties of P(APC1) and hP(APC1) for cerium (Ce) and neodymium (Nd) (the two most abundant REEs in the earth) were evaluated to compare the influence of the alkyloxy and hydroxy groups borne by the phosphorous atom on the complexing property for the REEs. DiAPC1, APC1 and hAPC1 monomers were also evaluated for Ce and Nd to compare monomeric and polymeric chemical structures. It is important to notice that P(DiAPC1) was not studied because of its non-water-soluble character. The Isothermal Titration Calorimetry (ITC) technique was then used to characterize the complexation interactions. It permitted to rapidly and indirectly evaluate the sorption efficiency, and above all to compare the complexing property of the monomers and polymers even for relatively weak interactions. All the experimental results obtained are reported in the following article.



Scheme 9. Chemical structures of diisopropyl(acryloyloxymethyl) phosphonate (DiAPC1), dimethyl(acryloyloxymethyl) phosphonate (APC1) monomers, and the hydrolyzed hAPC1 derivative; corresponding P(DiAPC1) (non-water-soluble) and P(APC1) polymers, together with their hydrolyzed hP(APC1) derivative

Evaluation of Oxymethylphosphonated-based Monomers and Polymers by Isothermal Titration Calorimetry (ITC) for the Complexation of Cerium and Neodymium

Abstract: Monomers and polymers bearing different phosphorous-based complexing moieties were prepared and studied for the complexation of lanthanides(III). Diisopropyl(acryloyloxymethyl) phosphonate (DiAPC1), dimethyl(acryloyloxymethyl) phosphonate (APC1) and acryloyloxymethyl phosphonic acid (hAPC1) were first prepared. Then, DiAPC1 and APC1 were polymerized by free radical polymerization to lead to corresponding P(DiAPC1) and P(APC1), respectively. These polymers were further hydrolyzed to afford water-soluble hP(APC1) phosphonic acid-based polymer. The complexing properties of monomers and polymers for cerium (Ce) and neodymium (Nd) were studied by Isothermal Titration Calorimetry (ITC). The influence of phosphonated group chemical structure on complexing properties was determined comparing different monomers and polymers when the latter were water-soluble. Only the hydrolyzed hP(APC1) polymer showed good complexing properties towards both Ce(III) and Nd(III), demonstrating both the interest of phosphonic acid derivatives and of the polymeric structure in comparison with the monomeric ones.

Keywords: phosphonated-based monomers, phosphonated-based polymers, cerium, neodymium, Isothermal Titration Calorimetry

1. Introduction

Nowadays, the lanthanides (Ln), which are the majority of the rare-earth elements (REEs), play a crucial role in many top-technologies [38, 39, 209, 210]. For instance, their applications vary from super-conductors [36], Magnetic Resonance Imaging (MRI) contrast agents [34], to fuel cells and fuel additives in nuclear field [43]. However, only a few countries possess abundant REEs resources and are able to produce high quantities of pure REEs [1]. As a result, separation and recovery of the lanthanides from mineral or industrial effluents is an important subject for both environment protection and economic benefit.

The lanthanides are indeed broadly distributed in the Earth's crust, but in relatively small concentrations (10-300 ppm) and always in mixture with other species. Cerium (Ce) is the most abundant lanthanide element in the Earth's crust, with abundance of 60-68 ppm. For neodymium (Nd) and gadolinium (Gd), abundance is about 30-35 ppm and 5-10 ppm, respectively [35, 51]. Because of the small concentrations and the presence of other contaminants, separating and refining the lanthanides individually is still a challenge. Nowadays, the methods for separating the lanthanides mainly include solvent extraction, heterogeneous systems based on non-water-soluble polymers (known as Solid Phase Extraction (SPE) process) [76], and the use of water-soluble chelating polymers coupled with ultrafiltration (known as Polymer Enhanced Ultrafiltration (PEUF) process) [65]. Among these methods, the use of water-soluble polymeric sorbents appears as interesting for its absence of organic solvent, fast kinetics, good efficiency and capacity, together with a possible selectivity of some polymers in complexing some metal ions [66, 76, 80, 81]. Amongst the polymers functionalized with different binding groups, those with phosphonated ester or phosphonic acid groups have shown interesting complexing property for various metal ions [9, 96-101], including the lanthanides(III) [188, 189, 211]. Gomes Rodrigues *et al* [146] has succeeded synthesizing a phosphonate-based acrylamide monomer and the corresponding thermosensitive homopolymer, prepared by free radical polymerization. The monomer, namely the diethyl-6-(acrylamido)hexylcarbamoylmethyl phosphonate (CPAAM6C), contained a valuable carbamoylmethyl phosphonated moiety, which brought complexing property, and the acrylamide function induced P(CPAAM6C) thermosensitive behavior. The cloud point value was equal to about 42 °C in Milli-Q water and could be modulated by

adjusting the pH. P(CPAAm6C) proved to be selective for gadolinium (Gd(III)) in Gd/Ni mixture aqueous solution [147]. With the thermosensitivity of P(CPAAm6C), its complexes with Gd(III) could be precipitated by heating the aqueous solution over the cloud point. In a more recent work [149], P(CPAAm6C) and its hydrolyzed phosphonic acid-based hP(CPAAm6C) derivative, which was not thermosensitive anymore, were both tested in Gd/Th/U mixture aqueous solutions. P(CPAAm6C) showed selectivity for Th(IV) and hP(CPAAm6C) selectively flocculated with U(VI) at pH=1. Experimental results demonstrated that both P(CPAAm6C) and hP(CPAAm6C) were selective for the actinides over the lanthanides. In another example, Graillot *et al* [127] has developed P(NnPAAm-stat-hMAPC1) thermosensitive copolymers which bore complexing phosphonic acid groups. This copolymer showed selectivity for Al(III) over other divalent metal ions, Ni(II), Ca(II) and Cd(II). Many other studies involving phosphonic acid as binding group in polymers with different physical forms have also demonstrated the good complexing properties of the phosphonic groups [97, 102, 111, 112, 114].

In such context, in order to develop an efficient and refining REEs separation procedure, the objective of this contribution was to prepare and evaluate different water-soluble phosphonated monomers and polymers able to selectively and efficiently complex the Ln(III). Concerning phosphorous atom environment, we focused on oxymethyl phosphonate group (-OCH₂PO(OR)₂), not studied to our knowledge so far in polymeric structures, to complex the Ln(III). Herein, we wished to prepare three different monomer chemical structures: an acrylate bearing diisopropyl(oxymethyl) phosphonated group and an acrylate dimethyl(oxymethyl) phosphonated group. In addition, monomers were hydrolyzed to produce phosphonic acid groups. Diisopropyl and dimethyl phosphonate-based monomers were then polymerized to produce corresponding polymers, which were also hydrolyzed to afford identical hP(APC1) polymer. The complexing properties of the different monomers and polymers developed were studied by Isothermal Titration Calorimetry (ITC) with cerium (Ce) and neodymium (Nd) as lanthanides. The influence of the alkyloxy group (diisopropoxy or dimethoxy) borne by the phosphorous atom on the sorption properties was studied and compared to the phosphonic acid group in the monomers and the polymers.

2. Experimental section

2.1. Materials and methods

2.1.1. Materials

Zinc bromide (Sigma-Aldrich, 99.999%), paraformaldehyde (Sigma-Aldrich, 99% reagent degree), thionyl chloride (Sigma-Aldrich, 99%), calcium chloride (Sigma-Aldrich), triisopropyl phosphite (Sigma-Aldrich, 98%), potassium phthalimide (Sigma-Aldrich, $\geq 99\%$), diisopropyl phosphite (TLC, 98%), hydrazine hydrate (Sigma-Aldrich, reagent grade, 50-60%), triethylamine (Sigma-Aldrich, $\geq 99\%$), acryloyl chloride (97%, Sigma Aldrich), bromotrimethyl silane (Sigma-Aldrich, 97%), potassium carbonate (Sigma-Aldrich), concentrated (65%) nitric acid (Carlo Erba), cerium(III) nitrate hexahydrate ($\text{Ce}(\text{NO}_3)_3 \cdot 6\text{H}_2\text{O}$, Aldrich, 99.99% metal basis trace), neodymium(III) nitrate hexahydrate ($\text{Nd}(\text{NO}_3)_3 \cdot 6\text{H}_2\text{O}$, Aldrich, 99.99% metal basis trace), were used without further purification. Azobisisobutyronitrile (Sigma-Aldrich, 98%) was recrystallized before use. All solvents (Sigma-Aldrich) used in the synthesis were technique grade. Only acetonitrile was dried before utilization. All the aqueous solutions of cations, of monomers and polymers were prepared using Milli-Q water (18.2 M Ω .cm).

2.1.2. Characterizations

Nuclear Magnetic Resonance (NMR) was carried out with Bruker Avance 400 (400 MHz) to record ^1H and ^{31}P NMR spectra using deuterated chloroform (CDCl_3) or dimethylsulfoxide ($\text{DMSO}-d_6$) as deuterated solvents purchased from Eurisotop. For ^1H NMR, chemical shifts were referenced to the corresponding hydrogenated solvent residual peaks at 7.26 ppm and 2.50 ppm, for CDCl_3 and $\text{DMSO}-d_6$, respectively. H_3PO_4 was used as a reference for ^{31}P NMR.

Size Exclusion Chromatography (SEC) was performed with a PL-GPC 50 apparatus (Agilent) equipped with a RI refractive index detector. PolarGel M column was used at 50 °C with a flow of 0.8 mL \cdot min $^{-1}$ calibrated with PMMA standards. Elution solvent used was DMAc (+0.1wt% LiCl).

2.2. Synthesis

2.2.1. Synthesis of diisopropyl(acryloyloxymethyl) phosphonate monomer (DiAPC1)

Diisopropyl(acryloyloxymethyl) phosphonate (DiAPC1) was prepared in a two steps procedure. Diisopropyl phosphite (5.01 g, 0.03 mol), paraformaldehyde (0.99 g, 0.033 mol, 1.1 eq), and potassium carbonate (0.21 g, 1.5 mmol, 0.05 eq) were dissolved in methanol (20 mL). The mixture was then stirred at room temperature for 2 hours. Methanol was evaporated under vacuum to lead to diisopropyl hydroxymethyl phosphonate (4.46 g, yield: 76 %).

^1H NMR (400 MHz, δ (ppm), CDCl_3): 1.33-1.34 (m, $-\text{CH}_3$), 3.82-3.84 (d, $-\text{OCH}_2$), 4.73-4.75 (m, $-\text{OCH}$) (Figure SI 11)

^{31}P NMR (400 MHz, δ (ppm), CDCl_3): 22.20 (Figure SI 12)

Mass spectra (positive mode, ESI) $m/z=197.1$ (Figure SI 13)

In a second step, diisopropyl hydroxymethyl phosphonate (1.75 g, 8.9 mmol) was dissolved in anhydrous acetonitrile (10 mL). Then triethylamine (Et_3N) (1.80 g, 17.8 mmol, 2 eq) was slowly added into the reaction solution at 0 °C. Reaction was stirred for 3 hours at room temperature. Acryloyl chloride (1.21 g, 13.3 mmol, 1.5 eq) dissolved in anhydrous acetonitrile (10 mL) was then added dropwise at 0 °C into the reactional mixture. Reaction lasted for 6 hours at room temperature. After filtration and removal of acetonitrile, the crude material was dissolved in dichloromethane to achieve chromatographic column with a gradient eluent using pentane and ethyl acetate (AcOEt) mixture going from 50/50 to 20/80 (v/v). The retardation factor (R_f) value of thin-layer chromatography (TLC-eluent: pentane/AcOEt (50/50)) was equal to 0.35. Diisopropyl(acryloyloxymethyl) phosphonate monomer (1.3 g, yield: 59%) was obtained as a transparent liquid.

^1H NMR (400 MHz, δ (ppm), CDCl_3): 1.32-1.35 (m, $-\text{CH}_3$), 4.38-4.41 (d, $-\text{PCH}_2$), 4.73-4.81 (m, $-\text{OCH}$), 5.88-8.91 (d, $-\text{CCH}$), 6.14-6.21 (m, $-\text{CCH}_2$), 6.45-6.49 (d, $-\text{CCH}_2$)

^{31}P NMR (400 MHz, δ (ppm), CDCl_3): 16.76 (Figure SI 14)

Mass spectra (positive mode, ESI,) $m/z=251.11$ (Figure SI 15)

2.2.2. Synthesis of dimethyl(acryloyloxymethyl) phosphonate monomer (APC1)

Dimethyl(acryloyloxymethyl) phosphonate monomer (APC1) was prepared according to procedure previously reported in the literature [212].

2.2.3. Synthesis of acryloyloxymethyl phosphonic acid monomer (hAPC1)

Acryloyloxymethyl phosphonic acid was obtained by hydrolysis of the diisopropyl(acryloyloxymethyl) phosphonate or dimethyl(acryloyloxymethyl) phosphonate monomer. In a typical experiment, trimethylsilyl bromide (3.2 g, 26.4 mmol) was added to a solution of diisopropyl(acryloyloxymethyl) phosphonate (100 mg, 0.40 mmol) in anhydrous dichloromethane (30 mL). After stirring for 3 hours at room temperature, the mixture was concentrated under reduced pressure. Methanol (30 mL) was added and the mixture was stirred for 1 hour at room temperature. The solvent was evaporated and the hAPC1 (41 mg, yield: 90 %) was dried under vacuum, obtained as transparent liquid.

^1H NMR (400 MHz, δ (ppm), CDCl_3): 4.46 (d, - PCH_2), 5.91-5.93 (d, -CCH), 6.15-6.19 (m, - CHCH_2), 6.47-6.52 (d, - CHCH_2), 6.77 (m, -OH) (Figure SI 16)

^{31}P NMR (400 MHz, δ (ppm), CDCl_3): 19.99 (Figure SI 17)

2.2.4. Synthesis of poly(diisopropyl(acryloyloxymethyl) phosphonate) (P(DiAPC1))

Diisopropyl(acryloyloxymethyl) phosphonate (DiAPC1) (51.6 mg, 0.206 mmol) and azobisisobutyronitrile (AIBN) (0.62 mg, 0.0037 mmol, 0.02 eq) were dissolved in dimethylsulfoxide (DMSO) (5 mL). After 3 cycles of N_2 -vacuum, the reaction solution was put in oil bath heated at 70 °C. The polymerization reached 100% after 24 hours. Purification was carried out through dialysis using a 2 kD cut-off membrane during 5 days, and the P(DiAPC1) (49 mg, yield: 95 %) was obtained as a slightly yellow solid.

^1H NMR (400 MHz, δ (ppm), CDCl_3): 1.33 (m, - CH_3 and - CHCH_2), 1.79-1.80 (m, -CCH), 4.28-4.32 (m, - PCH_2), 4.73 (m, - CH_3)

^{31}P NMR (400 MHz, δ (ppm), CDCl_3): 16.84 (Figure SI 19)

SEC (DMAc): $M_n=4500 \text{ g}\cdot\text{mol}^{-1}$, $D=2.2$ (Figure SI 18)

2.2.5. Synthesis of poly(dimethyl(acryloyloxymethyl) phosphonate) (P(APC1))

Dimethyl(acryloyloxymethyl) phosphonate (APC1) (1 g, 5.17 mmol) and azobisisobutyronitrile (AIBN) (0.025 g, 0.152 mmol) were dissolved in dimethylsulfoxide (DMSO) (13 mL). After 3 cycles of N₂-vacuum, the reaction solution was put in oil bath heated at 70 °C. The polymerization reached 100% after 20 hours. Purification was carried out through dialysis using a 2 kD cut-off membrane during 4 days, and the P(APC1) (0.95 g, yield: 96 %) was obtained as a white solid.

¹H NMR (400 MHz, δ (ppm), CDCl₃): 1.63-2.35 (m, -CHCH₂ and -CCH), 3.68-3.70 (m, -CH₃), 4.31 (m, -PCH₂) (Figure SI 21)

³¹P NMR (400 MHz, δ (ppm), CDCl₃): 21.70 (Figure SI 22)

SEC (DMAc): M_n=9800 g·mol⁻¹, \bar{D} =1.5 (Figure SI 20)

2.2.6. Synthesis of poly(acryloyloxymethyl phosphonic acid) (hP(APC1))

P(DiAPC1) (150 mg, 0.96 mmol) was dissolved in anhydrous dichloromethane (DCM) (6 mL). The solution was bubbled with N₂ for 1 hour. Then, bromotrimethylsilane (TMSBr) (0.58 g, 4.78 mmol, 5 eq) was added dropwise. Reaction was stirred overnight at room temperature. DCM was removed under vacuum. Methanol (15 mL) was added and the reactional mixture was stirred at room temperature for 4 hours. The hP(APC1) (130 mg, yield: 96%) was obtained as a white powder after removing methanol under reduced pressure.

¹H NMR (400 MHz, δ (ppm), DMSO-*d*₆): 1.65-2.37 (m, -CHCH₂ and -CCH), 4.17 (m, -PCH₂), 6.06 (m, -OH)

³¹P NMR (400 MHz, δ (ppm), DMSO-*d*₆): 14.42 (Figure SI 23)

2.3. Sorption experiments with Isothermal Titration Calorimetry (ITC)

2.3.1. Preparation of monomer and polymer aqueous solutions

APC1, DiAPC1 and hAPC1 monomer aqueous solutions with a concentration equal to 14.35 mmol·L⁻¹ were prepared by respectively dissolving APC1, DiAPC1, hAPC1 in Milli-Q water. P(APC1) and hP(APC1) polymer aqueous solutions with a concentration equal to

14.35 mmol·L⁻¹ were also prepared by respectively dissolving P(APC1) and hP(APC1) in Milli-Q water. The concentrations were here expressed taking into account the concentrations of the monomer unit. Then, the pH of all the prepared solutions was adjusted to pH=1 using a 1 mol·L⁻¹ HNO₃ solution, which was prepared by diluting concentrated (65%) HNO₃. The new concentrations of all these aqueous solutions were recalculated after the pH modification.

2.3.2. Preparation of metal ions aqueous solutions

Two different concentrations of 63 and 17 mmol·L⁻¹ were chosen for each type of metal ion (Ce(III) and Nd(III)) aqueous solutions to adapt to different sorbents for obtaining optimal experimental signals. Ce(III) and Nd(III) aqueous solutions were prepared by dissolving Ce(NO₃)₃·6H₂O or Nd(NO₃)₃·6H₂O in Milli-Q water, respectively. Then, the pH of all aqueous solutions was modified to pH=1 using a 1 mol·L⁻¹ HNO₃ solution. The new concentrations of all these aqueous solutions were recalculated after the pH modification for metal ions speciation calculations.

2.3.3. Isothermal Titration Calorimetry (ITC) experiments

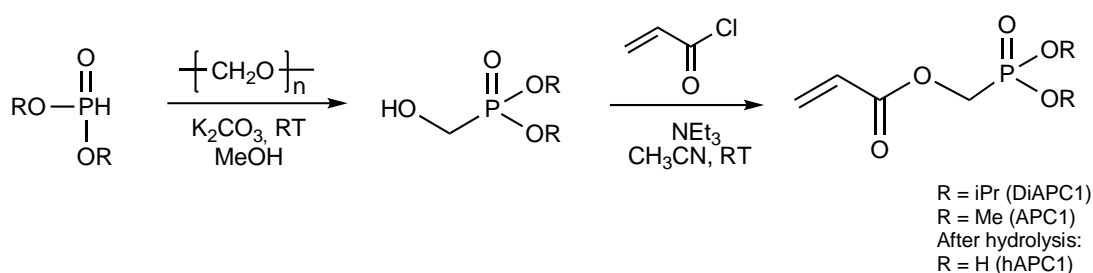
ITC experiments were performed with a TAM III multi-channel calorimetric device, which was equipped with Nanocalorimeters and Micro Reaction System. The experimental system comprised a computer-controlled micro-syringe injection device. A stock solution (metal cation solutions in this work) was injected in a controlled manner to stainless steel sample ampoule serving as a calorimetric cell. The sample cell was filled with the ligand solution for a sorption experiment. Similar experiment was performed with metal successive injection in the solvent (acidified aqueous solution without ligand), in order to remove the thermal effect due to the dilution. The initial volume in the cell (of the ligand or of the acidified water) is 800 μL. Measurements were carried out at 298 K. A complete experiment consisted in a series of 25 injections of 10 μL (injection duration of 10 seconds). The time between two injections was 45 minutes to ensure complete return to the baseline before the next injection. Homogeneity of the solutions was maintained using a gold stirrer at 95 rpm.

3. Results and discussions

3.1. Synthesis of monomers and polymers

3.1.1. Synthesis of monomers

Diisopropyl(acryloyloxymethyl) phosphonate (DiAPC1) and dimethyl(acryloyloxymethyl) phosphonate (APC1) were prepared using the same reactional procedure (Scheme 10).



Scheme 10. Reactional pathway for the synthesis of diisopropyl(acryloyloxymethyl) phosphonate (DiAPC1) and dimethyl(acryloyloxymethyl) phosphonate (APC1) monomers, hydrolysis to produce acryloyloxymethyl phosphonic acid (hAPC1)

In the first step, diisopropyl phosphite or dimethyl phosphite were added to paraformaldehyde and potassium carbonate in methanol at room temperature to produce diisopropyl(hydroxymethyl) phosphonate (DihMP) or dimethyl(hydroxymethyl) phosphonate (hMP), respectively (see Supporting information, ^1H NMR of DihMP in Figure SI 11, ^{31}P NMR of DihMP in Figure SI 12, mass spectrum of DihMP in Figure SI 13). Then, monomers were prepared by acryloylation reaction with acryloyl chloride at 0 °C in acetonitrile in the presence of triethylamine. In particular, diisopropyl(acryloyloxymethyl) phosphonate (DiAPC1) was purified by passing through a chromatographic column using gradient proportions (50/50 to 20/80 (v/v)) of pentane/ethyl acetate mixture as eluent and obtained with 59% yield. ^1H NMR spectrum of DiAPC1 showed the presence of the isopropyl group at 1.32-1.35 and 4.73-4.81 ppm (methyl and methine groups, respectively), the methylene in α -position of the phosphorus atom at 4.38-4.41 ppm, and the protons of the acryloyl moiety at 5.88-8.91, 6.14-6.21, and 6.45-6.49 (Figure 20). ^{31}P NMR also showed one signal at 16.76 ppm (see Supporting information, Figure SI 14). Finally, mass spectroscopy confirmed that the reaction was successful, with m/z equal to 251 (see Supporting information, Figure SI 15).

Diisopropyl(acryloyloxymethyl) phosphonate (DiAPC1) and dimethyl(acryloyloxymethyl) phosphonate (APC1) were hydrolyzed to produce acryloyloxymethyl phosphonic acid monomer (hAPC1). Reaction took place in the presence of trimethylsilyl bromide followed by hydrolysis in methanol. hAPC1 monomer was obtained with a yield equal to 90% and was characterized by NMR. ^1H NMR (see Supporting information, Figure SI 16) notably showed the disappearance of the isopropyl group (when DiAPC1 was used for the hydrolysis reaction) and the appearance of a signal at 6.77 ppm corresponding to the -OH of the phosphonic acid groups. ^{31}P NMR signal (see Supporting information, Figure SI 17) shifted from 16.76 to 20 ppm after hydrolysis.

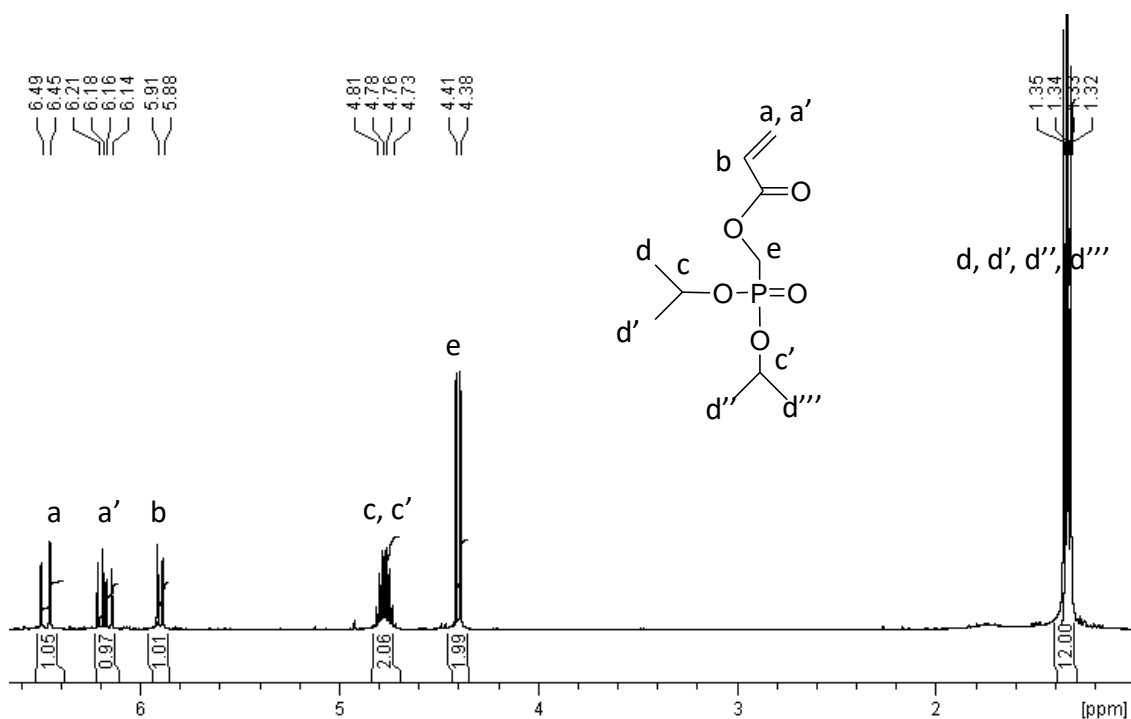
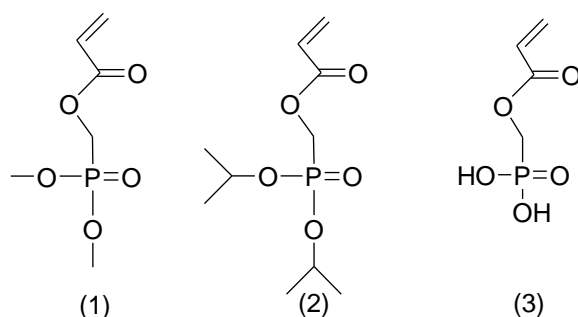


Figure 20. ^1H NMR spectrum (400 MHz, CDCl_3) of diisopropyl(acryloyloxymethyl) phosphonate (DiAPC1)

To conclude, three different monomers were prepared (Scheme 11) and will be further studied for the sorption of cerium and neodymium.



Scheme 11. Chemical structures of oxymethylphosphonated monomers studied for the sorption properties of cerium and neodymium: dimethyl(acryloyloxymethyl) phosphonate (APC1) (1), diisopropyl(acryloyloxymethyl) phosphonate (DiAPC1) (2) and acryloyloxymethyl phosphonic acid (hAPC1) (3)

3.1.2. Synthesis of polymers

Diisopropyl(acryloyloxymethyl) phosphonate (DiAPC1) and dimethyl(acryloyloxymethyl) phosphonate (APC1) monomers synthesized were used to produce corresponding poly(diisopropyl(acryloyloxymethyl) phosphonate) (P(DiAPC1)) and poly(dimethyl(acryloyloxymethyl) phosphonate) (P(APC1)) polymers, respectively. Reaction was achieved by free radical polymerization in the presence of azobisisobutyronitrile (AIBN) as initiator under nitrogen at 70 °C in DMSO. Purification of the polymers was carried out through dialysis using a 2 kD cut-off membrane. Analysis of P(DiAPC1) by size exclusion chromatography (SEC) allowed determining the molecular weight (M_n) and the dispersity (\mathcal{D}) equal to 4500 g·mol⁻¹ and 2.2, respectively (see Supporting information, Figure SI 18). ¹H NMR spectrum (Figure 21) logically showed the disappearance of the signals corresponding to the acryloyl moiety coming from the monomer. All other signals were broadened, which is characteristic when polymerization occurs. Only one signal was observed in ³¹P NMR spectrum at around 17 ppm (see Supporting information, Figure SI 19). Concerning poly(dimethyl(acryloyloxymethyl) phosphonate) (P(APC1)), SEC showed a molecular weight (M_n) and dispersity (\mathcal{D}) equal to 9800 g·mol⁻¹ and 1.5, respectively (see Supporting information, Figure SI 20). ¹H and ³¹P NMR (see Supporting information, Figure SI 21 and Figure SI 22, respectively) also allowed to conclude that the polymerization reaction was successful. In particular, ³¹P NMR signal was found at 21.7 ppm. Finally, hydrolysis of the phosphonated ester moieties on P(DiAPC1) allowed the obtaining of the poly(acryloyloxymethyl phosphonic acid) (hP(APC1)). Reaction conditions were similar to

those employed for the hydrolysis of the DiAPC1 monomer (trimethylsilyl bromide followed by methanolysis). hP(APC1) was not characterized by SEC as phosphonic acid groups could be retained on SEC columns. ^1H NMR spectrum (Figure 22) showed the disappearance of the isopropyl groups and signal on ^{31}P NMR (see Supporting information, Figure SI 23) shifted from 17 to 14.4 ppm when hydrolysis occurred.

Figure 21. ^1H NMR spectrum (400 MHz, CDCl_3) of poly(diisopropyl(acryloyloxymethyl) phosphonate) (P(DiAPC1))

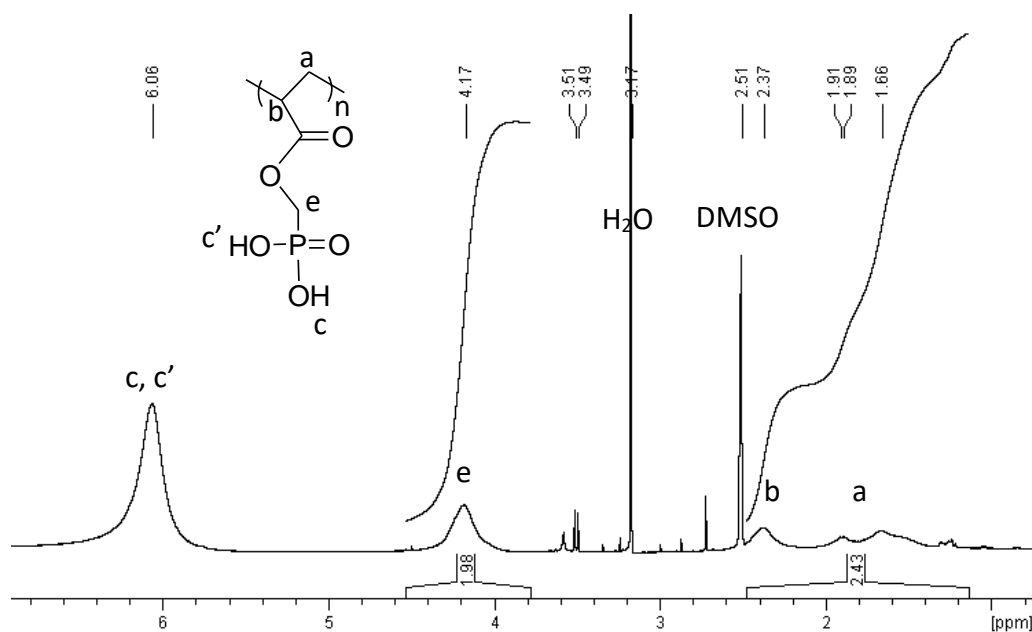
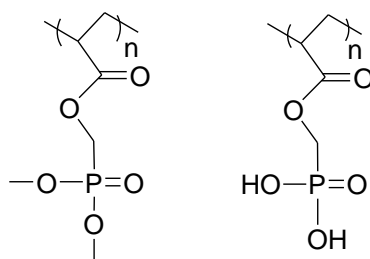


Figure 22. ^1H NMR spectrum (400 MHz, $\text{DMSO}-d_6$) of poly(acryloyloxymethyl phosphonic acid) (hP(APC1))

Finally, it was important to consider water solubility of the three polymers synthesized, as they will be potentially employed as water-soluble materials to complex the lanthanides contained in effluents. Water solubility depended on the nature of the alkyloxy group borne by the phosphorous atom. Indeed, poly(diisopropyl(acryloyloxymethyl) phosphonate) (P(DiAPC1)) proved to be insoluble in water and, as a result, was not further studied. On the reverse, poly(dimethyl(acryloyloxymethyl) phosphonate) (P(APC1)) was soluble in water. Poly(acryloyloxymethyl phosphonic acid) (hP(APC1)) was logically soluble in water too, due to the presence of highly hydrophilic phosphonic acid moieties. To conclude, both P(APC1) and hP(APC1) (Scheme 12) were evaluated for the sorption of lanthanides, especially Ce(III) and Nd(III).



Scheme 12. Chemical structures of water-soluble poly(dimethyl(acryloyloxymethyl) phosphonate) (P(APC1)) (left) and poly(acryloyloxymethyl phosphonic acid) (hP(APC1)) (right) employed for the complexation of the lanthanides

3.2. Sorption study

ITC technique was used to evaluate the interaction between a given ligand (monomer or polymer) and a given cation (for Ce(III) or Nd(III)), and thus try to indirectly assess the complexing property of the three APC1, DiAPC1 and hAPC1 monomers (see the structures in Scheme 11), in comparison with the two polymers P(APC1) and hP(APC1) (see the structures in Scheme 12). The P(DiAPC1) polymer was not tested because of its non-water-soluble character. Before these measurements, the repartition of the various species for a given element was determined to confirm that the ions are hydrolyzed nor crystallized. The speciation diagrams of Ce(III) aqueous solutions of 63 and 17 mmol·L⁻¹ are shown in Supporting information, Figure SI 24 and Figure SI 25, respectively; that for Nd(III) aqueous solutions of 63 and 17 mmol·L⁻¹ are shown in Supporting information, Figure SI 26 and Figure SI 27, respectively. As mentioned in the experimental part, all measurements were carried

out at pH=1, for the sorbents and for the adsorbates alone. This was in connection with the application of the separation process to extract cations dissolved from ores in acidic media [191, 192]. The speciation calculations have revealed that at pH=1 no solids were present, and only free species had to be considered. For Ce(III), the main species at pH=1 were Ce^{3+} and CeNO_3^{2+} . Depending on the concentration in the solution to be injected, the repartition between Ce^{3+} and CeNO_3^{2+} was 70 and 30% respectively for the lowest concentration, and 50%-50% for the highest concentration. For Nd(III), the main species at pH=1 were Nd^{3+} and NdNO_3^{2+} . The repartition was 60% of Nd^{3+} and 40% for NdNO_3^{2+} for the lowest concentration, whereas it was 35% and 55% respectively for higher concentration. In all cases, all species were in ionic form.

3.2.1. Sorption results with Ce(III)

Firstly, the sorption of the polymers has been characterized for Ce(III) and compared to the corresponding monomers and DiAPC1. Figure 23 illustrates the raw ITC thermograms for the P(APC1)/Ce(III) system (Figure 23(a)) or the hP(APC1)/Ce(III) (Figure 23(b)) system, with the superposition of the sorption experiment at pH=1 together with the dilution measured on acidified Milli-Q water. The successive injections resulted in a raw heat rate record as a function of time. The thermograms of the sorption experiments carried out under the same condition between Ce(III) and the three monomers APC1, DiAPC1 and hAPC1 are shown in Supporting information, Figure SI 28.

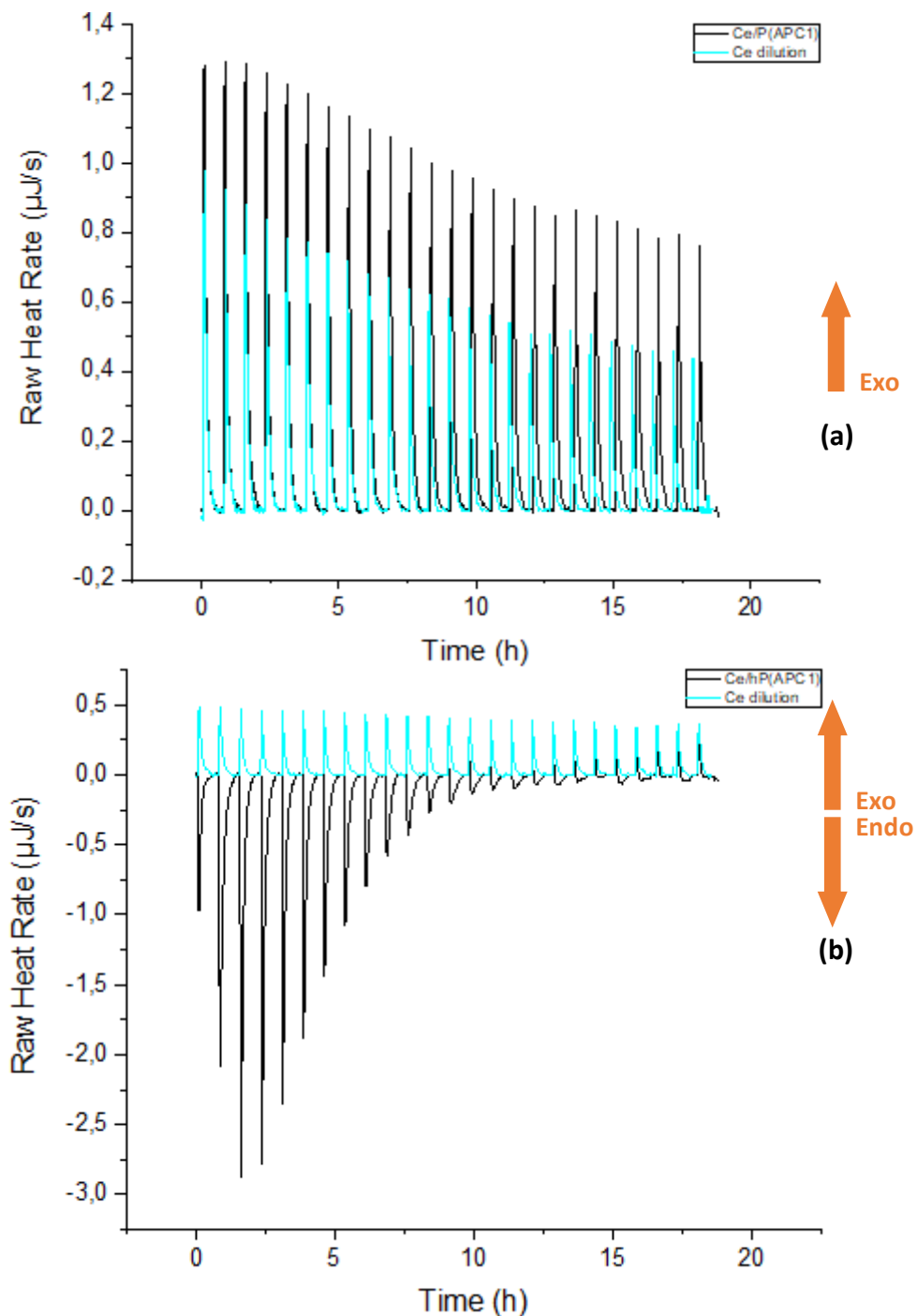


Figure 23. Processed thermal profiles Ce(III) ITC measurements on the P(APC1) (a) or hP(APC1) (b) aqueous solution of $14.35 \text{ mmol}\cdot\text{L}^{-1}$ (sorption experiment) together with the dilution experiment carried out with acidified Milli-Q water. The P(APC1) system is titrated with $63 \text{ mmol}\cdot\text{L}^{-1}$ $\text{Ce}(\text{NO}_3)_3\cdot 6\text{H}_2\text{O}$ aqueous solution, whereas the hP(APC1) is titrated with $17 \text{ mmol}\cdot\text{L}^{-1}$ $\text{Ce}(\text{NO}_3)_3\cdot 6\text{H}_2\text{O}$ aqueous solution. Experiments carried out at 298 K and $\text{pH}=1$, with 25 successive injections recorded with $10 \mu\text{L}$ for each injection of Ce(III) stock solution into $800 \mu\text{L}$ of polymer (P(APC1) or hP(APC1) aqueous solution or acidified Milli-Q water.

As shown in Figure 23(a), the sorption experiment between Ce(III) and P(APC1) and the dilution of Ce(III) showed both exothermic signals with a similar decreasing tendency. The signals of P(APC1) had intensity from $1.3 \mu\text{J}\cdot\text{s}^{-1}$ to $0.8 \mu\text{J}\cdot\text{s}^{-1}$, which were slightly higher than that of the dilution ($0.25\text{-}0.35 \mu\text{J}\cdot\text{s}^{-1}$). The very small difference between these two signals indicated the pretty weak interaction between Ce(III) and the dimethyl phosphonate P(APC1) polymer. In addition, this difference in signals was still too weak to be fitted for further thermodynamic calculation. It was clearly impossible to extract any binding constant. Meanwhile, the sorption experiment between Ce(III) and hP(APC1) shown in Figure 23(b) was fully different, with higher intensities, and two parts shown in the curve. It showed first endothermic signals with increasing tendency (in absolute value) till about $-3 \mu\text{J}\cdot\text{s}^{-1}$. Then after the 4th injection, an inversion was observed and the global heat effect decreased, till no variation of the intensity for the last peaks. For the 8-10 last injections, only dilution effect remained at the end. These relatively strong endothermic signals for the first peaks were completely different from the exothermic signals of the dilution experiment. It demonstrated an important complexation interaction between Ce(III) and the hP(APC1) phosphonic acid polymer. The succession of the two tendencies in the signals indicated that there were probably two contributions to the interaction mechanism [180, 194, 195].

The P(APC1) phosphonated ester polymer and the three monomers did not show apparent complexing property for Ce(III). On the reverse, the hP(APC1) phosphonic acid polymer showed significant signals and thus possible complexing property for Ce(III). This meant that the acryloyloxymethyl phosphonic acid was not able to complex when it was alone and free in solution (monomer), but when engaged in a polymer form, as in the case for phosphonic acid poly(acryloyloxymethyl phosphonic acid) (hP(APC1)) polymer, the complexation occurred. This was not the case for the ester form.

3.2.2. Sorption results with Nd(III)

The complexing property of the APC1, DiAPC1 and hAPC1 monomers (see the structures in Scheme 11), together with that of the polymers P(APC1) and hP(APC1) (see the structures in Scheme 12) for Nd(III) was studied as well using ITC. Only the raw data thermogram of the ITC sorption experiment between Nd(III) and hP(APC1), carried out at 298 K and pH=1, is reported in Figure 24. It shows the calorimetric results of the titration by Nd(III) aqueous

solution for the hP(APC1) polymer aqueous solution (sorption experiment), in comparison with the dilution experiment. The thermograms of the other sorption experiments under the same experimental condition of Nd(III) with the APC1, DiAPC1, hAPC1 monomers and the P(APC1) polymer are shown in Supporting information, Figure SI 29 and Figure SI 30, respectively.

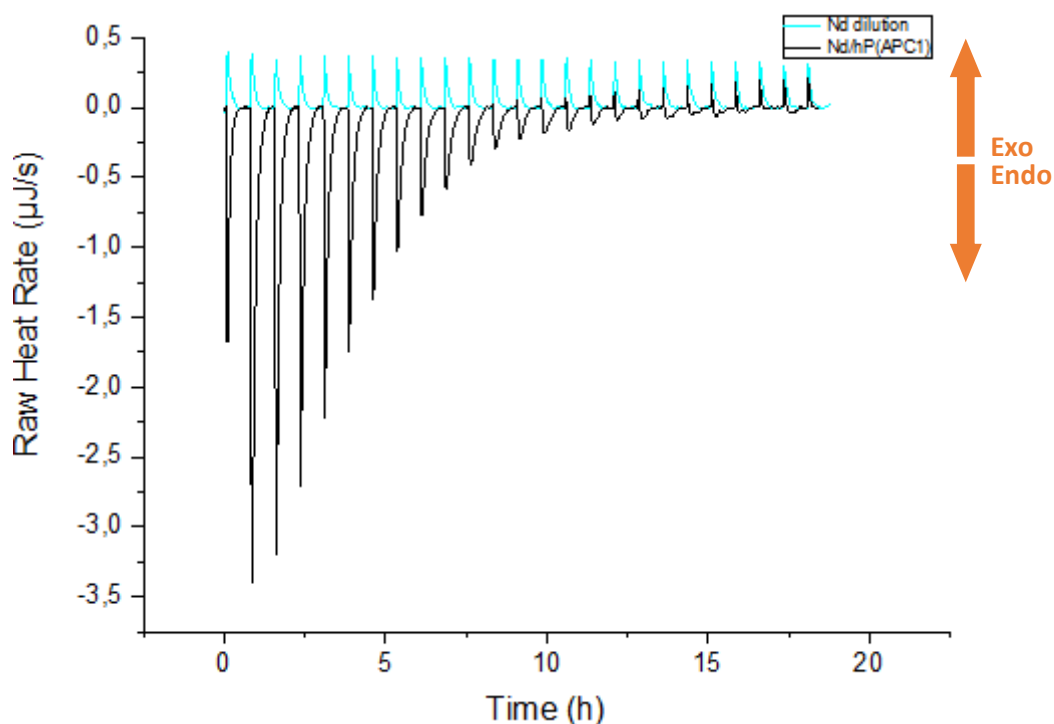


Figure 24. Processed thermal profiles at 298 K and pH=1 for injections of $17 \text{ mmol}\cdot\text{L}^{-1}$ Nd(III) stock solution into acid Milli-Q water (Nd dilution) and injections of the same Nd(III) stock solution into $14.35 \text{ mmol}\cdot\text{L}^{-1}$ hP(APC1) aqueous solution: 25 successive injections recorded with $10 \mu\text{L}$ for each injection of the $\text{Nd}(\text{NO}_3)_3\cdot 6\text{H}_2\text{O}$ solution with pH=1 into a 1 mL stainless ampoule containing initially $800 \mu\text{L}$ of Milli-Q water with pH=1 (dilution experiment) or $800 \mu\text{L}$ hP(APC1) aqueous solutions with pH=1 (sorption experiment).

As shown in Figure 24, the sorption experiment between Nd(III) and the hP(APC1) polymer showed relatively intense endothermic signals until the 16th peak, from which the dilution effect became dominant. As observed for Ce(III), two parts in the curves could be distinguished. There was first increase of the endothermic part, till $-3.5 \mu\text{J}\cdot\text{s}^{-1}$, and then it returned to weaker values. Meanwhile, the Nd(III) dilution experiment showed exothermic signals with much less intensity. This significant difference in thermic signals showed interaction between Nd(III) and hP(APC1). The succession of the two tendencies in the signals indicated that two reactions contributed to the interaction mechanism. As in the case

for Ce(III), it was also the acryloyloxymethyl phosphonic acid hP(APC1) polymer that exhibited the strongest interaction or complexing property for Nd(III). For the APC1, DiAPC1 and hAPC1 monomers and also the P(APC1) polymer, the sorption and the dilution curves were similar, meaning that these materials did not show obvious complexing property for Nd(III).

Similar trends were concluded for the effect of the polymeric form, with the hAPC1 monomer that exhibited no different heat effect, and thus probably no interactions, whereas ITC for hP(APC1) revealed interactions. The acryloyloxymethyl phosphonic acid was not able to complex when it was alone and free in solution, but when engaged in a polymer form, as this was the case for phosphonic acid polymer hydrolyzed, it seemed to exhibit interaction.

In both cases for Ce(III) or Nd(III), the polymer with phosphonic acid moieties (hP(APC1)) exhibited complexation abilities, but P(APC1), that differs only with the presence of the methyl group, was not able to complex with high intensity of interactions. The presence of the hydroxy groups borne by the phosphorous atom on the acryloyloxymethyl phosphonic acid polymer stands for the greater complexation. This was not the case for the phosphonated ester P(APC1) polymer, which did not demonstrate any interactions, and thus probably any sorption or complexation. It was also interesting to notice that the ligand in the polymeric form was more efficient to complex. This meant that the complexation was possible only with the polymeric form. The polymeric structure favored the interactions with the cations and stabilized the complexes. This could be deciphered as a 'trapping effect' of the polymer chains. This stability brought by polymer chains has already been reported by Chen *et al* [213]. The chelating vinyl monomer glycidyl methacrylate (GMA)-iminodiacetic acid (IDA), and various polymeric chelating structures were synthesized. The stability constants between the monomer or chelating monomer and some transitions-metal ions (Ni(II), Zn(II), and Co(II)) were determined. The homopolymer PGMA-IDA corresponding to the initial monomer, the copolymer with methyl acrylate (PGI-co-MA) and the copolymer with acrylamide (PGI-co-AM) were compared. The monomer showed smaller stability constants than the three copolymers in binding Ni(II), Zn(II) and Co(II). The better stability of

the polymer complexes was explained in terms of the stereo and entanglement structure of the polymers.

The good complexing/chelating property of hP(APC1) for both Ce(III) and Nd(III) might be due to the affinity of the phosphonic acid for the lanthanides(III) [97, 102, 111, 112, 114, 189, 214]. Taking into account the hard-soft acid-base theory, lanthanides, as hard acids, tend to form chemical bonds with hard base atoms [34]. Thus, interactions between the phosphonic acids groups (hard ligand) and the Ln(III) were favoured. Our experimental results confirmed the complexing property of phosphonic acid towards the Ln(III). In addition, phosphonic acids exhibit two dissociation constants ($pK_{a1}=2-3$ and $pK_{a2}=6-7$) [94, 95], which make them different from other functional group and bring them better sorption capacity at low pH compared to other functional groups.

3.2.3. Complexation of hydrolyzed poly(acryloyloxymethyl phosphonate) (hP(APC1)) for Ce(III) and Nd(III) comparison

Figure 25 displays the ITC heat data as a function of the molar ratio between the cation and the ligand in the polymer. This corresponds to the titration of 25 injections in the sorption experiment between Ce(III) and hP(APC1) and also in the sorption experiment between Nd(III) and hP(APC1), after removal of the dilution contribution. It gives a general comparison of the interaction of the phosphonic acid hP(APC1) polymer for Ce(III) and Nd(III). The two groups of ITC heat data both showed two tendencies with a little more difference in the first stage. However, they were similar in general, it indicated the similar complexing property of hP(APC1) for Ce(III) and Nd(III). Such behavior has already been observed in previous works. The studied extractant were carbamoylmethylphosphonate, (benzimidazol-2-yl)pyridine-6-carboxamide, and diglycolamide based materials (mainly oxapentanediamide). The authors have generally reported the high affinity but bad selectivity of the hard donor ligands towards the Ln(III) [214-216]. In our present study, the phosphonic acid group in the hP(APC1), as a hard ligand, showed efficiency in complexing both Ce(III) and Nd(III), but did not show selectivity between the two Ln(III). Additionally, the two possible contributions, with increasing and then decreasing signal could be due either to the various species of cations, or to the successive reactions with one or two ligands group per cation, with a possible partial release of water molecules or nitrates.

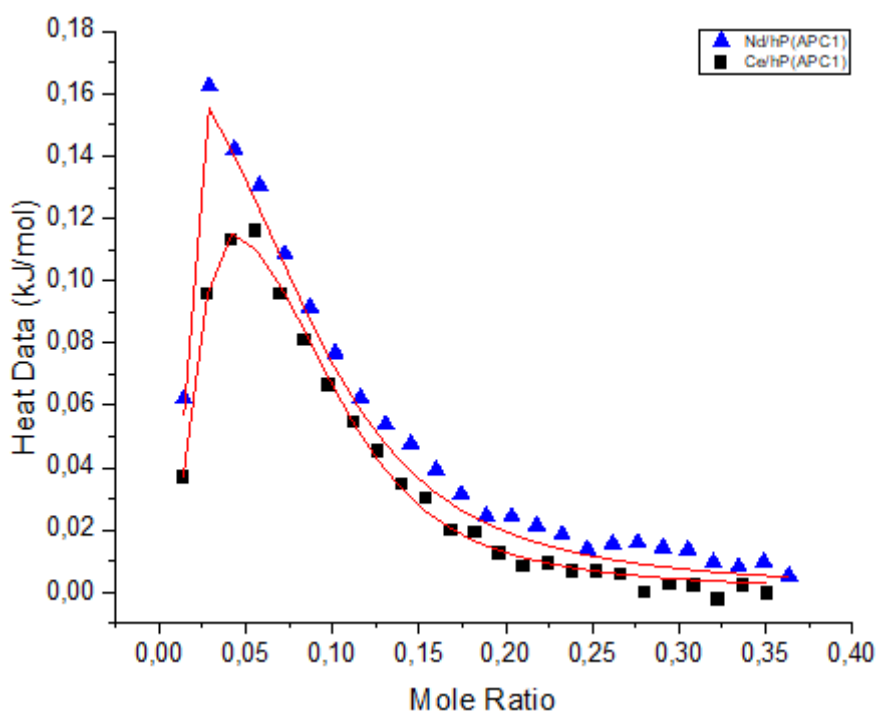


Figure 25. Superposition of the heat data corresponding to Ce(III) and Nd(III) ITC experiments (298 K and pH=1) of the hP(APC1) polymer aqueous solution titrated by $\text{Nd}(\text{NO}_3)_3 \cdot 6\text{H}_2\text{O}$ stock solution ($17 \text{ mmol} \cdot \text{L}^{-1}$ $\text{Nd}(\text{NO}_3)_3 \cdot 6\text{H}_2\text{O}$ or $17 \text{ mmol} \cdot \text{L}^{-1}$ $\text{Ce}(\text{NO}_3)_3 \cdot 6\text{H}_2\text{O}$ stock solution into $14.35 \text{ mmol} \cdot \text{L}^{-1}$ hP(APC1) aqueous solution).

4. Conclusion

Acrylate and phosphonate containing monomers, namely diisopropyl(acryloyloxymethyl) phosphonate (DiAPC1) and dimethyl(acryloyloxymethyl) phosphonate (APC1) were first prepared. These monomers were polymerized by free radical polymerization to lead to poly(diisopropyl(acryloyloxymethyl) phosphonate) (P(DiAPC1)) and poly(dimethyl(acryloyloxymethyl) phosphonate) (P(APC1)), respectively. Additionally, both DiAPC1 and APC1 were hydrolyzed, leading to the same hAPC1 monomer. Finally, P(DiAPC1) or P(APC1) polymers were also hydrolyzed leading to the same poly(acryloyloxymethyl phosphonic acid) (hP(APC1)) polymer. Then, Isothermal Titration Calorimetry (ITC) technique was tested to characterize the complexation efficiency for cerium (Ce) and neodymium (Nd).

The various (acryloyloxymethyl) phosphonate monomers in the dimethyl form (APC1), the diisopropyl form (DiAPC1) or the hydrolyzed form (hAPC1) did not complex Ce(III) and Nd(III) in our experimental conditions. The phosphonated ester P(APC1) polymer did not show obvious complexing property for Ce(III) or Nd(III). Only the hydrolyzed hP(APC1) phosphonic

acid polymer showed significant complexing property for both Ce(III) and Nd(III) without clear differences between the two cations. This demonstrates the effect of the hydroxy groups borne by the phosphorous atom on the complexing property for the REEs, and in particular the effect of the charge to favor the interactions in acidic pH conditions. In addition, for the hydrolyzed form, the hAPC1 ligand alone did not show any clear interactions, whereas the hP(APC1) polymer chains seem to exhibit a trapping effect, in which the ligand revealed a stronger chelating effect, thus illustrating the improvement of the extraction performance. This confirmed the additional value of the present work, *i.e.* fixing a ligand on a polymeric structure enhances the interaction, and facilitates the separation and the recovery of the lanthanides.

Appendix

Synthesis of bis(chloromethyl)ether (BCME)

Paraformaldehyde (56.29 g, 1.87 mol, 2 eq) and thionyl chloride (68 mL, 0.93 mol) were mixed. Then, zinc bromide (4.50 g, 19.9 mmol, 0.023 eq) was added slowly. Reaction mixture was protected from humidity with calcium chloride (CaCl₂). The reaction lasted one day at 80 °C. Bis(chloromethyl)ether (BCME) (82.71 g, yield: 77%) was isolated by cryo-distillation at room temperature.

¹H NMR (400 MHz, δ (ppm), CDCl₃): 5.56 (s, -OCH₂) (Figure Appendix 1)

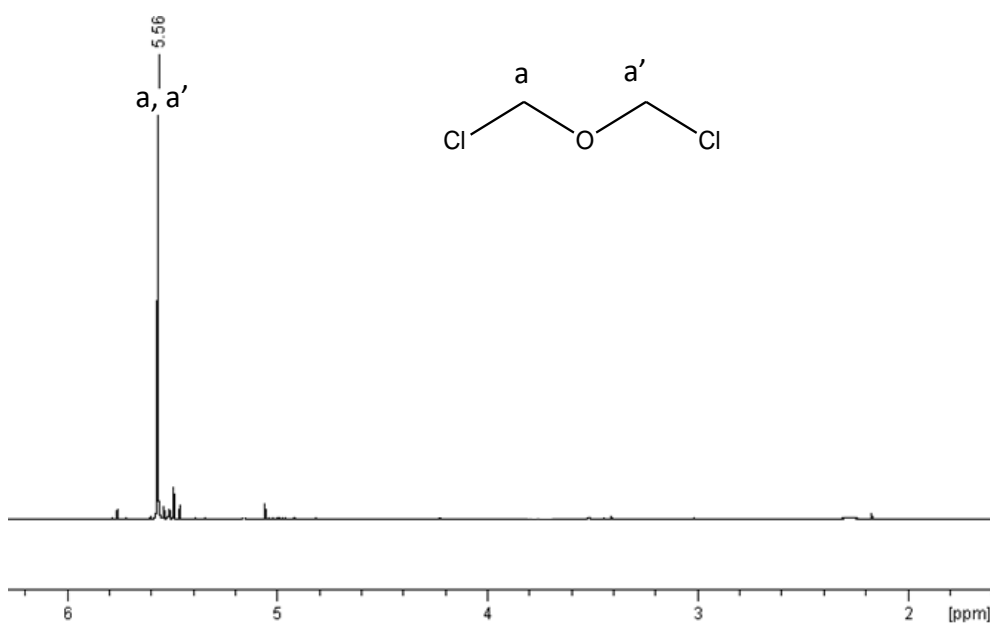


Figure Appendix 1. ¹H NMR spectrum (400 MHz, CDCl₃) of bis(chloromethyl)ether (BCME)

Diisopropyl(chloromethoxy)methyl phosphonate (DiCMP)

BCME (81.61 g, 0.71 mol, 20 eq) was heated to 105°C, then triisopropyl phosphite (8.83 mL, 0.0354 mol) was slowly added dropwise. Reaction lasted 15 hours under reflux. After evaporating remaining BCME, fractional cryo-distillation was achieved and Diisopropyl(chloromethoxy)methyl phosphonate (5.5 g, yield: 60%) was recovered at 80 °C under 0.1 mbar as a transparent liquid.

Chapter 3

^1H NMR (400 MHz, δ (ppm), CDCl_3): 1.33-1.35 (m, $-\text{CH}_3$), 3.90-3.92 (d, $-\text{PCH}_2$), 4.74-4.79 (m, $-\text{OCH}$), 5.52 (s, ClCH_2) (Figure Appendix 2)

^{31}P NMR (400 MHz, δ (ppm), CDCl_3): 17.06 (Figure Appendix 3)

Mass spectroscopy (positive mode, ESI) $m/z=245.02$ (Figure Appendix 4)

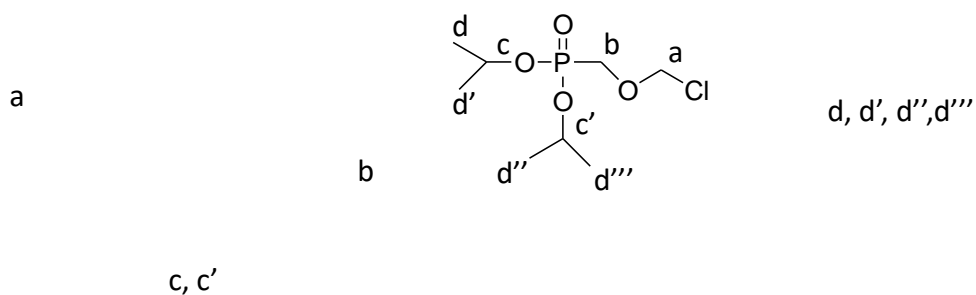


Figure Appendix 2. ^1H NMR spectrum (400 MHz, CDCl_3) of diisopropyl(chloromethoxy)methyl phosphonate (DiCMP)

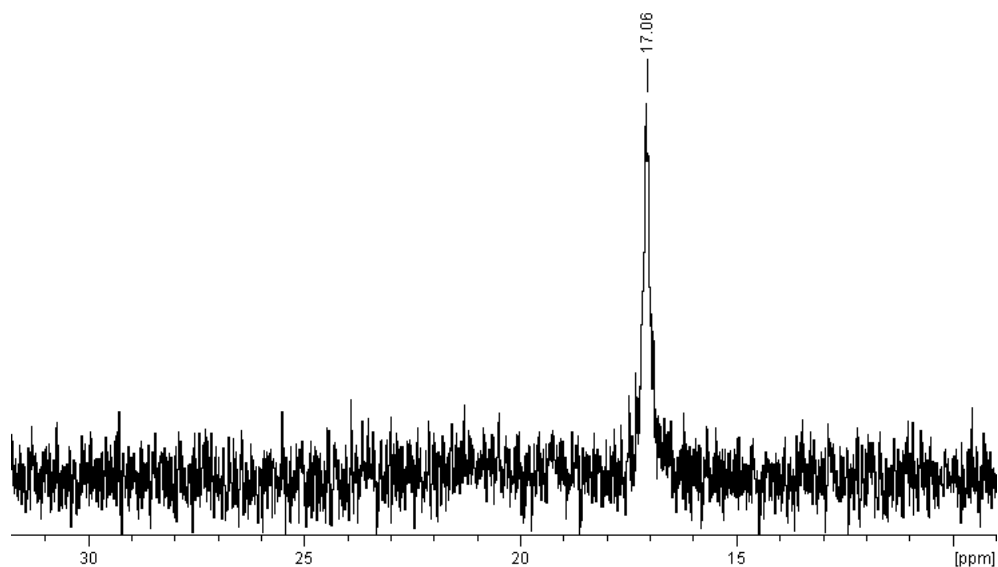


Figure Appendix 3. ^{31}P NMR spectrum (400 MHz, CDCl_3) of diisopropyl(chloromethoxy)methyl phosphonate (DiCMP)

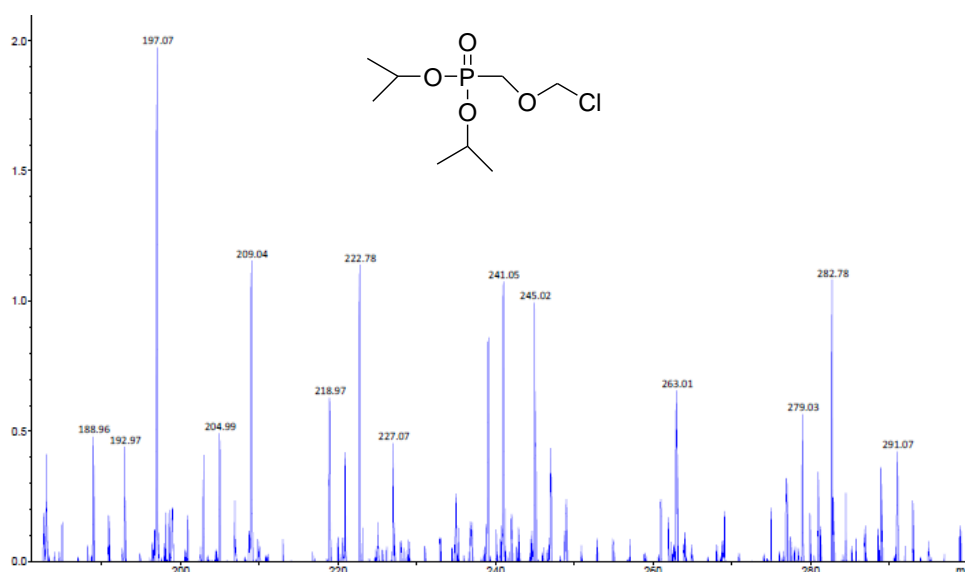


Figure Appendix 4. Mass spectrum in positive mode (+MS) of diisopropyl(chloromethoxy)methyl phosphonate (DiCMP) by Amazon speed instrument, ion source: ESI, intensity: $\times 10^6$; scan with maximum resolution from 50 1000 m/z . Product found at $m/z=245.02$.

Diisopropyl [(1,3-dioxisoindol-2-yl)methoxy] methyl phosphonate (DiOMP)

DiCMP (2.3 g, 9.4 mmol) and potassium phthalimide (8.7 g, 0.047 mol, 5 eq) were dissolved in anhydrous acetonitrile (40 mL). The reactional mixture was bubbled with N_2 and then heated to 80 °C overnight. It was filtered and acetonitrile was removed under reduced pressure. The crude material was then dissolved in ethanol for precipitating impurities. Diisopropyl [(1,3-dioxisoindol-2-yl)methoxy] methyl phosphonate (DiOMP) (2.7 g, yield: 80%) was recovered as a transparent viscous oil.

1H NMR (400 MHz, δ (ppm), $CDCl_3$): 1.33-1.35 (m, $-CH_3$), 3.88-3.91 (d, $-PCH_2$), 4.74 (m, $-OCH$), 5.22-5.25 (d, $-NCH_2$), 7.75 (m, $NCCHCHCH$), 7.90 (m, $NCCHCH$) (Figure Appendix 5)

^{31}P NMR (400 MHz, δ (ppm), $CDCl_3$): 18.22 (Figure Appendix 6)

Mass spectroscopy (positive mode, ESI) $m/z=356.1$ (Figure Appendix 7)

Figure Appendix 5. ^1H NMR spectrum (400 MHz, CDCl_3) of diisopropyl [(1,3-dioxoisindol-2-yl)methoxy] methyl phosphonate (DiOMP)

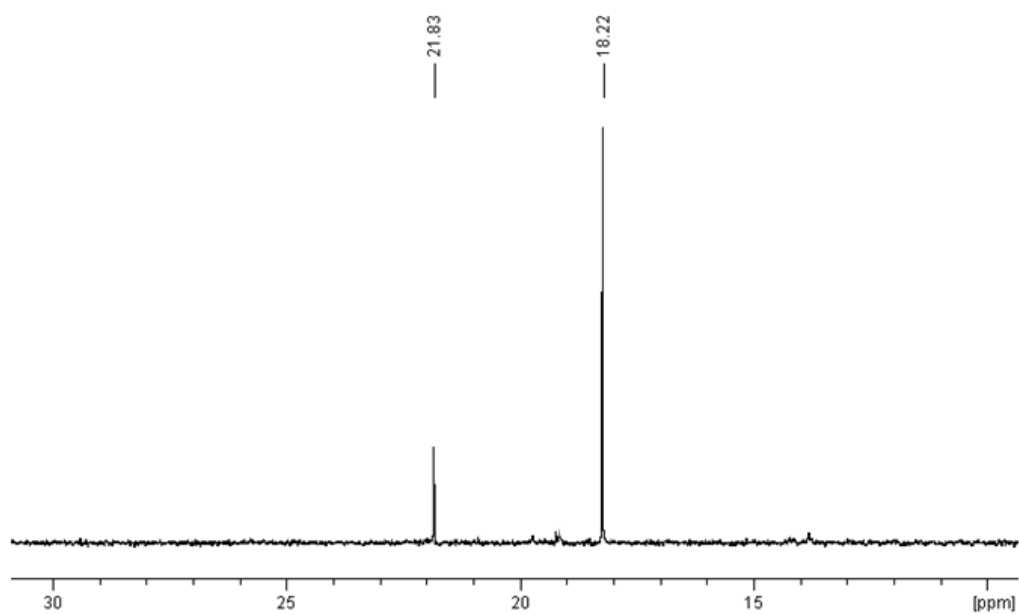


Figure Appendix 6. ^{31}P NMR spectrum (400 MHz, CDCl_3) of diisopropyl [(1,3-dioxoisindol-2-yl)methoxy] methyl phosphonate (DiOMP)

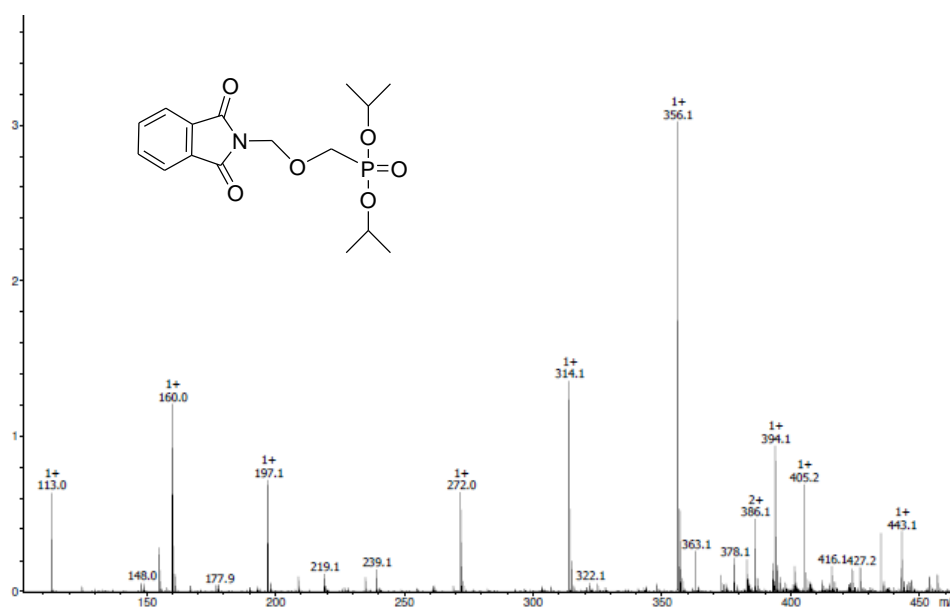


Figure Appendix 7. Mass spectrum of positive mode (+MS) of diisopropyl [(1,3-dioxoisindol-2-yl)methoxy] methyl phosphonate (DiOMP) by micrOTOF-Q instrument, ion source: ESI, intensity: $\times 10^5$; scan with maximum resolution from 50 to 2200 m/z . Product found at $m/z=356.1$.

Conclusion

In this chapter, we developed oxymethylphosphonated-based monomers and polymers for the complexation of cerium and neodymium. For such purpose, we first focused on the synthesis of an acrylamide monomer to try combining complexing properties of the phosphorous moiety of the monomer with polyacrylamide nature of the polymer in order to favor thermosensitivity. Unfortunately, synthesis was difficult to perform. As a consequence, we focused on the study of oxymethylphosphonated-based acrylate. Three different monomers and polymers were prepared. Firstly, monomers differed from the nature of the phosphorous moiety as we prepared diisopropoxy, dimethoxy phosphonated ester and phosphonic acid monomers. Diisopropyl(acryloyloxymethyl) phosphonate and dimethyl(acryloyloxymethyl) phosphonate were then polymerized by free radical polymerization to afford poly(diisopropyl(acryloyloxymethyl) phosphonate) (P(DiAPC1)) and poly(dimethyl(acryloyloxymethyl) phosphonate) (P(APC1)), respectively. These polymers were also hydrolyzed to obtain poly(acryloyloxymethyl phosphonic acid) (hP(APC1)). One important parameter to be taken in consideration was the water solubility of the different (macro)molecules synthesized. All monomers were soluble in water. On the reverse, only poly(dimethyl(acryloyloxymethyl) phosphonate) and poly(acryloyloxymethyl phosphonic acid) were water-soluble. So, sorption properties were studied for three monomers (DiAPC1, APC1, hAPC1) and two polymers (P(APC1) and hP(APC1)).

Sorption properties were evaluated in the presence of Ce(III) and Nd(III). The Isothermal Titration Calorimetry (ITC) technique was tested to characterize the complexation or chelation efficiency for cerium (Ce) and neodymium (Nd). This methodology was here used to evaluate the interaction between a given ligand (monomer or polymer) and a given cation, and thus try to indirectly assess the complexing property of the three APC1, DiAPC1 and hAPC1 monomers, in comparison with the two P(APC1) and hP(APC1) polymers, the P(DiAPC1) being not tested because of its non-water-solubility.

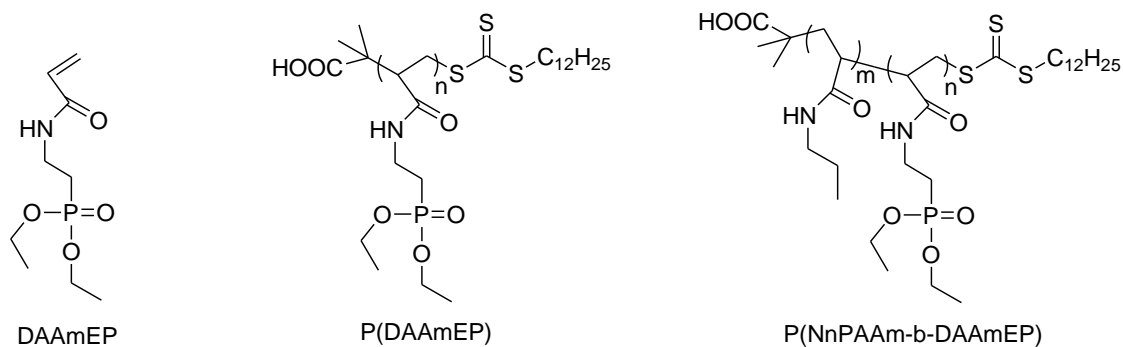
The various (acryloyloxymethyl) phosphonate monomers in the dimethyl form (APC1), the diisopropyl form (DiAPC1) or the hydrolyzed form (hAPC1) did not complex Ce(III) and Nd(III) in our experimental conditions. The phosphonated ester P(APC1) polymer did not show

obvious complexing property for Ce(III) or Nd(III). Only the phosphonic acid hP(APC1) hydrolyzed polymer showed significant complexing property for both Ce(III) and Nd(III). The intensity of interaction was similar for the two considered cations. Two contributions were observed on the ITC curves, which could be due either to the various species of cations, or to the successive reactions with one or two ligands group per cations. The comparison of hP(APC1) and P(APC1) has evidenced the influence of the alkyloxy and hydroxy groups borne by the phosphorous atom on the complexing property for the REEs. For the alkyloxy form, no interaction (or athermic) was detected, and the P(APC1) was not efficient for complexion. The comparison between monomer and polymer demonstrated a trapping effect of the polymer chains where the ligand had a stronger chelating effect, when it was localized in a polymer. This indeed indicated a stronger stabilization of the cations due to the loss of mobility when the polymer was used.

**Chapter 4: Thermosensitive phosphonate-based acrylamide
polymers: complexation with Ln(III) and Th(IV) studied by
Isothermal Titration Calorimetry (ITC)**

Introduction

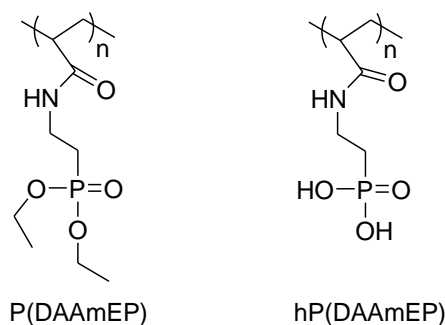
The objective of the chapter 3 was the synthesis of an oxymethylphosphonated-based acrylamide monomer in order to combine complexing property and thermosensitive character. Unfortunately, synthesis was very difficult and we did not obtain targeted structure. In this chapter, the objective was to prepare thermosensitive phosphonate-based polyacrylamide for the sorption of lanthanides and/or actinides. For such purpose, an acrylamide and phosphonate containing monomer, namely diethyl-2-(acrylamido)ethyl phosphonate (DAAmEP) (Scheme 13) [217] and now commercially available, was used.



Scheme 13. Chemical structures of diethyl-2-(acrylamido)ethyl phosphonate (DAAmEP) monomer, P(DAAmEP) polymer and thermosensitive P(NnPAAm-*b*-DAAmEP) copolymers developed by Graillot *et al* [217]

This monomer was interesting for its complexing properties brought by the phosphonate group and the potential thermosensitivity brought by the acrylamide group. It has already been polymerized by reversible addition-fragmentation transfer (RAFT) polymerization using two different trithiocarbonate chain transfer agents to obtain P(DAAmEP) (Scheme 13) with controlled molecular weight and low dispersity [217]. Synthesis of P(NnPAAm-*b*-DAAmEP) diblock copolymers (Scheme 13) was also achieved using poly(N-*n*-propylacrylamide) (P(NnPAAm)) as macro-chain transfer agent with a similar RAFT procedure. The P(NnPAAm-*b*-DAAmEP) diblock copolymer proved to be thermosensitive with a cloud point measured at around 22 °C in Milli-Q water for a 80/20 NnPAAm/DAAmEP molar ratio of monomers in the copolymer. However, it is important to notice that the thermosensitivity of P(DAAmEP) homopolymer and its complexing properties have not been studied yet.

In the present chapter, polymers combining thermosensitivity and complexing property were developed. Diethyl-2-(acrylamido)ethyl phosphonate (DAAmEP) was polymerized by free radical polymerization, leading to P(DAAmEP) homopolymer (Scheme 14). Its thermosensitive behavior was studied. Then, P(DAAmEP) was hydrolyzed to lead to poly(2-(acrylamido)ethyl phosphonic acid) (hP(DAAmEP)) (Scheme 14).

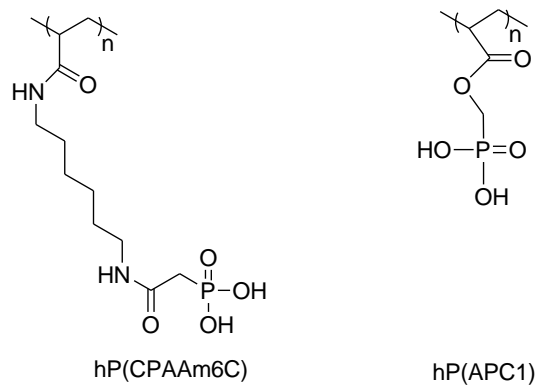


Scheme 14. Chemical structures of poly(diethyl-2-(acrylamido)ethyl phosphonate) (P(DAAmEP)) and poly(2-(acrylamido)ethyl phosphonic acid) (hP(DAAmEP))

Both P(DAAmEP) and hP(DAAmEP) were evaluated for complexing gadolinium (Gd), cerium (Ce) and neodymium (Nd), which are the three most abundant REEs in minerals, in order to compare the complexing properties of these polymers for REEs. To evaluate their potential to treat effluents containing radioactive contaminants, their complexation for thorium (Th) was also studied, as thorium is an actinide (Ac) that can be considered as representative of contaminants.

Finally, the three phosphonic acid containing polymers which have shown interesting complexing property for Ln(III) or An in previous works were compared: hP(DAAmEP) (Scheme 14), hP(CPAAm6C) and hP(APC1) (Scheme 15). In this particular case, polymers were not thermosensitive but we already saw that they could potentially flocculate when complexing specific metal ions. As a consequence, this property could represent another interesting way to explore to develop new process for lanthanide separation and recovery. Acidic polymers were all evaluated for complexation of Gd(III), Ce(III) and Nd(III). The objective was to study and compare the influence of phosphonic acid binding sites on complexing the Ln(III). Isothermal Titration Calorimetry (ITC) was still the technique chosen to study the sorption efficiency and the complexing interactions. In particular, binding

constant was the main parameter used to compare the complexing properties of the synthesized polymers.



Scheme 15. Chemical structures of poly(6-(acrylamido)hexylcarbamoylmethyl phosphonic acid) (hP(CPAAm6C)) and poly(acryloyloxymethyl phosphonic acid) (hP(APC1))

Experimental results are reported in the following article.

Study of Ln(III) and Th(IV) complexation by Isothermal Titration Calorimetry on thermosensitive/flocculant phosphonated-based polyacrylamide: a new opportunity for water treatment

Abstract: In the present contribution, poly(diethyl-2-(acrylamido)ethyl phosphonate) (P(DAAmEP)) and its hydrolyzed form, namely poly(2-(acrylamido)ethyl phosphonic acid) (hP(DAAmEP)), were synthesized by free radical polymerization and hydrolysis, respectively. Then, complexation of Gd(III), Ce(III), Nd(III) and Th(IV) on both P(DAAmEP) and hP(DAAmEP) were studied and compared. P(DAAmEP) proved to be thermosensitive but did not show efficient lanthanide complexation. The hydrolyzed hP(DAAmEP) polymer showed much better sorption for all the four metal ions tested. Additionally, the complexes of Th(IV) and hP(DAAmEP) flocculated in aqueous solution at acid and natural pH, which would also allow an easy separation step of the metal-polymer complexes. Finally, as phosphonic acid-based polymers proved to be of great interest, two other phosphonic acid polymers, namely poly(6-(acrylamido)hexylcarbamoylmethyl phosphonic acid) (hP(CPAAm6C)) and poly(acryloyloxymethyl phosphonic acid) (hP(APC1), were also tested and showed good complexing properties for Gd(III), Ce(III) and Nd(III). All acidic polymers were compared: hP(DAAmEP) turned to have better affinity with the three Ln(III) than hP(CPAAm6C) and hP(APC1).

Keywords: phosphonic acid, water-soluble polymer, lanthanide, thorium

1. Introduction

Purification and separation of rare-earth elements (REEs) have been much studied because of the important role of REEs in advanced technologies [38, 39, 209, 210]. Indeed, nowadays, REEs are used in various fields owing to their excellent physical and chemical properties, such as super-conductors [36], hydrogen storage [37], permanent magnets [39], lasers [40], and magneto-optic data recording [35]. However, the resources of REEs over the world is own by a few countries. According to U.S. Geological Survey's mineral commodity summaries in January 2020, documented rare-earths production of China represented 65% of the worldwide production in 2019, and its reserves was about 40% of the world [1]. Europe needs to import more than 90% of REEs mainly from China due to the lack of internal supply [2]. In order to better treat the REEs resources and recycling the REEs, techniques for purifying and separating them more efficiently are intensively requested. The difficulties encountered in the REEs separation are the small concentrations of the REEs salts in the minerals, and the presence of various contaminants, which are mainly thorium (Th) and uranium (U).

Different methods to separate REEs from mineral and industrial effluents have been developed, including solvent extraction, Solid Phase Extraction (SPE) [5, 51, 76] using non-water-soluble polymeric sorbents, and Polymer Enhanced Ultrafiltration (PEUF) [65], involving water-soluble polymeric sorbents. Solvent extraction methods showed drawbacks such as an important consumption of solvent, many repetitions needed to obtain pure product and residual traces of solvent in the products. The SPE methods have generally slow kinetics and bad efficiency. In the PEUF procedures, water-soluble polymers functionalized with different binding sites showed efficiency, fast kinetic and selectivity in some cases [28, 29]. Among the polymers functionalized with binding groups, phosphonate and phosphonic acid ones have been reported for their good complexing property for various metal ions. For instance, the phosphonic polymeric sorbents with polyethylenimine backbone was much used to the recovery of metals such as Fe(III), U(IV) [105-107], and Cu(II) [100]. Tokuyama *et al* [103] described the synthesis of phosphonic acid polymeric sorbents in gel state, which allowed the complexation of In(III) and Zn(II) ions. Prabhakaran *et al* chemically modified an Amberlite resin® with a phosphonic derivative for the selective complexation of U(VI), Th(IV)

and La(III) [102, 111]. Additionally, considering the cost of the ultrafiltration technique used in PEUF procedure, other methods for isolating metal-polymer complexes were developed. In particular, thermosensitive polymers proved to be valuable for its precipitation character over a specific temperature in aqueous solution, called Lower Critical Solution Temperature (LCST) [144]. The LCST of these polymers was generally between 25-40 °C, which showed that they could be potentially used in water treatment processes. For example, Graillot *et al* [127, 144, 145] developed an innovative thermosensitive copolymer, namely poly(*N-n*-propylacrylamide-*stat*-(dimethoxyphosphoryl)methyl-2-methylacrylate) (P(*Nn*PAAm-*stat*-MAPC1)). MAPC1 moieties were then hydrolyzed to afford phosphonic acid complexing groups. Resulting P(*Nn*PAAm-*stat-h*MAPC1) copolymers were characterized and used for the sorption of metal ions. These copolymers showed different LCST values depending on the molar ratio of both monomers. Copolymer with 20% of phosphonic acid groups was selected as it combined relatively high content of complexing groups with appropriate LCST value (around 25 °C in Milli-Q water). Sorption experiments demonstrated its efficiency for complexing Ni(II), Cd(II) and Al(III) metal ions. Thermosensitive character of the copolymer allowed an easy separation of the metal-polymer complexes, in particular for the case of Al(III). Experimental results led to the development of a new process for removal of heavy metals from wastewater named 'Thermosensitive polymer Enhanced Filtration' (TEF process) [144]. Another commercially available monomer containing acrylamide and phosphonate, namely diethyl-2-(acrylamido)ethyl phosphonate (DAAmEP) [217], was of great interest for the potential complexing properties and thermosensitivity that could bring to the corresponding polymer. This monomer was polymerized using reversible addition-fragmentation transfer (RAFT) polymerization [217] and allowed obtaining P(DAAmEP) with controlled molecular weight and low dispersity. The DAAmEP monomer was also used to obtain another thermosensitive copolymer with poly(*N-n*-propylacrylamide), namely P(*Nn*PAAm-*b*-DAAmEP). Its LCST value was about 21.7 °C. However, to date, thermosensitivity and the complexing property of P(DAAmEP) homopolymer has not been studied.

In the present contribution, complexing properties of water-soluble phosphonate-based polymers were studied in order to optimize complexation efficiency and capacity towards the lanthanides. For such purpose, diethyl-2-(acrylamido)ethyl phosphonate (DAAmEP) was

polymerized by free radical polymerization, leading to thermosensitive polyacrylamide P(DAAmEP), bearing complexing moieties. Then, P(DAAmEP) was hydrolyzed to obtain its hydrolyzed derivative (hP(DAAmEP)). The complexing properties of P(DAAmEP) and hP(DAAmEP) towards Gd(III), Ce(III) and Nd(III), the three most abundant Ln(III) in minerals, were studied. Then, complexing properties of P(DAAmEP) and hP(DAAMEP) towards Th(IV), which represented the radioactive contaminants found in lanthanides mineral solutions, were also studied, to compare with those for Ln(III). Finally, two other phosphonic acid containing polymers were also considered for the complexation of the three Ln(III): poly(6-(acrylamido)hexylcarbamoymethyl phosphonic acid) (hP(CPAAm6C)) and poly(acryloyloxymethyl phosphonic acid) (hP(APC1)). Isothermal Titration Calorimetry (ITC) was used to study the complexing interactions, and binding constant for each interaction was calculated for comparison.

2. Experimental section

2.1. Materials and methods

Gadolinium(III) nitrate hexahydrate ($\text{Gd}(\text{NO}_3)_3 \cdot 6\text{H}_2\text{O}$, Aldrich, 99.99% metal basis trace), cerium(III) nitrate hexahydrate ($\text{Ce}(\text{NO}_3)_3 \cdot 6\text{H}_2\text{O}$, Aldrich, 99.99% metal basis trace), neodymium(III) nitrate hexahydrate ($\text{Nd}(\text{NO}_3)_3 \cdot 6\text{H}_2\text{O}$, Aldrich, 99.99% metal basis trace) and thorium(IV) nitrate hydrate ($\text{Th}(\text{NO}_3)_4 \cdot \text{H}_2\text{O}$, puriss. spez. Aktivität: 0.0467 uCi/g) were used as received. Concentrated nitric acid (65% HNO_3) was bought from Carlo Erba. Diethyl-2-(acrylamido)ethyl phosphonate (DAAmEP) was bought from Specific Polymers (Castries, France). All solution for sorption and ITC were prepared with Milli-Q water (18.2 M Ω .cm). All other products, catalysts and solvents employed in the syntheses were bought from Sigma-Aldrich and were used as received, without further purification.

Nuclear Magnetic Resonance (NMR) was carried out with Bruker Avance 400 (400 MHz) to record ^1H and ^{31}P NMR spectra with deuterated chloroform (CDCl_3), deuterium oxide (D_2O), or deuterated dimethylsulfoxide ($\text{DMSO}-d_6$) as deuterated solvents purchased from Eurisotop. For ^1H NMR, chemicals shift were referenced to the corresponding hydrogenated solvent residual peaks at 7.26, 4.79 or 2.50 ppm, respectively. H_3PO_4 was used as a reference for ^{31}P NMR.

Size Exclusion Chromatography (SEC) was performed using a PL-GPC 50 (Agilent) apparatus equipped with a RI refractive index detector. PolarGel M column was used at 50 °C with a flow of 0.8 mL·min⁻¹ calibrated with PMMA standards. Elution solvent used was dimethylacetamide (DMAc) (+0.1 wt% LiCl).

Cloud point (CP) measurement was performed using a PerkinElmer Lambda 35 UV/VIS spectrometer coupled with PerkinElmer Peltier temperature programmer system. The polymer aqueous solution of 10 g·L⁻¹ was prepared by dissolution of the polymer in Milli-Q water. Experiment was performed in a temperature ranging from 18 to 60 °C at 0.1 °C·min⁻¹. The wavelength was fixed at 500 nm.

2.2. Synthesis

2.2.1. Synthesis of poly(diethyl-2-(acrylamido)ethyl phosphonate) (P(DAAmEP))

Diethyl-2-(acrylamido)ethyl phosphonate (DAAmEP) monomer (1 g, 4.25 mmol) was dissolved in dimethylsulfoxide (DMSO) (8.5 mL) containing azobisisobutyronitrile (AIBN) (0.02 g, 0.124 mmol). After three of N₂-vacuum cycles, reaction solution was put in oil bath heated at 70 °C. Polymerization lasted for 8 hours to reach 100% conversion. Poly(diethyl-2-(acrylamido)ethyl phosphonate) (P(DAAmEP)) (0.96 g, yield: 96%) was obtained through dialysis with 3.5 kD cut-off membrane in distilled water for five days.

¹H NMR (400 MHz, δ (ppm), CDCl₃): 1.35 (m, -CH₃, -CHCH₂), 2.09 (m, -PCH₂), 2.33 (m, -COCH), 3.51 (m, -NHCH₂), 4.12 (m, CH₃CH₂O)

³¹P NMR (400 MHz, δ (ppm), CDCl₃): 29.37 (Figure SI 31)

2.2.2. Synthesis of poly(2-(acrylamido)ethyl phosphonic acid) (hP(DAAmEP))

Poly(diethyl-2-(acrylamido)ethyl phosphonate) (P(DAAmEP)) (0.302 g, 1.28 mmol) was dissolved in anhydrous dichloromethane (DCM) (5 mL) under nitrogen. After one hour, trimethylsilyl bromide (TMSBr) (0.572 g, 6.48 mmol) was added dropwise. The reaction was stirred overnight at room temperature. DCM was removed and methanol (30 mL) was added. Reaction lasted for 4 hours at room temperature. Poly(2-(acrylamido)ethyl phosphonic acid) (hP(DAAmEP)) (0.23 g, yield: 100%) was obtained after evaporation of methanol under reduced pressure.

^1H NMR (400 MHz, δ (ppm), D_2O): 1.48 (m, $-\text{CHCH}_2$), 1.64 (m, $-\text{PCH}_2$), 1.96 (m, $-\text{COCH}$), 3.35 (m, $-\text{NHCH}_2$)

^{31}P NMR (400 MHz, δ (ppm), D_2O): 26.63 (Figure SI 33)

2.2.3. Synthesis of poly(6-(acrylamido)hexylcarbamoylmethyl phosphonic acid) (hP(CPAAm6C))

Poly(diethyl-6-(acrylamido)hexylcarbamoylmethyl phosphonate) (P(CPAAm6C)) was prepared following the experimental procedure already described in the literature [146]. Hydrolysis of P(CPAAm6C) was carried out following the experimental procedure reported in the literature [112]. P(CPAAm6C) (0.38 g, 1.09 mmol), and TMSBr (0.87 g, 5.68 mmol) were dissolved in DCM (5 mL). The reaction was stirred overnight at room temperature. DCM was removed and methanol (25 mL) was then added. Reaction lasted for 4 hours at room temperature. Poly(6-(acrylamido)hexylcarbamoylmethyl phosphonic acid) (hP(CPAAm6C)) (0.26 g, yield: 100%) was obtained after evaporation of methanol under reduced pressure.

^1H NMR (400 MHz, δ (ppm), D_2O): 1.36 (m, $-\text{CHCH}_2$, $-\text{NHCH}_2\text{CH}_2\text{CH}_2$), 1.54 (m, $-\text{COCH}$, $-\text{NHCH}_2\text{CH}_2$), 2.85 (m, $-\text{PCH}_2$), 3.21 (m, $-\text{NHCH}_2$) (Figure SI 34)

^{31}P NMR (400 MHz, δ (ppm), D_2O): 17.32 (Figure SI 35)

2.2.4. Synthesis of poly(acryloyloxymethyl phosphonic acid) (hP(APC1))

Poly(diisopropyl(acryloyloxymethyl) phosphonate) (P(DiAPC1)) (0.15 g, 0.96 mmol) and TMSBr (0.58 g, 3.79 mmol) were dissolved in DCM (5 mL). The reaction was stirred overnight at room temperature. DCM was removed and methanol (15 mL) was added. Reaction lasted for 4 hours at room temperature. Poly(acryloyloxymethyl phosphonic acid) (hP(APC1)) (0.14 g, yield: 96%) was obtained after evaporation of methanol under reduced pressure.

^1H NMR (400 MHz, δ (ppm), $\text{DMSO}-d_6$): 1.65-2.37 (m, $-\text{CHCH}_2$, $-\text{CCH}$), 4.17 (m, $-\text{PCH}_2$), 6.06 (m, $-\text{OH}$)

^{31}P NMR (400 MHz, δ (ppm), $\text{DMSO}-d_6$): 14.42 (Figure SI 23)

2.3. Sorption experiments by Isothermal Titration Calorimetry (ITC)

2.3.1. Preparation of metal ions and polymers aqueous solutions

The aqueous solutions of Gd(III), Ce(III), Nd(III) and Th(IV) were prepared by dissolving respectively $\text{Gd}(\text{NO}_3)_3 \cdot 6\text{H}_2\text{O}$, $\text{Ce}(\text{NO}_3)_3 \cdot 6\text{H}_2\text{O}$, $\text{Nd}(\text{NO}_3)_3 \cdot 6\text{H}_2\text{O}$, and $\text{Th}(\text{NO}_3)_4 \cdot \text{H}_2\text{O}$ in Milli-Q water. P(DAAmEP), hP(DAAmEP), hP(CPAAm6C) and hP(APC1) aqueous solutions were prepared by dissolving the polymer in Milli-Q water. The concentrations were expressed taking into account the concentrations of the monomer unit. The different combinations for the concentrations of polymer or metal ion aqueous solutions are summarized in Table 7. The pH of the metal ions or polymers aqueous solutions was modified to pH=1 with $1 \text{ mol} \cdot \text{L}^{-1}$ HNO_3 solution (prepared from the dilution of concentrated HNO_3 (65%)). The dilution after pH adjustment was carefully considered and the new concentrations of ions or polymers aqueous solutions were recalculated and were taken into account for speciation and thermodynamic calculation.

[P]* \ [C]*	Gd	Ce	Nd	Th
P(DAAmEP)	63 14.35	63 14.35	63 14.35	63 31
hP(DAAmEP)	17 14.35	17 14.35	17 14.35	17 14.35
hP(CPAAm6C)	17 14.35	38 36	38 36	
hP(APC1)	17 14.35	17 14.35	17 14.35	

* Unit is $\text{mmol} \cdot \text{L}^{-1}$

Table 7. Polymers and metal ions aqueous solution concentrations used in sorption experiment.

2.3.2. Isothermal Titration Calorimetry (ITC) experiments

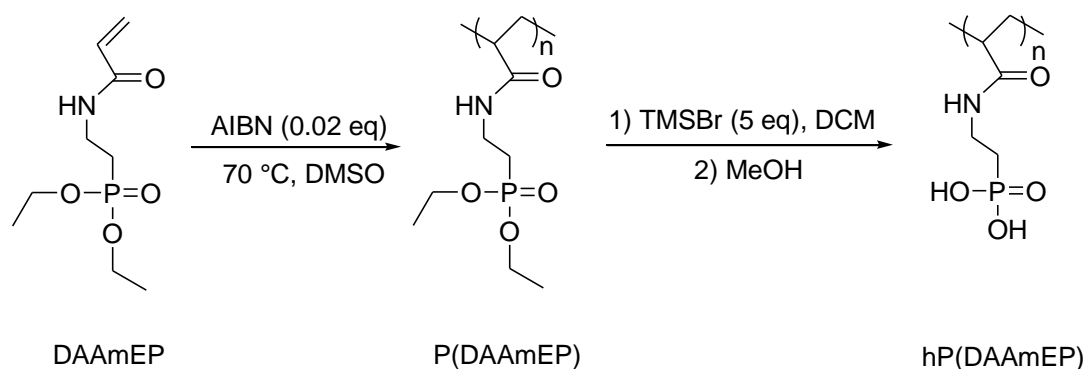
ITC experiments were performed with a TAM III multi-channel calorimetric device, which was equipped with Nanocalorimeters and Micro Reaction System. The experimental system

comprised a computer-controlled micro-syringe injection device. A stock solution of a given metal cation solutions was injected in a controlled manner to stainless steel sample ampoule serving as a calorimetric cell. The sample cell was filled with the ligand solution of a given polymer for a sorption experiment. Similar experiment was performed with metal successive injection in the solvent (acidified aqueous solution without ligand), in order to remove the thermal effect due to the dilution. The initial volume in the cell (of the ligand or of the acidified water) was 800 μL . Measurements were carried out at 298 K. A complete experiment consisted in a series of 25 injections of 10 μL (injection duration of 10 seconds). The time between two injections was 45 minutes to ensure complete return to the baseline before the next injection. Homogeneity of the solutions was maintained using a gold stirrer at 95 rpm.

3. Results and discussion

3.1. Polymer synthesis

First work dealt with the synthesis of various phosphorous-based polyacrylamides. In particular, polymerization of diethyl-2-(acrylamido)ethyl phosphonate (DAAmEP) by free radical polymerization in the presence of AIBN at 70 °C in DMSO allowed the obtaining of the corresponding poly(diethyl-2-(acrylamido)ethyl phosphonate) (P(DAAmEP)) (Scheme 16).



Scheme 16. Polymerization of diethyl-2-(acrylamido)ethyl phosphonate (DAAmEP) leading to P(DAAmEP), and hydrolysis leading to hP(DAAmEP)

^1H NMR spectrum (Figure 26) showed that the polymerization was successful, with the presence of the peaks corresponding to the P(DAAmEP) chemical structure. ^{31}P NMR (see

Supporting information, Figure SI 31) also showed one single peak at 29.3 ppm. Characterization by SEC (see Supporting information, Figure SI 32) permitted to determine the molecular weight (M_n) and the dispersity (\mathcal{D}) of the P(DAAmEP), equal to 9000 g·mol⁻¹ and 3, respectively.

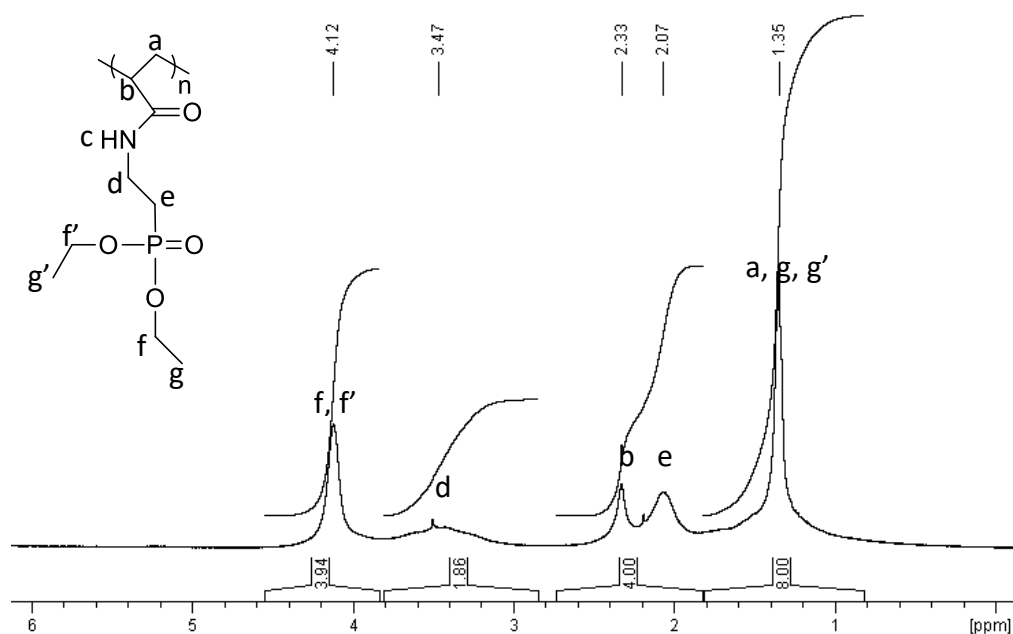


Figure 26. ¹H NMR spectrum (400 MHz, CDCl₃) of poly(diethyl-2-(acrylamido)ethyl phosphonate) (P(DAAmEP))

Thermosensitivity of the P(DAAmEP) was studied by measuring the transmittance of the polymer aqueous solution as a function of the temperature (Figure 27). The latter proved to have a cloud point (CP) equal to 23 °C in Milli-Q water. This result is valuable as it means that metal-polymer complexes could be separated from the water by increasing the temperature above the CP, leading to a possible easy filtration step.

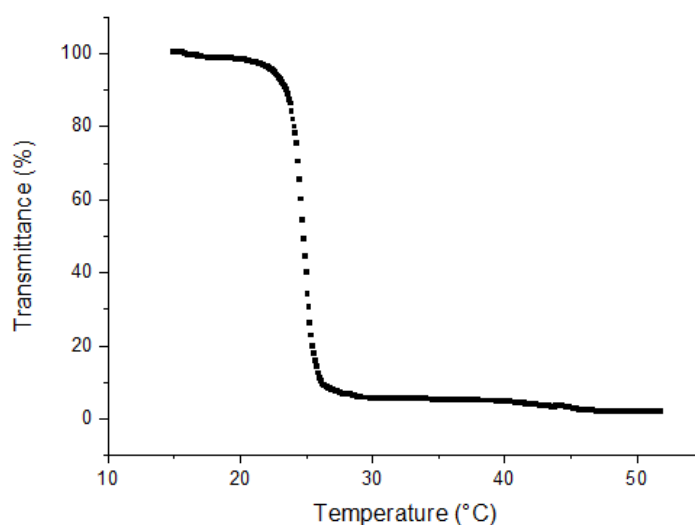


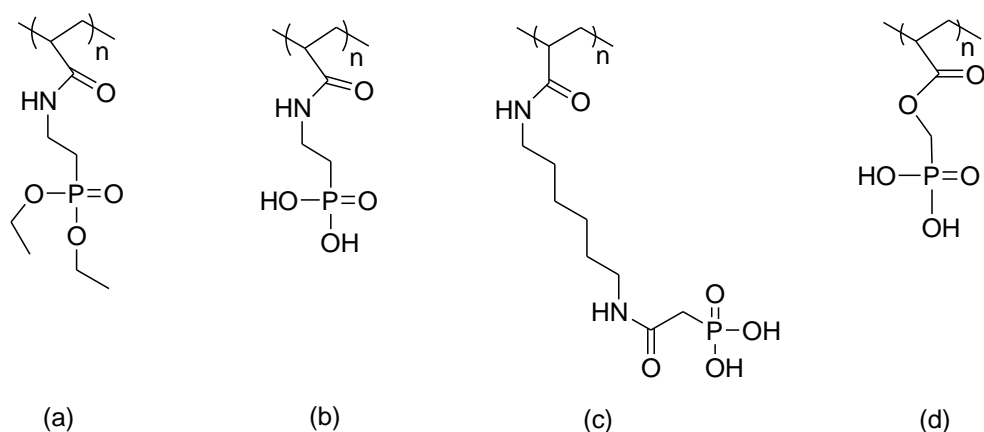
Figure 27. Transmittance in a function of the temperature for aqueous solution ($10 \text{ g}\cdot\text{L}^{-1}$) of poly(diethyl-2-(acrylamido)ethyl phosphonate) (P(DAAmEP)). Ramp of temperature was $0.1 \text{ }^\circ\text{C}\cdot\text{min}^{-1}$ from 15 to $55 \text{ }^\circ\text{C}$.

In order to study the influence of the phosphonate moiety on the sorption properties, hydrolysis of P(DAAmEP) was carried out (Scheme 16), using experimental procedure already described in the literature [217]. Reaction was carried out in the presence of trimethylsilyl bromide (TMSBr) followed by a methanolysis. Resulting poly(2-(acrylamido)ethyl phosphonic acid) (hP(DAAmEP)) was characterized by ^1H and ^{31}P NMR (Figure 28 and see Supporting information, Figure SI 33, respectively). ^1H NMR spectrum confirmed that the hydrolysis was successful as signals corresponding to the ethoxy groups borne by the phosphorous atom in the initial P(DAAmEP) have disappeared. ^{31}P NMR showed a shift of the signal from 29.3 to 26.6 ppm, going from P(DAAmEP) to hP(DAAmEP) polymer. Analysis of the transmittance as a function of the temperature proved that the hP(DAAmEP) polymer was not thermosensitive due to the high hydrophilic character of the phosphonic acid moieties. Even if hP(DAAmEP) was not thermosensitive, it was important to study as phosphonic acid groups proved to be of great interest for the sorption of lanthanides or actinides [97, 102, 111, 112, 114, 189, 214]. Additionally, phosphonic acid-based polymers can flocculate in water after the complexation of cations, which has already been proven for instance in the case of poly(6-(acrylamido)hexylcarbamoylmethyl phosphonic acid) (hP(CPAAm6C)) [149], and, as a result, it appeared to be interesting to also study this possibility in the case of hP(DAAmEP) polymer.

Figure 28. ^1H NMR spectrum (400 MHz, D_2O) of poly(2-(acrylamido)ethyl phosphonic acid) (hP(DAAmEP))

To achieve an exhaustive study on phosphonic acid-based polymers, poly(6-(acrylamido)hexylcarbamoylmethyl phosphonic acid) (hP(CPAAm6C)) and poly(acryloyloxymethyl phosphonic acid) (hP(APC1)) were synthesized, following already reported experimental procedures [112, 218]. hP(CPAAm6C) was prepared from poly(diethyl-6-(acrylamido)hexylcarbamoylmethyl phosphonate) (P(CPAAm6C)), which showed a molecular weight (M_n) and a dispersity (\mathcal{D}), determined by SEC, equal to $16000 \text{ g}\cdot\text{mol}^{-1}$ and 1.6, respectively. Concerning hP(APC1), starting poly((diisopropyl(acryloyloxymethyl) phosphonate) (P(DiAPC1)) had a molecular weight (M_n) and a dispersity (\mathcal{D}) equal to $5000 \text{ g}\cdot\text{mol}^{-1}$ and 1.8, respectively. hP(CPAAm6C) and hP(APC1) could not be characterized by SEC as phosphonic acid groups could be retained on the chromatographic column used.

To conclude, different polymers were prepared (Scheme 17): P(DAAmEP) polyacrylamide bore a phosphonated ester complexing group and was thermosensitive, hP(DAAmEP) polyacrylamide was not thermosensitive but could lead to flocculation after complexation. Two other polymers were synthesized and compared to the first ones: hP(CPAAm6C) polyacrylamide proved to flocculate after complexation of uranium [149] and hP(APC1) acrylate showed complexation property for lanthanides [218].



Scheme 17. Chemical structures of P(DAAmEP) (a), hP(DAAmEP) (b), hP(CPAAm6C) (c) and hP(APC1) (d) studied for their sorption properties

Complexation interactions were studied using calorimetric tool, in the present case using Isothermal Titration Calorimetry (ITC) technique. It permitted to indirectly and rapidly characterize thermodynamically the complexation through the evaluation of the heat effect associated to the complexation/chelation when a given cation was injected in a solution containing a given polymer. It was used here to characterize the complexing properties of the four synthesized polymers with Gd(III), Ce(III), Nd(III) and Th(IV).

Beforehand, the speciation diagrams of Gd(III), Ce(III), Nd(III) and Th(IV) aqueous solutions with the corresponding concentrations, are reported in Supporting information (see Supporting information, Figure SI 5 to Figure SI 8, Figure SI 24 to Figure SI 27, Figure SI 36 and Figure SI 37). This allowed verifying that there was no hydrolysis and no precipitation of the cations.

3.2. Sorption results of P(DAAmEP) and hP(DAAmEP) with Gd(III), Ce(III) and Nd(III)

The complexing properties of phosphonated ester P(DAAmEP) polymer and phosphonic acid hP(DAAmEP) polymer (structures in Scheme 17) for Gd(III), Ce(III) and Nd(III) was studied using ITC. Figure 29 illustrates the thermograms obtained in ITC sorption experiment of P(DAAmEP) and hP(DAAmEP) with Gd(III) at 298 K and pH=1. Figure 29(a) shows the thermogram of calorimetric titration of P(DAAmEP) by Gd(III) together with the dilution experiment and Figure 29(b) reports that of calorimetric titration of hP(DAAmEP) by Gd(III).

The thermograms of the other sorption experiments of P(DAAmEP) and hP(DAAmEP) with Ce(III) and Nd(III) are shown in Supporting information (see Supporting information, Figure SI 40 to Figure SI 43).

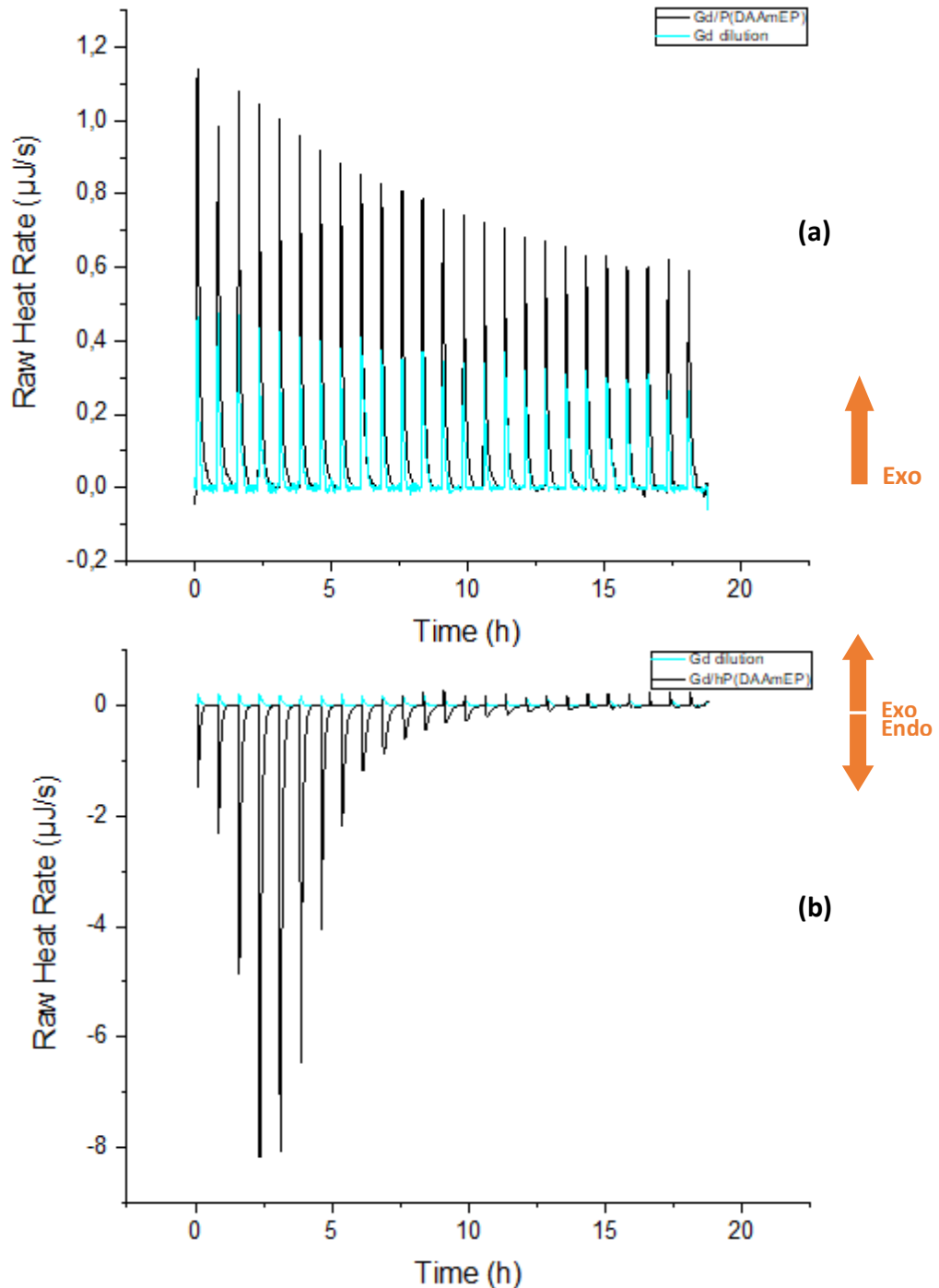
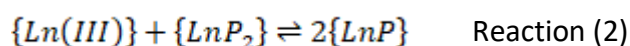
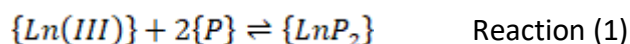


Figure 29. Processed thermal profiles Gd(III) ITC measurements on the P(DAAmEP) (a) or hP(DAAmEP) (b) aqueous solution of $14.35 \text{ mmol}\cdot\text{L}^{-1}$ (sorption experiment) together with the dilution experiments carried out with acidified water. The P(DAAmEP) system was titrated with $63 \text{ mmol}\cdot\text{L}^{-1}$ $\text{Gd}(\text{NO}_3)_3\cdot 6\text{H}_2\text{O}$ aqueous solution, whereas the hP(DAAmEP) was titrated with $17 \text{ mmol}\cdot\text{L}^{-1}$ $\text{Gd}(\text{NO}_3)_3\cdot 6\text{H}_2\text{O}$ aqueous solution. Experiments carried out at 298 K and $\text{pH}=1$, with 25 successive injections recorded with $10 \mu\text{L}$ for each injection of Gd(III) stock solution into $800 \mu\text{L}$ of P(DAAmEP) or hP(DAAmEP) polymer aqueous solution or acid water.

As shown in Figure 29(a), the dilution of Gd(III) aqueous solution and the sorption experiment between Gd(III) and P(DAAmEP) showed both exothermic character with a decreasing tendency, and with signals for the sorption being two times more intense. The small difference between the two signals indicated an interaction between Gd(III) and P(DAAmEP) relatively low in intensity. In Figure 29(b), the sorption experiment between Gd(III) and hP(DAAmEP) showed much stronger endothermic signals. The intense endothermic signals clearly demonstrated the interaction between Gd(III) and hP(DAAmEP). In addition, two tendencies were observed in the signals of interaction between Gd(III) and hP(DAAmEP). The intensity of endothermic signals increased in the four first injections, then the signals intensity decreased till there were only exothermic signals almost without variation at the end. The two tendencies in the signals indicated that there were probably two reactions in the complexation interaction between Gd(III) and hP(DAAmEP) [180, 193-195]. Based on the binding studies of the phosphonic acid or amine containing molecules in the literature [196, 197], a ‘successive binding sites model’ turned to be better adapted to our system, with two successive reactions taken into account:



To establish the relevant equation reactions, hP(DAAmEP) is indicated $\{P\}$; $\{Ln(III)\}$ represents the Ln(III) involved (Gd(III), Ce(III) or Nd(III)), as the exact species participating in the mechanism were not identified, they are noted $\{Ln(III)\}$. These reactions corresponded first to the beginning of titration, where there was an excess of phosphonic group $\{P\}$ in the cell and thus the reaction (1) was favourable; then, as Gd(III) moieties were added, the reaction (2) became dominant. Herein, thermodynamic parameters of interaction between Gd(III) and the h(PDAAmEP) was estimated by fitting experimental ITC data with the ‘successive binding sites model’ using the Levenberg–Marquardt non-linear curve-fitting algorithm.

Similar behaviours were observed for Ce(III) and Nd(III). For the P(DAAmEP) polymer, the thermograms (see Supporting information, Figure SI 40 and Figure SI 41(a)) exhibit small difference in the sorption and the dilution. For hP(DAAmEP) titrated by Ce(III) or Nd(III), the

particular shape of the thermograms (see Supporting information, Figure SI 42(a) and Figure SI 43(a), respectively) was also observed, with increase and decrease of the endothermic signals.

All these experimental data were fitted. For the three cations (Gd(III), Ce(III) and Nd(III)) with hP(DAAmEP), two successive reactions were used to fit the data with successive binding sites mode. The two K_a in the interactions of hP(DAAmEP) with the three Ln(III) corresponded respectively to the formation of $\{LnP_2\}$ (Reaction (1)) and the formation of $\{LnP\}$ (Reaction (2)). The results of the fit are shown in Supporting information (see Supporting information, Figure SI 39, Figure SI 42(b) and Figure SI 43(b) for Gd(III), Ce(III) and Nd(III) respectively).

For P(DAAmEP), one reaction was necessary to fit the data, 'independent model' from the Nanoanalyze software was used, and the fit are shown in Figure SI 38 for Gd(III) and Figure SI 41(b) for Nd(III)). Table 8 summarized the binding constant (K_a , representing the affinity of ligand) calculated for P(DAAmEP) and hP(DAAmEP) with Gd(III), Ce(III) and Nd(III).

Polymers	Metal ions	K_a (M^{-1})
P(DAAmEP)	Gd	$2.8 \cdot 10^1$
	Ce	signals too weak to be fitted
	Nd	$2.4 \cdot 10^2$
hP(DAAmEP)	Gd	$4.6 \cdot 10^4$
		$2.2 \cdot 10^5$
	Ce	$8.3 \cdot 10^4$
		$2.6 \cdot 10^5$
	Nd	$4.7 \cdot 10^4$
		$2.3 \cdot 10^5$

Table 8. Thermodynamic parameters at 298 K and under pH=1 condition of complexation of P(DAAmEP) for Gd(III), Ce(III) and Nd(III), and of complexation of hP(DAAmEP) with Gd(III), Ce(III) and Nd(III), results are calculated by fitting corresponding ITC heat data with 'independent model' for P(DAAmEP) in Nanoanalyze software; 'successive binding sites model' for hP(DAAmEP) with Levenberg–Marquardt non-linear curve-fitting algorithm in Microsoft Excel.

As shown in Table 8, for each metal ion, the two K_a values in the interaction with hP(DAAmEP) were both more important than those with P(DAAmEP). Even P(DAAmEP) and hP(DAAmEP) showed different mechanisms in complexing the Ln(III), hP(DAAmEP) still

showed much better affinity with the three Ln(III). In addition, the signals in the sorption experiment between Ce(III) and P(DAAmEP) were too weak to be fitted, it indicated that P(DAAmEP) probably did not complex Ce(III), or in a small extend. Comparing the K_a values of hP(DAAmEP) with the three Ln(III), pretty similar K_a values in corresponding successive reactions were remarked, the K_a for forming $\{LnP_2\}$ was around $5 \cdot 10^4$ and the K_a for forming $\{LnP\}$ was around $2 \cdot 10^5$. It meant that hP(DAAmEP) did not show much selectivity among Gd(III), Ce(III) and Nd(III). For P(DAAmEP), it showed complexing property for Gd(III) and Nd(III) but not for Ce(III). The K_a for Nd(III) was higher than the one for Gd(III), which may indicate its slight selectivity with Nd(III).

In general, the phosphonic acid hP(DAAmEP) polymer showed better affinity for Gd(III), Ce(III) and Nd(III) than the phosphonated ester P(DAAmEP) polymer. The complexing properties of hP(DAAmEP) for the three Ln(III) were pretty similar and hP(DAAmEP) did not show selectivity among Gd(III), Ce(III) and Nd(III). Meanwhile, P(DAAmEP) showed different performances in complexing the three Ln(III). We can conclude that the different complexing performances of P(DAAmEP) for the three Ln(III) was probably brought by the diethyl phosphonate group (structures in Scheme 17), whose phosphonic oxygen is a softer donor than that in phosphonic acid group. The phosphonic acid group, as a hard ligand, might make the hP(DAAmEP) polymer showing good and pretty similar performances in complexing Gd(III), Ce(III) and Nd(III) [189, 214].

3.3. Sorption results of P(DAAmEP) and hP(DAAmEP) with Th(IV)

Besides the three Ln(III), Th(IV) as the metal selected to represent the radioactive contaminants in effluents, was also tested with phosphonated ester P(DAAmEP) polymer and hP(DAAmEP) phosphonic acid polymer. The thermograms of ITC sorption experiments of P(DAAmEP) and hP(DAAmEP) with Th(IV) are reported in Figure 30. It shows the thermogram of calorimetric titration of P(DAAmEP) or hP(DAAmEP) by Th(IV) (sorption experiment) in acidified water (pH=1) together with the dilution experiment.

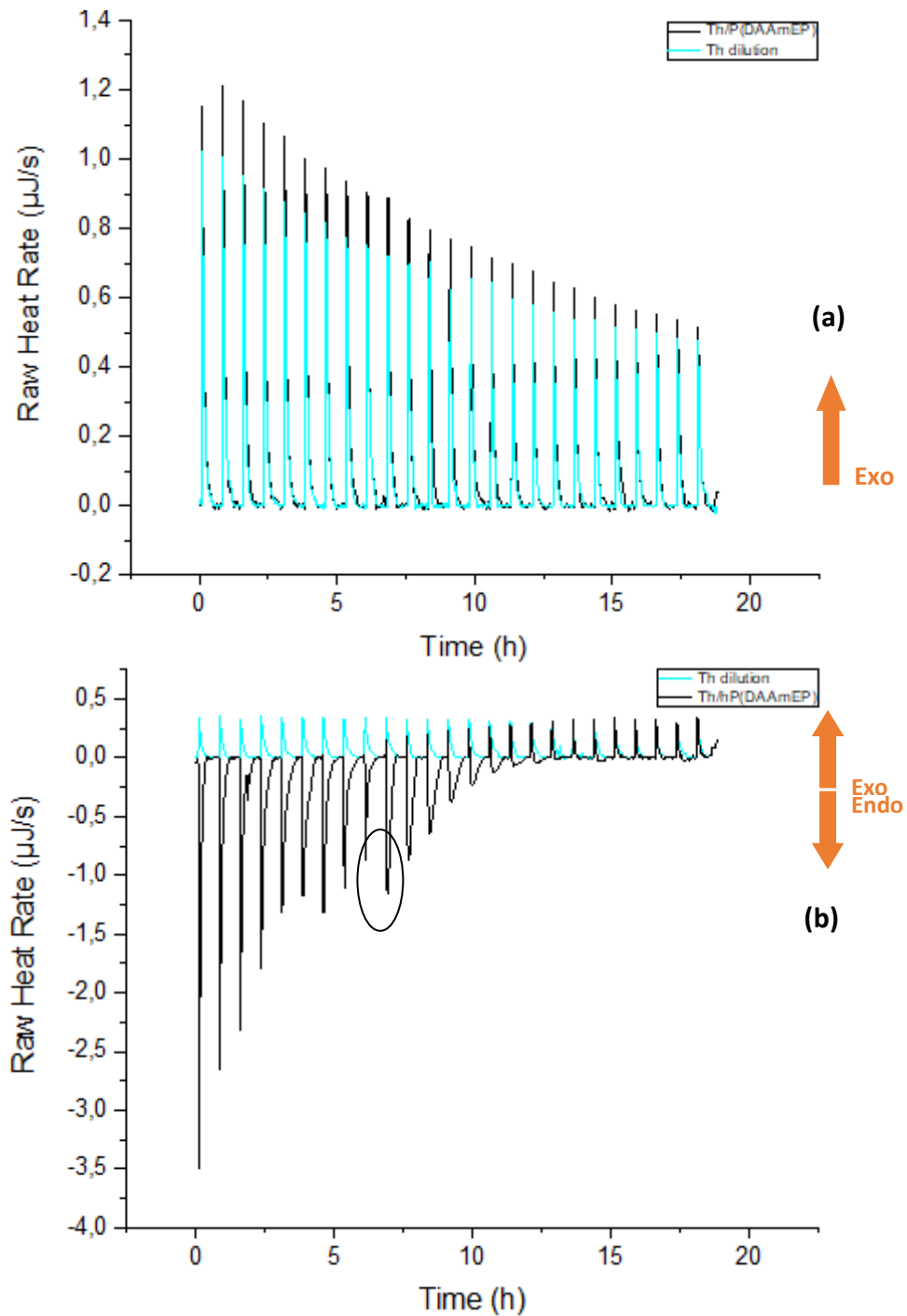
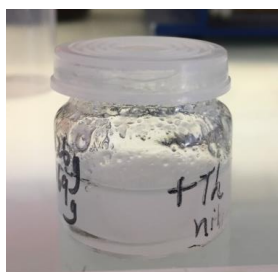


Figure 30. Processed thermal profiles Th(IV) ITC measurements on the P(DAAmEP) ($31 \text{ mmol}\cdot\text{L}^{-1}$) (a) or hP(DAAmEP) ($14.35 \text{ mmol}\cdot\text{L}^{-1}$) (b) aqueous solution (sorption experiment) together with the dilution experiments carried out with acidified water. The P(DAAmEP) system was titrated with $63 \text{ mmol}\cdot\text{L}^{-1}$ $\text{Th}(\text{NO}_3)_4\cdot\text{H}_2\text{O}$ aqueous solution, whereas the hP(DAAmEP) was titrated with $17 \text{ mmol}\cdot\text{L}^{-1}$ $\text{Th}(\text{NO}_3)_4\cdot\text{H}_2\text{O}$ aqueous solution. Experiments carried out at 298 K and $\text{pH}=1$, with 25 successive injections recorded with $10 \mu\text{L}$ for each injection of Th(IV) stock solution into $800 \mu\text{L}$ of P(DAAmEP) or hP(DAAmEP) polymer aqueous solution or acidified water.

As shown in Figure 30(a), the exothermic signals of the sorption experiment between Th(IV) and P(DAAmEP) showed similar intensity and tendency to that of the dilution experiment of Th(IV). The ITC heat data of sorption experiment of P(DAAmEP) with Th(IV) turned to be too weak to be fitted. It showed that there was almost no complexation between P(DAAmEP) and Th(IV).

For the sorption experiment between hP(DAAmEP) and Th(IV), as shown in Figure 30(b), strong endothermic signals were observed until there was only dilution effect of Th(IV) aqueous solution at the end. It demonstrated the relatively strong complexation interaction between Th(IV) and hP(DAAmEP). Furthermore, irregular but reproducible evolution of the decreasing in intensity was noticed from the 10th injection, as marked in Figure 30(b). Since flocculation was observed in the sample cells at the end of the sorption experiment, it might be caused by the appearance of the flocculation of the complexes of Th(IV) and hP(DAAmEP). After more tests by adding hP(DAAmEP) polymer aqueous solution into Th(NO₃)₄·H₂O aqueous solution at acidic pH and natural pH, the flocculation of the complexes of Th-hP(DAAmEP) was confirmed, as shown in Picture 1. This behaviour was not observed for the other cations. This could be due to the mechanism and to the various species involved in the interactions. Indeed, the speciation diagram obtained for Th(IV) exhibited different species distribution compared to the Ln(III). In particular, the speciation corresponding to the Th(IV) concentration of Figure 30 is displayed in Supporting information, Figure SI 7. This speciation diagram evidenced that the main moieties were ThNO₃³⁺ and Th⁴⁺, with the repartition of 94% and 6%, respectively. This was not the case for Gd(III), Nd(III) or Ce(III), where the ions were mainly present in their trivalent form (except for Nd at high concentration, see Supporting information, Figure SI 26) where NdNO₃²⁺ was 55% and Nd³⁺ 45%.



Picture 1. Flocculation of complexes of Th(IV) and poly(2-(acrylamido)ethyl phosphonic acid) (hP(DAAmEP)) observed by adding hP(DAAmEP) (14.35 mmol·L⁻¹) to Th(NO₃)₄·H₂O (17 mmol·L⁻¹) aqueous solution.

Because of the presence of flocculation during the experiment of hP(DAAmEP) with Th(IV), the recorded heat included not only the heat variation caused by the dilution and complexation, but also the flocculation. The concentration of the polymer solution in the sample cells decreased because of the flocculation. Thus, the ITC data obtained could not be properly fitted to extract the thermodynamic parameters of the complexation reaction between hP(DAAmEP) and Th(IV). Nonetheless, the ITC heat data is shown in Supporting information, Figure SI 44, the second tendency from the 10th point was also remarked in this graph, which demonstrated the impact of the appearance of flocculation on the ITC heat data measured.

As preliminary conclusions, it was demonstrated that the hP(DAAmEP) phosphonic acid containing polymer showed significant complexing properties for Th(IV), whereas the phosphonated ester containing P(DAAmEP) polymer did not show complexing property for Th(IV). Additionally, owing to the flocculation of the complexes of Th(IV) and hP(DAAmEP), hP(DAAmEP) might be used to separate Th(IV) from the Ln(III) and simplify the isolation of the complexes. However, the selectivity of hP(DAAmEP) between Th(IV) and Ln(III) should be verified with other methods.

To conclude, the complexing properties of P(DAAmEP) and hP(DAAmEP) towards Gd(III), Ce(III), Nd(III) (three Ln(III)) and Th(IV) (actinide) were evaluated. The phosphonic acid containing polymer (hP(DAAmEP)) showed much better complexing properties for Gd(III), Ce(III), Nd(III) and Th(IV) than the phosphonated ester containing polymer (P(DAAmEP)). hP(DAAmEP) showed pretty similar complexing property for Gd(III), Ce(III) and Nd(III), with no selectivity among the three Ln(III). It also showed good complexing properties for Th(IV) and their complexes flocculated at acid and natural pH. These results of hP(DAAmEP) confirmed the good affinity of phosphonic acid group for the lanthanides and actinides, as reported in literature [184, 189]. However, as a hard ligand, it did not show selectivity for different Ln(III). This is also the case for many hard ligands [214-216], like amide oxygen, ether oxygen... Concerning the flocculation of Th(IV)-hP(DAAmEP) complexes, it might be related to the higher coordination number of Th(IV) in aqueous solution containing nitrate [219], which is between 8 and 10. For P(DAAmEP), its phosphonated ester group is a softer ligand thus exhibits lower affinity for the Ln(III) compared to hP(DAAmEP) [189, 214].

Besides, P(DAAmP) did not complex Th(IV), however, another phosphonated ester polymer, namely poly(diethyl(6-acrylamido)hexylcarbamoylmethyl phosphonate) (P(CPAAm6C)), has showed selectivity for Th(IV) over Gd(III) [220]. The different complexing properties for Th(IV) of the two phosphonate-based polymers was explained by the carbamoylmethylphosphonate group, which proved to be efficient ligand for both lanthanides and actinides, whereas this was not observed for acrylamidoethyl group in the P(DAAmEP). The affinity range of hP(DAAmEP) between Th(IV) and Ln(III) is to be verified since no binding constant could be extracted for Th(IV). However, even the interactions between the phosphonated ester P(DAAmEP) polymer and the three Ln(III) were relatively weak, its thermosensitivity and different performances in complexing Gd(III) and Nd(III) might be interesting for specific applications.

3.4. Sorption results of hP(DAAmEP), hP(CPAAm6C) and hP(APC1) for Gd(III), Ce(III) and Nd(III)

Various structures of phosphonic acid binding sites (with ethylamine, acetamide or oxymethyl group) have finally been compared for their complexation of Ln(III). The following polymers hP(DAAmEP), hP(CPAAm6C) and hP(APC1) (Scheme 17) were tested with Gd(III), Ce(III) and Nd(III).

As in the case of hP(DAAmEP), the hP(CPAAm6C) and hP(APC1) phosphonic acid polymers exhibited two parts in the thermograms, therefore with two contributions for all the three Ln(III). All the thermograms and ITC heat curves are shown in the Supporting information, with the numbers of figures indicated in Table 9. Depending on the ion and ligand type, the two successive reactions on ITC heat curves were more or less clearly observed (see the discussion below for the Ce/hP(CPAAm6C) system). The corresponding ITC heat data curves were fitted as well with 'successive binding sites model' using Levenberg–Marquardt non-linear curve-fitting algorithm. The binding constant (K_a , the affinity of ligands for the metal ion) calculated by fitting the corresponding ITC sorption experiments data are regrouped with those of hP(DAAmEP) in Table 9.

Polymers	Metal ions	K_a (M^{-1})
hP(DAAmEP)	Gd Figure 29(b) and Figure SI 39	$4.6 \cdot 10^4$
		$2.2 \cdot 10^5$
	Ce Figure SI 42 (a and b)	$8.3 \cdot 10^4$
		$2.6 \cdot 10^5$
	Nd Figure SI 43 (a and b)	$4.7 \cdot 10^4$
		$2.3 \cdot 10^5$
hP(CPAAm6C)	Gd Figure SI 45 (a and b)	$6.9 \cdot 10^3$
		$3.3 \cdot 10^4$
	Ce Figure SI 46 (a and b)	$1.0 \cdot 10^3$
		$9.9 \cdot 10^3$
	Nd Figure SI 47 (a and b)	$5.0 \cdot 10^3$
		$1.2 \cdot 10^4$
hP(APC1)	Gd Figure SI 48 (a and b)	$9.1 \cdot 10^3$
		$2.1 \cdot 10^4$
	Ce Figure SI 49 (a and b)	$3.0 \cdot 10^3$
		$1.1 \cdot 10^4$
	Nd Figure SI 50 (a and b)	$9.9 \cdot 10^3$
		$1.1 \cdot 10^4$

Table 9. Binding constant (K_a) and stoichiometry (n) of complexation interactions of hP(DAAmEP), hP(CPAAm6C) and hP(APC1) polymers with Gd(III), Ce(III) and Nd(III) (at 298 K and under pH=1 condition), calculated by fitting corresponding ITC heat data with 'successive binding sites model' using Levenberg–Marquardt non-linear curve-fitting algorithm. For all systems (cation/polymer) the figures corresponding to the ITC thermograms and heat data curves are indicated.

In the previous paragraph (3.2.), similar complexing performance of hP(DAAmEP) for the three Ln(III) has been demonstrated. As shown in Table 9, hP(DAAmEP) showed higher K_a values in the two corresponding successive reactions for each Ln(III) compared to hP(CPAAm6C) and hP(APC1). This indicated the better affinity of hP(DAAmEP) with Gd(III), Ce(III) and Nd(III) than the two other polymers. For hP(CPAAm6C) and hP(APC1), their two K_a values for each Ln(III) were generally similar. In addition, in every complexation interaction reported in Table 9, the formation of $\{LnP\}$ (Reaction (2)) had a K_a higher than the formation of $\{LnP_2\}$ (Reaction (1)). This meant that the bi-ligand complex were only intermediate species. Then, when the metal quantity increased along the titration, the 1:1 species were more stabilized. This has to be correlated with the speciation diagram, which have shown that the nitrate counterions have also to be considered in the mechanism. hP(CPAAm6C) polymer showed slightly difference in corresponding K_a value for the interactions with the

three Ln(III), but stayed generally with $\times 10^3$ range for the first reaction and $\times 10^4$ range for the second reaction. In the case of Ce(III), even though this was clear in the thermogram (see Supporting information, Figure SI 46(a)), the successive binding mechanism on ITC heat curve (see Supporting information, Figure SI 46(b)) was less obvious than the others. Weaker binding constants K_a in both successive reactions was obtained. It might indicate that hP(CAAm6C) had less affinity for Ce(III) among the three Ln(III). For the hP(APC1) polymer, it also had K_a values of $\times 10^3$ range for the first successive reaction and $\times 10^4$ for the second one for each Ln(III). It showed as well relatively less affinity with Ce(III).

Overall, the three phosphonic acid containing polymers (hP(DAAmEP), hP(CPAAm6C) and hP(APC1)) demonstrated significant complexing properties for Gd(III), Ce(III) and Nd(III). hP(DAAmEP) showed clearly better affinity with all studied Ln(III) than the two other polymers. However, the selectivity of each polymer among Gd(III), Ce(III) and Nd(III) was hard to be concluded based on the K_a values obtained. As mentioned previously, the phosphonic acid groups are hard ligands and showed generally good affinity for the Ln(III) [184, 189], but without clear selectivity [214-216]. Concerning ion-ligand affinities, hard-soft acid-base character is one of the important criteria to consider, together with protonation of ligand and hydration which also could impact the chelating affinity [189]. The better affinity of hP(DAAmEP) for the studied Ln(III) was probably due to its different structure without oxygen atom besides the phosphonic acid group. In order to verify the selectivity of each polymer, increasing titration points in ITC sorption experiments to obtain more precious K_a values could be carried out. This could be confirmed with further measurements with increasing the number of data points for the first injections, for molar ratio lower than 0.02. In addition, sorption experiments with other methods, *e.g.* dialysis coupled with ICP-MS, will be necessary.

4. Conclusion

In this contribution, appropriate polymers for the complexation of metal ions were prepared. We focused on polyacrylamides as they could lead to thermosensitive or flocculating properties after complexation. Poly(diethyl-2-(acrylamido)ethyl phosphonate) (P(DAAmEP)) and its hydrolyzed form, namely poly(2-(acrylamido)ethyl phosphonic acid) (hP(DAAmEP)), were prepared by free radical polymerization followed by a hydrolysis,

respectively. Two other phosphonic acid polymers, namely poly(6-(acrylamido)hexylcarbamoylmethyl phosphonic acid) (hP(CPAAm6C)) and poly(acryloyloxymethyl phosphonic acid) (hP(APC1)), were also prepared in order to compare their complexing properties with those of the P(DAAmEP) and hP(DAAmEP) polyacrylamides. hP(CPAAm6C) was interesting to consider as it was already proved that this polymer could flocculate after sorption in some conditions. hP(APC1) was used to compare polyacrylamide and polyacrylate chemical nature of the polymers.

The sorption efficiency and more precisely the complexation interactions were analysed using calorimetric tool, in the present case Isothermal Titration Calorimetry (ITC) technique. It permitted to indirectly and rapidly thermodynamically characterize the complexation through the evaluation of the heat effect associated to the complexation/chelation. K_a calculated values based on the ITC heat data have been helpful for better understanding the influence of binding site structures on the selectivity of the ligands for some metal ions. In particular, it has been demonstrated that the poly(2-(acrylamido)ethyl phosphonic acid) (hP(DAAmEP)) showed much better complexing properties for Gd(III), Ce(III) and Nd(III) and Th(IV) than its corresponding diethyl phosphonated polymer (P(DAAmEP)). Nevertheless, the hP(DAAmEP) did not show obvious selectivity among the three Ln(III). In the particular case of Th(IV), the Th(IV)-hP(DAAmEP) complexes flocculated in aqueous solution at acidic or natural pH, which may simplify the complexes recovery. However, selectivity between the Ln(III) and Th(IV) has to be determined with other methods. Even if P(DAAmEP) showed relatively weak complexing property, its thermosensitivity could still be interesting for some specific applications.

The other two phosphonic acid polymers, poly(6-(acrylamido)hexylcarbamoylmethyl phosphonic acid) (hP(CPAAm6C)) and poly(acryloyloxymethyl phosphonic acid) (hP(APC1)) also showed good complexing properties for Gd(III), Ce(III) and Nd(III), but without much selectivity neither. In addition, hP(CPAAm6C) and hP(APC1) did not flocculate with Th(IV) in aqueous solution at any pH. To conclude, from all results obtained, the most interesting phosphonic acid-based polymer was poly(2-(acrylamido)ethyl phosphonic acid) (hP(DAAmEP)) as it showed efficient complexation and flocculating behavior. Further

Chapter 4

experiments have to be achieved to deeply study selectivity of this polymer towards a mixture containing Gd(III), Ce(III), Nd(III) and Th(IV) metal ions.

Conclusion

In this chapter, phosphonated-based polyacrylamides were synthesized for complexing the REEs and/or contaminants in effluents, in order to be applied in a new REEs separation procedure. Acrylamide group was considered as it could bring thermosensitive or flocculating property after the polymerization, which could simplify the recovery of metal-polymer complexes from water effluents. Poly(diethyl-2-(acrylamido)ethyl phosphonate) (P(DAAmEP)) was firstly synthesized using DAAmEP monomer. Free radical polymerization was used to limit the synthesis cost. Then, the hydrolyzed derivative, namely poly(2-(acrylamido)ethyl phosphonic acid) (hP(DAAmEP)), was prepared to be compared with the phosphonated ester form (P(DAAmEP)) in terms of complexing properties. Gadolinium (Gd), cerium (Ce) and neodymium (Nd), as most abundant REEs in minerals, were selected to be evaluated with P(DAAmEP) and hP(DAAmEP). Thorium (Th), representing the radioactive contaminants, was also considered with the two polymers. In addition, previous related work has demonstrated some complexing properties of two other phosphonic acid polymers, poly(6-(acrylamido)hexylcarbamoylethyl phosphonic acid) (hP(CPAAm6C)) and poly(acryloyloxymethyl phosphonic acid) (hP(APC1)). hP(CPAAm6C) proved to selectively flocculate with uranium (U) in Gd/Th/U mixture aqueous solution. hP(APC1) showed complexing properties towards Ce and Nd. In order to better understand the influence of different phosphonic acid structures on complexing metal ions, particularly the REEs, hP(CPAAm6C) and hP(APC1) were also prepared and evaluated with Gd, Ce and Nd in this chapter, and compared to hP(DAAmEP). All the sorption experiments were carried out using Isothermal Titration Calorimetry (ITC). The ITC data allowed calculating binding constant, which permitted comparison of complexing properties of the polymers. K_a binding constant have been helpful to better understand the influence of binding site structures, notably on the selectivity of the ligands for the metal ions.

Comparing the thermosensitive P(DAAmEP) polyacrylamide with its hydrolyzed hP(DAAmEP) derivative, the phosphonic acid-based polymer (not thermosensitive) showed much better complexing properties towards Gd(III), Ce(III), Nd(III) and Th(IV). For the three Ln(III), hP(DAAmEP) had pretty similar binding constants for all the three cations, which

indicated that it did not show selectivity among the three Ln(III). For Th(IV), hP(DAAmEP) showed flocculation property once complexing Th(IV), and it was confirmed at acidic and natural pH. Thus, even if hP(DAAmEP) was not thermosensitive, its flocculation character with Th(IV) might be used for simplifying the purification of REEs. However, the selectivity of hP(DAAmEP) between the Ln(III) and Th(IV) is to be further studied with other methods, *e.g.* dialysis coupled with ICP-MS technique. Concerning P(DAAmEP), even if it showed less strong complexing properties for Gd(III) and Nd(III), its thermosensitivity still could be interesting for simplifying the recovery of its complexes. In addition, P(DAAmEP) did not show complexing property for Ce(III) and Th(IV).

Two other phosphonic acid-based polymers, hP(CPAAm6C) and hP(APC1), were also evaluated with the selected Ln(III) for comparison with hP(DAAmEP), in order to better understand the influence of different phosphonic acid binding sites on complexing affinity. hP(CPAAm6C) and hP(APC1) both showed good complexing properties for Gd(III), Ce(III) and Nd(III). There was not much difference in their binding constants for each cation. A general comparison showed that hP(DAAmEP) had a little better affinity for all the three Ln(III) than the two other phosphonic acid polymers. However, because of the presence of two successive reactions in the complexation interactions between the phosphonic acid polymers and the Ln(III), it was difficult to compare their binding constants to conclude on the influence of chemical structures on their affinity for the Ln(III). Nevertheless, hP(CPAAm6C) and hP(APC1) did not show flocculation property. Thus, hP(DAAmEP) appeared as a good potential sorbent for Ln(III) and An.

General conclusion and prospect

As techniques for REEs purification and separation is currently being intensively demanded and studied for recycling the REEs, the present work aimed at synthesizing original water-soluble phosphorous-based polymers for complexing the REEs or the contaminants found in the effluents. The phosphorous polymers were specifically designed to selectively complex the lanthanides (the major REEs) or the actinides (the major contaminants). Additionally, in order to simplify the recovery of complexes from effluents by changing the solubility of polymers, thermosensitive (insolubility over cloud point) or flocculating (after complexing cations) properties of polymers were also considered. Concerning the targeted metal ions, gadolinium (Gd), cerium (Ce) and neodymium (Nd), as the three most abundant REEs in minerals, were studied; thorium (Th), as one of the main contaminants, was also evaluated.

Some original polymers have been developed in our team (thesis of Dr Gomes Rodrigues) and proved to be interesting in REEs purification. Thermosensitive poly(diethyl-6-(acrylamido)hexylcarbamoylmethyl phosphonate) (P(CPAAm6C)) (LCST=42 °C in Milli-Q water) notably demonstrated to be selective for Th(IV) in a Gd/Th/U mixture aqueous solution at acidic pH; its hydrolyzed hP(CPAAm6C) derivative has shown selective flocculation property with uranium (U) in Gd/Th/U mixture aqueous solution at acidic pH [149].

Based on these results, an innovative process was designed to extract the REEs using the synthesized water-soluble and chelating polymers, where the strategy was to separate the REEs from the contaminants and/or individually through the selectivity of these phosphorous polymers (Figure 31). The polymer 1 (P(CPAAm6C)) was thermosensitive, the polymer 2 (hP(CPAAm6C)) flocculated with U(VI) in aqueous solution. Therefore, when putting the two polymers in effluents containing Gd, Ce, Nd (REEs) and Th, U (contaminants), the complexes of polymer 2 and U(VI) could be isolated by filtration at the first time, and the complexes of polymer 1 with Th(IV) could be isolated by precipitation after heating. Then, a third polymer (polymer 3) will be thus necessary to selectively complex the lanthanides (Gd, Nd and Ce), with thermosensitive or flocculating properties.

Figure 31. Designed phosphorous polymers and ideal process to be developed for separating and isolating REEs from phosphorous water-soluble polymeric sorbents

For such purpose, we firstly continued the previous work on P(CPAAm6C) derivatives. P(CPAAm6C) was prepared and then mono-hydrolyzed for the first time leading to mhP(CPAAm6C). Both polymers were evaluated with Gd(III) and Th(IV). ITC and dialysis coupled of ICP-MS sorption experiments confirmed the selectivity of P(CPAAm6C) with Th(IV) and demonstrated the selectivity of mhP(CPAAm6C) with Gd(III). Additionally, mhP(CPAAm6C) (not thermosensitive) also showed flocculation properties in Gd/Th/U mixture solution. Therefore, a further study should be carried out to check the selectivity of mhP(CPAAm6C) amongst Gd(III), Th(IV) and U(VI), and the type of metal ion involved (Gd or U) in the flocculated complexes with mhP(CPAAm6C). Depending on the future results, mhP(CPAAm6C) could be decided to be applied in the innovative REEs separation procedure (Figure 31, polymer 3) to recover Gd(III) or not.

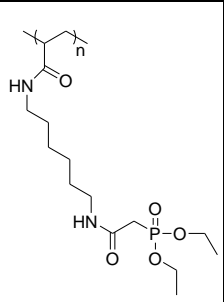
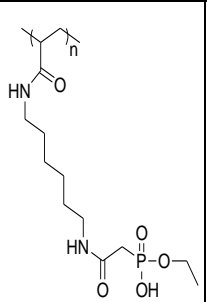
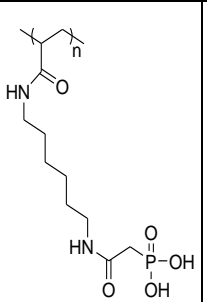
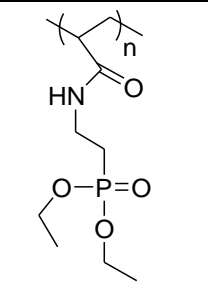
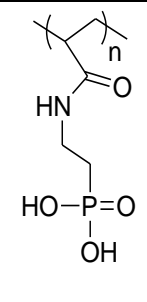
Then, other phosphonate-based polymers were developed and studied for selectively complex the REEs. The targeted polymer should bear an acrylamide and an oxymethyl phosphonate group, which had not been tested yet with the REEs. Unfortunately, the ideal monomer was not synthesized (chapter 3) but different oxymethyl phosphonate acrylate monomers, bearing diisopropyl (DiAPC1), dimethyl (APC1), or phosphonic acid (hAPC1) groups were prepared at last. Only the water-soluble corresponding P(APC1) and hP(APC1) polymers, together with the three monomers, were evaluated for the complexation of

valuable REEs, Ce(III) and Nd(III). ITC sorption experiments results demonstrated significant complexing properties of the phosphonic acid polymer (hP(APC1)) for both Ce(III) and Nd(III). The phosphonated ester polymer (P(APC1)) and the three monomers did not show complexation for Ce(III) and Nd(III). However, hP(APC1) was not thermosensitive. These results demonstrated again the good complexing properties of phosphonic acid group in the polymer, even without much selectivity. Thus, phosphonic acid polymers could be efficient sorbent for the Ln(III) but lack of thermosensitivity or flocculation should lead to their use in polymer enhanced ultrafiltration precesses.

In the last chapter, the use of phosphonate acrylamide containing monomer, namely diethyl-2-(acrylamido)ethyl phosphonate (DAAmEP) was highlighted. It could possibly lead to thermosensitivity after polymerization and complexing properties owing to phosphonated ester functional groups. P(DAAmEP) homopolymer obtained with free radical polymerization proved to be thermosensitive with a cloud point around 23 °C measured in Milli-Q water. P(DAAmEP) was then fully hydrolyzed to lead to hP(DAAmEP). Both P(DAAmEP) and hP(DAAmEP) were evaluated towards Gd(III), Ce(III), Nd(III) and Th(IV), in order to study their ability to complex and possibly separate the REEs. By comparing the binding constants calculated from ITC data, the phosphonic acid hP(DAAmEP) polymer showed much better complexation for the Ln(III) tested than the phosphonated ester P(DAAmEP) polymer. hP(DAAmEP) had pretty similar binding constants in complexing the three Ln(III), which meant that it had almost no selectivity among them. It also proved to complex Th(IV) and, in that case, the resulting complexes flocculated in aqueous solution at acidic and natural pH. This flocculation property could be applied in the REEs purification process, however, its affinity between the Ln(III) and Th(IV) should be checked to confirm that it will selectively flocculate with Th(IV) in effluents. On the reverse, thermosensitive P(DAAmEP) showed less strong complexing property for Gd(III) and Nd(III) than hP(DAAmEP) and did not complex Ce(III) and Th(IV). Its thermosensitivity and different complexing performances in complexing the Ln(III) and An could be still interesting for some applications. It is also important to mention that P(DAAmEP) was the only thermosensitive polymer in our study to show selectivity for some Ln(III) over An (even if U has to be tested). As a candidate for being used to complex the REEs in the new process (Figure 31), the challenge will be to improve its efficiency, playing on experimental conditions.

Finally, three phosphonic acid polymers (hP(DAAmEP), hP(CPAAm6C) and h(APC1)) were compared for the complexation of Gd(III), Ce(III) and Nd(III). Since the phosphonic acid polymers showed generally good complexing property for various metal ions, an insight of their chemical structures connected with their affinity for different Ln(III) was interesting to consider. ITC experiments showed that hP(CPAAm6C) and hP(APC1) showed both significant and similar complexing properties for the three Ln(III). hP(DAAmEP) showed a little better affinity than the two others for the three Ln(III).

All the valuable polymers evaluated and their complexing results obtained are summarized in the following table:

Polymeric chemical structure	 P(CPAAm6C)	 mhP(CPAAm6C)	 hP(CPAAm6C)	 P(DAAmEP)	 hP(DAAmEP)
Selectivity	Thorium	Gadolinium	Uranium	Gadolinium, Neodymium	Thorium
Character	Thermosensitive	Flocculating	Flocculating	Thermosensitive	Flocculating

Based on the innovative REEs purification and separation process shown in Figure 31, P(CPAAm6C) and hP(CPAAm6C) could be used for removing the radioactive contaminants (Th and U) and their complexes could be isolated by heating the effluent or filtration, respectively. With integrating the results of the present work, hP(DAAmEP) could also be used for removing Th after confirming its selectivity between the Ln(III) and the An; mhP(CPAAm6C) might be used for separating the Gd(III) after checking its selectivity between Gd(III) and U(VI); P(DAAmEP) could be used for selectively recovering Gd(III) and Nd(III), even with less efficiency, after being evaluated with U(VI) to confirm its selectivity for the Ln(III).

Thus, in future work, the sorption experiments that have to be carried out, mainly to confirm the selectivity of these valuable polymers are: i) for hP(DAAMEP), sorption experiments with dialysis coupled with ICP-MS by immersing hP(DAAMEP) into Gd/Th/U mixture aqueous solution, and measurements of the Gd, Th and U concentrations before and after dialysis might indicate its selectivity between the Ln(III) and An; ii) for mhP(CPAAM6C), similar sorption experiments could be carried out for confirming its selectivity in the mixture of Gd/Th/U aqueous solution; iii) for P(DAAMEP), ITC sorption experiments with U(VI) could be an efficient way to calculate its binding constant that could be compared with those for Gd(III) and Nd(III), in order to confirm its selectivity for Ln(III). Sorption experiments using dialysis with Gd/Nd/U aqueous solution mixture might be another way to check its selectivity between Ln(III) and An. Then, depending on the results of these sorption experiments, the innovative REEs purification and separation process (Figure 31) will be more finalized and complexing properties of these valuable polymers will be better understood to develop more competitive polymeric sorbents.

To conclude, several new valuable polymers were developed and studied for a potential application in an innovative REEs purification and separation process. This innovative process will be more and more accurate and efficient, involving different thermosensitive or flocculating polymeric sorbents. There are still developments to perform to better understand the complexing properties of these polymers and to improve the innovative REEs purification and separation process.

Supporting information

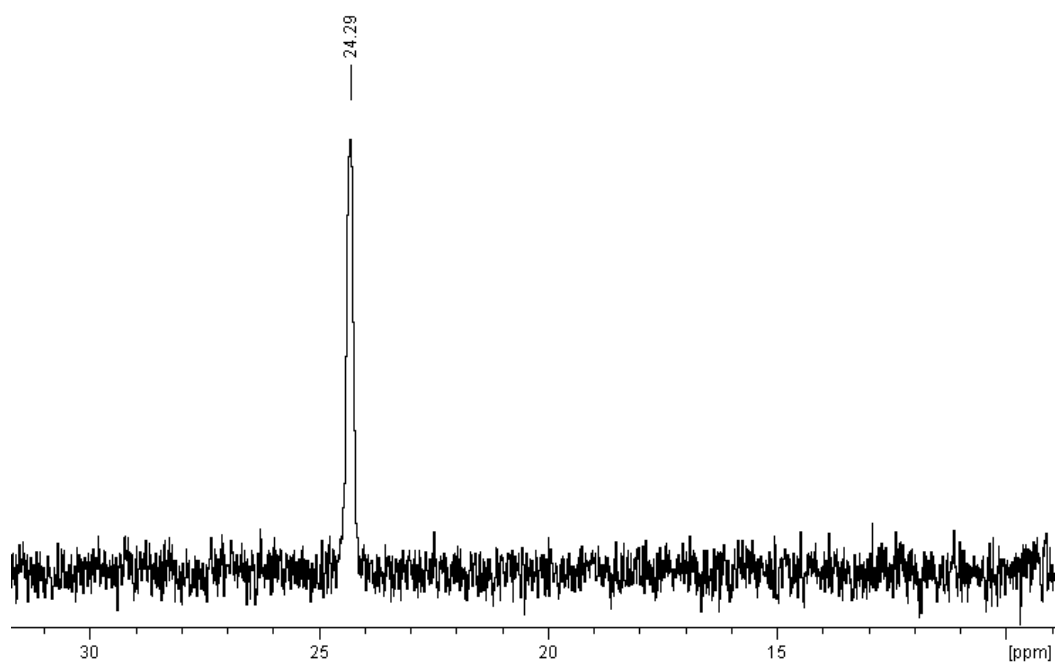


Figure SI 1. ^{31}P NMR spectrum (400 MHz, D_2O) of poly(diethyl-6-(acrylamido)hexylcarbamoylmethyl phosphonate) (P(CPAAm6C))

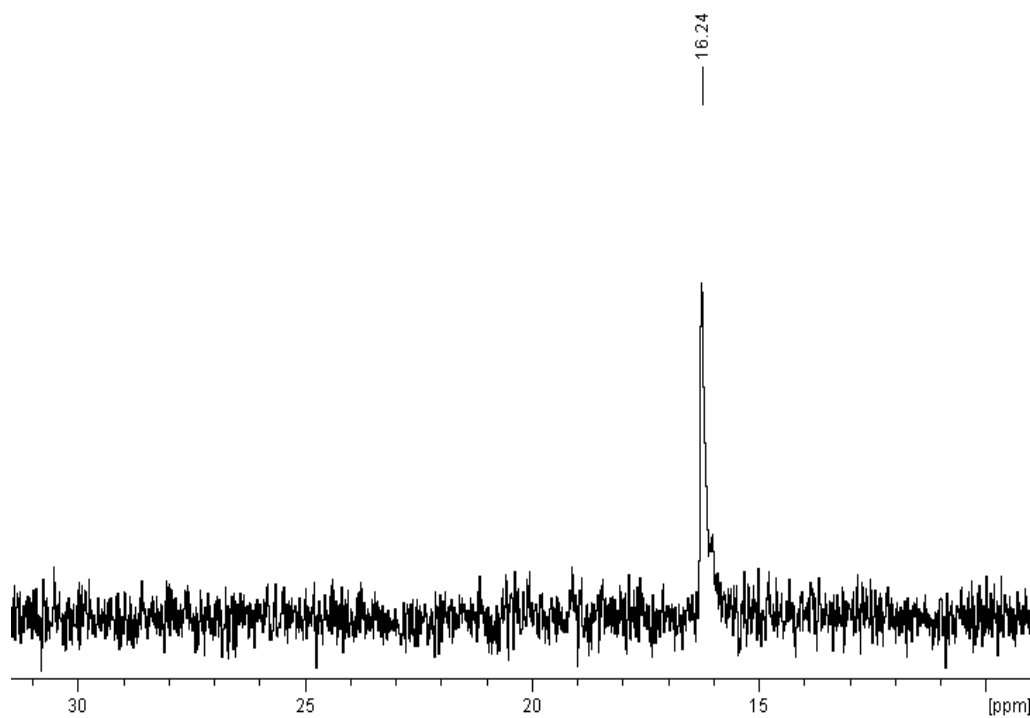


Figure SI 2. ^{31}P NMR spectrum (400 MHz, D_2O) of poly(6-(acrylamido)hexylcarbamoylmethyl phosphonic monoacid) (mhP(CPAAm6C))

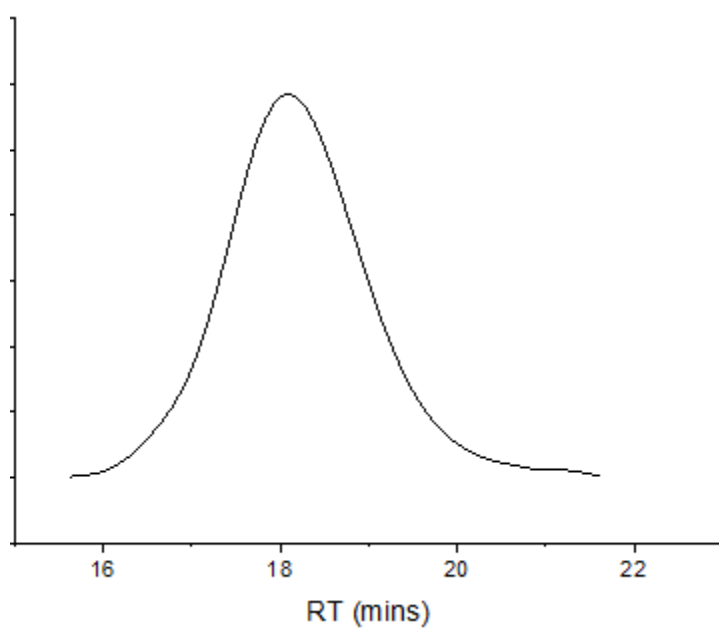


Figure SI 3. Size exclusion chromatogram of poly(diethyl-6-(acrylamido)hexylcarbamoylmethyl phosphonate) (P(CPAAm6C)) (DMAc eluent +LiCl 0.1% at 0.8 mL·L⁻¹; PMMA standards): $M_n=16000$ g·mol⁻¹, $\bar{D}=1.6$.

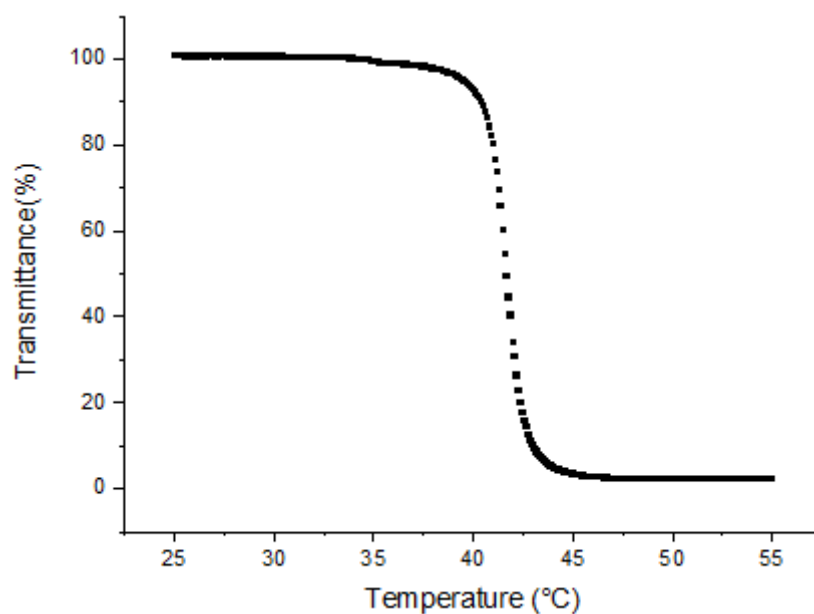


Figure SI 4. Transmittance curve as a function of temperature for aqueous solution (10 g·L⁻¹) of poly(diethyl-6-(acrylamido)hexylcarbamoylmethyl phosphonate) (P(CPAAm6C)): ramp of temperature was 0.1 °C·min⁻¹ from 25 to 55 °C.

Supporting information

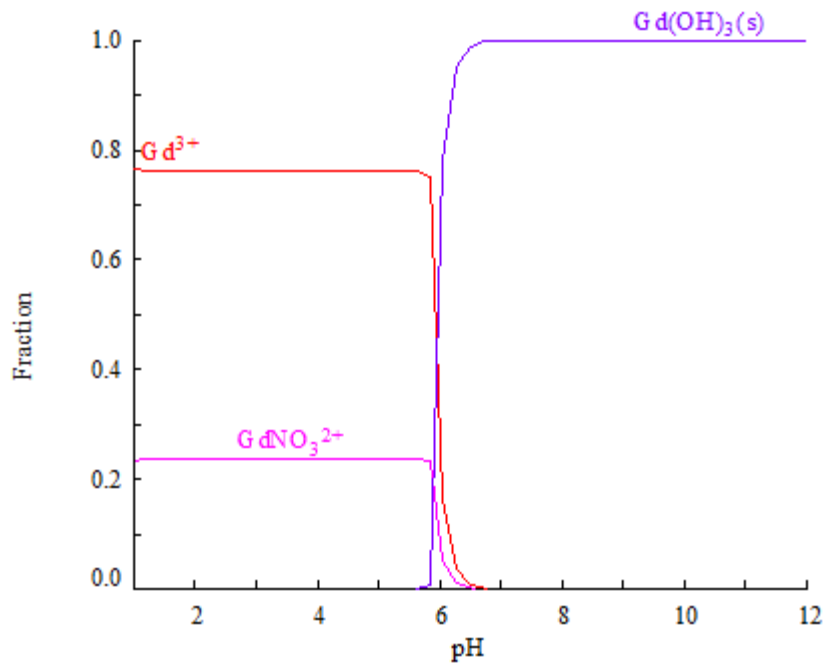


Figure SI 5. Speciation diagram of gadolinium nitrate ($Gd(NO_3)_3 \cdot 6H_2O$) in Milli-Q water containing nitrate acid: $[Gd^{3+}] = 15.97 \text{ mmol} \cdot L^{-1}$, $[NO_3^-] = 108.66 \text{ mmol} \cdot L^{-1}$; diagram was obtained with Medusa freeware.

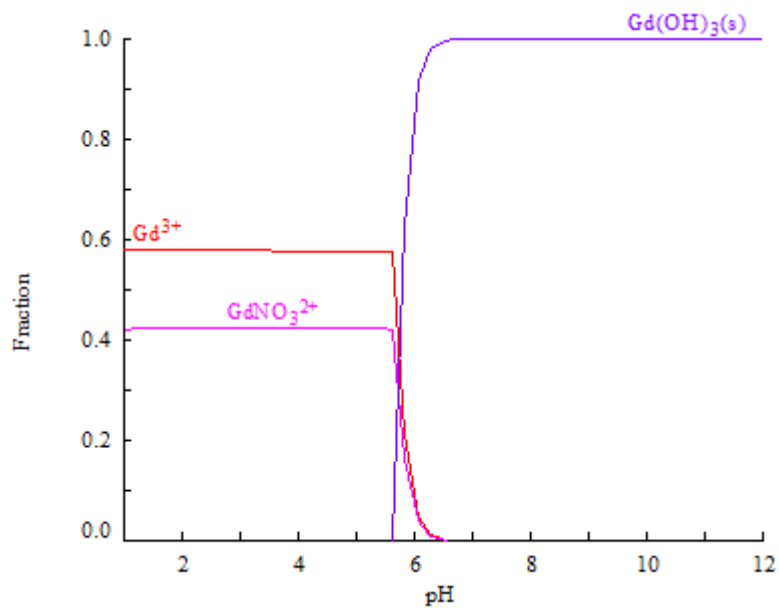


Figure SI 6. Speciation diagram of gadolinium nitrate ($Gd(NO_3)_3 \cdot 6H_2O$) in Milli-Q water containing nitrate acid: $[Gd^{3+}] = 56.69 \text{ mmol} \cdot L^{-1}$, $[NO_3^-] = 271.84 \text{ mmol} \cdot L^{-1}$; diagram was obtained with Medusa freeware.

Supporting information

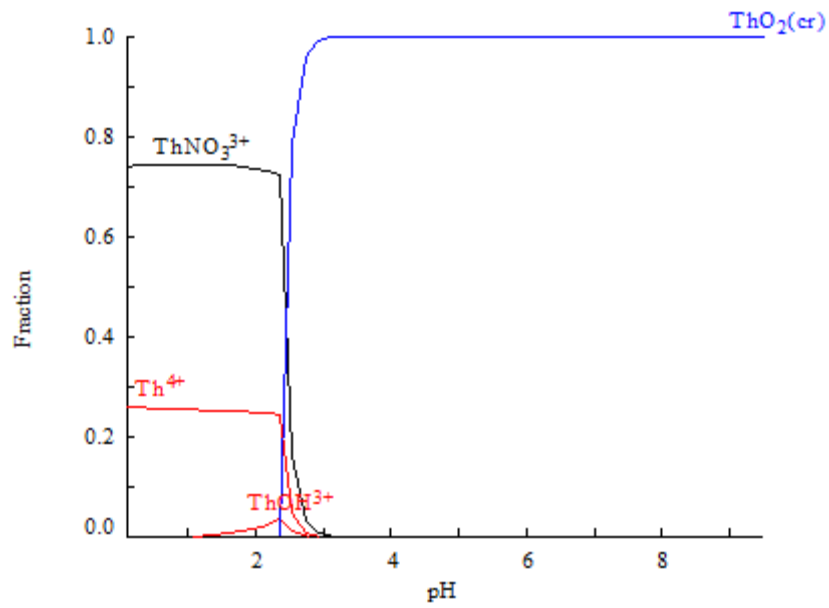


Figure SI 7. Speciation diagram of thorium nitrate ($\text{Th}(\text{NO}_3)_4 \cdot \text{H}_2\text{O}$) in Milli-Q water containing nitrate acid: $[\text{Th}^{3+}] = 16.788 \text{ mmol} \cdot \text{L}^{-1}$, $[\text{NO}_3^-] = 107.152 \text{ mmol} \cdot \text{L}^{-1}$; diagram was obtained with Medusa freeware using database 'sit.dat'.

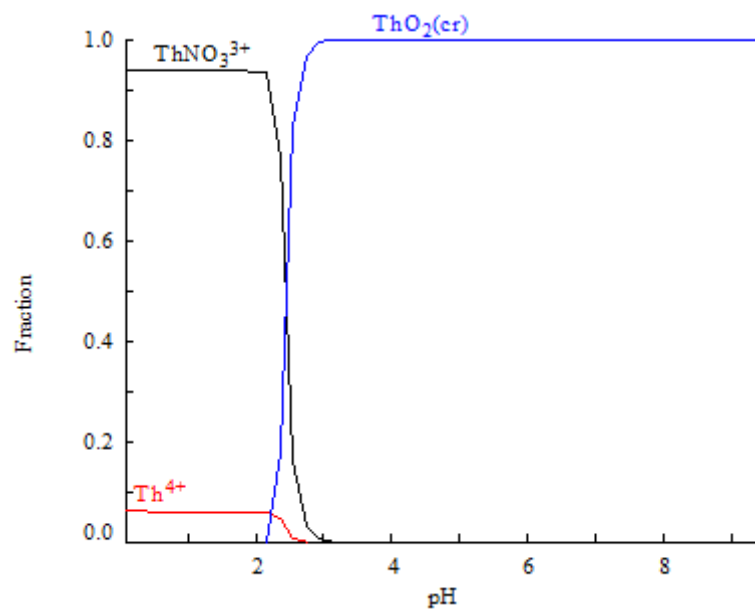


Figure SI 8. Speciation diagram of thorium nitrate ($\text{Th}(\text{NO}_3)_4 \cdot \text{H}_2\text{O}$) in Milli-Q water containing nitrate acid: $[\text{Th}^{3+}] = 59.353 \text{ mmol} \cdot \text{L}^{-1}$, $[\text{NO}_3^-] = 280.245 \text{ mmol} \cdot \text{L}^{-1}$; diagram was obtained with Medusa freeware using database 'sit.dat'.

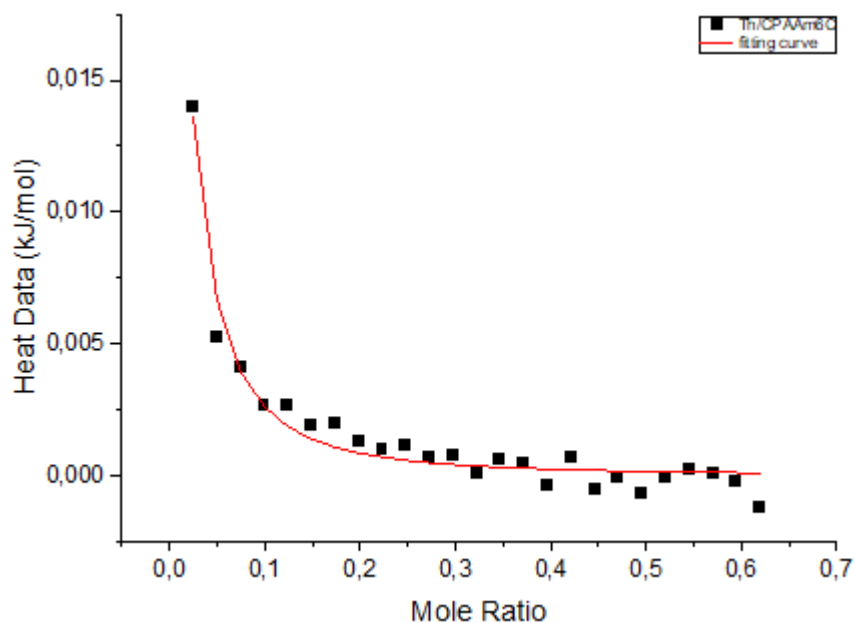


Figure SI 9. ITC heat data corresponding to the Th(IV) ITC experiment (298 K and pH=1) of the CPAAm6C monomer ($31 \text{ mmol}\cdot\text{L}^{-1}$) aqueous solution titrated by $\text{Th}(\text{NO}_3)_4\cdot\text{H}_2\text{O}$ ($63 \text{ mmol}\cdot\text{L}^{-1}$) stock solution, together with the fitting curve obtained with 'independent model' in Nanoanalyze software.

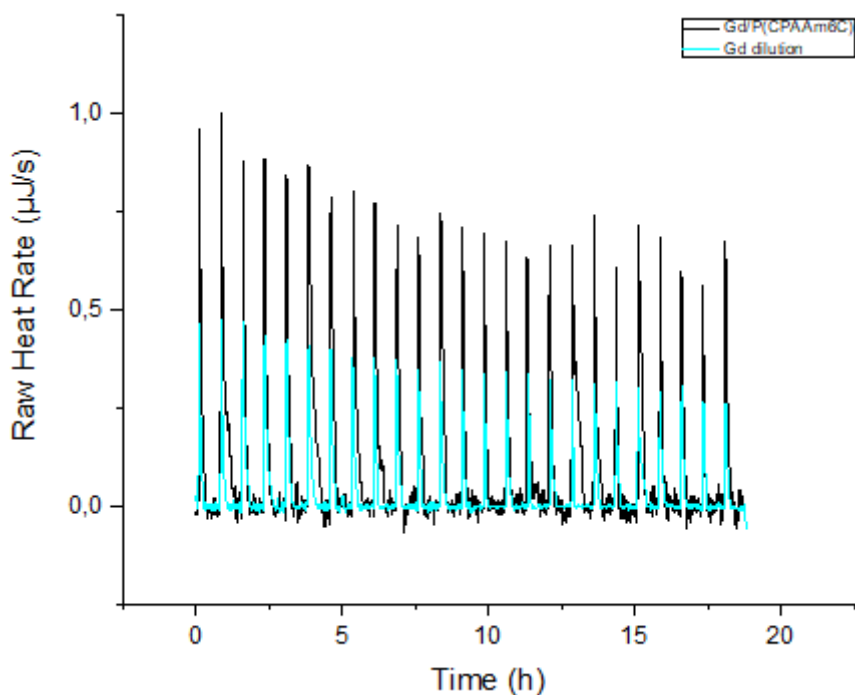


Figure SI 10. Processed thermal profiles for the Gd(III) ITC experiment of the P(CPAAm6C) polymer aqueous solution of $31 \text{ mmol}\cdot\text{L}^{-1}$ (sorption experiment) and acidified Milli-Q water (dilution experiment) titrated by $63 \text{ mmol}\cdot\text{L}^{-1}$ $\text{Gd}(\text{NO}_3)_3\cdot 6\text{H}_2\text{O}$ aqueous solution. Experiments carried out at 298 K and pH=1, with 25 successive injections recorded with $10 \mu\text{L}$ for each injection of Gd(III) stock solution into $800 \mu\text{L}$ of P(CPAAm6C) polymer solution or acidified Milli-Q water.

Supporting information

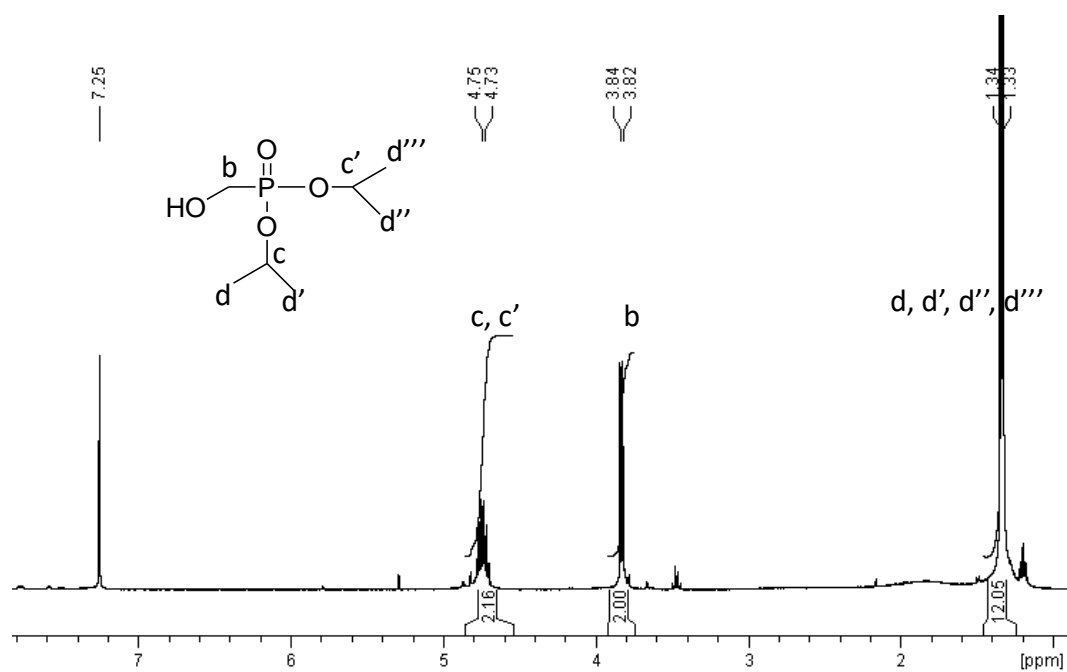


Figure SI 11. ¹H NMR spectrum (400 MHz, CDCl₃) of diisopropyl hydroxymethyl phosphonate (DihMP)

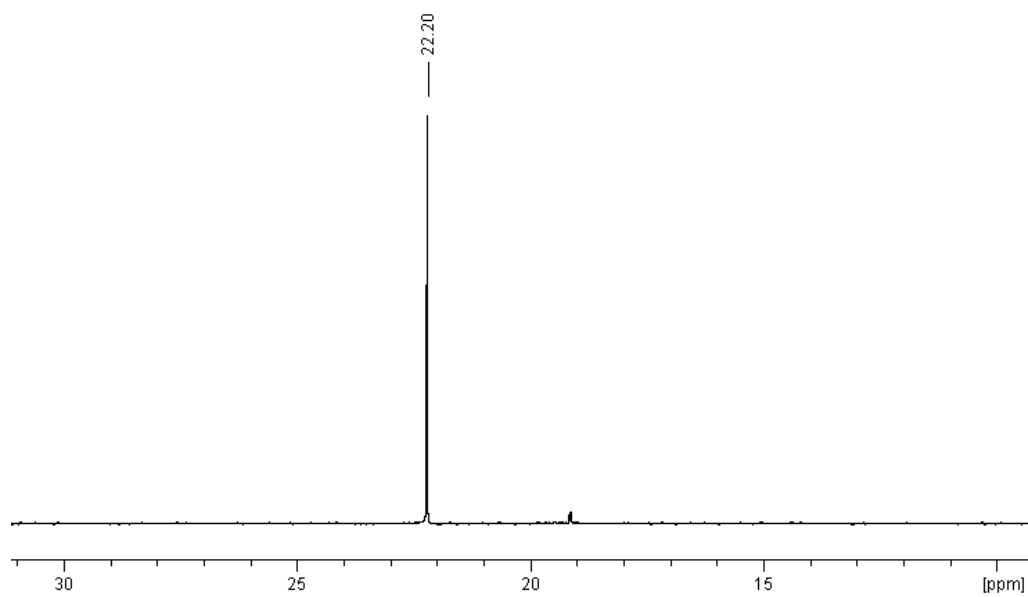


Figure SI 12. ³¹P NMR spectrum (400 MHz, CDCl₃) of diisopropyl hydroxymethyl phosphonate (DihMP)

Supporting information

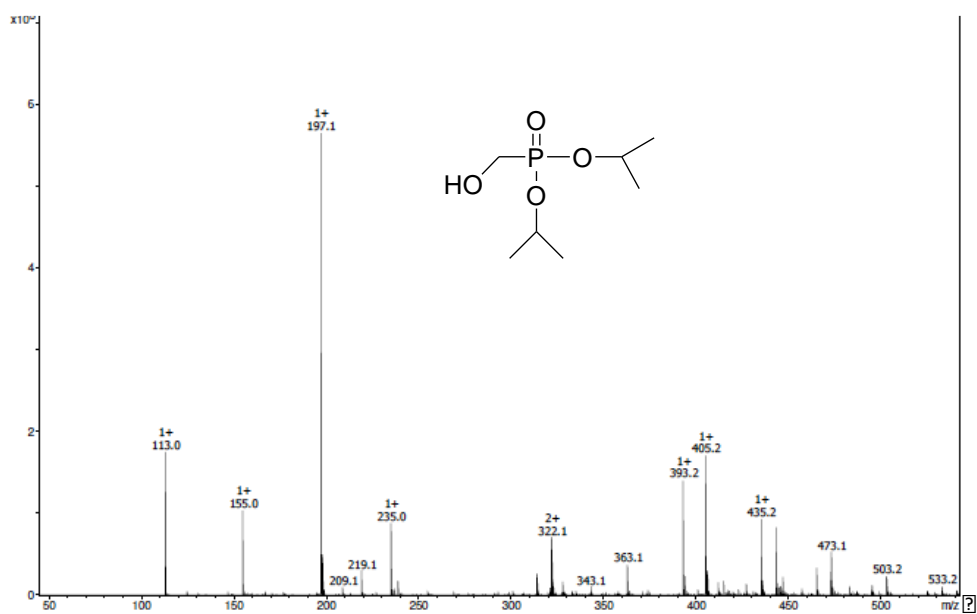


Figure SI 13. Mass spectrum of positive mode (+MS) of diisopropyl hydroxymethyl phosphonate (DihMP) by micrOTOF-Q instrument, ion source: ESI, intensity $\times 10^5$; scan with maximum resolution from 50 to 2200 m/z . Product found at $m/z=197.1$.

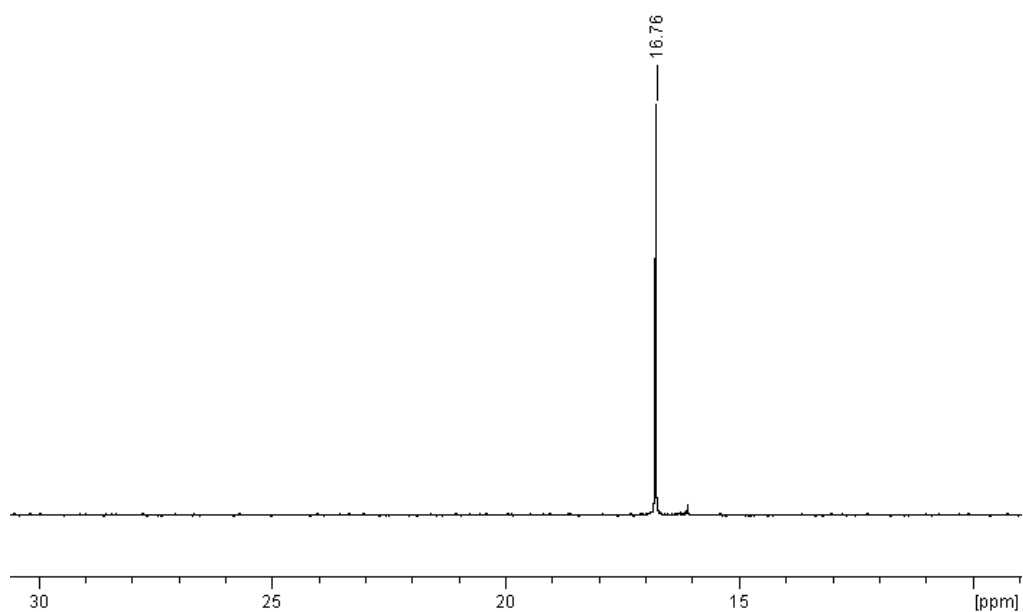


Figure SI 14. ^{31}P NMR spectrum (400 MHz, CDCl_3) of diisopropyl(acryloyloxymethyl) phosphonate (DiAPC1).

Supporting information

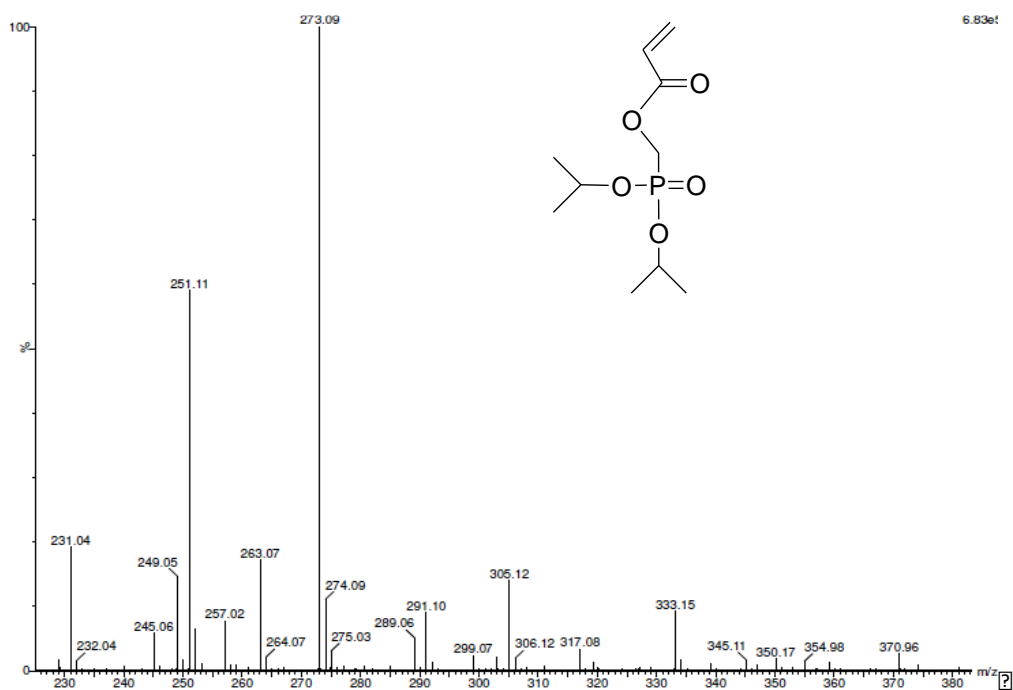


Figure SI 15. Mass spectrum of positive mode (+MS) of diisopropyl(acryloyloxymethyl) phosphonate (DiAPC1) by TOF instrument, ion source: ESI; scan from 50 to 1500 m/z . Product appeared at $m/z=251.11$.

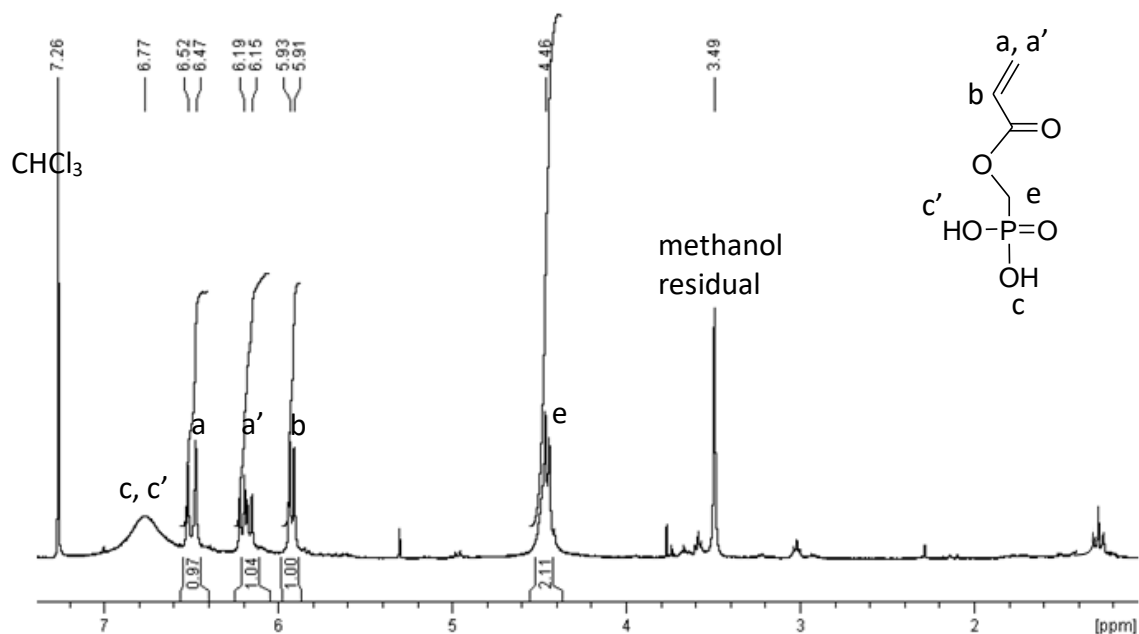


Figure SI 16. ^1H NMR spectrum (400 MHz, CDCl_3) of acryloyloxymethyl phosphonic acid (hAPC1)

Supporting information

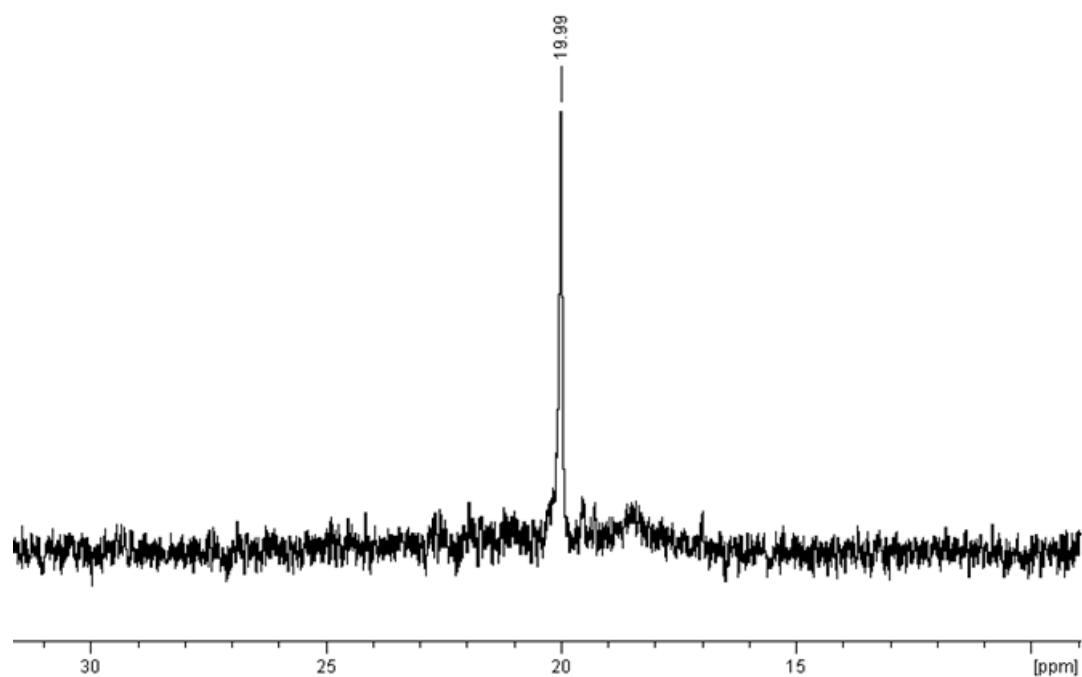


Figure SI 17. ^{31}P NMR spectrum (400 MHz, CDCl_3) of acryloyloxymethyl phosphonic acid (hAPC1)

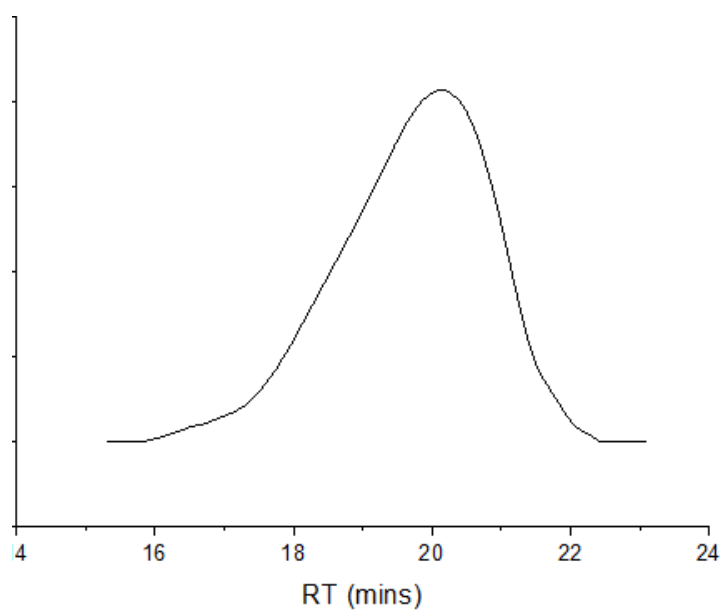


Figure SI 18. Size exclusion chromatogram of poly(diisopropyl(acryloyloxymethyl) phosphonate) (P(DiAPC1)) (DMAC eluent +LiCl 0.1% at $0.8 \text{ mL}\cdot\text{L}^{-1}$, PMMA standards): $M_n=4500 \text{ g}\cdot\text{mol}^{-1}$, $D=2.2$.

Supporting information

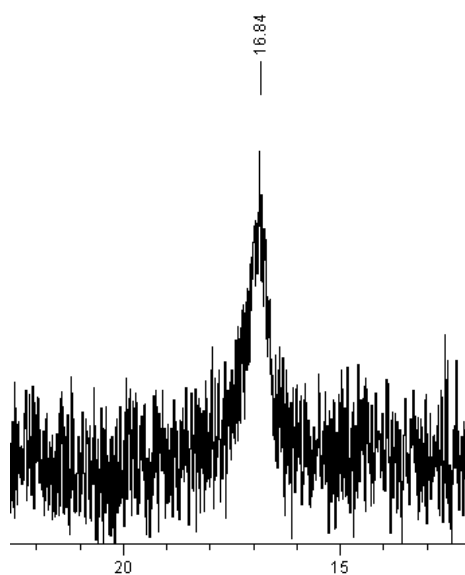


Figure SI 19. ^{31}P NMR spectrum (400 MHz, δ (ppm), CDCl_3) of poly(diisopropyl(acryloyloxymethyl)phosphonate) (P(DiAPC1))

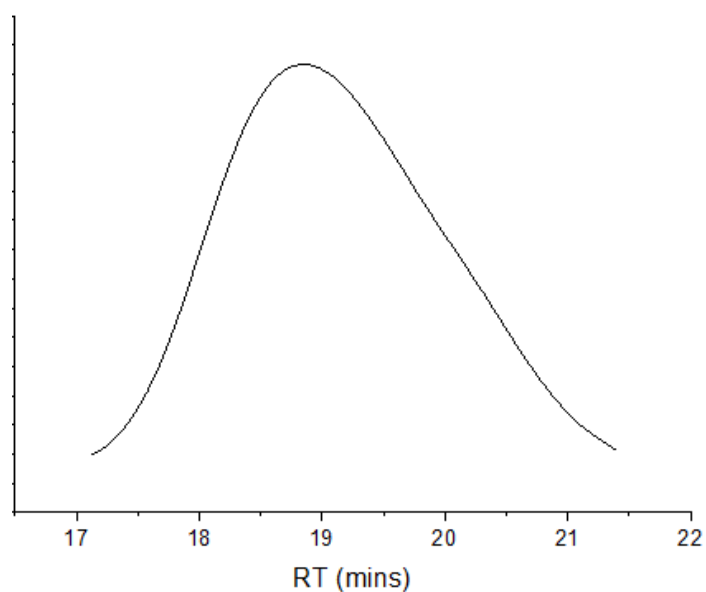


Figure SI 20. Size exclusion chromatogram of poly(dimethyl(acryloyloxymethyl)phosphonate) (P(APC1)) (DMAC eluent +LiCl 0.1% at $0.8 \text{ mL}\cdot\text{L}^{-1}$, PMMA standards); $M_n=9800 \text{ g}\cdot\text{mol}^{-1}$, $D=1.5$.

Figure SI 21. ^1H NMR spectrum (400 MHz, CDCl_3) of poly(dimethyl(acryloyloxymethyl) phosphonate) (P(APC1))

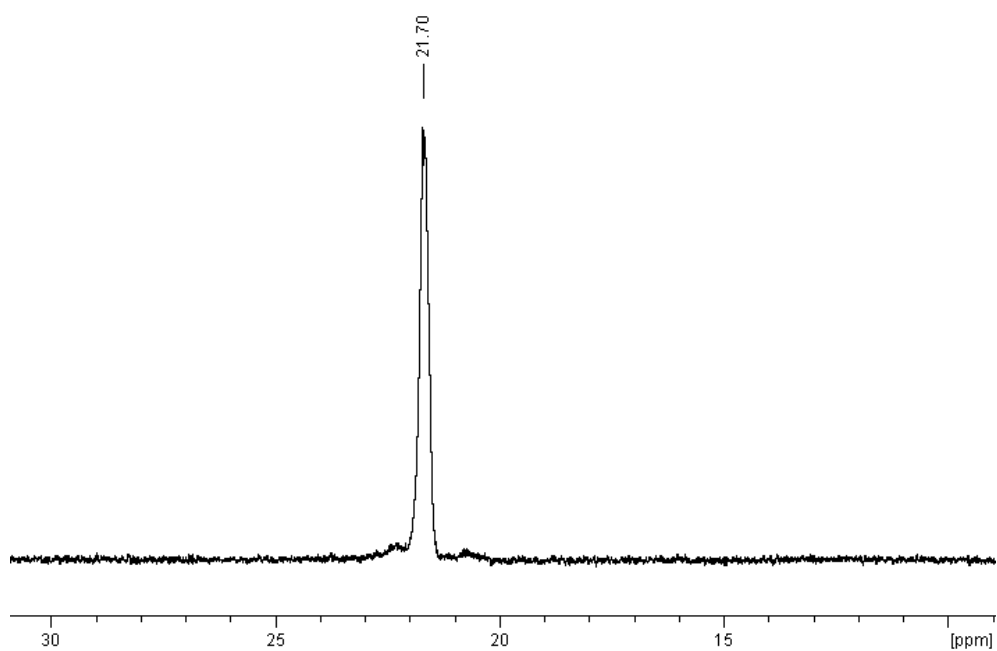


Figure SI 22. ^{31}P NMR spectrum (400 MHz, CDCl_3) of poly(dimethyl(acryloyloxymethyl) phosphonate) (P(APC1))

Supporting information

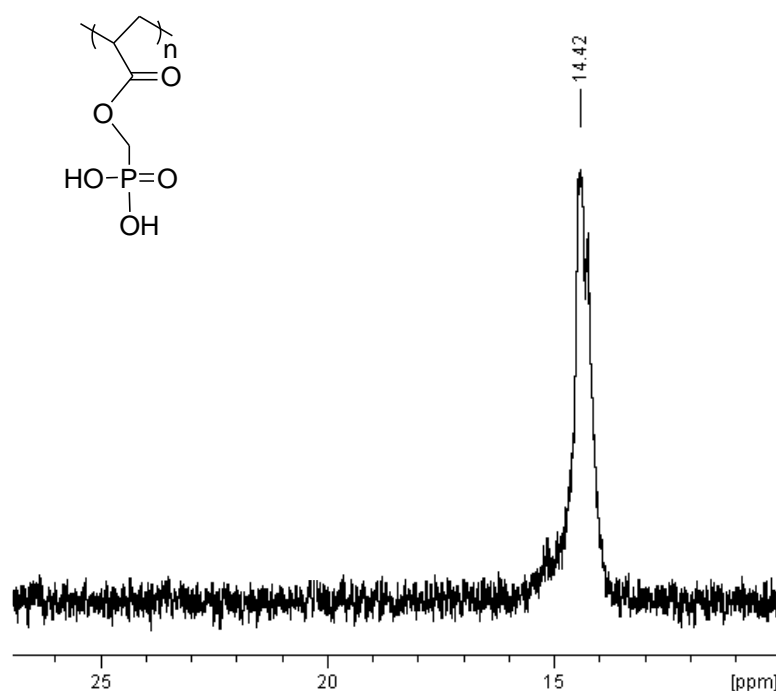


Figure SI 23. ^{31}P NMR spectrum (400 MHz, $\text{DMSO-}d_6$) of poly(acryloyloxymethyl phosphonic acid) (hP(APC1))

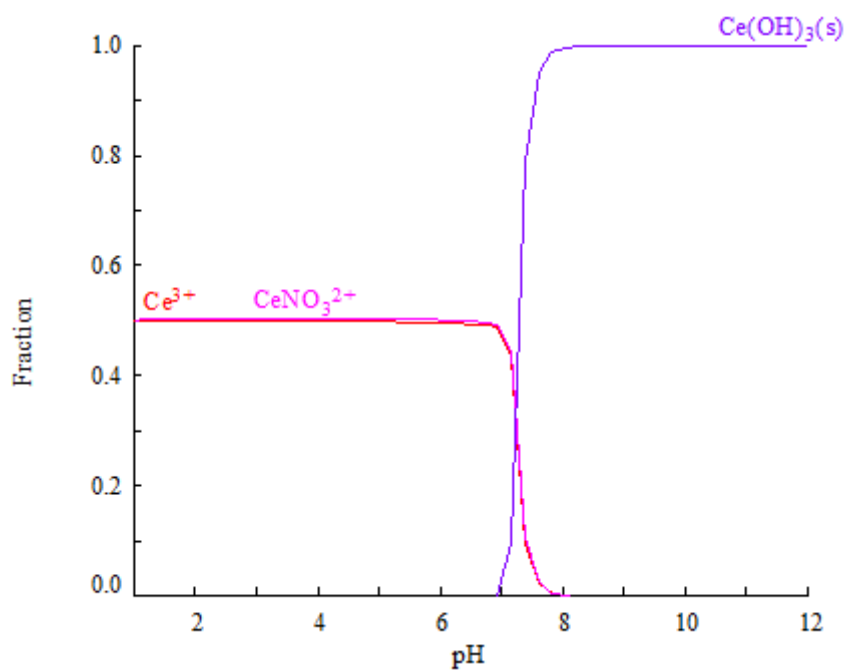


Figure SI 24. Speciation diagram of cerium nitrate ($\text{Ce}(\text{NO}_3)_3 \cdot 6\text{H}_2\text{O}$) in Milli-Q water containing nitrate acid: $[\text{Ce}^{3+}] = 60.7 \text{ mmol} \cdot \text{L}^{-1}$, $[\text{NO}_3^-] = 236.6 \text{ mmol} \cdot \text{L}^{-1}$; diagram was obtained with Medusa freeware.

Supporting information

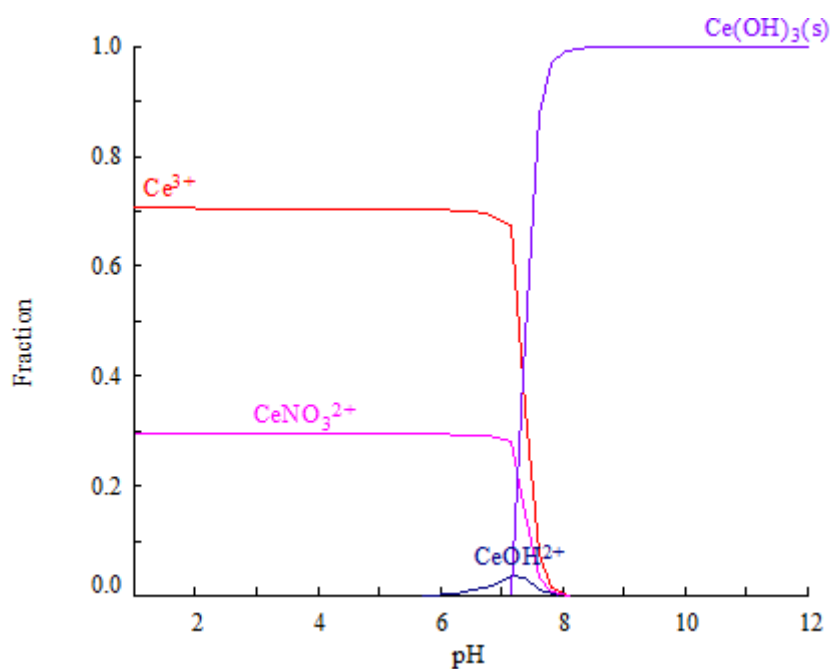


Figure SI 25. Speciation diagram of cerium nitrate ($\text{Ce(NO}_3)_3 \cdot 6\text{H}_2\text{O}$) in Milli-Q water containing nitrate acid: $[\text{Ce}^{3+}] = 16.8 \text{ mmol}\cdot\text{L}^{-1}$, $[\text{NO}_3^-] = 90.2 \text{ mmol}\cdot\text{L}^{-1}$; diagram was obtained with Medusa freeware.

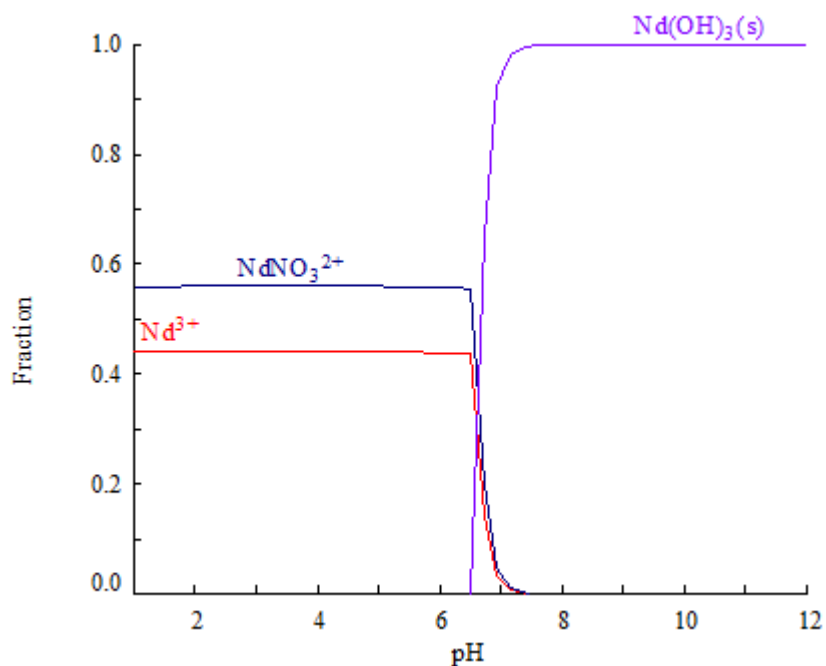


Figure SI 26. Speciation diagram of neodymium nitrate ($\text{Nd(NO}_3)_3 \cdot 6\text{H}_2\text{O}$) in Milli-Q water containing nitrate acid: $[\text{Nd}^{3+}] = 60.8 \text{ mmol}\cdot\text{L}^{-1}$, $[\text{NO}_3^-] = 240.2 \text{ mmol}\cdot\text{L}^{-1}$; diagram was obtained with Medusa freeware.

Supporting information

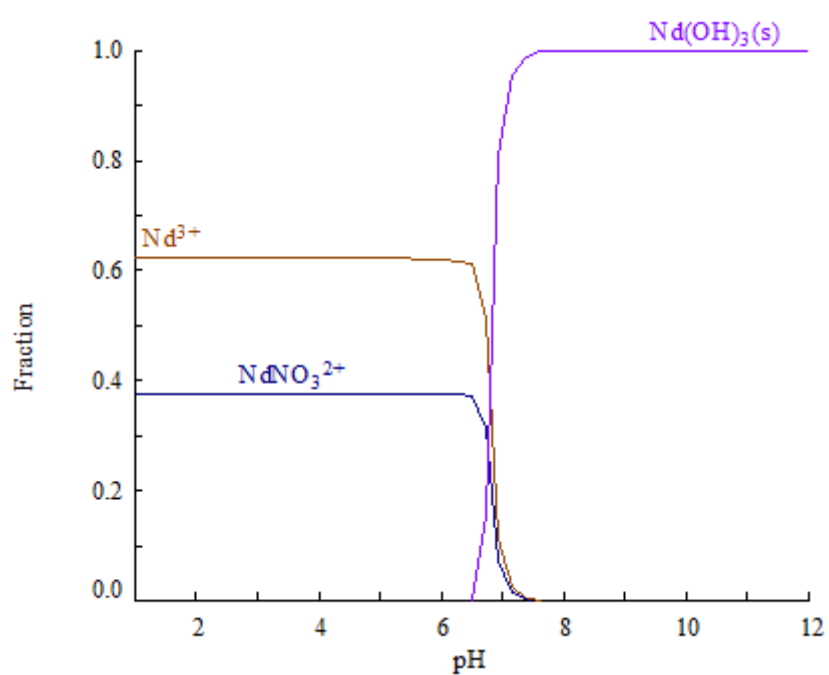


Figure SI 27. Speciation diagram of neodymium nitrate ($\text{Nd(NO}_3)_3 \cdot 6\text{H}_2\text{O}$) in Milli-Q water containing nitrate acid: $[\text{Nd}^{3+}] = 17.13 \text{ mmol} \cdot \text{L}^{-1}$, $[\text{NO}_3^-] = 104.7 \text{ mmol} \cdot \text{L}^{-1}$; diagram was obtained with Medusa freeware.

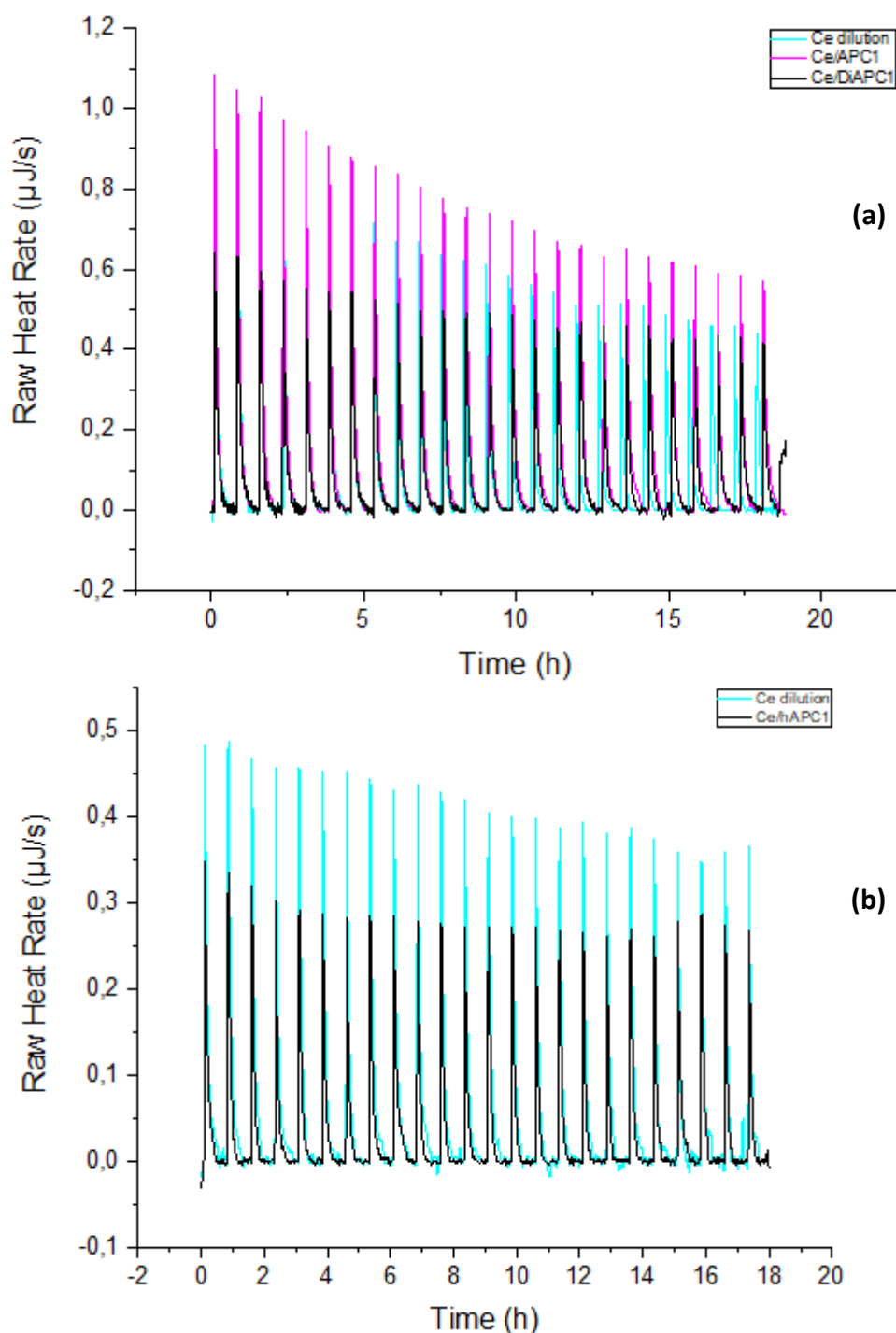


Figure SI 28. (a) Processed thermal profiles for Ce(III) ITC experiment of the APC1 or DiAPC1 monomer aqueous solution of $14.35 \text{ mmol}\cdot\text{L}^{-1}$ (sorption experiment) together with acidified Milli-Q water (dilution experiment) titrated by $63 \text{ mmol}\cdot\text{L}^{-1} \text{ Ce}(\text{NO}_3)_3\cdot 6\text{H}_2\text{O}$ aqueous solution; (b) Similar measurements with $14.35 \text{ mmol}\cdot\text{L}^{-1}$ hAPC1 aqueous solution titrated with $17 \text{ mmol}\cdot\text{L}^{-1} \text{ Ce}(\text{NO}_3)_3\cdot 6\text{H}_2\text{O}$ aqueous solution. Experiments carried out at 298 K and $\text{pH}=1$, with 25 successive injections recorded with $10 \mu\text{L}$ for each injection of Ce(III) stock solution into $800 \mu\text{L}$ of monomer aqueous solution or acidified Milli-Q water.

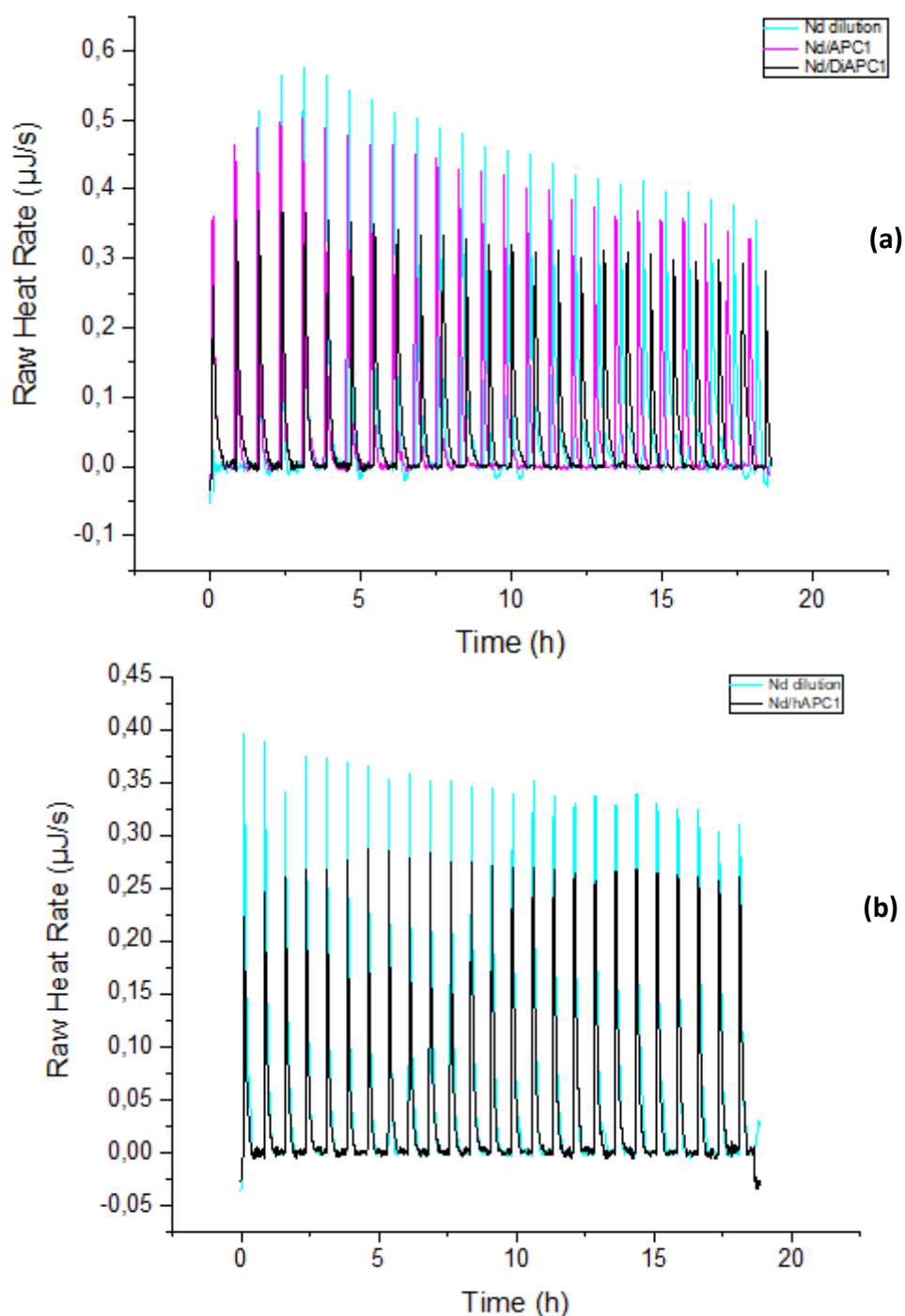


Figure SI 29. (a) Processed thermal profiles for Nd(III) ITC experiment of the APC1 or DiAPC1 monomer aqueous solution of $14.35 \text{ mmol}\cdot\text{L}^{-1}$ (sorption experiment) together with acidified Milli-Q water (dilution experiment) titrated by $\text{Nd}(\text{NO}_3)_3\cdot 6\text{H}_2\text{O}$ aqueous solution of $63 \text{ mmol}\cdot\text{L}^{-1}$; (b) Similar measurements with hAPC1 aqueous solution of $14.35 \text{ mmol}\cdot\text{L}^{-1}$ titrated with $17 \text{ mmol}\cdot\text{L}^{-1}$ $\text{Nd}(\text{NO}_3)_3\cdot 6\text{H}_2\text{O}$ aqueous solution. Experiments carried out at 298 K and $\text{pH}=1$, with 25 successive injections recorded with $10 \mu\text{L}$ for each injection of Nd(III) stock solution into $800 \mu\text{L}$ of monomer aqueous solution or acidified Milli-Q water.

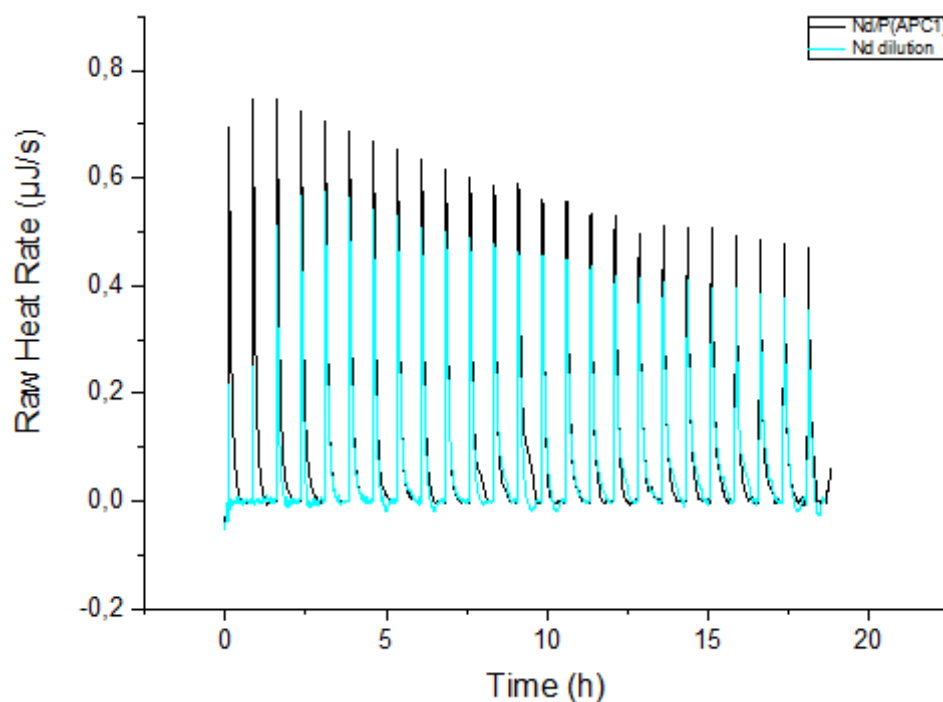


Figure SI 30. Processed thermal profiles for Nd(III) ITC experiment of the P(APC1) polymer aqueous solution of $14.35 \text{ mmol}\cdot\text{L}^{-1}$ (sorption experiment) together with acidified Milli-Q water (dilution experiment) titrated by $\text{Nd}(\text{NO}_3)_3\cdot 6\text{H}_2\text{O}$ aqueous solution of $63 \text{ mmol}\cdot\text{L}^{-1}$. Experiments carried out at 298 K and $\text{pH}=1$, with 25 successive injections recorded with $10 \mu\text{L}$ for each injection of Nd(III) stock solution into $800 \mu\text{L}$ of polymer aqueous solution or acidified Milli-Q water.

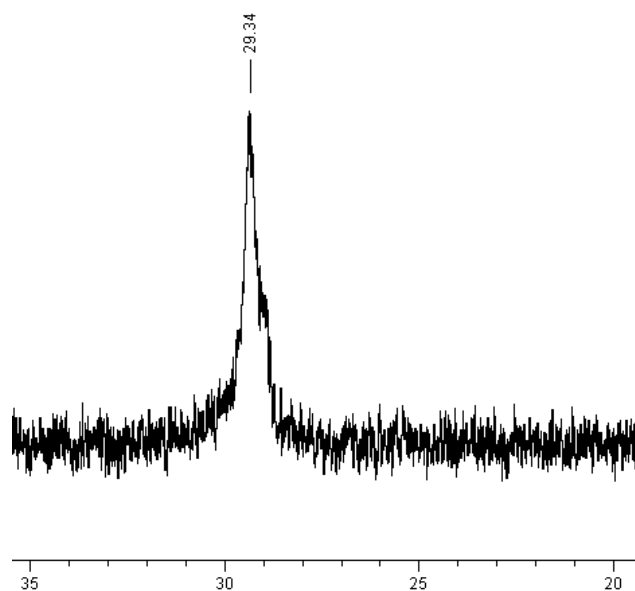


Figure SI 31. ^{31}P NMR spectra (400 MHz, δ (ppm), CDCl_3) of poly(diethyl-2-(acrylamido)ethyl phosphonate) (P(DAAmEP))

Supporting information

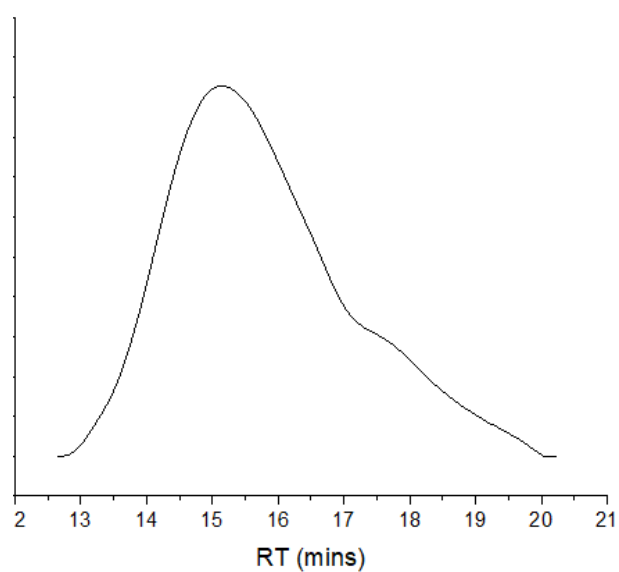


Figure SI 32. Size exclusion chromatogram of poly(diethyl-2-(acrylamido)ethyl phosphonate) (P(DAAmEP)) (DMAC eluent +LiCl 0.1% at 0.8 mL·L⁻¹, PMMA standards)

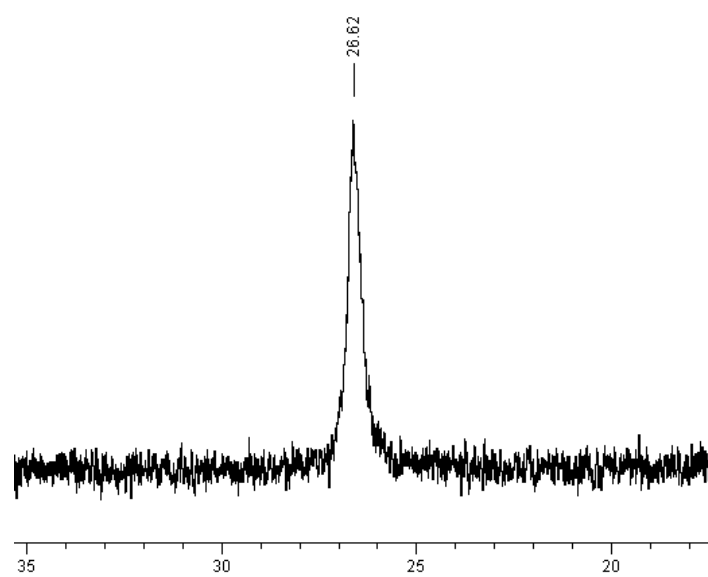


Figure SI 33. ³¹P NMR spectrum (400 MHz, δ(ppm), D₂O) of poly(2-(acrylamido)ethyl phosphonic acid) (hP(DAAmEP))

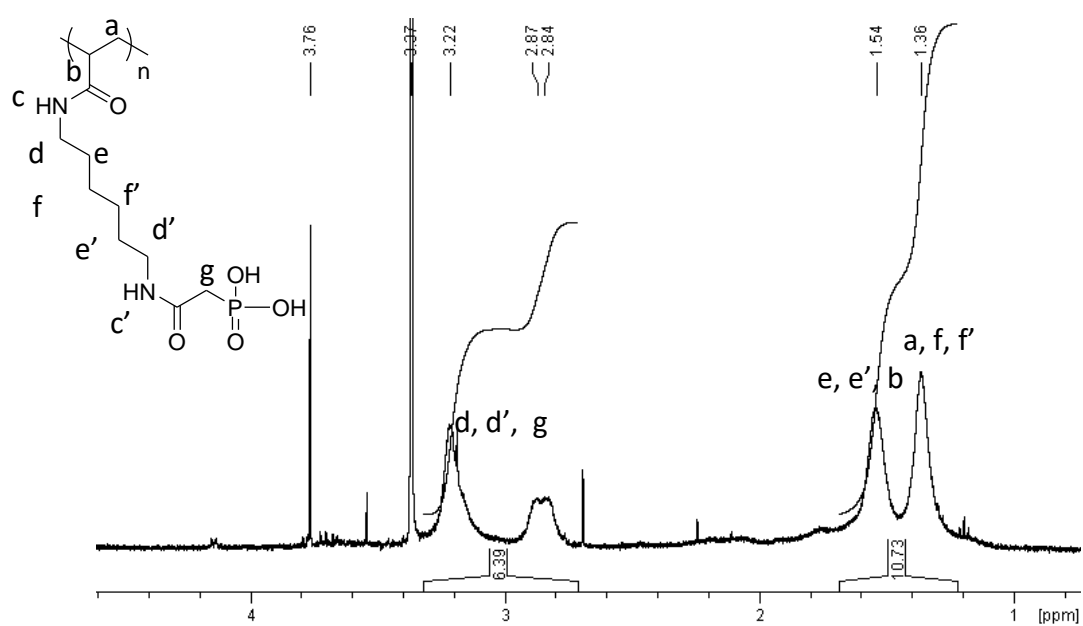


Figure SI 34. ^1H NMR spectrum (400 MHz, D_2O) of poly(6-(acrylamido)hexylcarbamoylmethyl phosphonic acid) (hP(CPAAm6C))

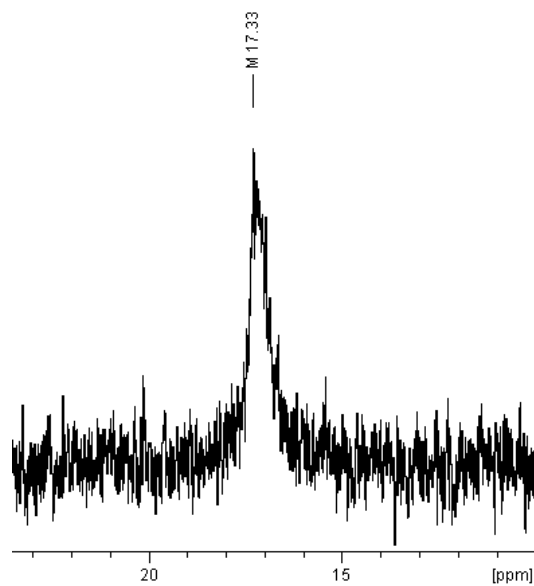


Figure SI 35. ^{31}P NMR spectrum (400 MHz, D_2O) of poly(6-(acrylamido)hexylcarbamoylmethyl phosphonic acid) (hP(CPAAm6C))

Supporting information

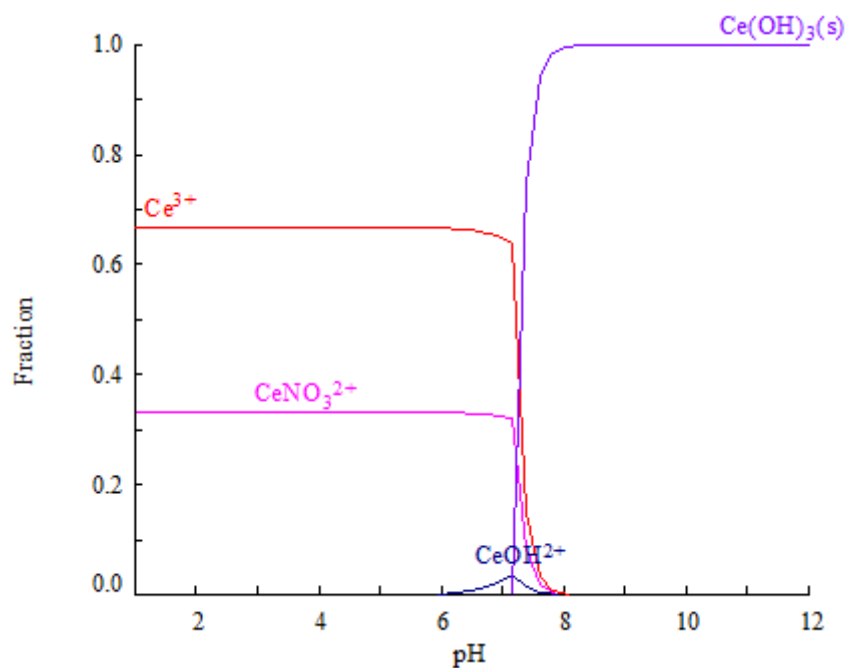


Figure SI 36. Speciation diagram of cerium nitrate ($\text{Ce(NO}_3)_3 \cdot 6\text{H}_2\text{O}$) in Milli-Q water containing nitrate acid: $[\text{Ce}^{3+}] = 37.8 \text{ mmol}\cdot\text{L}^{-1}$, $[\text{NO}_3^-] = 114.3 \text{ mmol}\cdot\text{L}^{-1}$; diagram was obtained with Medusa freeware.

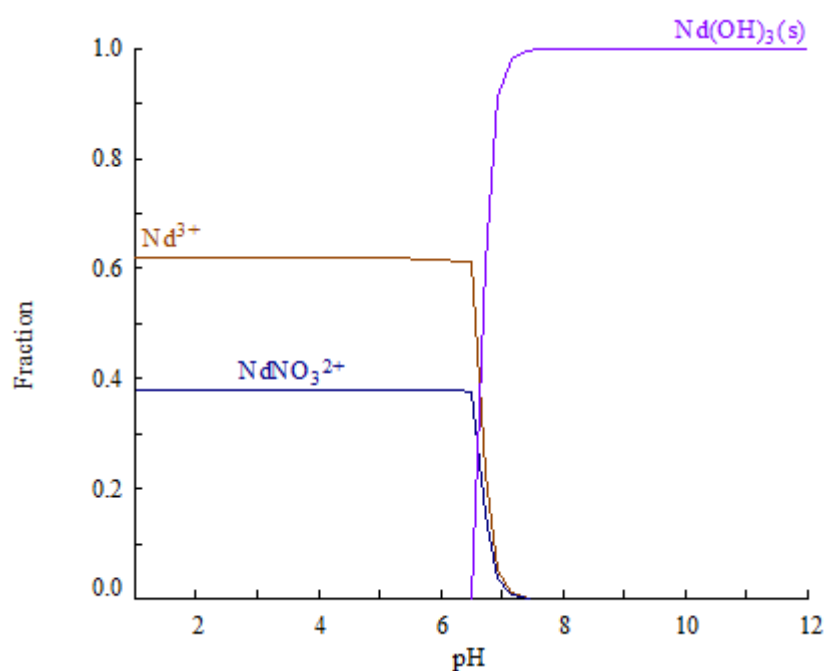


Figure SI 37. Speciation diagram of neodymium nitrate ($\text{Nd(NO}_3)_3 \cdot 6\text{H}_2\text{O}$) in Milli-Q water containing nitrate acid: $[\text{Nd}^{3+}] = 38 \text{ mmol}\cdot\text{L}^{-1}$, $[\text{NO}_3^-] = 114 \text{ mmol}\cdot\text{L}^{-1}$; diagram was obtained with Medusa freeware.

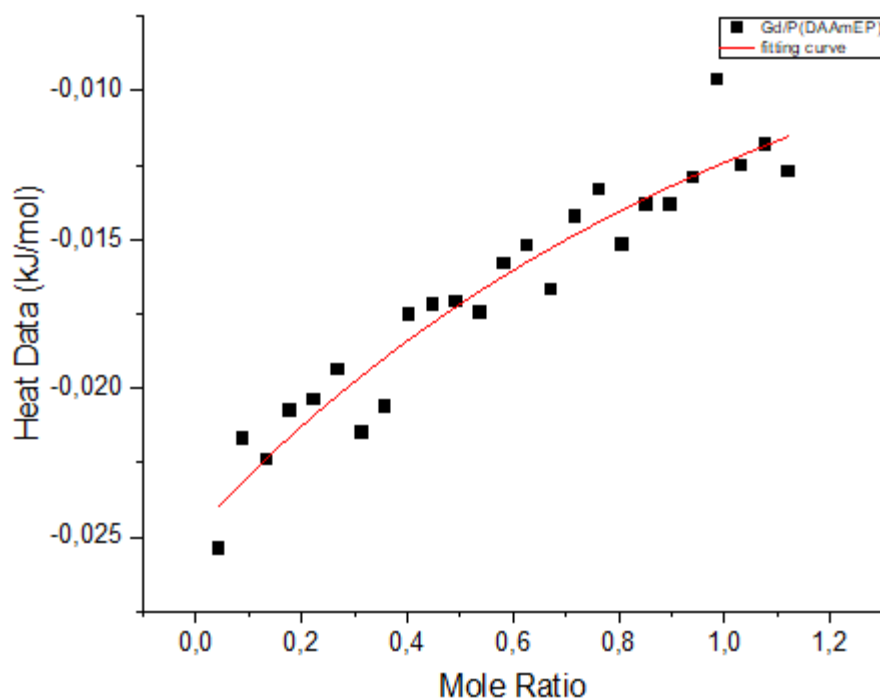


Figure SI 38. ITC heat data corresponding to the Gd(III) ITC experiment (298 K and pH=1) of the P(DAAmEP) polymer ($14.35 \text{ mmol}\cdot\text{L}^{-1}$) aqueous solution titrated by $\text{Gd}(\text{NO}_3)_3\cdot 6\text{H}_2\text{O}$ stock solution ($63 \text{ mmol}\cdot\text{L}^{-1}$), together with the fitting curve obtained with 'independent model' in Nanoanalyze software.

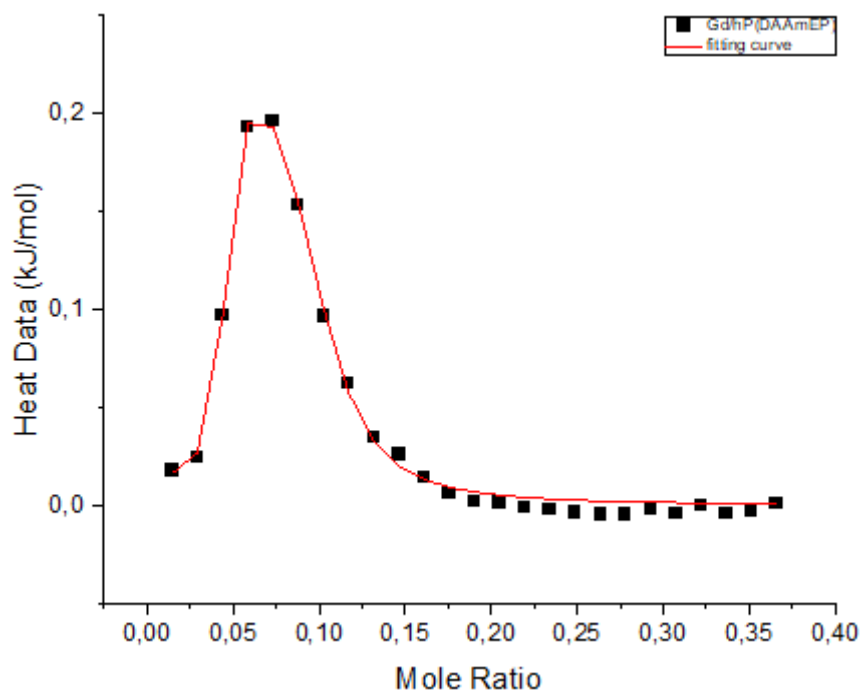


Figure SI 39. ITC heat data corresponding to the Gd(III) ITC experiment (298 K and pH=1) of the hP(DAAmEP) polymer ($14.35 \text{ mmol}\cdot\text{L}^{-1}$) aqueous solution titrated by $\text{Gd}(\text{NO}_3)_3\cdot 6\text{H}_2\text{O}$ stock solution ($17 \text{ mmol}\cdot\text{L}^{-1}$), together with the fitting curve obtained with 'successive binding sites model' using the Levenberg–Marquardt non-linear curve-fitting algorithm.

Supporting information

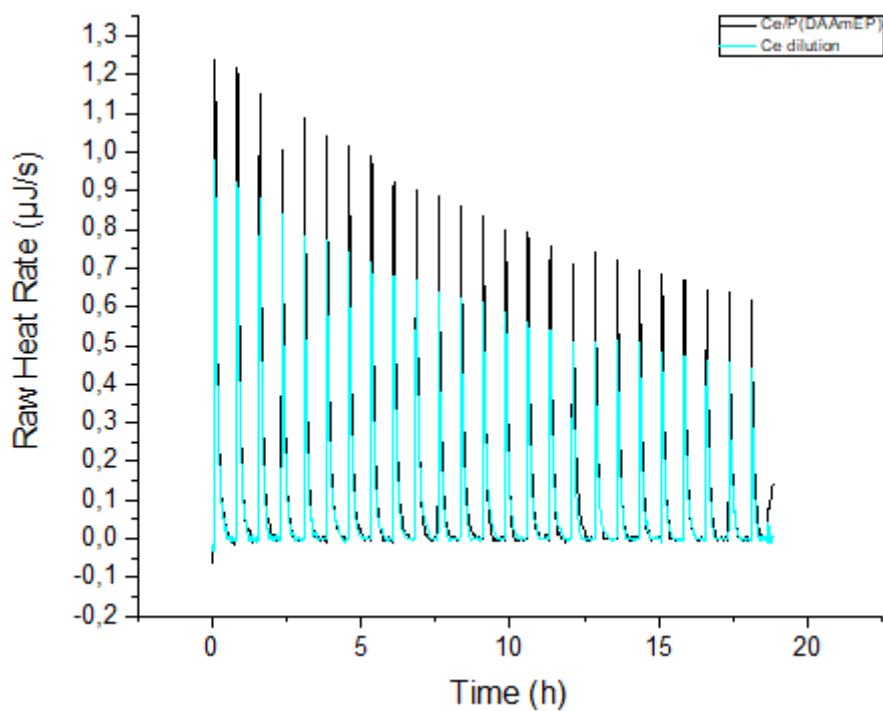


Figure SI 40. Processed thermal profiles at 298 K and under pH=1 for injections of $63 \text{ mmol}\cdot\text{L}^{-1}$ Ce(III) stock solution into acidified water (Ce dilution) and injections of the same Ce(III) solution into $14.35 \text{ mmol}\cdot\text{L}^{-1}$ P(DAAmEP) polymer aqueous solution: 25 successive injections recorded with $10 \mu\text{L}$ for each injection of the $\text{Ce}(\text{NO}_3)_3\cdot 6\text{H}_2\text{O}$ aqueous solution with pH=1 into a 1 mL stainless ampoule containing initially $800 \mu\text{L}$ of acidified water (dilution experiment) or $800 \mu\text{L}$ P(DAAmEP) aqueous solution with pH=1 (sorption experiment).

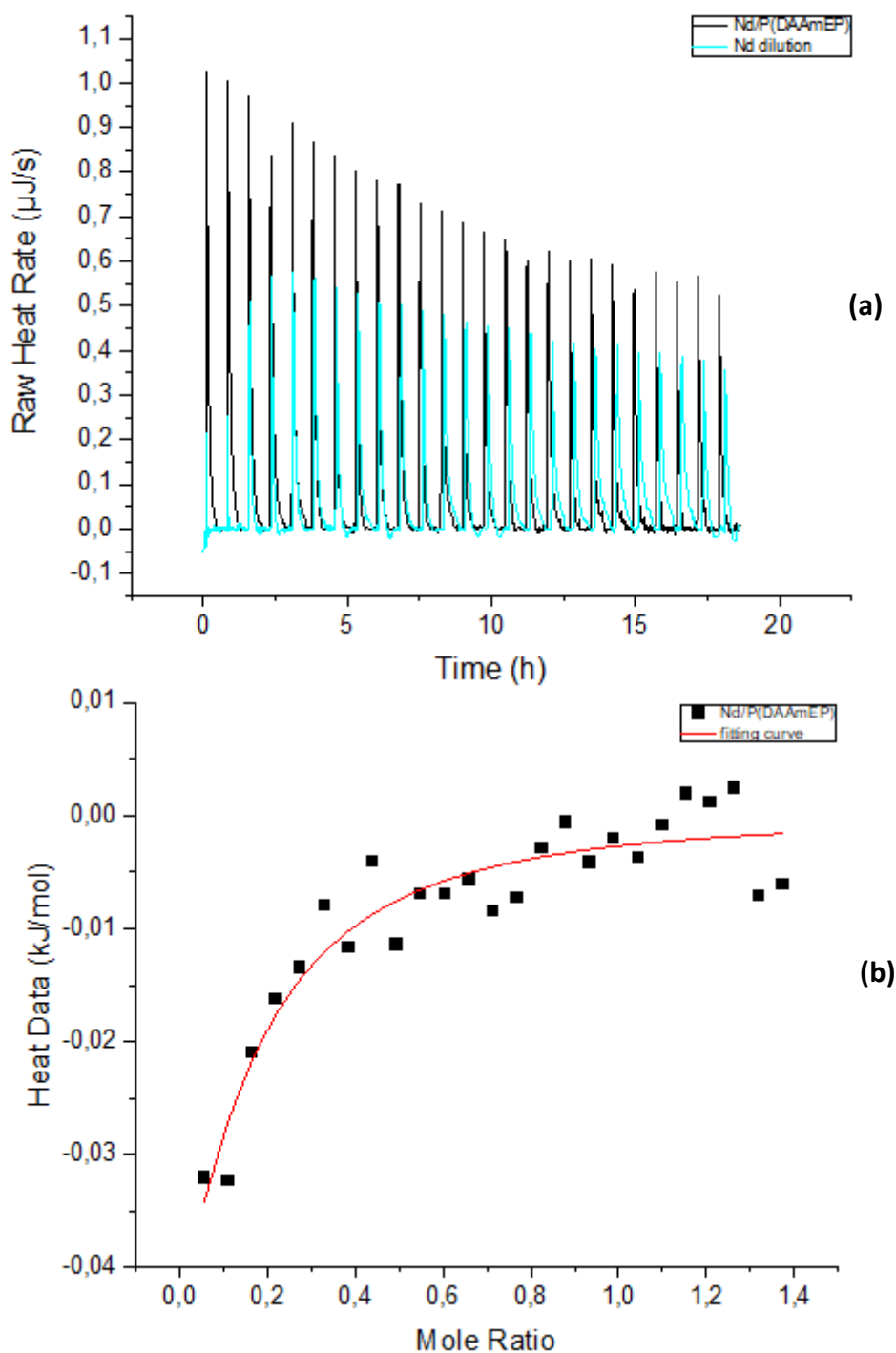


Figure SI 41. (a) Processed thermal profiles at 298 K and under pH=1 for injections of $63 \text{ mmol}\cdot\text{L}^{-1}$ Nd(III) stock solution into acidified water (Nd dilution) and injections of the same Nd(III) solution into $14.35 \text{ mmol}\cdot\text{L}^{-1}$ P(DAAmEP) aqueous solution: 25 successive injections recorded with $10 \mu\text{L}$ for each injection of the $\text{Nd}(\text{NO}_3)_3\cdot 6\text{H}_2\text{O}$ aqueous solution with pH=1 into a 1 mL stainless ampoule containing initially $800 \mu\text{L}$ of acidified water (dilution experiment) or $800 \mu\text{L}$ P(DAAmEP) aqueous solution with pH=1 (sorption experiment); (b) ITC heat data corresponding to the Nd(III) ITC experiments (298 K and pH=1) of the P(DAAmEP) polymer aqueous solution titrated by $\text{Nd}(\text{NO}_3)_3\cdot 6\text{H}_2\text{O}$ stock solution, together with the fitting curve obtained with 'independent model' in Nanoanalyze software.

Supporting information

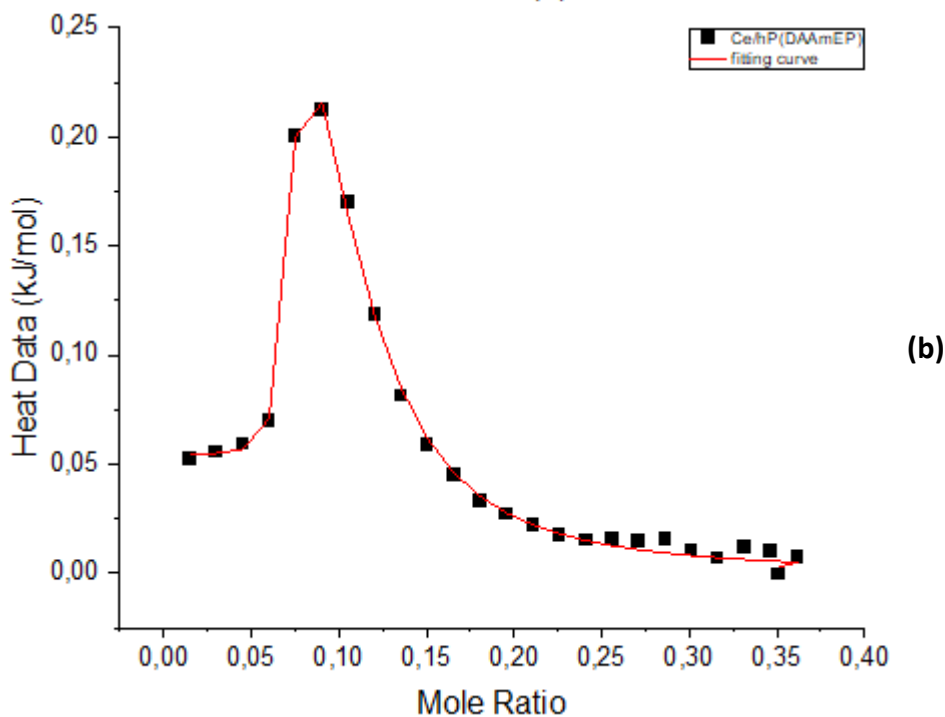
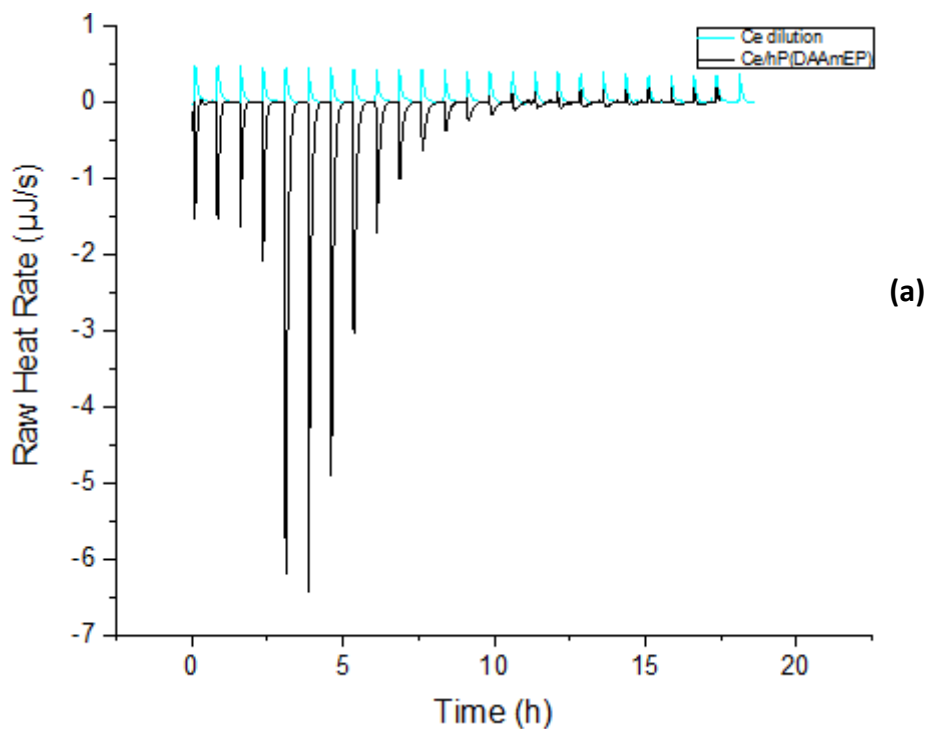


Figure SI 42. (a) Processed thermal profiles at 298 K and under pH=1 for injections of $17 \text{ mmol}\cdot\text{L}^{-1}$ Ce(III) stock solution into acidified water (Ce dilution) and injections of the same Ce(III) solution into $14.35 \text{ mmol}\cdot\text{L}^{-1}$ hP(DAAmEP) aqueous solution: 25 successive injections recorded with $10 \mu\text{L}$ for each injection of the $\text{Ce}(\text{NO}_3)_3\cdot 6\text{H}_2\text{O}$ aqueous solution with pH=1 into a 1 mL stainless ampoule containing initially $800 \mu\text{L}$ of acidified water (dilution experiment) or $800 \mu\text{L}$ hP(DAAmEP) aqueous solution with pH=1 (sorption experiment); (b) ITC heat data corresponding to the Ce(III) ITC experiments (298 K and pH=1) of the hP(DAAmEP) polymer ($14.35 \text{ mmol}\cdot\text{L}^{-1}$) aqueous solution titrated by $\text{Ce}(\text{NO}_3)_3\cdot 6\text{H}_2\text{O}$ ($17 \text{ mmol}\cdot\text{L}^{-1}$) stock solution, together with the fitting curve obtained with 'successive binding sites model' using the Levenberg–Marquardt non-linear curve-fitting algorithm.

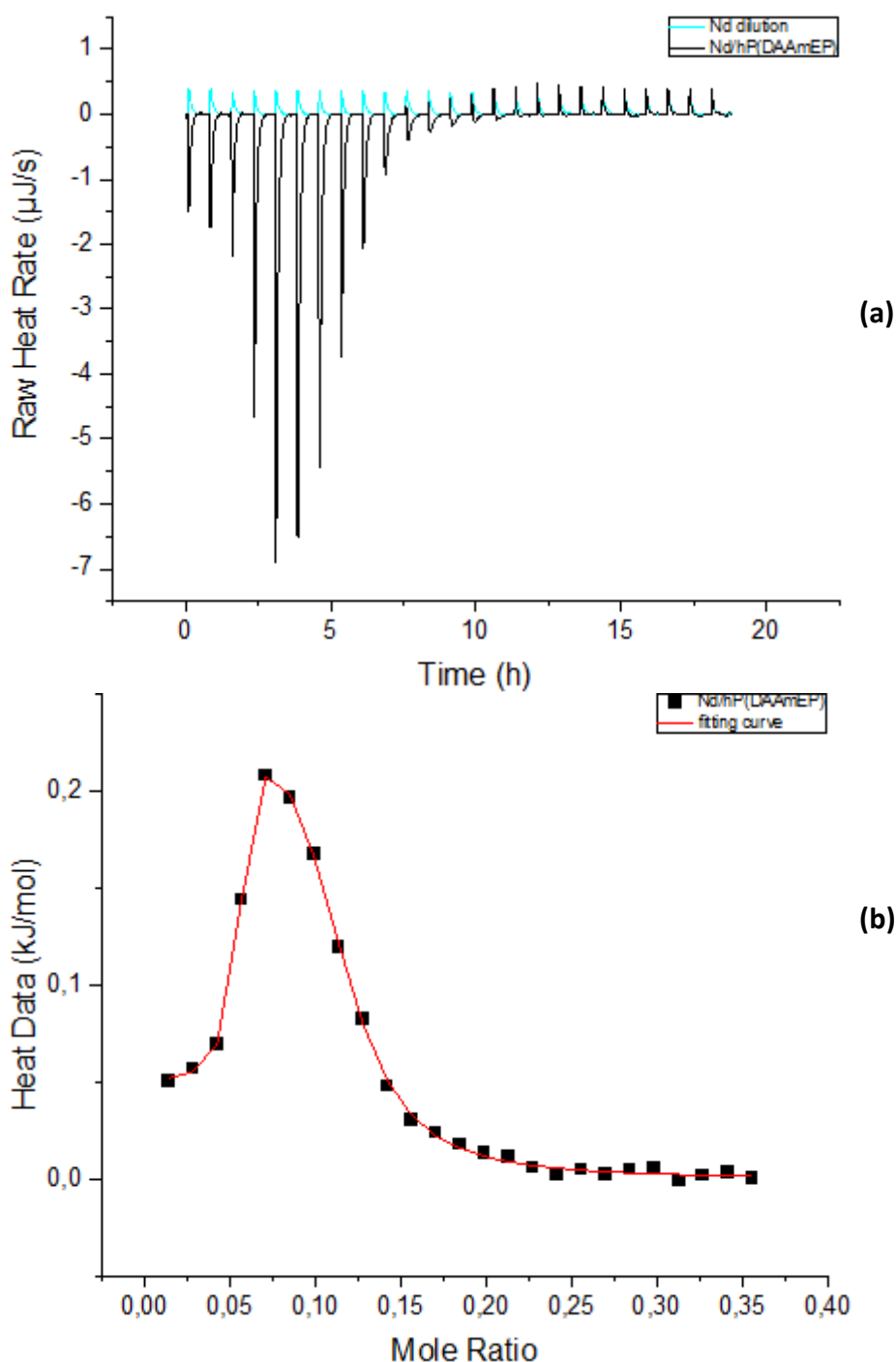


Figure SI 43. (a) Processed thermal profiles at 298 K and under pH=1 for injections of $17 \text{ mmol}\cdot\text{L}^{-1}$ Nd(III) stock solution into acidified water (Nd dilution) and injections of the same Nd(III) solution into $14.35 \text{ mmol}\cdot\text{L}^{-1}$ hP(DAAmEP) aqueous solution: 25 successive injections recorded with $10 \mu\text{L}$ for each injection of the $\text{Nd}(\text{NO}_3)_3\cdot 6\text{H}_2\text{O}$ aqueous solution with pH=1 into a 1 mL stainless ampoule containing initially $800 \mu\text{L}$ of acidified water (dilution experiment) or $800 \mu\text{L}$ hP(DAAmEP) aqueous solution with pH=1 (sorption experiment); (b) ITC heat data corresponding to the Nd(III) ITC experiments (298 K and pH=1) of the hP(DAAmEP) polymer ($14.35 \text{ mmol}\cdot\text{L}^{-1}$) aqueous solution titrated by the $\text{Nd}(\text{NO}_3)_3\cdot 6\text{H}_2\text{O}$ ($17 \text{ mmol}\cdot\text{L}^{-1}$) stock solution, together with the fitting curve obtained with 'successive binding sites model' using the Levenberg–Marquardt non-linear curve-fitting algorithm.

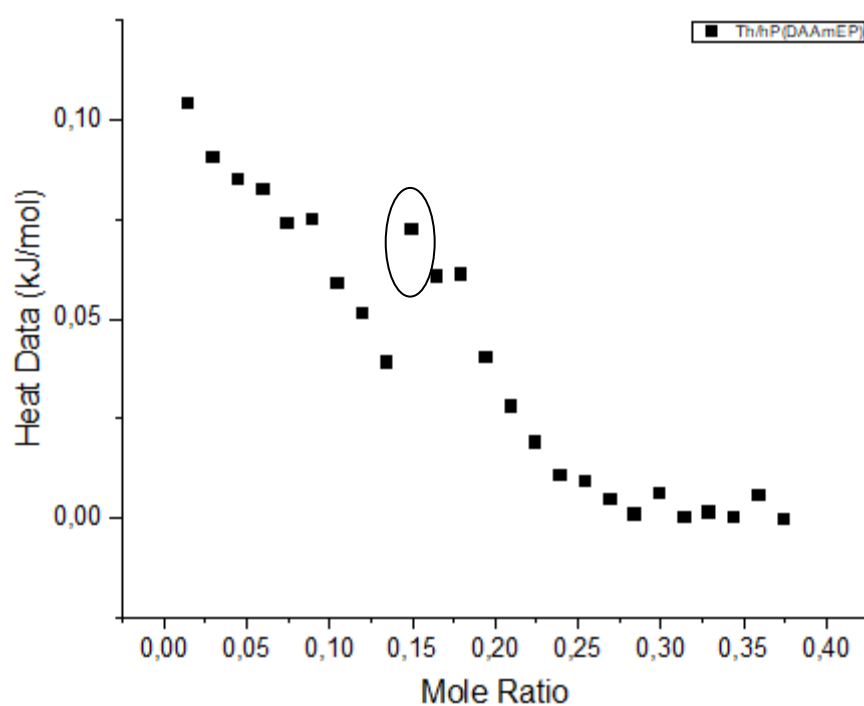


Figure SI 44. ITC heat data corresponding to the Th(IV) ITC experiments (298 K and pH=1) of the hP(DAAmEP) polymer ($14.35 \text{ mmol}\cdot\text{L}^{-1}$) aqueous solution titrated by $\text{Th}(\text{NO}_3)_4\cdot\text{H}_2\text{O}$ ($17 \text{ mmol}\cdot\text{L}^{-1}$) stock solution, without fitting because of the presence of precipitation of Th-hP(DAAmEP) complexes.

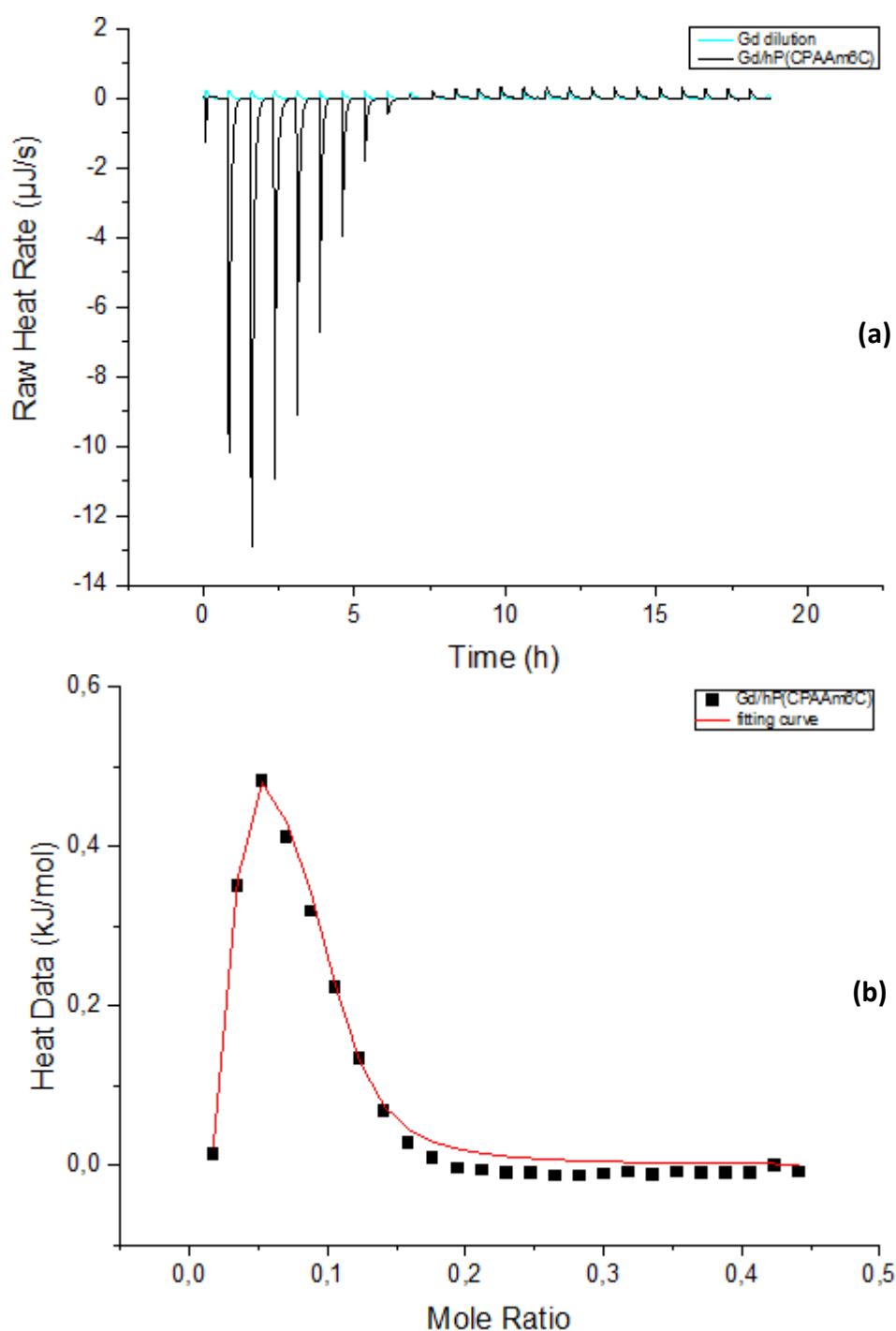


Figure SI 45. (a) Processed thermal profiles at 298 K and under pH=1 for injections of $17 \text{ mmol}\cdot\text{L}^{-1}$ Gd(III) stock solution into acidified water (Gd dilution) and injections of the same Gd(III) solution into $14.35 \text{ mmol}\cdot\text{L}^{-1}$ hP(DAAmEP) aqueous solution: 25 successive injections recorded with $10 \mu\text{L}$ for each injection of the $\text{Gd}(\text{NO}_3)_3\cdot 6\text{H}_2\text{O}$ aqueous solution with pH=1 into a 1 mL stainless ampoule containing initially $800 \mu\text{L}$ of acidified water (dilution experiment) or $800 \mu\text{L}$ hP(DAAmEP) aqueous solution with pH=1 (sorption experiment); (b) ITC heat data corresponding to the Gd(III) ITC experiments (298 K and pH=1) of the hP(DAAmEP) polymer ($14.35 \text{ mmol}\cdot\text{L}^{-1}$) aqueous solution titrated by the $\text{Gd}(\text{NO}_3)_3\cdot 6\text{H}_2\text{O}$ ($17 \text{ mmol}\cdot\text{L}^{-1}$) stock solution, together with the fitting curve obtained with 'successive binding sites model' using the Levenberg–Marquardt non-linear curve-fitting algorithm.

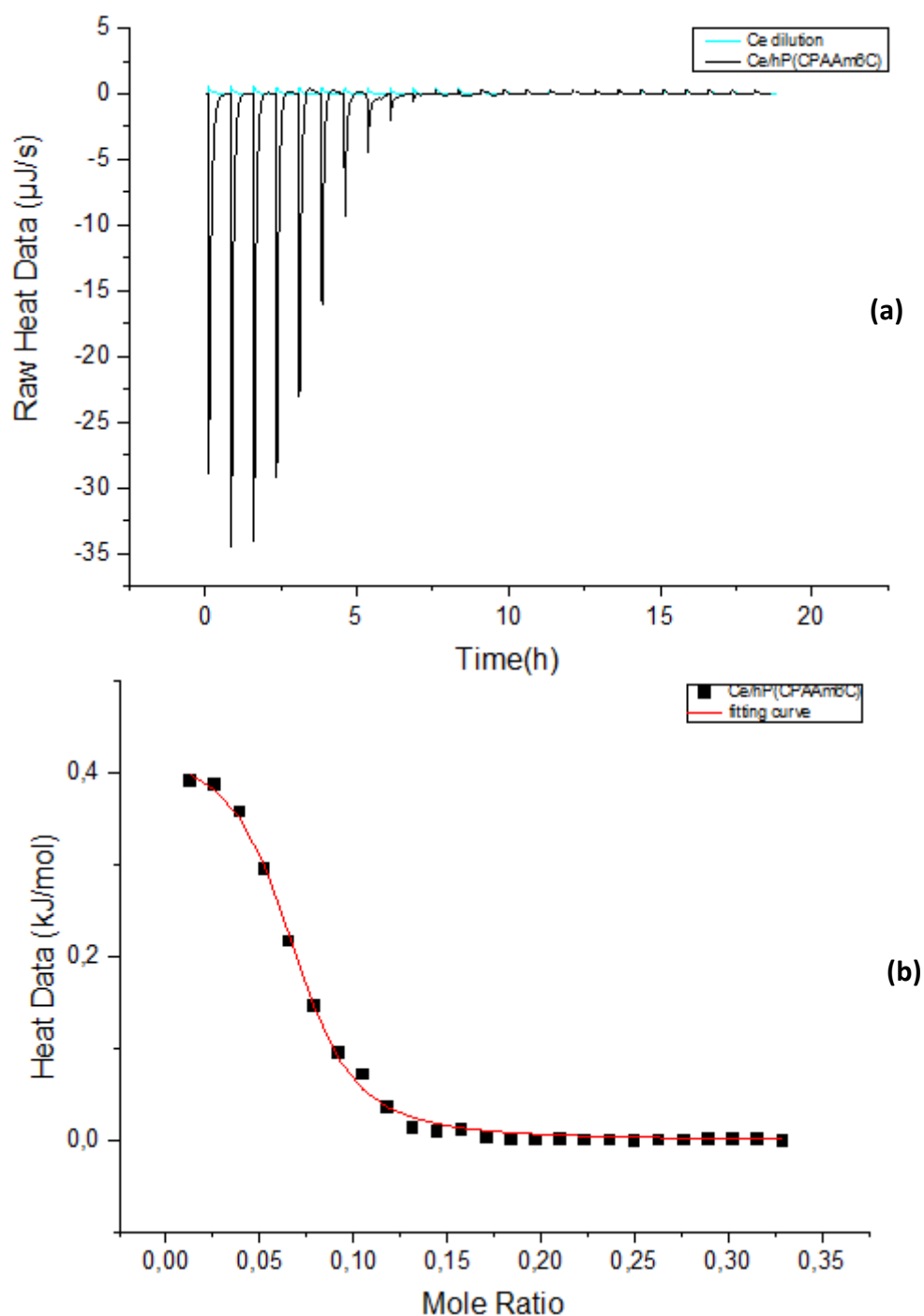


Figure SI 46. (a) Processed thermal profiles at 298 K and under pH=1 for injections of $17 \text{ mmol}\cdot\text{L}^{-1}$ Ce(III) stock solution into acidified water (Ce dilution) and injections of the same Ce(III) solution into $14.35 \text{ mmol}\cdot\text{L}^{-1}$ hP(CPAAm6C) aqueous solution: 25 successive injections recorded with $10 \mu\text{L}$ for each injection of the $\text{Ce}(\text{NO}_3)_3\cdot 6\text{H}_2\text{O}$ aqueous solution with pH=1 into a 1 mL stainless ampoule containing initially $800 \mu\text{L}$ of acidified water (dilution experiment) or $800 \mu\text{L}$ hP(CPAAm6C) aqueous solution with pH=1 (sorption experiment); (b) ITC heat data corresponding to the Ce(III) ITC experiments (298 K and pH=1) of the hP(CPAAm6C) polymer ($14.35 \text{ mmol}\cdot\text{L}^{-1}$) aqueous solution titrated by $\text{Ce}(\text{NO}_3)_3\cdot 6\text{H}_2\text{O}$ ($17 \text{ mmol}\cdot\text{L}^{-1}$) stock solution, together with the fitting curve obtained with 'successive binding sites model' using the Levenberg–Marquardt non-linear curve-fitting algorithm.

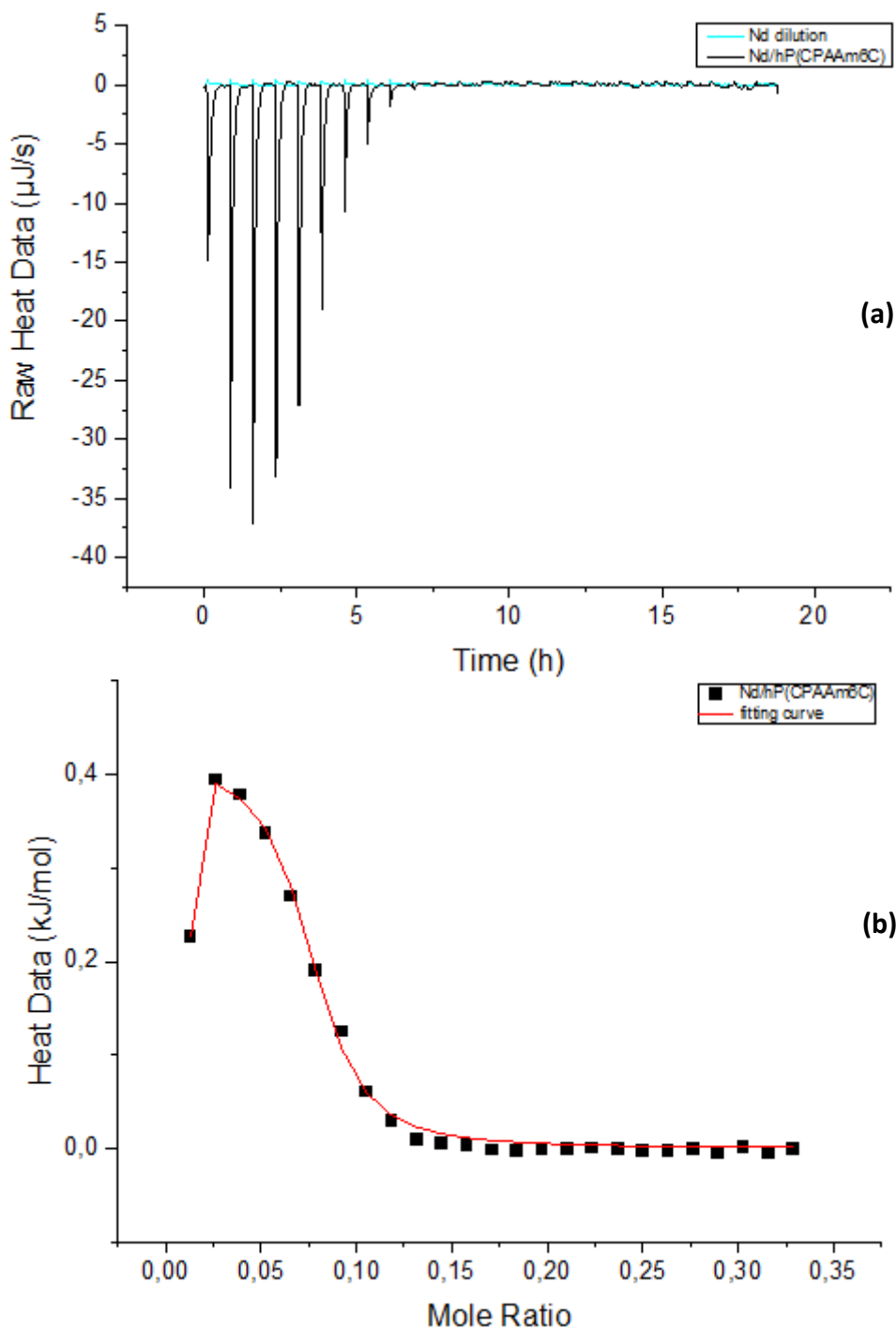


Figure SI 47. (a) Processed thermal profiles at 298 K and under pH=1 for injections of $17 \text{ mmol}\cdot\text{L}^{-1}$ Nd(III) stock solution into acidified water (Nd dilution) and injections of the same Nd(III) solution into $14.35 \text{ mmol}\cdot\text{L}^{-1}$ hP(CPAAm6C) aqueous solution: 25 successive injections recorded with $10 \mu\text{L}$ for each injection of the $\text{Nd}(\text{NO}_3)_3\cdot 6\text{H}_2\text{O}$ aqueous solution with pH=1 into a 1 mL stainless ampoule containing initially $800 \mu\text{L}$ of acidified water (dilution experiment) or $800 \mu\text{L}$ hP(CPAAm6C) aqueous solution with pH=1 (sorption experiment); (b) ITC heat data corresponding to the Nd(III) ITC experiments (298 K and pH=1) of the hP(CPAAm6C) polymer ($14.35 \text{ mmol}\cdot\text{L}^{-1}$) aqueous solution titrated by $\text{Nd}(\text{NO}_3)_3\cdot 6\text{H}_2\text{O}$ ($17 \text{ mmol}\cdot\text{L}^{-1}$) stock solution, together with the fitting

Supporting information

curve obtained with 'successive binding sites model' using the Levenberg–Marquardt non-linear curve-fitting algorithm.

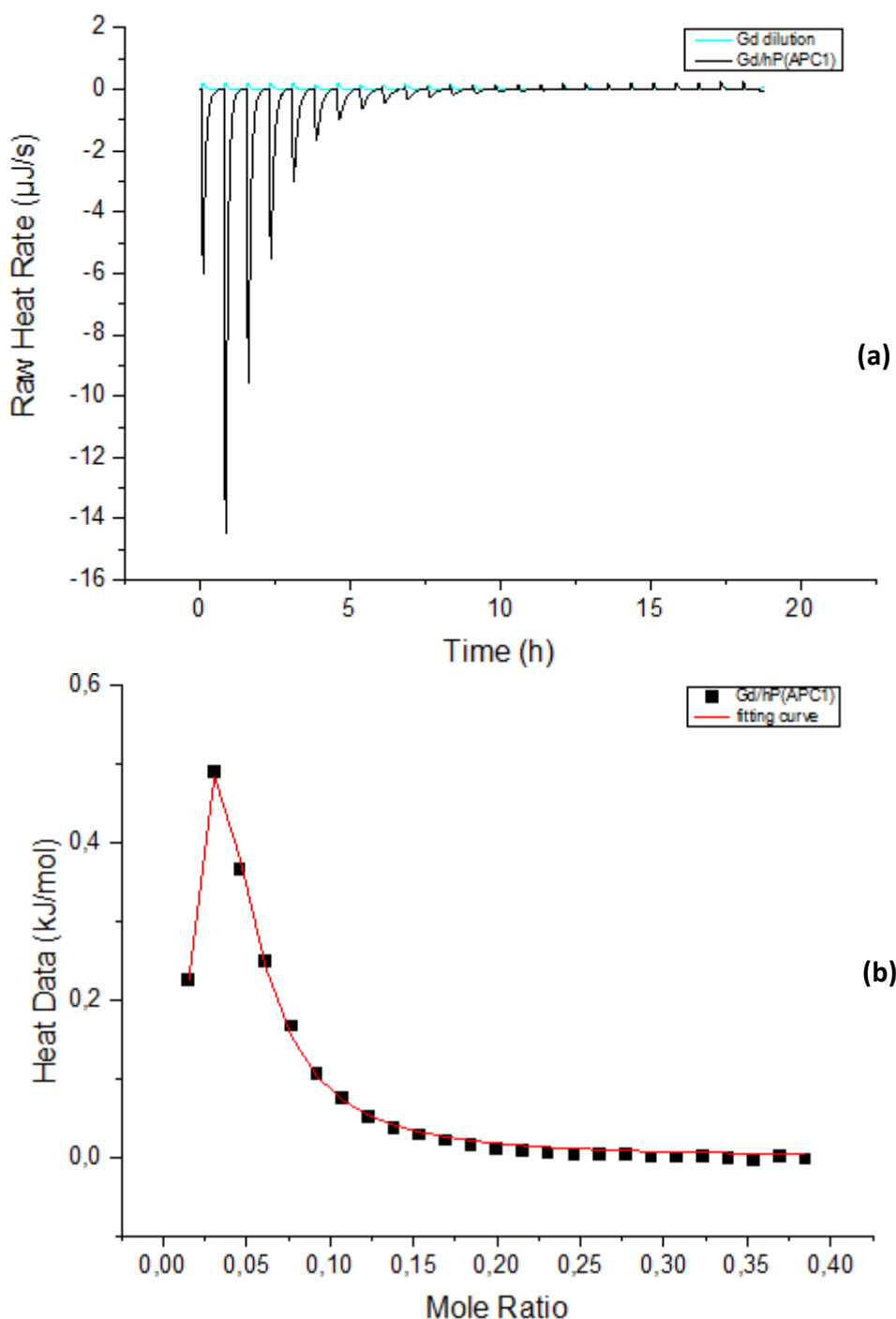


Figure SI 48. (a) Processed thermal profiles at 298 K and under pH=1 for injections of $17 \text{ mmol}\cdot\text{L}^{-1}$ Gd(III) stock solution into acidified water (Gd dilution) and injections of the same Gd(III) solution into $14.35 \text{ mmol}\cdot\text{L}^{-1}$ hP(APC1) aqueous solution: 25 successive injections recorded with $10 \mu\text{L}$ for each injection of the $\text{Gd}(\text{NO}_3)_3\cdot 6\text{H}_2\text{O}$ aqueous solution with pH=1 into a 1 mL stainless ampoule containing initially $800 \mu\text{L}$ of acidified water (dilution experiment) or $800 \mu\text{L}$ hP(APC1) aqueous solution with pH=1 (sorption experiment); (b) ITC heat data corresponding to the Gd(III) ITC experiments (298 K and pH=1) of the hP(APC1) polymer ($14.35 \text{ mmol}\cdot\text{L}^{-1}$) aqueous solution titrated by the $\text{Gd}(\text{NO}_3)_3\cdot 6\text{H}_2\text{O}$ ($17 \text{ mmol}\cdot\text{L}^{-1}$) stock solution, together with the fitting curve

Supporting information

obtained with 'successive binding sites model' using the Levenberg–Marquardt non-linear curve-fitting algorithm.

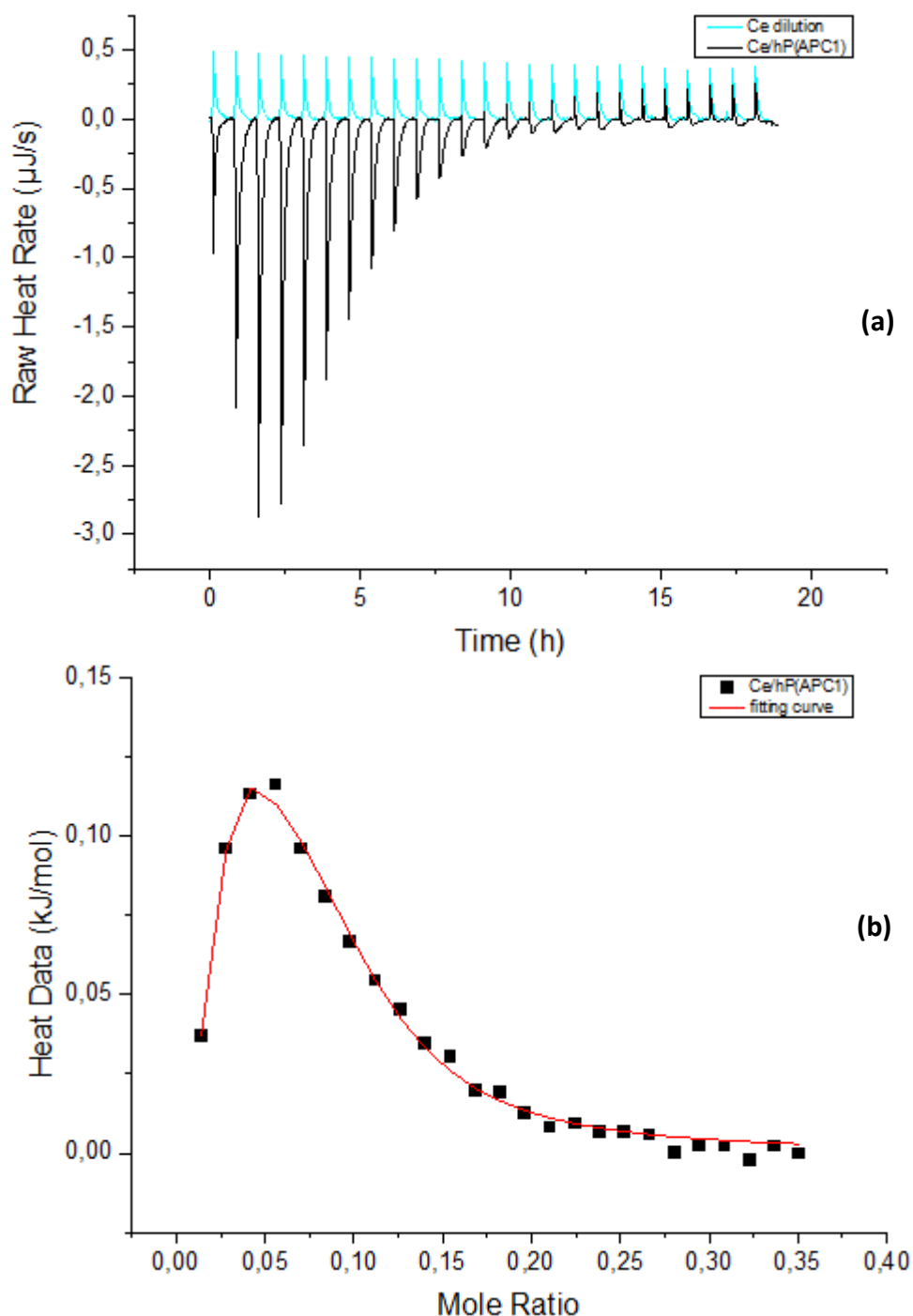


Figure SI 49. (a) Processed thermal profiles at 298 K and under pH=1 for injections of $17 \text{ mmol}\cdot\text{L}^{-1}$ Ce(III) stock solution into acidified water (Ce dilution) and injections of the same Ce(III) solution into $14.35 \text{ mmol}\cdot\text{L}^{-1}$ hP(APC1) aqueous solution: 25 successive injections recorded with $10 \mu\text{L}$ for each injection of the $\text{Ce}(\text{NO}_3)_3\cdot 6\text{H}_2\text{O}$ aqueous solution with pH=1 into a 1 mL stainless ampoule containing initially $800 \mu\text{L}$ of acidified water (dilution experiment) or $800 \mu\text{L}$ hP(APC1) aqueous solution with pH=1 (sorption experiment); (b) ITC heat data corresponding to the Ce(III) ITC experiments (298 K and pH=1) of the hP(APC1) polymer ($14.35 \text{ mmol}\cdot\text{L}^{-1}$) aqueous solution titrated by $\text{Ce}(\text{NO}_3)_3\cdot 6\text{H}_2\text{O}$ stock solution, together with the fitting curve obtained with 'successive binding sites model' using the Levenberg–Marquardt non-linear curve-fitting algorithm.

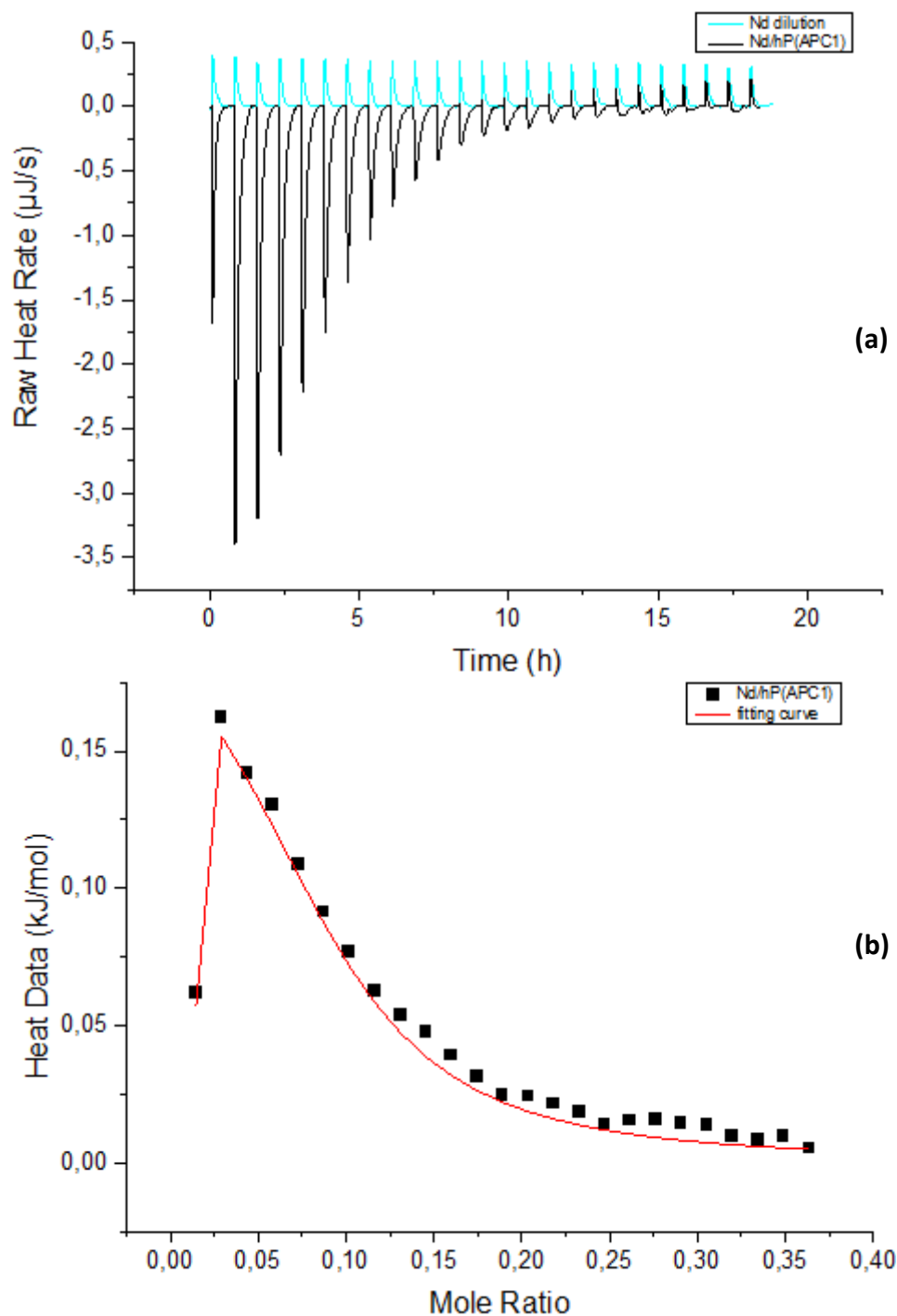


Figure SI 50. (a) Processed thermal profiles at 298 K and under pH=1 for injections of $17 \text{ mmol}\cdot\text{L}^{-1}$ Nd(III) stock solution into acidified water (Nd dilution) and injections of the same Nd(III) solution into $14.35 \text{ mmol}\cdot\text{L}^{-1}$ hP(APC1) aqueous solution: 25 successive injections recorded with $10 \mu\text{L}$ for each injection of the $\text{Nd}(\text{NO}_3)_3\cdot 6\text{H}_2\text{O}$ aqueous solution with pH=1 into a 1 mL stainless ampoule containing initially $800 \mu\text{L}$ of acidified water (dilution experiment) or $800 \mu\text{L}$ hP(APC1) aqueous solution with pH=1 (sorption experiment); (b) ITC heat data corresponding to the Nd(III) ITC experiments (298 K and pH=1) of the hP(APC1) polymer ($14.35 \text{ mmol}\cdot\text{L}^{-1}$)

Supporting information

aqueous solution titrated by $\text{Nd}(\text{NO}_3)_3 \cdot 6\text{H}_2\text{O}$ stock solution, together with the fitting curve obtained with 'successive binding sites model' using the Levenberg–Marquardt non-linear curve-fitting algorithm.

References

- [1] Mineral commodity summaries 2020, in: Mineral Commodity Summaries, Reston, VA, 2020, pp. 204.
- [2] Strengthening of the European Rare Earth Supply Chain - Challenges and policy options in, European Rare Earths Competency Network (ERECON), 2019.
- [3] B.L. Rivas, E. Pereira, A. Maureira, Functional water-soluble polymers: polymer–metal ion removal and biocide properties, *Polymer International*, 58 (2009) 1093-1114.
- [4] J.J. Pittman, V. Klep, I. Luzinov, R.K. Marcus, Extraction of metals from aqueous systems employing capillary-channeled polymer (C-CP) fibers modified with poly(acrylic acid) (PAA), *Analytical Methods*, 2 (2010) 461-469.
- [5] R.A. Beauvais, S.D. Alexandratos, Polymer-supported reagents for the selective complexation of metal ions: an overview, *Reactive and Functional Polymers*, 36 (1998) 113-123.
- [6] I.G. Dakova, I.B. Karadjova, V.T. Georgieva, G.S. Georgiev, Polycarboxylic microsphere polymer gel for solid phase extraction of trace elements, *Microchimica Acta*, 164 (2009) 55-61.
- [7] J. Deng, X. Kang, L. Chen, Y. Wang, Z. Gu, Z. Lu, A nanofiber functionalized with dithizone by co-electrospinning for lead (II) adsorption from aqueous media, *Journal of Hazardous Materials*, 196 (2011) 187-193.
- [8] S.D. Alexandratos, D.W. Crick, Polymer-Supported Reagents: Application to Separation Science, *Industrial & Engineering Chemistry Research*, 35 (1996) 635-644.
- [9] A. Popa, C.-M. Davidescu, P. Negrea, G. Ilia, A. Katsaros, K.D. Demadis, Synthesis and Characterization of Phosphonate Ester/Phosphonic Acid Grafted Styrene–Divinylbenzene Copolymer Microbeads and Their Utility in Adsorption of Divalent Metal Ions in Aqueous Solutions, *Industrial & Engineering Chemistry Research*, 47 (2008) 2010-2017.
- [10] L. Yang, Y. Li, X. Jin, Z. Ye, X. Ma, L. Wang, Y. Liu, Synthesis and characterization of a series of chelating resins containing amino/imino-carboxyl groups and their adsorption behavior for lead in aqueous phase, *Chemical Engineering Journal*, 168 (2011) 115-124.
- [11] L. Lebrun, F. Vallée, B. Alexandre, Q.T. Nguyen, Preparation of chelating membranes to remove metal cations from aqueous solutions, *Desalination*, 207 (2007) 9-23.

References

- [12] L. Pelit, F.N. Ertaş, A.E. Eroğlu, T. Shahwan, H. Tural, Biosorption of Cu(II) and Pb(II) ions from aqueous solution by natural spider silk, *Bioresource Technology*, 102 (2011) 8807-8813.
- [13] D. Prabhakaran, M.S. Subramanian, Selective extraction of U(VI), Th(IV), and La(III) from acidic matrix solutions and environmental samples using chemically modified Amberlite XAD-16 resin, *Analytical and Bioanalytical Chemistry*, 379 (2004) 519-525.
- [14] B.L. Rivas, C. Muñoz, Synthesis and metal ion adsorption properties of poly(4-sodium styrene sulfonate-co-acrylic acid), *Journal of Applied Polymer Science*, 114 (2009) 1587-1592.
- [15] M. Wongkaew, A. Imyim, P. Eamchan, Extraction of heavy metal ions from leachate of cement-based stabilized waste using purpurin functionalized resin, *Journal of Hazardous Materials*, 154 (2008) 739-747.
- [16] M. Tabakci, M. Yilmaz, Sorption characteristics of Cu(II) ions onto silica gel-immobilized calix[4]arene polymer in aqueous solutions: Batch and column studies, *Journal of Hazardous Materials*, 151 (2008) 331-338.
- [17] P.A. Kumar, S. Chakraborty, Fixed-bed column study for hexavalent chromium removal and recovery by short-chain polyaniline synthesized on jute fiber, *Journal of Hazardous Materials*, 162 (2009) 1086-1098.
- [18] E.E. Laney, J.H. Lee, J.S. Kim, X. Huang, Y. Jang, H.-S. Hwang, T. Hayashita, R.A. Bartsch, Sorption of lead(II) by proton-ionizable polyether resins, *Reactive and Functional Polymers*, 36 (1998) 125-134.
- [19] Z. Ajji, A.M. Ali, Separation of copper ions from iron ions using PVA-g-(acrylic acid/N-vinyl imidazole) membranes prepared by radiation-induced grafting, *Journal of Hazardous Materials*, 173 (2010) 71-74.
- [20] H. Bessbousse, J.-F. Verchère, L. Lebrun, Characterisation of metal-complexing membranes prepared by the semi-interpenetrating polymer networks technique. Application to the removal of heavy metal ions from aqueous solutions, *Chemical Engineering Journal*, 187 (2012) 16-28.
- [21] Y. Jiang, W.-C. Wang, Functional membranes prepared by layer-by-layer assembly and its metal ions adsorption property, *Polymers for Advanced Technologies*, 22 (2011) 2509-2516.

References

- [22] B. Gupta, N. Anjum, Preparation of ion-exchange membranes by the hydrolysis of radiation-grafted polyethylene-g-polyacrylamide films: Properties and metal-ion separation, *Journal of Applied Polymer Science*, 90 (2003) 3747-3752.
- [23] J.D. Lamb, A.Y. Nazarenko, Selective Metal Ion Sorption and Transport Using Polymer Inclusion Membranes Containing Dicyclohexano-18-crown-6, *Separation Science and Technology*, 32 (1997) 2749-2764.
- [24] G.E. Fryxell, W. Chouyyok, R.D. Rutledge, Design and synthesis of chelating diamide sorbents for the separation of lanthanides, *Inorganic Chemistry Communications*, 14 (2011) 971-974.
- [25] C. Gérente, P. Couespel du Mesnil, Y. Andrès, J.-F. Thibault, P. Le Cloirec, Removal of metal ions from aqueous solution on low cost natural polysaccharides: Sorption mechanism approach, *Reactive and Functional Polymers*, 46 (2000) 135-144.
- [26] B.L. Rivas, B.F. Urbano, J. Sánchez, Water-Soluble and Insoluble Polymers, Nanoparticles, Nanocomposites and Hybrids With Ability to Remove Hazardous Inorganic Pollutants in Water, *Frontiers in Chemistry*, 6 (2018).
- [27] F. Gao, An Overview of Surface-Functionalized Magnetic Nanoparticles: Preparation and Application for Wastewater Treatment, *ChemistrySelect*, 4 (2019) 6805-6811.
- [28] L. Dambies, A. Jaworska, G. Zakrzewska-Trznadel, B. Sartowska, Comparison of acidic polymers for the removal of cobalt from water solutions by polymer assisted ultrafiltration, *Journal of Hazardous Materials*, 178 (2010) 988-993.
- [29] S. Verbych, M. Bryk, M. Zaichenko, Water treatment by enhanced ultrafiltration, *Desalination*, 198 (2006) 295-302.
- [30] B.L. Rivas, E.D. Pereira, M. Palencia, J. Sánchez, Water-soluble functional polymers in conjunction with membranes to remove pollutant ions from aqueous solutions, *Progress in Polymer Science*, 36 (2011) 294-322.
- [31] É. Fenyvesi, K. Barkács, K. Gruiz, E. Varga, I. Kenyeres, G. Záray, L. Szenté, Removal of hazardous micropollutants from treated wastewater using cyclodextrin bead polymer – A pilot demonstration case, *Journal of Hazardous Materials*, 383 (2020) 121181.
- [32] S. Syed, Recovery of gold from secondary sources—A review, *Hydrometallurgy*, 115-116 (2012) 30-51.
- [33] International year of the periodic table, in, philipharris.co.uk.

References

- [34] Z.B. Chunhui Huang, *Rare Earth Coordination Chemistry: Fundamental and Applications* John Wiley & Sons (Asia) Pte Ltd, Singapore, 2010.
- [35] J.-C.G. Bünzli, Lanthanides, *Kirk-Othmer Encyclopedia of Chemical Technology*, (2013) 1-43.
- [36] A. Keren, W. Crump, B.P.P. Mallett, S.V. Chong, I. Keren, H. Luetkens, J.L. Tallon, Relevance of magnetism to cuprate superconductivity: Lanthanides versus charge-compensated cuprates, *Physical Review B*, 100 (2019) 144512.
- [37] J. Henao, Y. Pacheco, O. Sotelo, M. Casales, L. Martinez-Gómez, Lanthanum titanate nanometric powder potentially for rechargeable Ni-batteries: Synthesis and electrochemical hydrogen storage, *Journal of Materials Research and Technology*, 8 (2019) 759-765.
- [38] R. Kawalla, V. Brichkin, V.Y. Bazhin, T. Litvinova, Ways of rare earth application for iron and steel production technologies, in: *Innovation-Based Development of the Mineral Resources Sector: Challenges and Prospects: Proceedings of the 11th Russian-German Raw Materials Conference*, November 7-8, 2018, Potsdam, Germany, CRC Press, 2018, pp. 359.
- [39] H. Nakamura, The current and future status of rare earth permanent magnets, *Scripta Materialia*, 154 (2018) 273-276.
- [40] B. Tian, A. Fernandez-Bravo, H. Najafiaghdam, N.A. Torquato, M.V.P. Altoe, A. Teitelboim, C.A. Tajon, Y. Tian, N.J. Borys, E.S. Barnard, M. Anwar, E.M. Chan, P.J. Schuck, B.E. Cohen, Low irradiance multiphoton imaging with alloyed lanthanide nanocrystals, *Nature Communications*, 9 (2018) 3082.
- [41] K.H. Thompson, C. Orvig, Editorial: Lanthanide compounds for therapeutic and diagnostic applications, *Chemical Society Reviews*, 35 (2006) 499-499.
- [42] I. Kostova, Lanthanides as Anticancer Agents, *Current Medicinal Chemistry - Anti-Cancer Agents*, 5 (2005) 591-602.
- [43] J.T. Dahle, Y. Arai, Environmental geochemistry of cerium: applications and toxicology of cerium oxide nanoparticles, *International journal of environmental research and public health*, 12 (2015) 1253-1278.
- [44] G.A. Molander, Application of lanthanide reagents in organic synthesis, *Chemical Reviews*, 92 (1992) 29-68.

References

- [45] W. Li, M. Xue, F. Xu, J. Tu, Y. Zhang, Q. Shen, Synthesis, characterization of bridged bis(amidinate) lanthanide amides and their application as catalysts for addition of amines to nitriles for monosubstituted N-arylamidines, *Dalton Transactions*, 41 (2012) 8252-8260.
- [46] E. Kirillov, A.K. Dash, A.-S. Rodrigues, J.-F. Carpentier, Ansa-metallocene and half-sandwich complexes of group-3 metals and lanthanides incorporating fluorenyl-based ligands: from synthesis to catalytic applications, *Comptes Rendus Chimie*, 9 (2006) 1151-1157.
- [47] J. Dowsland, F. McKerlie, D.J. Procter, Convenient preparation of ytterbium(III) chalcogenolate complexes by insertion of ytterbium into chalcogen-chalcogen bonds. Application in the ring-opening of epoxides, *Tetrahedron Letters*, 41 (2000) 4923-4927.
- [48] H. Noss, M. Oberthür, C. Fischer, W.P. Kretschmer, R. Kempe, Complexes of Group 3 Metals and Lanthanides That Contain Siloxane-Bridged Bisaminopyridinato Ligands: Synthesis, Structure, and Application in the Ring-Opening Polymerization of Lactones, *European Journal of Inorganic Chemistry*, 1999 (1999) 2283-2288.
- [49] K. Nie, L. Fang, Y. Yao, Y. Zhang, Q. Shen, Y. Wang, Synthesis and Characterization of Amine-Bridged Bis(phenolate)lanthanide Alkoxides and Their Application in the Controlled Polymerization of rac-Lactide and rac- β -Butyrolactone, *Inorganic Chemistry*, 51 (2012) 11133-11143.
- [50] W. Li, Z. Zhang, Y. Yao, Y. Zhang, Q. Shen, Control of Conformations of Piperazine-Bridged Bis(phenolato) Groups: Syntheses and Structures of Bimetallic and Monometallic Lanthanide Amides and Their Application in the Polymerization of Lactides, *Organometallics*, 31 (2012) 3499-3511.
- [51] L. Wang, X. Huang, Y. Yu, L. Zhao, C. Wang, Z. Feng, D. Cui, Z. Long, Towards cleaner production of rare earth elements from bastnaesite in China, *Journal of Cleaner Production*, 165 (2017) 231-242.
- [52] S. Cotton, Introduction to the Actinides, in: *Lanthanide and Actinide Chemistry*, 2006, pp. 145-153.
- [53] K.L. Nash, J.C. Braley, Challenges for Actinide Separations in Advanced Nuclear Fuel Cycles, in: *Nuclear Energy and the Environment*, American Chemical Society, 2010, pp. 19-38.

References

- [54] S. Cotton, Coordination Chemistry of the Actinides, in: Lanthanide and Actinide Chemistry, 2006, pp. 173-199.
- [55] M.S. Fred, Spectra and Electronic Structure of Free Actinide Atoms and Ions, in: J.J. Katz, G.T. Seaborg, L.R. Morss (Eds.) The Chemistry of the Actinide Elements: Volume 2, Springer Netherlands, Dordrecht, 1986, pp. 1196-1234.
- [56] J. Leduc, M. Frank, L. Jürgensen, D. Graf, A. Raauf, S. Mathur, Chemistry of Actinide Centers in Heterogeneous Catalytic Transformations of Small Molecules, ACS Catalysis, 9 (2019) 4719-4741.
- [57] M.I. Ojovan, W.E. Lee, S.N. Kalmykov, Chapter 16 - Treatment of Radioactive Wastes, in: M.I. Ojovan, W.E. Lee, S.N. Kalmykov (Eds.) An Introduction to Nuclear Waste Immobilisation (Third Edition), Elsevier, 2019, pp. 231-269.
- [58] K. Bobrowski, K. Skotnicki, T. Szreder, Application of radiation chemistry to some selected technological issues related to the development of nuclear energy, in: Applications of Radiation Chemistry in the Fields of Industry, Biotechnology and Environment, Springer, 2017, pp. 147-194.
- [59] S.G. McAdams, A.-M. Ariciu, A.K. Kostopoulos, J.P.S. Walsh, F. Tuna, Molecular single-ion magnets based on lanthanides and actinides: Design considerations and new advances in the context of quantum technologies, Coordination Chemistry Reviews, 346 (2017) 216-239.
- [60] Y. Gao, B. Wang, Y. Lei, B.K. Teo, Z. Wang, Actinide-embedded gold superatom models: Electronic structure, spectroscopic properties, and applications in surface-enhanced Raman scattering, Nano Research, 9 (2016) 622-632.
- [61] K.-Q. Hu, Z.-W. Huang, Z.-H. Zhang, L. Mei, B.-B. Qian, J.-P. Yu, Z.-F. Chai, W.-Q. Shi, Actinide-Based Porphyrinic MOF as a Dehydrogenation Catalyst, Chemistry – A European Journal, 24 (2018) 16766-16769.
- [62] A. Kumar, M. Ali, R.S. Ningthoujam, P. Gaikwad, M. Kumar, B.B. Nath, B.N. Pandey, The interaction of actinide and lanthanide ions with hemoglobin and its relevance to human and environmental toxicology, Journal of Hazardous Materials, 307 (2016) 281-293.
- [63] S. Barath Kumar, R.K. Padhi, K.K. Satpathy, P.K. Parida, Ultra-structural alterations in gill tissues of *Scylla serrate* (mud crab) on exposure to uranium, Indira Gandhi Centre for Atomic Research, India, 2017.

References

- [64] P. Iryna, Toxicity of Radionuclides in Determining Harmful Effects on Humans and Environment, *Journal of Environmental Science and Public Health*, 01 (2017) 115-119.
- [65] J.A. Thompson, Using Water-soluble Polymers to Remove Dissolved Metal Ions, *Filtration & Separation*, (1999) 28-32.
- [66] B.L. Rivas, E.D. Pereira, I. Moreno-Villoslada, Water-soluble polymer–metal ion interactions, *Progress in Polymer Science*, 28 (2003) 173-208.
- [67] J. Su, R. Xu, S. Ni, F. Li, X. Sun, A cost-effective process for recovering thorium and rare earths from radioactive residues, *Journal of Cleaner Production*, 254 (2020) 119931.
- [68] Y. Hu, J. Florek, D. Larivière, F.-G. Fontaine, F. Kleitz, Recent Advances in the Separation of Rare Earth Elements Using Mesoporous Hybrid Materials, *The Chemical Record*, 18 (2018) 1261-1276.
- [69] X. Zhang, P. Gu, Y. Liu, Decontamination of radioactive wastewater: State of the art and challenges forward, *Chemosphere*, 215 (2019) 543-553.
- [70] U.F. Hugo Royen, Rare Earth Elements-Purification, Separation and Recycling, in, IVL Swedish Environmental Research Institute Stockholm, Sweden, 2016.
- [71] H. Jin, D.W. Reed, V.S. Thompson, Y. Fujita, Y. Jiao, M. Crain-Zamora, J. Fisher, K. Scalzone, M. Griffel, D. Hartley, J.W. Sutherland, Sustainable Bioleaching of Rare Earth Elements from Industrial Waste Materials Using Agricultural Wastes, *ACS Sustainable Chemistry & Engineering*, 7 (2019) 15311-15319.
- [72] V.L. Brisson, W.-Q. Zhuang, L. Alvarez-Cohen, Bioleaching of rare earth elements from monazite sand, *Biotechnology and Bioengineering*, 113 (2016) 339-348.
- [73] S. Ilyas, M.-s. Kim, J.-c. Lee, Integration of microbial and chemical processing for a sustainable metallurgy, *Journal of Chemical Technology & Biotechnology*, 93 (2018) 320-332.
- [74] H. Hou, J. Xu, Y. Wang, J. Chen, Solvent extraction of lanthanum and cerium ions from hydrochloric acidic aqueous solutions using partly saponified 2-ethylhexyl phosphonic acid mono-2-ethylhexyl ester, *Chinese Journal of Chemical Engineering*, 24 (2016) 79-85.
- [75] C. Tunsu, Y. Menard, D.Ø. Eriksen, C. Ekberg, M. Petranikova, Recovery of critical materials from mine tailings: A comparative study of the solvent extraction of rare earths using acidic, solvating and mixed extractant systems, *Journal of Cleaner Production*, 218 (2019) 425-437.

References

- [76] V. Beaugeard, J. Muller, A. Graillot, X. Ding, J.-J. Robin, S. Monge, Acidic polymeric sorbents for the removal of metallic pollution in water: A review, *Reactive and Functional Polymers*, (2020) 104599.
- [77] J.A. Marinsky, Selectivity and Ion Speciation in Cation-Exchange Resins, in: *Mass Transfer and Kinetics of Ion Exchange*, Springer, 1983, pp. 75-120.
- [78] Y. Ren, J. Zhang, J. Guo, F. Chen, F. Yan, Porous Poly(Ionic Liquid) Membranes as Efficient and Recyclable Absorbents for Heavy Metal Ions, *Macromolecular Rapid Communications*, 38 (2017) 1700151.
- [79] A. Nowik-Zajac, I. Zawierucha, C. Kozłowski, Selective removal of silver(i) using polymer inclusion membranes containing calixpyrroles, *RSC Advances*, 9 (2019) 31122-31132.
- [80] R. Camarillo, Á. Pérez, P. Cañizares, A. de Lucas, Removal of heavy metal ions by polymer enhanced ultrafiltration: Batch process modeling and thermodynamics of complexation reactions, *Desalination*, 286 (2012) 193-199.
- [81] B.L. Rivas, C. Espinosa, J. Sánchez, Application of the liquid-phase polymer-based retention technique to the sorption of molybdenum(VI) and vanadium(V), *Polymer Bulletin*, 76 (2019) 539-552.
- [82] J. Wang, H. Li, L. Tang, C. Zhong, Y. Liu, L. Lu, T. Qiu, H. Liu, Behavior and mechanism of low-concentration rare earth ions precipitated by the microbial humic-like acids, *Environmental Science and Pollution Research*, (2020).
- [83] T. Kegl, A. Košak, A. Lobnik, Z. Novak, A.K. Kralj, I. Ban, Adsorption of rare earth metals from wastewater by nanomaterials: A review, *Journal of Hazardous Materials*, 386 (2020) 121632.
- [84] N.K. Gupta, A. Sengupta, A. Gupta, J.R. Sonawane, H. Sahoo, Biosorption-an alternative method for nuclear waste management: a critical review, *Journal of Environmental Chemical Engineering*, 6 (2018) 2159-2175.
- [85] E.S. Aziman, A.H.J. Mohd Salehuddin, A.F. Ismail, Remediation of Thorium (IV) from Wastewater: Current Status and Way Forward, *Separation & Purification Reviews*, (2019) 1-26.
- [86] J. Wang, S. Zhuang, Cesium separation from radioactive waste by extraction and adsorption based on crown ethers and calixarenes, *Nuclear Engineering and Technology*, 52 (2020) 328-336.

References

- [87] V. Luca, J. Veliscek-Carolan, New insights into the radiolytic stability of metal(iv) phosphonate hybrid adsorbent materials, *Physical Chemistry Chemical Physics*, 22 (2020) 17027-17032.
- [88] O. Sedlacek, J. Kucka, B.D. Monnery, M. Slouf, M. Vetric, R. Hoogenboom, M. Hruby, The effect of ionizing radiation on biocompatible polymers: From sterilization to radiolysis and hydrogel formation, *Polymer Degradation and Stability*, 137 (2017) 1-10.
- [89] G. Crini, N. Morin-Crini, N. Fatin-Rouge, S. Déon, P. Fievet, Metal removal from aqueous media by polymer-assisted ultrafiltration with chitosan, *Arabian Journal of Chemistry*, 10 (2017) S3826-S3839.
- [90] E.C. Aka, M.C. Nongbe, T. Ekou, L. Ekou, V. Coeffard, F.-X. Felpin, A fully bio-sourced adsorbent of heavy metals in water fabricated by immobilization of quinine on cellulose paper, *Journal of Environmental Sciences*, 84 (2019) 174-183.
- [91] T. Kaliyappan, P. Kannan, Co-ordination polymers, *Progress in Polymer Science*, 25 (2000) 343-370.
- [92] M.B. Charlotte M. Sevrain, Hélène Couthon and Paul-Alain Jaffrès, Phosphonic acid: preparation and application, *Beilstein Journal of Organic Chemistry*, 13 (2017) 2186-2213.
- [93] J. Jiang, E. Yang, K.R. Reddy, D.M. Niedzwiedzki, C. Kirmaier, D.F. Bocian, D. Holten, J.S. Lindsey, Synthetic bacteriochlorins bearing polar motifs (carboxylate, phosphonate, ammonium and a short PEG). Water-solubilization, bioconjugation, and photophysical properties, *New Journal of Chemistry*, 39 (2015) 5694-5714.
- [94] K. Ohta, Prediction of pKa Values of Alkylphosphonic Acids, *Bulletin of the Chemical Society of Japan*, 65 (1992) 2543-2545.
- [95] A. Graillot, D. Bouyer, S. Monge, J.-J. Robin, C. Faur, Removal of nickel ions from aqueous solution by low energy-consuming sorption process involving thermosensitive copolymers with phosphonic acid groups, *Journal of hazardous materials*, 244 (2013) 507-515.
- [96] O.C.S. Al Hamouz, S.A. Ali, Removal of heavy metal ions using a novel cross-linked polyzwitterionic phosphonate, *Separation and Purification Technology*, 98 (2012) 94-101.
- [97] R.X. Liu, B.W. Zhang, H.X. Tang, Synthesis and characterization of poly(acrylamino-phosphonic-carboxyl-hydrazide) chelating fibre, *Reactive and Functional Polymers*, 39 (1999) 71-81.

References

- [98] S.D. Alexandratos, L.A. Hussain, Synthesis of α -, β -, and γ -Ketophosphonate Polymer-Supported Reagents: The Role of Intra-ligand Cooperation in the Complexation of Metal Ions, *Macromolecules*, 31 (1998) 3235-3238.
- [99] S.D. Alexandratos, S. Natesan, Ion-selective polymer-supported reagents: the principle of bifunctionality, *European Polymer Journal*, 35 (1999) 431-436.
- [100] N. Ferrah, O. Abderrahim, M.A. Didi, D. Villemin, Removal of copper ions from aqueous solutions by a new sorbent: Polyethyleneiminemethylene phosphonic acid, *Desalination*, 269 (2011) 17-24.
- [101] V. Kubíček, J. Kotek, P. Hermann, I. Lukeš, Aminoalkylbis(phosphonates): Their Complexation Properties in Solution and in the Solid State, *European Journal of Inorganic Chemistry*, 2007 (2007) 333-344.
- [102] D. Prabhakaran, M.S. Subramanian, Extraction of U(VI), Th(IV), and La(III) from acidic streams and geological samples using AXAD-16–POPDE polymer, *Analytical and Bioanalytical Chemistry*, 380 (2004) 578-585.
- [103] H. Tokuyama, T. Yoshida, L. He, Preparation of Novel Emulsion Gel Adsorbents and Their Adsorption Properties for Heavy-Metal Ions, *Industrial & Engineering Chemistry Research*, 50 (2011) 10270-10277.
- [104] T.P. Knepper, Synthetic chelating agents and compounds exhibiting complexing properties in the aquatic environment, *TrAC Trends in Analytical Chemistry*, 22 (2003) 708-724.
- [105] O. Abderrahim, M.A. Didi, B. Moreau, D. Villemin, A New Sorbent for Selective Separation of Metal: Polyethylenimine Methylene phosphonic Acid, *Solvent Extraction and Ion Exchange*, 24 (2006) 943-955.
- [106] O. Abderrahim, M. Didi, B. Moreau, D. Villemin, Selective separation of metals by a new sorbent, the polyethylenimine methylenephosphonic acid (PEIMPA), *Studii si Cercetari Stiintifice: Chimie si Inginerie Chimica, Biotehnologii, Industrie Alimentara (Universitatea Bacau)*, 8 (2007) 129-141.
- [107] O. Abderrahim, M.A. Didi, D. Villemin, A new sorbent for uranium extraction: Polyethyleniminephenylphosphonamidic acid, *Journal of Radioanalytical and Nuclear Chemistry*, 279 (2009) 237-244.

References

- [108] T. Nonaka, A. Yasunaga, T. Ogata, S. Kurihara, Formation of thermosensitive copolymer beads having phosphinic acid groups and adsorption ability for metal ions, *Journal of Applied Polymer Science*, 99 (2006) 449-460.
- [109] A.W. Trochimczuk, M. Streat, Novel chelating resins with aminothiophosphonate ligands, *Reactive and Functional Polymers*, 40 (1999) 205-213.
- [110] T. Kusunoki, M. Oshiro, F. Hamasaki, T. Kobayashi, Polyvinylphosphonic acid copolymer hydrogels prepared with amide and ester type crosslinkers, *Journal of Applied Polymer Science*, 119 (2011) 3072-3079.
- [111] D. Prabhakaran, M.S. Subramanian, Selective extraction of U(VI) over Th(IV) from acidic streams using di-bis(2-ethylhexyl) malonamide anchored chloromethylated polymeric matrix, *Talanta*, 65 (2005) 179-184.
- [112] D.G. Rodrigues, S. Monge, S. Pellet-Rostaing, N. Dacheux, D. Bouyer, C. Faur, A new carbamoylmethylphosphonic acid-based polymer for the selective sorption of rare earth elements, *Chemical Engineering Journal*, 371 (2019) 857-867.
- [113] V.I. Grachek, A.A. Shunkevich, R.V. Martsynkevich, Synthesis and sorption properties of new fibrous nitrogen- and phosphorus-containing ion exchangers, *Russian Journal of Applied Chemistry*, 84 (2011) 1335.
- [114] T. Vasudevan, A.K. Pandey, S. Das, P.K. Pujari, Poly(ethylene glycol methacrylate phosphate-co-2-acrylamido-2-methyl-1-propane sulfonate) pore-filled substrates for heavy metal ions sorption, *Chemical Engineering Journal*, 236 (2014) 9-16.
- [115] S.D. Alexandratos, M.-J. Hong, Enhanced metal ion affinities by supported ligand synergistic interaction in bifunctional polymer-supported aminomethylphosphonates, *Separation Science and Technology*, 37 (2002) 2587-2605.
- [116] S.D. Alexandratos, New polymer-supported ion-complexing agents: Design, preparation and metal ion affinities of immobilized ligands, *Journal of Hazardous Materials*, 139 (2007) 467-470.
- [117] S.D. Alexandratos, S.D. Smith, Intraligand cooperation in metal-ion binding by immobilized ligands: The effect of bifunctionality, *Journal of Applied Polymer Science*, 91 (2004) 463-468.

References

- [118] S.D. Alexandratos, A.W. Trochimczuk, E.P. Horwitz, R.C. Gatrone, Synthesis and characterization of a bifunctional ion exchange resin with polystyrene-immobilized diphosphonic acid ligands, *Journal of Applied Polymer Science*, 61 (1996) 273-278.
- [119] A. Rogina, A. Lončarević, M. Antunović, I. Marijanović, M. Ivanković, H. Ivanković, Tuning physicochemical and biological properties of chitosan through complexation with transition metal ions, *International Journal of Biological Macromolecules*, 129 (2019) 645-652.
- [120] M. Ajmal, R.A.K. Rao, S. Anwar, J. Ahmad, R. Ahmad, Adsorption studies on rice husk: removal and recovery of Cd(II) from wastewater, *Bioresour. Technol.*, 86 (2003) 147-149.
- [121] A. Graillet, C. Cojocariu, D. Bouyer, S. Monge, S. Mauchauffe, J.J. Robin, C. Faur, Thermosensitive polymer Enhanced Filtration (TEF) process: An innovative process for heavy metals removal and recovery from industrial wastewaters, *Sep. Purif. Technol.*, 141 (2015) 17-24.
- [122] M.R. Aguilar, C. Elvira, A. Gallardo, B. Vázquez, J. Román, Smart polymers and their applications as biomaterials, *Topics in tissue engineering*, 3 (2007).
- [123] A. Bordat, T. Boissenot, J. Nicolas, N. Tsapis, Thermoresponsive polymer nanocarriers for biomedical applications, *Advanced Drug Delivery Reviews*, 138 (2019) 167-192.
- [124] D. Roy, W.L.A. Brooks, B.S. Sumerlin, New directions in thermoresponsive polymers, *Chemical Society Reviews*, 42 (2013) 7214-7243.
- [125] L. Klouda, Thermoresponsive hydrogels in biomedical applications: A seven-year update, *European Journal of Pharmaceutics and Biopharmaceutics*, 97 (2015) 338-349.
- [126] R. Pelton, Temperature-sensitive aqueous microgels, *Advances in Colloid and Interface Science*, 85 (2000) 1-33.
- [127] A. Graillet, D. Bouyer, S. Monge, J.-J. Robin, P. Loison, C. Faur, Sorption properties of a new thermosensitive copolymeric sorbent bearing phosphonic acid moieties in multi-component solution of cationic species, *Journal of Hazardous Materials*, 260 (2013) 425-433.
- [128] P. Bass, L. Zhang, Z.Y. Cheng, Time-dependence of the electromechanical bending actuation observed in ionic-electroactive polymers, *Journal of Advanced Dielectrics*, 7 (2017) 1720002.
- [129] L. Zhang, Z. Liu, X. Lu, G. Yang, X. Zhang, Z.-Y. Cheng, Nano-clip based composites with a low percolation threshold and high dielectric constant, *Nano Energy*, 26 (2016) 550-557.

References

- [130] J. Ge, Y. Wang, S. Min, Degradable performance and bio-mineralization function of PLA-PEG-PLA/PLA tissue engineering scaffold in vitro and in vivo, *Sheng wu yi xue gong cheng xue za zhi= Journal of biomedical engineering= Shengwu yixue gongchengxue zazhi*, 27 (2010) 1070-1075.
- [131] Y. Zou, L. Zhang, L. Yang, F. Zhu, M. Ding, F. Lin, Z. Wang, Y. Li, "Click" chemistry in polymeric scaffolds: Bioactive materials for tissue engineering, *Journal of controlled release*, 273 (2018) 160-179.
- [132] M.R. Matanović, J. Kristl, P.A. Grabnar, Thermoresponsive polymers: Insights into decisive hydrogel characteristics, mechanisms of gelation, and promising biomedical applications, *International Journal of Pharmaceutics*, 472 (2014) 262-275.
- [133] C. Liu, J. Guo, W. Yang, J. Hu, C. Wang, S. Fu, Magnetic mesoporous silica microspheres with thermo-sensitive polymer shell for controlled drug release, *Journal of Materials Chemistry*, 19 (2009) 4764-4770.
- [134] Z.-Q. Zhang, S.-C. Song, Multiple hyperthermia-mediated release of TRAIL/SPION nanocomplex from thermosensitive polymeric hydrogels for combination cancer therapy, *Biomaterials*, 132 (2017) 16-27.
- [135] P. Zarrintaj, M. Jouyandeh, M.R. Ganjali, B.S. Hadavand, M. Mozafari, S.S. Sheiko, M. Vatankhah-Varnoosfaderani, T.J. Gutiérrez, M.R. Saeb, Thermo-sensitive polymers in medicine: A review, *European Polymer Journal*, 117 (2019) 402-423.
- [136] S. Chen, Y. Zhang, K. Wang, H. Zhou, W. Zhang, N-Ester-substituted polyacrylamides with a tunable lower critical solution temperature (LCST): the N-ester-substitute dependent thermoresponse, *Polymer Chemistry*, 7 (2016) 3509-3519.
- [137] D.G. Lessard, M. Ousalem, X. Zhu, Effect of the molecular weight on the lower critical solution temperature of poly(N,N-diethylacrylamide) in aqueous solutions, *Canadian Journal of Chemistry*, 79 (2011) 1870-1874.
- [138] J.-S. Park, K. Kataoka, Precise Control of Lower Critical Solution Temperature of Thermosensitive Poly(2-isopropyl-2-oxazoline) via Gradient Copolymerization with 2-Ethyl-2-oxazoline as a Hydrophilic Comonomer, *Macromolecules*, 39 (2006) 6622-6630.
- [139] V.H. Pino-Ramos, G. Cedillo, E. López-Barriguete, E. Bucio, Comonomer effect: Switching the lower critical solution temperature to upper critical solution temperature in

References

thermo-pH sensitive binary graft copolymers, *Journal of Applied Polymer Science*, 136 (2019) 48170.

[140] M.H. Futscher, M. Philipp, P. Müller-Buschbaum, A. Schulte, The Role of Backbone Hydration of Poly(N-isopropyl acrylamide) Across the Volume Phase Transition Compared to its Monomer, *Scientific Reports*, 7 (2017) 17012.

[141] W. Tachaboonyakiat, H. Ajiro, M. Akashi, Synthesis of a thermosensitive polycation by random copolymerization of N-vinylformamide and N-vinylbutyramide, *Polymer Journal*, 45 (2013) 971-978.

[142] E. Makhaeva, L. Thanh, S. Starodoubtsev, A. Khokhlov, Thermoshrinking behavior of poly(vinylcaprolactam) gels in aqueous solution, *Macromolecular Chemistry and Physics*, 197 (1996) 1973-1982.

[143] C.R. Becer, S. Hahn, M.W.M. Fijten, H.M.L. Thijs, R. Hoogenboom, U.S. Schubert, Libraries of methacrylic acid and oligo(ethylene glycol) methacrylate copolymers with LCST behavior, *Journal of Polymer Science Part A: Polymer Chemistry*, 46 (2008) 7138-7147.

[144] A. Graillot, C. Cojocariu, D. Bouyer, S. Monge, S. Mauchauffe, J.-J. Robin, C. Faur, Thermosensitive polymer Enhanced Filtration (TEF) process: An innovative process for heavy metals removal and recovery from industrial wastewaters, *Separation and Purification Technology*, 141 (2015) 17-24.

[145] A. Graillot, S. Djenadi, C. Faur, D. Bouyer, S. Monge, J.J. Robin, Removal of metal ions from aqueous effluents involving new thermosensitive polymeric sorbent, *Water Science and Technology*, 67 (2013) 1181-1187.

[146] D. Gomes Rodrigues, N. Dacheux, S. Pellet-Rostaing, C. Faur, D. Bouyer, S. Monge, The first report on phosphonate-based homopolymers combining both chelating and thermosensitive properties of gadolinium: Synthesis and evaluation, *Polym. Chem.*, 6 (2015).

[147] D. Gomes Rodrigues, S. Monge, S. Pellet-Rostaing, N. Dacheux, D. Bouyer, C. Faur, Sorption properties of carbamoylmethylphosphonated-based polymer combining both sorption and thermosensitive properties: New valuable hydrosoluble materials for rare earth elements sorption, *The Chemical Engineering Journal*, 355 (2019) 871-880.

[148] D. Gomes Rodrigues, S. Monge, S. Pellet-Rostaing, N. Dacheux, D. Bouyer, C. Faur, A new carbamoylmethylphosphonic acid-based polymer for the selective sorption of rare earth elements, *Chemical Engineering Journal*, (2019).

References

- [149] D. Gomes Rodrigues, S. Monge, N. Dacheux, S. Pellet-Rostaing, C. Faur, Highlighting the selective properties of carbamoylmethylphosphonated hydrosoluble polymers for Gd(III)/Th(IV)/U(VI) separation, *Separation and Purification Technology*, 254 (2021) 117260.
- [150] L. Ebdon, L. Pitts, R. Cornelis, H. Crews, P. Quevauviller, O. Donard, Trace element speciation for environment, food and health, Royal Society of Chemistry, 2001.
- [151] A. Gonzalez, M.L. Cervera, S. Armenta, M. de la Guardia, A review of non-chromatographic methods for speciation analysis, *Analytica Chimica Acta*, 636 (2009) 129-157.
- [152] F. Porcaro, S. Roudeau, A. Carmona, R. Ortega, Advances in element speciation analysis of biomedical samples using synchrotron-based techniques, *TrAC Trends in Analytical Chemistry*, 104 (2018) 22-41.
- [153] Y. Ogra, Biology and toxicology of tellurium explored by speciation analysis, *Metallomics*, 9 (2017) 435-441.
- [154] H. Kaasalainen, A. Stefánsson, G.K. Druschel, Geochemistry and speciation of Fe(II) and Fe(III) in natural geothermal water, Iceland, *Applied Geochemistry*, 87 (2017) 146-157.
- [155] P.M. Thanh, B. Ketheesan, Z. Yan, D. Stuckey, Trace metal speciation and bioavailability in anaerobic digestion: A review, *Biotechnology Advances*, 34 (2016) 122-136.
- [156] W. Quiroz, L. Aguilar, M. Barría, J. Veneciano, D. Martínez, M. Bravo, M.G. Lobos, L. Mercado, Sb(V) and Sb(III) distribution in human erythrocytes: Speciation methodology and the influence of temperature, time and anticoagulants, *Talanta*, 115 (2013) 902-910.
- [157] T.A. Maryutina, A.R. Timerbaev, Metal speciation analysis of petroleum: Myth or reality?, *Analytica Chimica Acta*, 991 (2017) 1-8.
- [158] J. Huang, F. Yuan, G. Zeng, X. Li, Y. Gu, L. Shi, W. Liu, Y. Shi, Influence of pH on heavy metal speciation and removal from wastewater using micellar-enhanced ultrafiltration, *Chemosphere*, 173 (2017) 199-206.
- [159] J. Guzman, I. Saucedo, J. Revilla, R. Navarro, E. Guibal, Copper sorption by chitosan in the presence of citrate ions: influence of metal speciation on sorption mechanism and uptake capacities, *International Journal of Biological Macromolecules*, 33 (2003) 57-65.
- [160] H. Xu, M. Ding, K. Shen, J. Cui, W. Chen, Removal of aluminum from drinking water treatment sludge using vacuum electrokinetic technology, *Chemosphere*, 173 (2017) 404-410.

References

- [161] R.H. Byrne, L.R. Kump, K.J. Cantrell, The influence of temperature and pH on trace metal speciation in seawater, *Marine Chemistry*, 25 (1988) 163-181.
- [162] Y. Jo, H.-K. Kim, J.-I. Yun, Complexation of $\text{UO}_2(\text{CO}_3)_3^{4-}$ with Mg^{2+} at varying temperatures and its effect on U(vi) speciation in groundwater and seawater, *Dalton Transactions*, 48 (2019) 14769-14776.
- [163] G.F. Koopmans, W.D.C. Schenkeveld, J. Song, Y. Luo, J. Japenga, E.J.M. Temminghoff, Influence of EDDS on Metal Speciation in Soil Extracts: Measurement and Mechanistic Multicomponent Modeling, *Environmental Science & Technology*, 42 (2008) 1123-1130.
- [164] P. Gundersen, E. Steinnes, Influence of pH and TOC concentration on Cu, Zn, Cd, and Al speciation in rivers, *Water Research*, 37 (2003) 307-318.
- [165] G. Morrison, G. Batley, T.M. Florence, Metal Speciation and Toxicity, *CHEM. BR.*, 25 (1989) 791-796.
- [166] R. Miravet, E. Hernández-Nataren, A. Sahuquillo, R. Rubio, J.F. López-Sánchez, Speciation of antimony in environmental matrices by coupled techniques, *TrAC Trends in Analytical Chemistry*, 29 (2010) 28-39.
- [167] J.M. VanBriesen, M. Small, C. Weber, J. Wilson, Modelling chemical speciation: thermodynamics, kinetics and uncertainty, *Modelling of Pollutants in Complex Environmental Systems*, 2 (2010) 135.
- [168] L.O. Öhman, S. Sjöberg, The experimental determination of thermodynamic properties for aqueous aluminium complexes, *Coordination Chemistry Reviews*, 149 (1996) 33-57.
- [169] T.P. Nigl, N.D. Smith, T. Lichtenstein, J. Gesualdi, K. Kumar, H. Kim, Determination of Thermodynamic Properties of Alkaline Earth-liquid Metal Alloys Using the Electromotive Force Technique, *Journal of visualized experiments : JoVE*, (2017) 56718.
- [170] T. Fridriksson, P.S. Neuhoff, B.E. Viani, D.K. Bird, Experimental determination of thermodynamic properties of ion-exchange in heulandite: Binary ion-exchange experiments at 55 and 85° C involving Ca^{2+} , Sr^{2+} , Na^{+} , and K^{+} , *American Journal of Science*, 304 (2004) 287-332.
- [171] F. Morel, J. Morgan, Numerical method for computing equilibriums in aqueous chemical systems, *Environmental Science & Technology*, 6 (1972) 58-67.

References

- [172] M. Di Bonito, S. Lofts, J.E. Groenenberg, Chapter 11 - Models of Geochemical Speciation: Structure and Applications, in: B. De Vivo, H.E. Belkin, A. Lima (Eds.) *Environmental Geochemistry (Second Edition)*, Elsevier, 2018, pp. 237-305.
- [173] S. Lantenois, B. Prélot, J.-M. Douillard, K. Szczodrowski, M.-C. Charbonnel, Flow microcalorimetry: Experimental development and application to adsorption of heavy metal cations on silica, *Applied Surface Science*, 253 (2007) 5807-5813.
- [174] D.L. Parkhurst, C.A.J. Appelo, Description of input and examples for PHREEQC version 3: a computer program for speciation, batch-reaction, one-dimensional transport, and inverse geochemical calculations, in: *Techniques and Methods*, Reston, VA, 2013, pp. 519.
- [175] L. Karimzadeh, H. Lippold, M. Stockmann, C. Fischer, Effect of DTPA on europium sorption onto quartz – Batch sorption experiments and surface complexation modeling, *Chemosphere*, 239 (2020) 124771.
- [176] V.V. Khutoryanskiy, R.Y. Smyslov, A.V. Yakimansky, *Modern Methods for Studying Polymer Complexes in Aqueous and Organic Solutions*, Polymer Science, Series A, 60 (2018) 553-576.
- [177] A. Thanassoulas, G. Nounesis, Isothermal Titration Calorimetry: A Powerful Tool for the Characterization of Molecular Interactions, in: C. Demetzos, N. Pippa (Eds.) *Thermodynamics and Biophysics of Biomedical Nanosystems: Applications and Practical Considerations*, Springer Singapore, Singapore, 2019, pp. 63-103.
- [178] V.K. Srivastava, R. Yadav, Chapter 9 - Isothermal titration calorimetry, in: G. Misra (Ed.) *Data Processing Handbook for Complex Biological Data Sources*, Academic Press, 2019, pp. 125-137.
- [179] S. Leavitt, E. Freire, Direct measurement of protein binding energetics by isothermal titration calorimetry, *Current Opinion in Structural Biology*, 11 (2001) 560-566.
- [180] V. Karlsen, E.B. Heggset, M. Sørli, The use of isothermal titration calorimetry to determine the thermodynamics of metal ion binding to low-cost sorbents, *Thermochimica Acta*, 501 (2010) 119-121.
- [181] F. Taube, B. Drobot, A. Rossberg, H. Foerstendorf, M. Acker, M. Patzschke, M. Trumm, S. Taut, T. Stumpf, Thermodynamic and Structural Studies on the Ln(III)/An(III) Malate Complexation, *Inorganic Chemistry*, 58 (2019) 368-381.

References

- [182] F.M. Lounis, J. Chamieh, L. Leclercq, P. Gonzalez, A. Geneste, B. Prelot, H. Cottet, Interactions between Oppositely Charged Polyelectrolytes by Isothermal Titration Calorimetry: Effect of Ionic Strength and Charge Density, *The Journal of Physical Chemistry B*, 121 (2017) 2684-2694.
- [183] J. Muller, X. Ding, A. Geneste, J. Zajac, B. Prelot, S. Monge, Complexation properties of water-soluble poly(vinyl alcohol) (PVA)-based acidic chelating polymers, *Separation and Purification Technology*, 255 (2021) 117747.
- [184] A. Clearfield, Coordination chemistry of phosphonic acids with special relevance to rare earths, *Journal of Alloys and Compounds*, 418 (2006) 128-138.
- [185] W. Bisset, H. Jacobs, N. Koshti, P. Stark, A. Gopalan, Synthesis and metal ion complexation properties of a novel polyethyleneimine N-methylhydroxamic acid water soluble polymer, *Reactive and Functional Polymers*, 55 (2003) 109-119.
- [186] G. Jarvinen, Water-soluble chelating polymers for removal of actinides from wastewater, in: Pacific Northwest Lab., Richland, WA (United States), Conference: Efficient separations and processing crosscutting program 1996 technical meeting, Gaithersburg, MD (United States), 16-19 Jan, 1996, pp. 52.
- [187] K.L. Nash, P.G. Rickert, E.P. Lessmann, M.D. Mendoza, J.F. Feil, J.C. Sullivan, New Water-Soluble Phosphonate and Polycarboxylate Complexants for Enhanced f Element Separations, in: K.L. Nash, G.R. Choppin (Eds.) *Separations of f Elements*, Springer US, Boston, MA, 1995, pp. 125-141.
- [188] G. Jarvinen, Water-soluble chelating polymers for removal of actinides from wastewater, in, United States, 1996.
- [189] Y. Yang, S.D. Alexandratos, Affinity of Polymer-Supported Reagents for Lanthanides as a Function of Donor Atom Polarizability, *Industrial & Engineering Chemistry Research*, 48 (2009) 6173-6187.
- [190] A. Graillet, S. Djenadi, C. Faur, D. Bouyer, S. Monge, J.-J. Robin, Removal of metal ions from aqueous effluents involving new thermosensitive polymeric sorbent, *Water science and technology*, 67 (2013) 1181-1187.
- [191] T. Hidalgo, L. Kuhar, A. Beinlich, A. Putnis, Effect of multistage solution–mineral contact in in-situ recovery for low-grade natural copper samples: Extraction, acid consumption, gangue-mineral changes and precipitation, *Minerals Engineering*, 159 (2020) 106616.

References

- [192] A.M. Eyal, R. Canari, pH dependence of carboxylic and mineral acid extraction by amine-based extractants: effects of pKa, amine basicity, and diluent properties, *Industrial & engineering chemistry research*, 34 (1995) 1789-1798.
- [193] C.F. Quinn, M.C. Carpenter, M.L. Croteau, D.E. Wilcox, Chapter One - Isothermal Titration Calorimetry Measurements of Metal Ions Binding to Proteins, in: A.L. Feig (Ed.) *Methods in Enzymology*, Academic Press, 2016, pp. 3-21.
- [194] B. Chen, J. Liu, L. Lv, L. Yang, S. Luo, Y. Yang, S. Peng, Complexation of Lanthanides with N,N,N',N'-Tetramethylamide Derivatives of Bipyridinedicarboxylic Acid and Phenanthrolinecarboxylic Acid: Thermodynamics and Coordination Modes, *Inorganic Chemistry*, 58 (2019) 7416-7425.
- [195] M. Karavan, F. Arnaud-Neu, V. Hubscher-Bruder, I. Smirnov, V. Kalchenko, Novel phosphorylated calixarenes for the recognition of f-elements, *Journal of Inclusion Phenomena and Macrocyclic Chemistry*, 66 (2010) 113-123.
- [196] M.A. Mostefa Side Larbi, C. Sauzet, P. Piccerelle, P. Cau, N. Levy, P. Gallice, D. Berge-Lefranc, Thermodynamic study of the interaction between calcium and zoledronic acid by calorimetry, *The Journal of Chemical Thermodynamics*, 97 (2016) 290-296.
- [197] K. Popov, H. Rönkkömäki, L.H. Lajunen, Critical evaluation of stability constants of phosphonic acids (IUPAC technical report), *Pure and applied chemistry*, 73 (2001) 1641-1677.
- [198] S. Pailloux, C.E. Shirima, K.A. Smith, E.N. Duesler, R.T. Paine, N.J. Williams, R.D. Hancock, Synthesis and Reactivity of (Benzoxazol-2-ylmethyl)phosphonic Acid, *Inorganic Chemistry*, 49 (2010) 9369-9379.
- [199] W. Liansheng, M. Casarci, G.M. Gasparini, THE EXTRACTION OF Eu(III) FROM ACIDIC MEDIA BY OCTYL(PHENYL)-N,N-DIISOBUTYL CARBAMOYLMETHYLPHOSPHINE OXIDE, *Solvent Extraction and Ion Exchange*, 8 (1990) 49-64.
- [200] E. Philip Horwitz, D.C. Kalina, H. Diamond, G.F. Vandegrift, W.W. Schulz, THE TRUEX PROCESS - A PROCESS FOR THE EXTRACTION OF THE TRANSURANIC ELEMENTS FROM NITRIC ACID WASTES UTILIZING MODIFIED PUREX SOLVENT*, *Solvent Extraction and Ion Exchange*, 3 (1985) 75-109.
- [201] E.P. Horwitz, R. Chiarizia, R.C. Gatrone, BEHAVIOR OF AMERICIUM IN THE STRIP STAGES OF THE TRUEX PROCESS, *Solvent Extraction and Ion Exchange*, 6 (1988) 93-110.

References

- [202] K.A. Martin, E.P. Horwitz, J.R. Ferraro, INFRARED STUDIES OF BIFUNCTIONAL EXTRACTANTS, *Solvent Extraction and Ion Exchange*, 4 (1986) 1149-1169.
- [203] W.W. Schulz, E.P. Horwitz, The Truex Process and the Management of Liquid Tru Uwaste, *Separation Science and Technology*, 23 (1988) 1191-1210.
- [204] K.L. Nash, A REVIEW OF THE BASIC CHEMISTRY AND RECENT DEVELOPMENTS IN TRIVALENT f-ELEMENTS SEPARATIONS, *Solvent Extraction and Ion Exchange*, 11 (1993) 729-768.
- [205] M. Mazzanti, R. Wietzke, J. Pécaut, J.-M. Latour, P. Maldivi, M. Remy, Structural and Density Functional Studies of Uranium(III) and Lanthanum(III) Complexes with a Neutral Tripodal N-Donor Ligand Suggesting the Presence of a U–N Back-Bonding Interaction, *Inorganic Chemistry*, 41 (2002) 2389-2399.
- [206] G.R. Choppin, Covalency in f-element bonds, *Journal of Alloys and Compounds*, 344 (2002) 55-59.
- [207] O. Páv, I. Košiová, I. Barvík, R. Pohl, M. Buděšínský, I. Rosenberg, Synthesis of oligoribonucleotides with phosphonate-modified linkages, *Organic & Biomolecular Chemistry*, 9 (2011) 6120-6126.
- [208] M. Fild, T. Oehmigen, M. Sebastian, M. Vahldiek, 1, 3, 4-Oxa-und 1, 3, 4-Thia-diphospholane aus Diphosphorsubstituierten 2-Oxa-und 2-Thia-propanen, *Zeitschrift für anorganische und allgemeine Chemie*, 589 (1990) 187-198.
- [209] S.M. McCutcheon, S.M. Kajiura, Electrochemical properties of lanthanide metals in relation to their application as shark repellents, *Fisheries Research*, 147 (2013) 47-54.
- [210] R.D. Teo, J. Termini, H.B. Gray, Lanthanides: Applications in Cancer Diagnosis and Therapy, *Journal of Medicinal Chemistry*, 59 (2016) 6012-6024.
- [211] K. Lv, C.-T. Yang, J. Han, S. Hu, X.-L. Wang, An initial demonstration of hierarchically porous niobium alkylphosphonates coordination polymers as potent radioanalytical separation materials, *Journal of Chromatography A*, 1504 (2017) 35-45.
- [212] B.T. Benkhaled, T. Montheil, V. Lapinte, S. Monge, Hydrosoluble phosphonic acid functionalized poly(2-ethyl-2-oxazoline) chelating polymers for the sorption of metallic cations, *Journal of Polymer Science*, n/a.

References

- [213] C.-Y. Chen, C.-Y. Chen, Stability constants of polymer-bound iminodiacetate-type chelating agents with some transition-metal ions, *Journal of Applied Polymer Science*, 86 (2002) 1986-1994.
- [214] T. Kobayashi, K. Akutsu, M. Nakase, S. Suzuki, H. Shiwaku, T. Yaita, Complexation properties and structural character of lanthanides complexes of O,N-hetero donor ligand BIZA, *Separation Science and Technology*, 54 (2019) 2077-2083.
- [215] E.P. Horwitz, A.C. Muscatello, D.G. Kalina, L. Kaplan, The Extraction of Selected Transplutonium(III) and Lanthanide(III) Ions by Dihexyl-N, N-diethylcarbamoylmethylphosphonate from Aqueous Nitrate Media, *Separation Science and Technology*, 16 (1981) 417-437.
- [216] Y. Sasaki, Y. Sugo, S. Suzuki, S. Tachimori, THE NOVEL EXTRACTANTS, DIGLYCOLAMIDES, FOR THE EXTRACTION OF LANTHANIDES AND ACTINIDES IN HNO₃-n-DODECANE SYSTEM, *Solvent Extraction and Ion Exchange*, 19 (2001) 91-103.
- [217] A. Graillot, S. Monge, C. Faur, D. Bouyer, J.-J. Robin, Synthesis by RAFT of innovative well-defined (co) polymers from a novel phosphorus-based acrylamide monomer, *Polymer Chemistry*, 4 (2013) 795-803.
- [218] X. DING, Synthèse et évaluation de polymères phosphorés pour le traitement d'effluents chargés en lanthanides et actinides - Chapter 3: Phosphonic acid monomers and polymers for the complexation of Cerium and Neodymium: evaluation by Isothermal Titration Calorimetry (ITC), in, Université de Montpellier, 2020, pp. 83-115.
- [219] G. Johansson, M. Magini, H. Ohtaki, Coordination around thorium(IV) in aqueous perchlorate, chloride and nitrate solutions, *Journal of Solution Chemistry*, 20 (1991) 775-792.
- [220] X. DING, Synthèse et évaluation de polymères phosphorés pour le traitement d'effluents chargés en lanthanides et actinides - Chapter 2: Comparison of Isothermal Titration Calorimetry (ITC) and Inductively Coupled Plasma Mass Spectroscopy (ICP-MS) to study sorption properties of polymers, in, Université de Montpellier, 2020, pp. 56-82.